

SORTING OUT CERAMICS

**Correlating Change in the Technology
of Ceramic Production with the Chronology
of 18th and early 19th century
Western BaTswana Towns**

Dana Drake Rosenstein

**A dissertation submitted in fulfilment of the requirements
for the Master of Science degree in the
Department of Archaeology, University of Cape Town**

February 2008

The copyright of this thesis vests in the author. No quotation from it or information derived from it is to be published without full acknowledgement of the source. The thesis is to be used for private study or non-commercial research purposes only.

Published by the University of Cape Town (UCT) in terms of the non-exclusive license granted to UCT by the author.

Acknowledgements

From its inception, this project has been interdisciplinary in design and collaborative in practice. It could not have been achieved without the time and effort of many people who helped me along the way.

At QUADRU, Stephan Woodborne, Marc Pienaar, John Vogel, Siep Talma, and Annemarie Fuls were always willing to answer questions regarding the intricacies of radiocarbon and optically stimulated luminescence dating. Luminescence sampling at the stone-walled towns would have been impracticable without the enthusiasm of the landowners: Pierre Retief at Olifantspoort, Casper Willemse at Molokwane and Paul van der Merwe at Kaditshwene. I greatly appreciate the assistance of Pia Bombardella and Duncan Miller for translating the field notes of HB Sentker from Afrikaans to English and of Thomas Huffman for sharing Revil Mason's files on Olifantspoort radiocarbon dates. Confirmation of Dirk Harris' talent in all things computer-related can be seen in many of the images in this thesis.

This research would not have been viable without the patience and expertise of Zenobia Jacobs, who guided me through the intricacies of optically stimulated luminescence dating and calculated our final results. Gill Collett and Jan Boeyens were willing partners for road trips to collect the samples.

Life in Cape Town is beautiful because of friends like Arvind Varsani. Duncan Miller was the first to show me around a materials laboratory, and he has been an inimitable mentor and friend ever since. Without Simon Hall, none of this would have been possible.

Life in Arizona would be dull without my (expanded) cohort. It would be impossible without David Killick, whose knowledge, encouragement and friendship is sustaining my graduate career.

And to my family, Mom, Dad and Jodi, thank you for your support and love.

Abstract

The archaeology of the 18th and 19th century western BaTswana towns in the Rustenburg-Zeerust region of North West Province, South Africa, is important and complex. This period, the late Moloko phase at the end of the Late Iron Age, was a time of significant upheaval. The colonial frontier was advancing, slowly hemming in the BaTswana population. In the mid-17th century, the climate became cooler and drier, resulting in widespread drought through the beginning of the 18th century. These factors increased inter-group competition over land, access to trade goods and control of agricultural and exchange networks.

The sociopolitical response to these political and environmental pressures was large-scale centralization, in which people moved from dispersed village homesteads into expansive stone-walled towns with populations in the thousands. Settlement aggregation had significant effects on the scale of production at these new centres. Whereas earlier, small populations were largely self-supporting in basic needs such as agriculture and pottery manufacture, large, centralized populations required controlled maintenance of food and other natural resources. This trend toward sustainable management likely spread to materials production, as well.

This research examines a shift in pottery manufacturing techniques that occurred between the early and late Moloko periods, as evidenced by inclusions of graphitic and lustrous, platy and fibrous tempers in ceramic samples from town sites that do not occur in ceramics from earlier sites. Comparatively, petrographic data of analyzed potsherds from Marothodi, an early 19th century BaTlokwa town, reveals only two of 42 ceramic samples containing lustrous inclusions and none made of graphitic clay. A number of concepts, drawn from materials science and ethnographic analogy, are put forth to help understand this variation. This shift must be examined in the broader context of aggregation. Craft specialization and standardization might be one solution for providing for the needs of a large population. There are underpinning technological, social, political, economic, environmental and ideological factors that must be considered in understanding and interpreting the production and use of an object. Also implicit in the *chaîne opératoire* of pottery manufacture is human

behaviour, technological choice, function, style and social identity. Changes in scale or type of ceramic manufacture must be evaluated in terms of the sociopolitical, cultural and technological context in which they took place.

These shifts in pottery production occurred over a relatively short time, but the exact sequence of change over the late Moloko is unknown. While the oral-historical record offers a general indication of when the large stone-walled towns were occupied and abandoned, the beginning and duration of settlement cannot be resolved. This is because radiocarbon, the most common archaeometric method for dating the Late Iron Age, is ineffectual during the late Moloko due to anomalies in atmospheric production of radiocarbon and acute De Vries effects in the time range AD 1650-1950. Bayesian radiocarbon calibration can help to refine radiocarbon results, but still the resolution is not precise enough to inform usefully on the late Moloko archaeological record.

An alternative dating method is optically stimulated luminescence (OSL), which determines the amount of time passed since a mineral grain was last exposed to heat or light. This research includes a pilot study in dating late Moloko sites by measuring OSL of quartz grains from furnace and midden features for which approximate age is already known through oral-historical records and ceramic seriation.

The results of this experiment in OSL dating of the recent past are promising. OSL provides chronological control with the resolution necessary for establishing the settlement and ceramic sequence of late Moloko sites. This constitutes a first step in the future construction of a master archaeomagnetic calibration curve for absolute dating of sites in this region using chronometric data obtained through OSL. Archaeomagnetism is potentially the best method for relative, and eventually absolute, dating of sites in this temporal and geographic context.

Table of Contents

i	Acknowledgements
ii	Abstract
viii	List of Figures
xv	List of Tables
xvii	List of Equations
1	Chapter 1 Introduction
4	THE IRON AGE IN SOUTHERN AFRICA
6	The Late Iron Age and the Moloko period
10	BaTswana sites of the late Moloko
11	<i>Olifantspoort</i>
13	<i>Molokwane</i>
14	<i>Kaditshwene</i>
15	<i>Marothodi</i>
16	Sorting out ceramics: contextualizing the chronological problem of the late Moloko
18	Chapter 2 Late Moloko Ceramic Research
18	STUDIES OF 16 th TO 19 th CENTURY MOLOKO CERAMICS
22	LATE MOLOKO CERAMIC ANALYSIS
24	Geology of the Rustenburg-Zeerust region
27	Petrography of early and late Moloko ceramics
29	Petrography of Marothodi ceramics
33	TECHNOLOGICAL AND SOCIAL ASPECTS OF LATE MOLOKO POTTERY PRODUCTION
33	Technological choice
39	Craft specialization

43	Technological style
44	Social identity
49	CERAMICS AT MAROTHODI: A STUDY IN VARIATION
52	Chapter 3 Dating Method One: Radiocarbon
52	CONSIDERATIONS FOR RADIOCARBON DATING
59	RADIOCARBON IN THE LATE MOLOKO
60	Conventional radiocarbon calibration of late Moloko dates
63	BAYESIAN RADIOCARBON CALIBRATION AT OLIFANTSPOORT AND KADITSHWENE
73	Chapter 4 Dating Method Two: The Oral-Historical Record
76	ORAL-HISTORICAL DATING FOR THE LATE MOLOKO
76	Olifantspoort
77	Molokwane
79	Kaditshwene
79	Marothodi
80	EVALUATING ORAL-HISTORICAL DATES
82	Chapter 5 Dating Method Three: Optically Stimulated Luminescence
82	OPTICALLY STIMULATED LUMINESCENCE DATING IN SOUTHERN AFRICA
82	Optical dating of old contexts in southern Africa
83	Optical dating of young contexts in southern Africa
85	CONSIDERATIONS FOR OPTICALLY STIMULATED LUMINESCENCE DATING

86	Principles of optical dating
90	Understanding and measuring equivalent dose
94	Understanding and measuring dose rate

106 Chapter 6 Late Moloko OSL: Sampling, Analysis and Results

106	OSL DATING THE LATE MOLOKO
108	Sample selection
112	Sample collection
115	Determining sample dosimetry
124	Sample pre-treatment
126	OSL MEASUREMENT AND RESULTS

136 Chapter 7 Optically Stimulated Luminescence: Interpretation and Discussion

136	OSL DATING OF THE LATE MOLOKO
137	Midden samples
138	<i>Olifantspoort</i>
139	<i>Molokwane</i>
139	<i>Kaditshwene</i>
140	<i>Marothodi</i>
142	Furnace samples
142	<i>Kaditshwene</i>
143	<i>Marothodi</i>
145	Archaeological and geological considerations for OSL dating in the Late Iron Age
147	THE FUTURE OF OSL DATING FOR THE LATE IRON AGE

150	Chapter 8	Conclusion
150	SORTING OUT CERAMICS	
151	FUTURE DIRECTIONS	
154	Appendix A	Table of Previous Early and Late Moloko Ceramics Analysed
157	Appendix B	Table of Early and Late Moloko Ceramic Data
167	Appendix C	Table of Marothodi Ceramics Analysed
171	Appendix D	Table of Marothodi Ceramic Data
177	References Cited	

List of Figures

1 Chapter 1 Introduction

- 3 Figure 1.1. Dating samples were collected from four late Moloko stone-walled sites (site locations drawn on Map 1994).
- 4 Figure 1.2. A vegetation map of the summer rainfall region in which the Moloko sites are located. The green lines enclose the agriculturally productive Bushveld zones (Hall et al. 2007: Figure 2, after Mucina & Rutherford 2006).
- 7 Figure 1.3. A diagrammatic representation of the Moloko settlement sequence in the Rustenburg-Zeerust region. Dispersed early Moloko villages characterize the 16th to mid-18th century. The first stone walling in this area, called Type N (Maggs 1976), occurs after about AD 1550. Late Moloko aggregation resulted in the large stone-walled towns of the early 19th century. Figure adapted from Maggs (1976) and an unpublished illustration courtesy of Simon Hall.
- 9 Figure 1.4. Variations over the last millennium in the oxygen isotope values of stalagmites in the Makapansgat Valley, approximately 300 km northeast of Rustenburg. Higher oxygen isotope values are associated with a warmer, wetter climate; lower values a cooler, drier climate. Figure adapted from Tyson *et al.* (2002: Figure 1b).
- 12 Figure 1.5. Artist's rendering of the late Moloko site on the farm Olifantspoort (Mason 1987: 71).
- 13 Figure 1.6. Aerial photograph of the centre section at Molokwane. Note the large cattle enclosure at the core of the *kgosing*. Photograph courtesy School of Geography, Archaeology and Environmental Studies, University of the Witwatersrand, Johannesburg.
- 15 Figure 1.7. 'Kurreechane from the East,' Campbell's field sketch of the hilltop *kgosing* at Kaditshwene (Campbell 1820a).
- 16 Figure 1.8. Site plan of Marothodi. Areas of copper and iron metallurgy are marked. Note the central cattle enclosure, the largest among late Moloko towns (Hall *et al.* 2006: Figure 2).

18 Chapter 2 Late Moloko Ceramic Research

- 19 Figure 2.1. Drawings of typical early Moloko (left) and late Moloko (right) pottery classes. Note the significant decline frequency of design elements represented with the shift to stone-walled architecture in the later period

(adapted from Hall 1998: 252-253).

- 20 Figure 2.2. Ceramic shapes and styles typical of early Moloko pottery (*Madikwe* types, modified from Huffman 2007a: Figure 15.20A).
- 21 Figure 2.3. Ceramic shapes and styles typical of late Moloko pottery (*Buispoort* types, modified from Huffman 2007a: Figure 15.21A). Compare to Figure 2.2; from the early to late Moloko, the stylistic complexity of vessels decreases (Hall 1998).
- 23 Figure 2.4. 1: 250 000 geologic map of the research region (adapted from Jansen *et al.* 1974; and Walraven 1981). The locations of the Moloko period Late Iron Age sites under discussion are located generally northwest to south of the Pilanesberg Complex, at centre.
- 24 Figure 2.5. An outcrop of weathered, dark grey graphitic schist at Kaditshwene, adjacent to a stone-walled enclosure.
- 25 Figure 2.6. Sampling a light-coloured, lustrous, talcaceous schist at Molokwane.
- 26 Figure 2.7. Map showing the geographic region under discussion and the location of early and late Moloko period Late Iron Age sites from which ceramic samples were analysed for Rosenstein (2002) and this thesis (map modified from Hall 1998: 237).
- 28 Figure 2.8. Photograph and petromicrograph (XPL, width = 7.5 mm) of a ceramic sherd from Rietfontein, an early Moloko site near Kaditshwene. Note the lack of prominent or atypical inclusions or added temper.
- 29 Figure 2.9. Photograph and petromicrograph (XPL, width = 7.5 mm) of a ceramic sherd from the late Moloko component at Olifantspoort. Note the presence of very coarse sand and pebble-sized grains of muscovite mica that were crushed and added as temper to the clay material. Also note the distinct sparkly effect the inclusion of mica has on the exterior of the ceramic.
- 31 Figure 2.10. XPL petromicrographs representing typical petrographic groups of Marothodi ceramics as defined in Table 2.2 and Appendix D. Scale bar = 1 mm.
- 34 Figure 2.11. Platy inclusions bridge the opening of a crack as it proceeds through the clay matrix, forcing crack closure and enhancing the fracture resistance of the clay (modified from Becher 1991: 258).
- 35 Figure 2.12. XPL petromicrograph of added mica inclusions aligned parallel to the working direction of the clay, or horizontally to an upright vessel, perpendicular to the exterior wall (VL-11-MDB).
- 42 Figure 2.13. 'The potter and her apprentice,' an ethnographic photograph taken at a homestead in Mochudi, Botswana, settled by the BaKgatla in AD

1871 (Duggan-Cronin 1929). The back courtyards are where primary pot construction takes place.

- 47 Figure 2.14. Engraving after an original 1812 portrait by Burchell of Mahútu, a BaTlapin woman. Burchell writes (as in original), "... the bonnet-like appearance on her head, is produced by the peculiar mode in which the Bachapin women dress their *hair*. The color here shown, is occasioned by the *sibiilo* with which it is powdered (Burchell 1824: 494, Plate 8).
- 48 Figure 2.15. Broken ceramic vessel with *sebito* still cached inside, excavated from the late Moloko site Olifantspoort (Mason 1987: 80).

52 Chapter 3 Dating Method One: Radiocarbon

- 53 Figure 3.1. Radiocarbon production and dating, after Taylor (1997: Figure 3.1).
- 54 Figure 3.2. Major carbon reservoirs on Earth (in 1012 kg), with carbon exchange rates (1012 kg/year) (adapted from Ruddiman 2001: Figure 2-32b). Radiocarbon is produced and released at a rate of about 7.5 kg/year.
- 56 Figure 3.3. The radiocarbon calibration curve for the Late Iron Age, 800-0 years before present (BP, where 14C 0 BP = cal AD 1950), in the southern hemisphere as developed with information from fourteen independent datasets (McCormac *et al.* 2004; Reimer *et al.* 2004). Suess and de Vries effects, or wiggles, can cause a single radiocarbon year (BP) to correspond to a range of calendar years (cal AD).
- 64 Figure 3.4. John Vogel, right, at a midden excavation at the site on Olifantspoort farm in October 1967, collecting material for radiocarbon age determination (Vogel 1971). OSL dating samples for this study were collected from a different section of this same large midden, as described in Chapter 6. Photograph courtesy QUADRU.
- 65 Figure 3.5. The large midden of the main *kgotla* at Kaditshwene, from the south. OSL dating samples for this study were collected from a different section of this same large midden, as described in Chapter 6. Photograph courtesy Jan Boeyens.
- 66 Figure 3.6. Radiocarbon date ranges for the middens at the site on Olifantspoort farm (above) and Kaditshwene (below). These results were calibrated with the Southern Hemisphere dataset (McCormac *et al.* 2004) of the CALIB 5.01 program (Stuiver & Reimer 1993), and the probability curves represent calculations made by traditional statistical methods, as presented in Table 3.1.
- 68 Figure 3.7. A graphical representation of chronological information entered in the BCal calibration program. Alpha 1 and beta 1 represent boundaries.

‘Midden’ represents the group of radiocarbon results, ordered according to stratigraphy.

70 Figure 3.8. Probability curves for Bayesian radiocarbon calibration of dates from the midden on Olifantspoort farm, as presented in Table 3.2. Note in (a) how the input of prior stratigraphic information increases the probability that deeper samples yield older calendar dates. In (b) an upper chronological boundary, a normally distributed mean around AD 1830 \pm 10, was added to the stratigraphic results, thus incorporating another type of prior information - the abandonment event of the *difaqane*.

71 Figure 3.9. Probability curves for Bayesian radiocarbon calibration of dates from the midden at Kaditshwene, as presented in Table 3.2. Note in (a) how the input of prior stratigraphic information increases the probability that deeper samples yield older calendar dates. In (b), an upper chronological boundary, an exact date of AD 1823, was added to the stratigraphic results to incorporate another type of prior information, the abandonment event of the *difaqane*.

73 Chapter 4 Dating Method Two: The Oral-Historical Record

75 Figure 4.1. Above, dispersal of BaTswana and neighbouring BaSotho chiefdoms through the 16th – 18th centuries. Below, distribution of groups around AD 1800 (Legassick 1969: Figures 5 and 6).

78 Figure 4.2. ‘Holding Peetso or general meeting;’ Campbell’s AD 1820 field sketch of the main *kgatla* in the *kgosing* of Kaditshwene. In the upper drawing, the ‘North side of Kurreechane Public Place,’ note the midden in the left corner (Campbell 1820b).

82 Chapter 5 Dating Method Three: Optically Stimulated Luminescence

89 Figure 5.1. A photograph and schematic of the Risø TL/OSL reader (modified from Risø DTU February 2008: cover, 2).

91 Figure 5.2. A typical decay curve for an aliquot from sample Kad 1, representing the number of OSL counts per second during exposure to blue LEDs. The shape of the curve reflects the rapid depletion of trapped electrons at first exposure.

92 Figure 5.3. A dose response curve for one aliquot of sample Kad 1. R 2 - R 7 refer to Run numbers as described on Table 5.1. $D_e = 2.7 \pm 0.2$ Gy. The recycling ratio for this aliquot, calculated by comparing the OSL signals from Run 2 and Run 7, is 0.95 ± 0.06 . For every aliquot measured successfully, the

D_e determined from its dose response curve is plotted on a radial diagram, as in Figures 6.14 - 6.17, to determine the mean D_e for the sample.

- 95 Figure 5.4. Sensitivity tests according to preheat temperature in the SAR protocol. Above, comparing the OSL measurement after the test dose T_X/T_N over 11 runs of different regenerative doses. Below, the change in D_e .
- 96 Figure 5.5. Recycling ratio test. An aliquot fails the test if the ratio of L_X/T_X from Run 7 to L_X/T_X from Run 2 is not within 10% error around unity, or 1.0. Here, aliquots 1, 7, 9 and 19 fail the recycling ratio test.
- 98 Figure 5.6. OSL IR depletion ratio test (Duller 2003). An aliquot fails the test if the ratio of L_X/T_X from Run 9 to L_X/T_X from Run 7 is not within two standard deviations of error around unity, or 1.0. Here, aliquots 5, 10 and 19 fail the OSL IR depletion ratio test.
- 100 Figure 5.7. Radiation accumulation by a sample measured to determine dose rate. Short-range alpha and beta particles from natural impurities in the sample comprise the internal component and long-range gamma particles and cosmic radiation from the surrounding environment comprise the external dose (Aitken 1998: Figure 2.2).
- 101 Figure 5.8. Positioning and environment of luminescence samples in relation to acquisition of environmental dose. Gamma radiation penetrates 30 cm. A good sample is 30 cm below an ancient ground surface and is not close to any objects or materials that might emit spurious radiation (Aitken 1997: Figure 7.2).
- 98 Figure 5.9. *In-situ* gamma spectrometry at an OSL sample location (Molo 1) in a Molokwane midden. The spectrometer, in the sample hole, is measuring U, Th and K concentrations from a 30 cm sphere around its sensitive crystal tip.

106 Chapter 6 Late Moloko OSL: Sampling, Analysis and Results

- 108 Figure 6.1. The white arrow points to the ash heap midden at the site on Olifantspoort farm excavated and radiocarbon dated by Revil Mason and John Vogel and where the OSL sample Olif 1 was collected (image adapted from Mason 1987: Fig. 36).
- 109 Figure 6.2. The black arrow points to the area in the central section of Molokwane, just east and down slope of the *kgosing*, where the midden sample Molo 1 was collected (image adapted from Pistorius 1994: Fig 3).
- 110 Figure 6.3. The black arrow indicates the position of the central midden at Kaditshwene from which OSL sample Kad 1 was collected. In John Campbell's field sketch (Figure 4.2), the midden is depicted in the upper left

corner. Note the symbol ©, to the left of the arrow here. This indicates the location of Campbell's wagon, drawn adjacent to the midden in the sketch. Sample Kad 2, a copper furnace wall, was collected on the northwest perimeter of this area in an unexcavated section of the site (image adapted from Boeyens 2003: Fig. 5).

- 111 Figure 6.4. At Marothodi, two samples were collected from SU25, marked by the black arrow at the north: Vlak 1, sediment from a midden, and Vlak 2, a copper furnace wall. For sample Vlak 3, sediment was collected from a midden in the area marked by the lower arrow, near the *kgosing* (image adapted from Hall *et al.* 2006: Fig. 2).
- 113 Figure 6.5. Collecting a midden sediment sample (Vlak 3) at Marothodi. The opaque PVC pipe, blocked at the far end with black plastic, is inserted horizontally into a cleaned section until the plastic appears at the near end.
- 114 Figure 6.6. Collecting a wall sample from a copper furnace (Kad 2) at Kaditshwene. The thick black plastic tarp ensures that the sample remains as much in the dark as possible. Photograph courtesy Jan Boeyens.
- 115 Figure 6.7. *In-situ* gamma spectrometry in the SU25 midden at Marothodi (Vlak 1). The deposit is sterile after 25 cm, thus it is not possible to collect a sample deep enough for the ideal 30 cm sphere of gamma ray penetration.
- 116 Figure 6.8. *In-situ* gamma spectrometry of a sampled copper furnace at Kaditshwene (Kad 2). The placement of this instrument is not ideal, because of the 30 cm spherical geometry over which the crystal collects information. Another option would be to place the spectrometer into an access hole dug behind the furnace wall before the sample is removed, however, this would have to be done before the furnace is excavated and its dimensions are known.
- 120 Figure 6.9. The Aptec spectrum for sample Olif 1. Counts under each peak are as follows: K 7783, U 1852 and Th 1569.
- 120 Figure 6.10. The Aptec spectrum for sample Molo 1. Counts under each peak are as follows: K 8283, U 1402 and Th 1231.
- 121 Figure 6.11. The Aptec spectra for samples Kad 1 and Kad 2. Counts under each peak for Kad 1 are as follows: K 3525, U 1382 and Th 1007; and for Kad 2: K 2731, U 991 and Th 917.
- 122 Figure 6.12. The Aptec spectra for samples Vlak 1, Vlak 2 and Vlak 3. Counts under each peak for Vlak 1 are as follows: K 2812, U 620 and Th 577; Vlak 2: K 1106, U 518 and Th 470; and Vlak 3: K 2882, U 424 and Th 384.
- 126 Figure 6.13. A 9.7 mm diameter aluminium sample disc sprayed with silicone oil through a 2 mm mask, on which quartz grains are mounted for luminescence measurement. Photograph courtesy of Marc Pienaar.

- 128 Figure 6.14. Radial plot of D_e for sample Olif 1 ($n = 37$). Because of high overdispersion, characteristic of partial bleaching, the minimum age model was used to estimate D_e .
- 128 Figure 6.15. Radial plot of D_e for sample Molo 1 ($n = 23$). The central age model was used to estimate D_e .
- 129 Figure 6.16a. Radial plot of D_e for sample Kad 1 ($n = 24$). The central age model was used to estimate D_e .
- 129 Figure 6.16b. Radial plot of D_e for sample Kad 2 ($n = 6$). The central age model was used to estimate D_e .
- 130 Figure 6.17a. Radial plot of D_e for sample Vlak 1 ($n = 38$). Because of high overdispersion, characteristic of partial bleaching, the minimum age model was used to estimate D_e .
- 130 Figure 6.17b. Radial plot of D_e for sample Vlak 2 ($n = 23$). The central age model was used to estimate D_e .
- 131 Figure 6.17c. Radial plot of D_e for sample Vlak 3 ($n = 40$). Because of high overdispersion, characteristic of partial bleaching, the minimum age model was used to estimate D_e .

List of Tables

- 27 Table 2.1. Summary of Appendix B: natural and added ceramic inclusion types in early and late Moloko potsherds (Rosenstein 2002).
- 30 Table 2.2. Marothodi ceramic sherd type according to petrographic group.
- 60 Table 3.1. Published radiocarbon dates on charcoal for late Moloko stone-walled sites.
- 61 Table 3.1 (continued). Published radiocarbon dates on charcoal for late Moloko stone-walled sites.
- 62 Table 3.1 (continued). Published radiocarbon dates on charcoal for late Moloko stone-walled sites.
- 69 Table 3.2. Bayesian calibrations for ordered radiocarbon data from the middens on Olifantspoort farm and at Kaditshwene.
- 74 Table 4.1. Comparing dating methods for late Moloko sites: radiocarbon dates calibrated with Bayesian statistics according to the beta 1 border of the *difaqane* and dates from the oral-historical record.
- 90 Table 5.1. Typical measurement cycle D_e determination for late Moloko sample aliquots using the single aliquot regenerative dose (SAR) protocol (Murray & Wintle 2000).
- 93 Table 5.2. The OSL measurements used to build the dose response curve for one aliquot (Disc 22) of sample Kad 1, as shown in Figure 5.3, using the single aliquot regenerative dose (SAR) protocol (see Table 5.1; Murray & Wintle 2000). The dose is administered in seconds (1 Gy per s). L_x/T_x is a measurement of OSL intensity.
- 107 Table 6.1. Comparing dating methods for late Moloko sites: radiocarbon dates calibrated with Bayesian statistics according to the beta 1 border of the *difaqane*, dates from the oral-historical record and OSL ages.
- 112 Table 6.2. Samples collected for OSL dating.
- 117 Table 6.3. Dose rates for late Moloko OSL samples.
- 118 Table 6.3 (continued). Dose rates for late Moloko OSL samples.
- 132 Table 6.4. Evaluation of the central and minimum age models (Galbraith *et al.* 1999) to determine final equivalent dose (D_e) for each late Moloko OSL sample.

List of Equations

- 67 *Equation 3.1* $\text{posterior} \propto \text{likelihood} \times \text{prior}$
- 87 *Equation 5.1* $\text{age estimate (ka)} = \frac{\text{equivalent dose (Gy)}}{\text{estimated dose rate (Gy/ka)}}$
- 123 *Equation 6.1* $\%K = \%K_2O \times 0.83$
- 123 *Equation 6.2* $\% \text{ weight loss} = \frac{\text{mass wet (g)} - \text{mass dry (g)}}{\text{mass dry (g)}} \times 100$

Chapter 1

Introduction

In the mid-18th century, Tswana speakers in what is now North West Province, South Africa, underwent a process of settlement aggregation that gave rise to large stone-walled town complexes. Some of these attained significant size, with populations of a few thousand to estimates of sixteen thousand people made by travellers at the time, for example, John Campbell when he visited the Hurutshe capital of Kaditshwene in the early 1820s (Campbell 1822b: 277). Kaditshwene and possibly other towns were more populous than contemporary Cape Town, the colonial capital in the southwest corner of the country. Prior to this, individual homesteads were relatively dispersed on this landscape. The development of these towns marked a period of intense political centralization in which chiefs progressively oversaw and directed complex economies and coordinated large-scale agriculture, specialized metal and ceramic production and regional trade, in which success was always threatened by competition from equally ambitious neighbours. The scale of settlement and political change during the 18th and early 19th century makes this a period of considerable importance in BaTswana history.

In archaeology, this era falls during the southern African Late Iron Age, within a ceramic tradition termed 'Moloko.' The identification of the Moloko is based on a stylistic analysis of Late Iron Age ceramics that also captures variability in this tradition through time and space (Evers 1981; Hall 1981; Mason 1986; Hall 1998).¹ More recent research also has contributed to identifying significant changes in ceramic production technology between the early Moloko, when settlement was in

¹ In this thesis, the term *early Moloko* refers to the Madikwe and Olifantspoort phases of the Moloko sequence, from roughly AD 1500-1700, and the associated ceramic types. (Note that while these are the earliest phases that occur in the Rustenburg-Zeerust region, in the overall Moloko sequence, Icon is 'early' and Madikwe and Olifantspoort are 'middle.') The term *late Moloko* refers to mid-18th century settlement aggregation of the Molokwane type and the Buispoort ceramics associated with large stone-walled towns. See Huffman (2007a).

dispersed homesteads, and the late Moloko, when people resettled in the large stone-walled towns (Rosenstein 2002).

To appropriately analyse this change over time, however, the ceramic and settlement data must be tied to the relative and absolute chronology of BaTswana occupation in the region. The chronology is critical to understand the process of aggregation, but radiocarbon dating, the most commonly available chronometric technique, is inadequate for use at sites occupied throughout the late Moloko phase. Because of anomalies in atmospheric production of radiocarbon in the time range 1650-1950 cal CE, a period with acute De Vries effects, a radiocarbon age in that period can fall statistically at any year in the 18th or 19th centuries.

The 'historic,' or generational, scale of occupation at these sites requires better chronological control of the aggregation and production processes. At the low level of chronometric resolution offered by radiocarbon, however, explaining the ceramic and settlement sequence becomes problematic. In the following chapters, analysis and interpretation of Moloko ceramic production is integrated with a critical discussion of techniques commonly used to determine dates of site occupation, and therefore pottery manufacture, during the Late Iron Age. This thesis presents a pilot study that contributes to resolving chronology with an alternative dating method to radiocarbon in order to better understand BaTswana history and genealogy, including settlement sequence, the timing of changes in material technologies, particularly ceramic and metal production, and periods of interaction and competition between and among regional groups.

Chapter 1 briefly introduces the Late Iron Age sequence, ethnography and material culture, with emphasis on BaTswana sites of the late Moloko. New research into ceramic technology during the Moloko period will be discussed in Chapter 2 and the need for more chronological precision in this specific area made explicit. Chapters 3 and 4 outline two methods available to obtain dates for late Moloko sites. These are conventional radiocarbon dating and the oral-historical record, neither of which provide the precision or accuracy needed for this research. Consequently, an experiment using optically stimulated luminescence (OSL) dating was carried out, and that chronometric technique is described in Chapter 5. Data, interpretation and

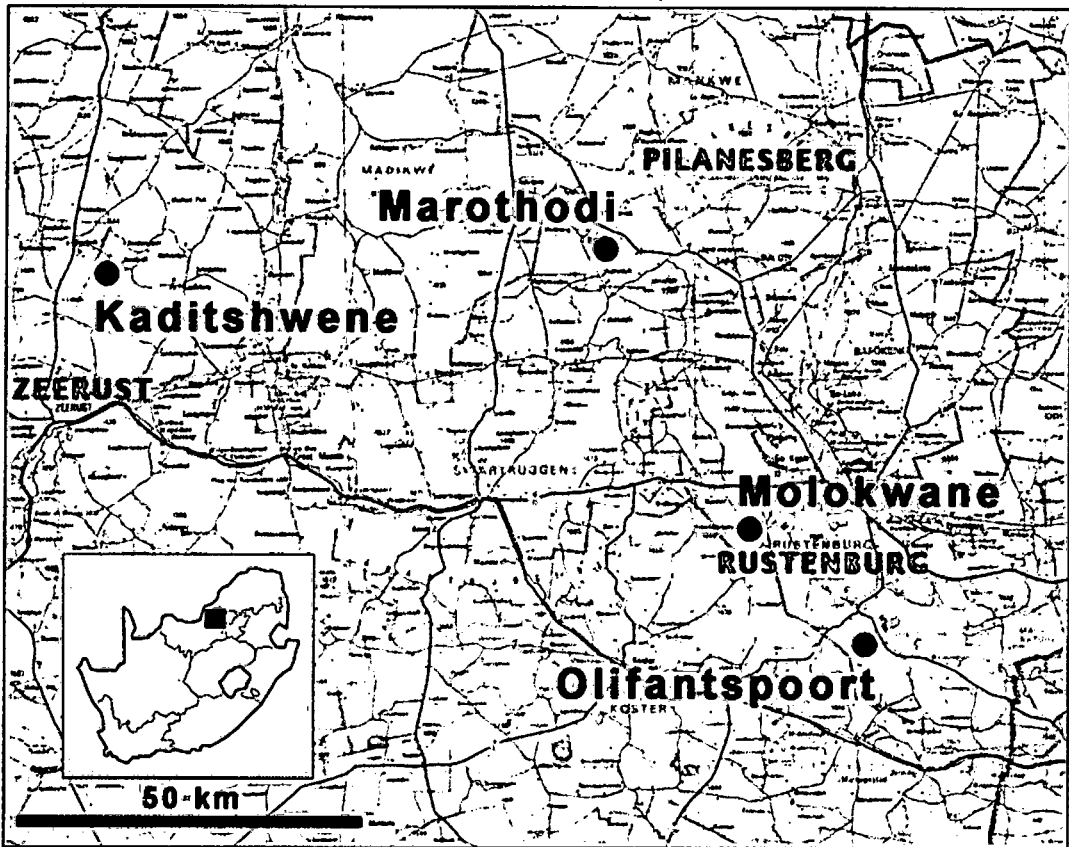


Figure 1.1. Dating samples were collected from four late Moloko stone-walled sites (site locations drawn on Map 1994).

discussion of the OSL experiment comprise Chapters 6 and 7. Chapter 8 offers concluding statements on the usefulness of OSL dating for both the Early and Late Iron Age periods in South Africa.

Dating samples were taken from four late Moloko sites: Olifantspoort, Molokwane, Kaditshwene and Marothodi. All sites are located in an area of North West Province roughly defined by Rustenburg in the southeast, the Pilanesberg in the northeast and Zeerust in the west, all west of Pretoria (Figure 1.1). This region is characterised by relatively high elevation and summer rainfall. The vegetation is diverse, and the location of Moloko sites reflects a preference for the agriculturally rich soils of the Zeerust Thornveld and the more wooded, grassy environment of the Swartruggens Mountain Bushveld. To the north and east are the Dwaalboom Thornveld and Sandy

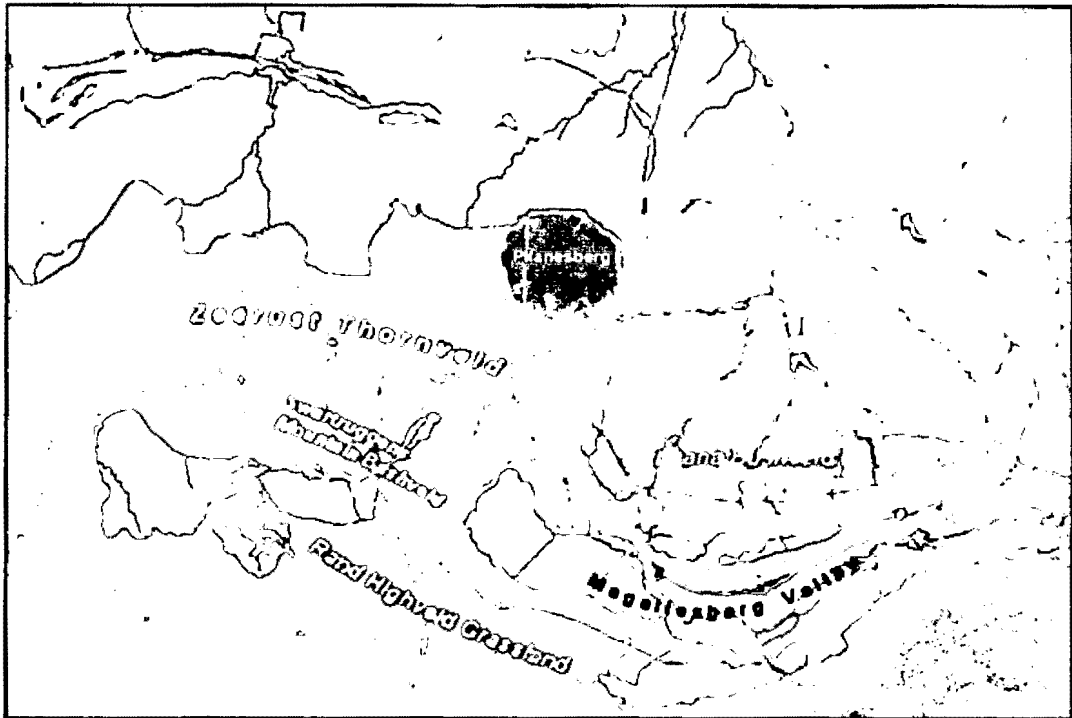


Figure 1.2. A vegetation map of the summer rainfall region in which the Moloko sites are located. The green lines enclose the agriculturally productive Bushveld zones (Hall *et al.* 2008: Plate 2, after Mucina & Rutherford 2006).

Bushveld, habitats more marginal for mixed farming (Figure 1.2; Mucina & Rutherford 2006; Hall *et al.* 2007, 2008).

THE IRON AGE IN SOUTHERN AFRICA

The start of the southern African Early Iron Age (EIA) is marked by traces of settled village life that was based upon cereal production and storage, animal husbandry and ceramic and metal production. All these attributes are significant innovations that did not develop within local indigenous hunter-gatherer populations. Stylistic analysis of ceramics has been fundamental in recognizing the advent of agricultural production into southern Africa (Huffman 1980, 1982, 1990). This pottery was brought by Bantu-speaking agro-pastoralists, and because in southern Africa their appearance was relatively sudden, it is important to consider the routes and timing of migration.

The earliest farmers in southern Africa, the Kwale branch of the Urewe tradition, took a route down the East African coast and date from about AD 300. The Nkope branch also is derived from the Urewe tradition, and those agro-pastoralists followed a more central line down into Zimbabwe, the Limpopo valley and eastern Botswana.

Kalundu, a second tradition, appears seemingly from the northwest around AD 600 that stratigraphically overlies and largely replaces Kwale branch communities where they overlapped. These are archaeological terms that refer to people who decorate their pottery in specific ways. There is not consensus, however, on the exact pattern of southward-moving 'ceramic streams' in this time period; the northern origins of agro-pastoralist peoples and the details of their lifestyle are still disputed (Phillipson 1977; Huffman 1982; Hall 1987; Denbow 1990). In southern Africa, the Early Iron Age is identified archaeologically by an Iron Age 'package,' first proposed by Tim Maggs (1984), that incorporates evidence from a range of disciplines, including anthropology, linguistics, history and ecology.

This 'package' includes evidence of sedentary life, with built structures organized into status-based villages that are distinctly different from the settlement and political structure of hunter-gatherer groups. Residues of domesticated sorghum and millet agriculture; use of grainbins for cereal storage; faunal remains of cattle, sheep and goat; areas for animal enclosures; and metal working also indicate agro-pastoralism, which requires time and effort invested annually in the successful cultivation of crops and husbandry of animals. Southern African Early Iron Age settlements are found only in the Bushveld areas of the summer rainfall regions in present-day northeast South Africa, southwest Botswana and southern Zimbabwe. These areas provided the climate to which sorghum and millet are best adapted.

Another attribute of agro-pastoralism was iron and copper production, indicated by artefacts and metal working debris. Iron tools were critical for farming and more efficient than wood and stone implements. Archaeological evidence for the production of very large ceramic vessels, used in cooking and long-term storage of food and liquids, is also associated with a sedentary lifestyle. In addition, pottery, the most ubiquitous artefact in Iron Age archaeology, served ritual contexts, as attested by the famous Lydenburg heads (Von Bezing & Inskeep 1966; Maggs & Davidson 1981), and in the Late Iron Age, was used also in metal working, as crucibles for

metal refinement. Iron and copper beads, wire and other jewellery comprise other metal artefacts found at Iron Age sites.

The Late Iron Age and the Moloko period

Between AD 1000-1300, there was a change in material remains that archaeologists distinguish by the terms 'Early' and 'Late' Iron Age. Linguistic, archaeological and ethnographic evidence suggests that the ancestors of present-day Sotho-Tswana and Nguni speakers, with their origins in eastern Africa, had migrated south of the Limpopo and into northern KwaZulu-Natal respectively. Ancestral Sotho-Tswana speakers had moved further southwards into the Rustenburg and Zeerust regions by AD 1500, and thereafter they and ancestral Nguni speakers were the first farmers to settle the predominantly grassland habitats further south (Phillipson 1977; Huffman 1982; Hall 1986; Huffman 1990; Lane 1994/95; Hall 1998; Huffman 1998, 2001, 2002, 2004).

Archaeological evidence for this movement is the appearance of new pottery types, the Moloko (Sotho-Tswana) and Blackburn (Nguni) ceramic traditions. The ceramic break with the EIA is significant, with some minor continuity between the 11th-13th century Early Iron Age Eiland tradition and Moloko (Evers 1983, 1984; Hall 1998). Radiocarbon dates from early Moloko sites confirm the presence of ceramics clearly ancestral to Sotho-Tswana ceramic styles south of the Limpopo river between AD 1300-1400 and further southwest from about AD 1500 (Hall 1998), and there is a parallel appearance of Nguni-speakers in KwaZulu-Natal (Huffman 2004). For a complex stylistic rendering of the complete Moloko ceramic sequence with a wider geographical focus, see Huffman (2002; 2007a).

For the Rustenburg-Zeerust region, Hall (1998) divides the Moloko tradition into three phases based on settlement size and the use of low stone walling to define spatial relations within the site (Figure 1.3), not to be confused with the ceramic stylistic phases developed and reviewed by Huffman (2002; 2007a). During the earliest Moloko phase in the Rustenburg-Zeerust region, roughly dated to AD 1500-1600, people lived in small, dispersed homesteads. The next period, roughly dated to AD 1600-1750, is characterized by the increasing clustering of homesteads, and

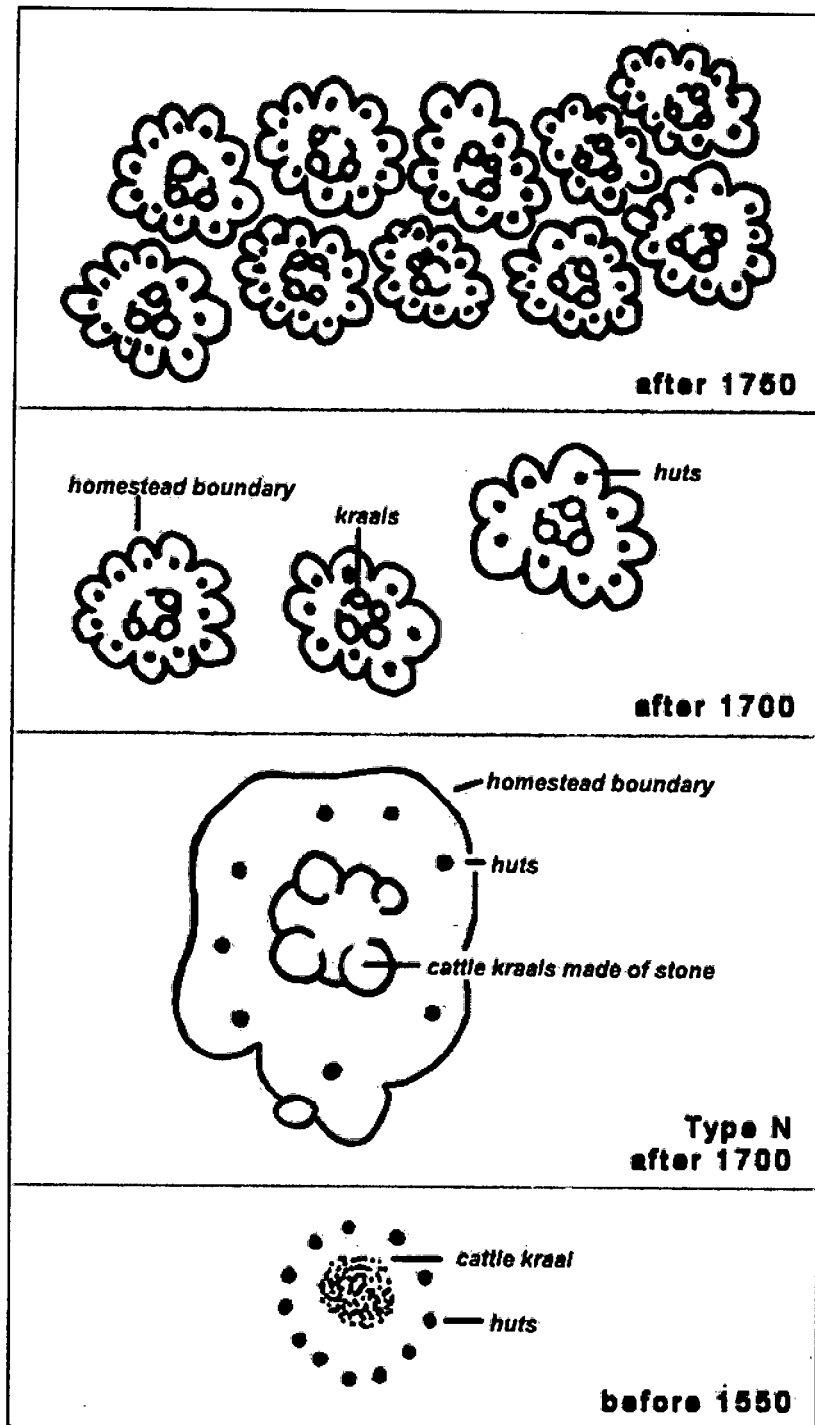


Figure 1.3. A diagrammatic representation of the Moloko settlement sequence in the Rustenburg-Zeerust region. Dispersed early Moloko villages characterize the 16th to mid-18th century. The first stone walling in this area, called Type N (Maggs 1976), occurs after about AD 1550. Late Moloko aggregation resulted in the large stone-walled towns of the early 19th century. Figure adapted from Maggs (1976) and an unpublished illustration courtesy of Simon Hall.

sparse stone walling was used to demarcate cattle enclosures and homestead boundaries. In the late Moloko, beginning around AD 1750, the scale of settlement changed dramatically, and large towns developed from this aggregation process. By the early 19th century, some of these centres had populations in the thousands, as documented by the first European travellers to the region (Hall 1998; Boeyens 2003).

For the late Moloko period, the relationship between the archaeological sites and the cultures described in traveller records is relatively direct. These records, combined with other ethnohistoric evidence, provide meaningful interpretation of the structure of late Moloko towns. For example, while the construction of some of the late Moloko towns on hilltops was a protective posture, the stone walling itself was not primarily defensive; most walls, remnants of which still stand at late Moloko archaeological sites, were less than 1 m in height. A distinctive boundary wall, made up of scallops marking the back courtyard wall of individual households, bordered each homestead. Households comprised sleeping huts, private back courtyards where granaries were built and more public front courtyards where, in some variants, kitchen enclosures are found. This domestic ring surrounded central cattle kraals, the court and craft spaces, such as metal working forges. The stone walls marked off and separated gendered activities; central cattle keeping, court activities and metal working were the preserve of initiated men, while cooking and initial ceramic production, the work of women, was organized within the encircling domestic area. Although one of the outcomes of homestead aggregation and the formation of large towns was increased centralized political control and greater social distance between commoner and elite homesteads, individual homesteads were responsible for their own production and social and judicial regulation (Hall 1998).

The shift to stone-walled settlements was the result of a complex interplay between environmental, historical and social factors. Climate records show that a period of cooler and drier conditions occurred in southern Africa beginning around AD 1600, culminating in widespread drought in the mid-18th century (Figure 1.4; Hall 1976; Tyson *et al.* 2000; Tyson *et al.* 2002; Norström *et al.* 2008). This is particularly significant regarding the spread of maize agriculture, which was introduced to the southern east African coast by the Portuguese. According to the appearance of characteristic maize grindstones in the archaeological record of the interior, the cereal

sparse stone walling was used to demarcate cattle enclosures and homestead boundaries. In the late Moloko, beginning around AD 1750, the scale of settlement changed dramatically, and large towns developed from this aggregation process. By the early 19th century, some of these centres had populations in the thousands, as documented by the first European travellers to the region (Hall 1998; Boeyens 2003).

For the late Moloko period, the relationship between the archaeological sites and the cultures described in traveller records is relatively direct. These records, combined with other ethnohistoric evidence, provide meaningful interpretation of the structure of late Moloko towns. For example, while the construction of some of the late Moloko towns on hilltops was a protective posture, the stone walling itself was not primarily defensive; most walls, remnants of which still stand at late Moloko archaeological sites, were less than 1 m in height. A distinctive boundary wall, made up of scallops marking the back courtyard wall of individual households, bordered each homestead. Households comprised sleeping huts, private back courtyards where granaries were built and more public front courtyards where, in some variants, kitchen enclosures are found. This domestic ring surrounded central cattle kraals, the court and craft spaces, such as metal working forges. The stone walls marked off and separated gendered activities; central cattle keeping, court activities and metal working were the preserve of initiated men, while cooking and initial ceramic production, the work of women, was organized within the encircling domestic area. Although one of the outcomes of homestead aggregation and the formation of large towns was increased centralized political control and greater social distance between commoner and elite homesteads, individual homesteads were responsible for their own production and social and judicial regulation (Hall 1998).

The shift to stone-walled settlements was the result of a complex interplay between environmental, historical and social factors. Climate records show that a period of cooler and drier conditions occurred in southern Africa beginning around AD 1600, culminating in widespread drought in the mid-18th century (Figure 1.4; Hall 1976; Tyson *et al.* 2000; Tyson *et al.* 2002; Norström *et al.* 2008). This is particularly significant regarding the spread of maize agriculture, which was introduced to the southern east African coast by the Portuguese. According to the appearance of characteristic maize grindstones in the archaeological record of the interior, the cereal

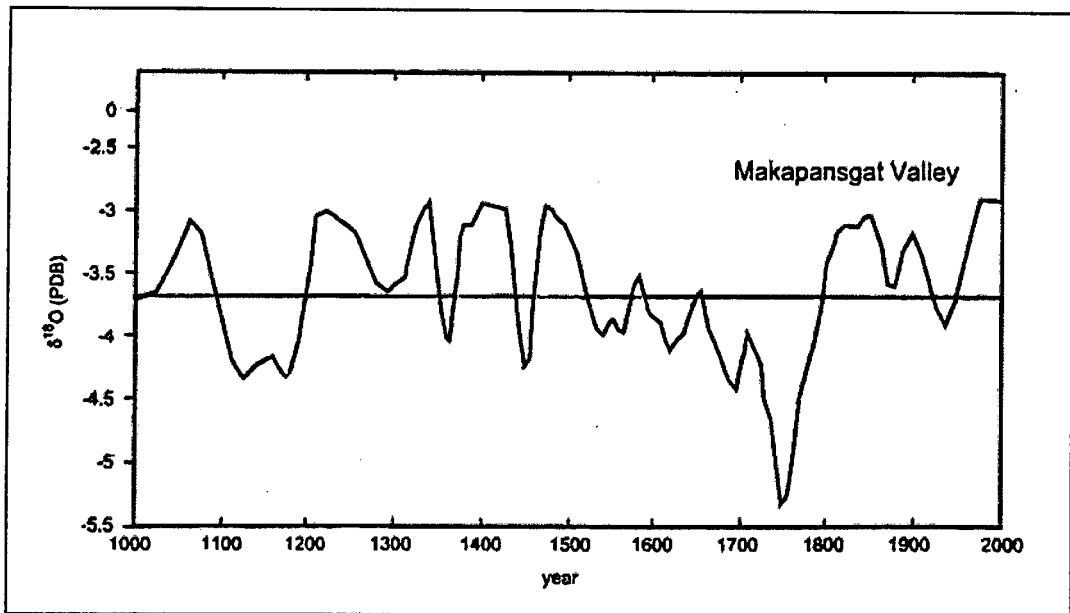


Figure 1.4. Variations over the last millennium in the oxygen isotope values of stalagmites in the Makapansgat Valley, approximately 300 km northeast of Rustenburg. Higher oxygen isotope values are associated with a warmer, wetter climate; lower values a cooler, drier climate. Figure adapted from Tyson *et al.* (2002: Figure 1b).

was adopted at least by the end of the 18th century as a complement to sorghum and millet, although some suggest that the introduction of maize took place even earlier (Huffman 2006), in the 17th century.

The improved yield of maize over sorghum and millet may have facilitated population growth in the mid-18th century, but in so doing, also created conditions for increased competition over food resources. Maize is less suited to dry conditions than are sorghum and millet; as conditions became drier through the mid-18th century, maize resources became scarcer, and famine ensued (Hall 1995; Huffman 1996; Boeyens 2003). Farming success in an agriculturally rich area, combined with competition over land and control of food production, amplified aggression between groups in the region. With the formation of the stone-walled towns and consolidation of political control, a new agricultural management strategy developed that addressed these concerns with food security.

Additionally, from about AD 1760 the encroaching colonial influence, driven by new demand for trade items (particularly ivory), further affected the BaTswana chiefs. Middlemen also exchanged furs, feathers, tobacco and iron, copper and tin metal for colonial goods such as beads, cloth, buttons and livestock. Wealthy chiefs were able to monopolize commerce, thereby attracting more trade and more followers. Increased competition for clients, coupled with droughts, shortage of good land for grazing and agriculture, and internal political strife over succession of leadership, greatly exacerbated conflict, particularly in the late 18th and early 19th centuries (Manson 1995).

By AD 1820 many BaTswana had been devastated by famine and conflict provoked by the unsustainable nature of these environmental, agricultural, colonial and political factors. Early missionaries wrote of poverty and emaciation, deserted towns, ongoing war and raiding, and the general despondence of the population (Campbell 1822b; Burchell 1824). The 'end' of the late Moloko period corresponds to the *difaqane*, or 'time of troubles,' which occurred through the 1820s. Mzilikazi, an AmaNdebele chief who broke away from the Zulu confederacy to establish his own state, pillaged the BaTswana, initially in the Rustenburg area. The power of Mzilikazi stabilized the region, which had been weakened by dissonant relations between BaTswana chiefs, but as a result, thousands were displaced, and many BaTswana shifted political and cultural allegiance to the AmaNdebele (Legassick 1970; Boeyens 2003).

BaTswana sites of the late Moloko

Numerous stone-walled, late Moloko sites in the study area were recorded during an extensive aerial photography project by Revil Mason (Mason 1968; Seddon 1968; Mason 1986); four of the largest were chosen for consideration in this study. Sites on the farm Olifantspoort (Mason 1973, 1986), Molokwane (Pistorius 1992, 1996, 1997) and Kaditshwene (Boeyens 1999, 2000, 2003) have been excavated over the past four decades. Material from Marothodi was excavated by and currently is being analysed by a multi-disciplinary team of researchers (Hall *et al.* 2006; Anderson forthcoming), of which the author is a member. The geographic and archaeological context of the four towns is described here. The chronologic context, as developed through radiocarbon dating, also is reported for Olifantspoort, Molokwane and Kaditshwene.

Because the radiocarbon technique failed to produce useful dates for those sites, the Marothodi research group decided to not submit samples from that site for radiocarbon dating. This subject will be explored further in Chapter 3.

Additionally, interpretation of the archaeology at Late Iron Age sites is greatly aided by the use of ethnographic comparison. This is especially cogent for Moloko period archaeology, where the historical and chronological relationships between the people who provide the ethnographic models and the BaTswana ancestors who lived at the archaeological sites are relatively direct and often traceable. One does not discount, however, the inevitable variability of culture that exists within and between groups of people and the importance of considering such differences when examining archaeological data.

Archaeological evidence occurs in many forms and at different scales, some of which cannot be directly compared or fall outside conventional comparative methods. It is apparent that scales of change in ceramic technology cannot be evaluated without scientific analysis for determining methods of pottery manufacture and direct chronological control over the timing of these innovations. The archaeologist is challenged to choose the appropriate scale of analysis for the data; in previous work (Rosenstein 2002) and in this thesis, I suggest that the changes in the technology of BaTswana ceramic manufacture reflect the processes and strategies of late Moloko settlement aggregation. These shifts emphasize the social, cultural and political atmosphere during this important era of BaTswana history, as the extent of involvement in aggregation across the region attests. We cannot properly interpret these shifts or make progress in understanding the details of this sequence, however, because the chronology of occupancy at late Moloko sites is not clear. Thus a principle aim of this research is to identify a useful method for absolute dating in this period, using the following four late Moloko sites as case studies.

Olifantspoort

Moloko sites from all three settlement and stone wall construction phases (Figure 1.3; Hall 1998) have been excavated on the farm Olifantspoort-328JQ (25°47'S: 27°15'E)

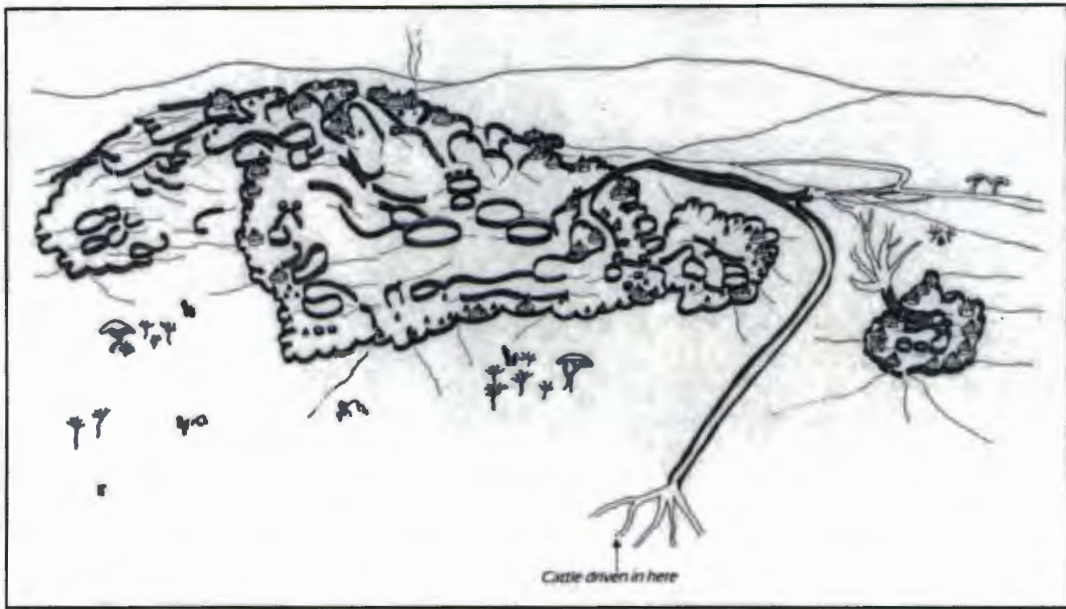


Figure 1.5. Artist's rendering of the late Moloko site on the farm Olifantspoort (Mason 1987: 71).

in the Rustenburg district (Mason 1973, 1986). Stone-walled architecture appears after AD 1600, in the middle Moloko phase (Figure 1.5). Radiocarbon dates on charcoal from middens and hut floors from the late Moloko site, however, range from the mid-15th to mid-19th centuries (Vogel 1971; Mason 1986: 68-69). This is due to the extensive fluctuations in the radiocarbon calibration curve during this time period, discussed in detail in Chapter 3. At a multi-component site such as Olifantspoort, where stratigraphic and ceramic evidence suggest long-term habitation, it is possible also that 15th-16th century radiocarbon dates accurately reflect earlier occupations at the site; at the other stone-walled sites in this study, there is no archaeological indication of earlier Moloko settlement.

Revil Mason suggested that the population resident on Olifantspoort during the stone wall phase were related to the BaKwena (Mason 1973), the BaTswana group who are traditionally associated with the Rustenburg area (Legassick 1969; Mason 1973: 487; Manson 1995; Hall *et al.* 2007, 2008).



Figure 1.6. Aerial photograph of the centre section at Molokwane. Note the large cattle enclosure at the core of the *kgosing*. Photograph courtesy School of Geography, Archaeology and Environmental Studies, University of the Witwatersrand, Johannesburg.

Molokwane

Molokwane (25°41'S: 27°04'E) is an extensive stone-walled town on the farm Selonskraal-317JQ near Rustenburg, ranging linearly for 3 km along the Ngwaritse (Selons) River (Pistorius 1992, 1996, 1997). The site is divided into three distinct settlement clusters. The centre section includes the *kgosing*, the main ward and residence of the 'chief,' recognisable because at its core is the largest cattle enclosure at a settlement (Figure 1.6). At the outer sections on either side of the *kgosing* are the commoner areas. Archaeological evidence, combined with radiocarbon dating and ethnohistorical records, initially indicated that the *kgosing* appeared in the mid-17th century (Pistorius 1997).

In ethnographic research, Breutz (1953) and Pistorius (1996) recorded the oral history of Tswana groups from the area. The BaKwena-ba-Modimosana were the inhabitants of both Molokwane and the large stone-walled town Boitsêmagano on the adjacent farm, Shylock-256JQ, continually from establishment until abandonment. The settlement reached its height under *kgosi* Kgasoane, who ruled c. AD 1770-1828, and was one of the most influential social and political BaTswana centres in the region. More recently, other scholars have argued that the *kgosing*, a direct expression of the power of a chief, reached its final, impressive size and form only at this early 19th century date (Hall *et al.* 2007, 2008), and not during the mid-17th century. This again emphasizes the difficulty with dating these sites. Using only radiocarbon and oral-historical records, it is not possible to understand exactly when and how the town aggregated. This will be further explored in Chapters 3 and 4. The circumstances of abandonment at Molokwane are undisputed, however; the Matabele, an AmaNdebele group under the leader Mzilikazi, destroyed the settlement during the *difaqane* in 1828 (Pistorius 1992, 1996).

Kaditshwene

The main stone-walled complex at Kaditshwene, in the Zeerust region (25°21'S: 26°10'E), is located on a large hill composed of two adjacent peaks spread over two farms, Kleinfontein (or Olifantspruit)-62JP and Bloemfontein-63JP, with the *kgosing* built on the southern peak (Boeyens 1999, 2000, 2003). Smaller divisions of the site extend to a third farm, Rietfontein-89JP, to the south. Radiocarbon dates on charcoal from middens and hut floors range from the mid-17th to mid-19th centuries (Boeyens 2000, 2003).

According to John Campbell, a traveller to the area in AD 1820, this BaHurutshe capital was populated by as many as 16 000 people at the time of his visit (MSB77 1820: 18; Campbell 1822b: 277). Campbell commissioned an artist to render many of his field sketches into paintings for the publication of his memoirs, but the original drawings, such as the image of the main hilltop *kgosing* depicted in Figure 1.7, survive in the South African Public Library in Cape Town (Campbell 1820a). The



Figure 1.7. ‘Kurreechane from the East,’ Campbell’s field sketch of the hilltop *kgosing* at Kaditshwene (Campbell 1820a).

known date of Campbell’s visit offers a precise point of chronological control at Kaditshwene that is important for assessing the value of the alternative dating techniques explored in this thesis. The inhabitants were forced to abandon the town only a few years later, when the Kololo of Sebetwane attacked the settlement during the *difaqane* (Legassick 1970: 328-331 in Boeyens 2000).

Marothodi

Revil Mason recorded a stone-walled settlement on a slight rise on the land straddling the farms Vlakfontein-207JP, Diamant-206JP and Bultfontein-204JP (25°19’S: 26°52’E), noting that the cattle enclosure there is the largest among late Moloko towns (1986). No scholarly work took place at this site, now known to be the BaTlokwa town of Marothodi (Boeyens 2003), until 2002, when an exploratory visit by archaeologists from the University of Cape Town revealed abundant surface scatters of iron and copper ores and slags (Figure 1.8; Hall *et al.* 2006; Anderson forthcoming). This suggestion of concentrated metal production at the site warranted closer examination, thus excavation by teams from the University of Cape Town (UCT) and University of South Africa (UNISA) took place in 2003, 2004 and 2005.

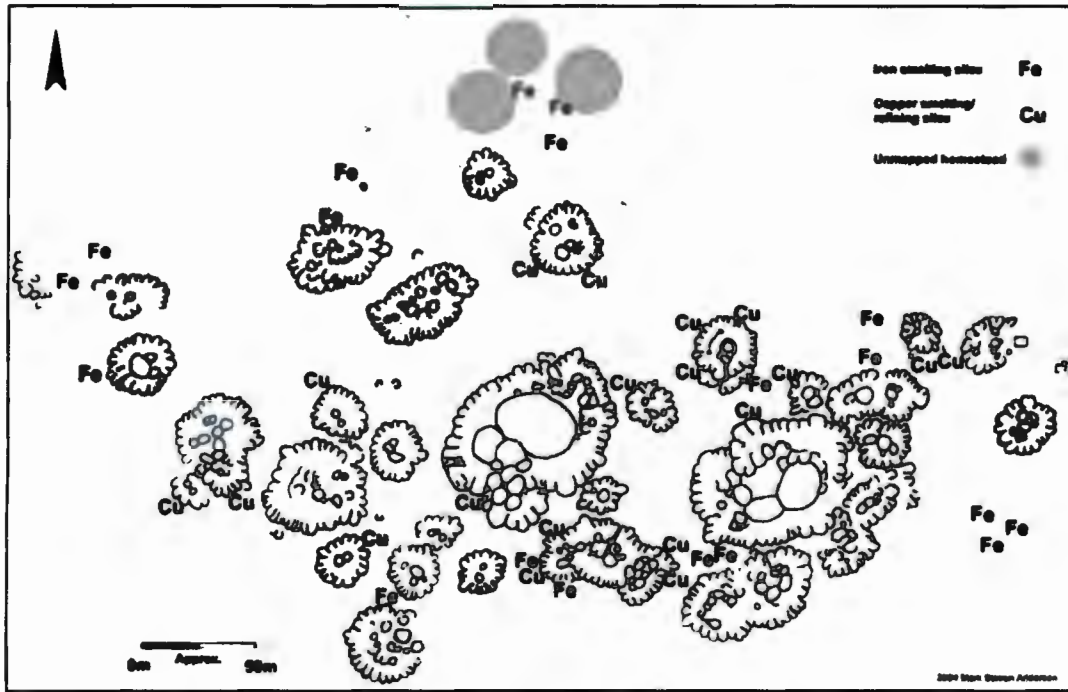


Figure 1.8. Site plan of Marothodi. Areas of copper and iron metallurgy are marked. Note the central cattle enclosure, the largest among late Moloko towns (Hall *et al.* 2006: Figure 2).

According to ethnography of BaTswana oral history, the BaTlokwa inhabited the site for only a short time in the early 19th century, c. AD 1810-1827, before being uprooted at the beginning of the *difaqane* (Ellenberger 1939; Breutz 1953, 1989; Boeyens 2004; Hall *et al.* 2008).

Sorting out ceramics: contextualizing the chronological problem of the late Moloko

The 18th century in the Rustenburg-Zeerust region was an era of significant change over a very short period of time. If we are to understand the process of transformation at this fine level of analysis, we must have high-resolution chronological control, reflecting time on a generational scale, rather than by century or half-century. Shifts in ceramic style are correlated with town living, and in this thesis, I suggest that changes in technology of manufacture similarly fit into this framework of action and reaction to social, cultural, political and environmental factors. The pace and timing

of these shifts in settlement plan and ceramic production are imprecise, however, and an alternative to radiocarbon dating for the late Moloko is essential.

An advantage of post-colonial archaeology is the oral-historical record. At Kaditshwene and Marothodi, for example, these records provide the dates of settlement, and travellers offer eyewitness accounts of town life in specific years of the early 1800s. Why, then, spend considerable time, effort and money to obtain chronometric dates from the archaeological sequence at these sites? Archaeometric information is valuable not only for the site at which it was obtained, but also as a point in a database for the entire region. Chronometric ages obtained by new methods can be compared to reliable oral-historical dates as a way to develop our techniques and refine our interpretations of the sequence of settlement and change in the Rustenburg-Zeerust region during this period.

I develop these issues in the following chapters, discussing late Moloko ceramic production, chronology and dating methods.

Chapter 2

Late Moloko Ceramic Research

The mid-18th century to early 19th century shift in settlement pattern of Late Iron Age Western Tswana groups, from early Moloko villages to late Moloko stone-walled towns, is the most significant archaeological characteristic of this period in the region. It gives rise to important issues regarding political, socio-economic, and technological changes that occur as members of a small-scale society adapt to life in large, politically centralized towns of several thousand or more people. One way to investigate socio-economic transformations and its chronology is to study the change in ceramic style and technology that occurred between the 16th and 19th century Moloko settlements.

STUDIES OF 16TH TO 19TH CENTURY MOLOKO CERAMICS

Hall (1998) has considered the way that ceramic style changed between the early and late Moloko phases (Figure 2.1). A general analysis was undertaken in order to measure a marked reduction through time in the decorative complexity of Moloko pottery that had been qualitatively recognized. Hall identified as many as fifteen Moloko ceramic classes, defined according to multivariate analyses of shape and decoration (Huffman 1980; Hall 1998: 250). See Huffman (2002; 2007a) for a detailed typological consideration of the complete Moloko ceramic sequence.

Generally, more than 50 percent of ceramics from pre-town phase early and middle Moloko sites are elaborately and ornately decorated over large portions of the vessel exteriors and interiors (Hanisch 1979; Hall 1981, 1985; Mason 1986). Black graphite and red ochre are used to liberally colour both the internal and external surfaces of the ceramics. Necks of pots and upper sections of bowls are incised with multiple bands of diagonal lines. In addition, shoulders and bodies of pots are decorated with chevrons and arcades (Figure 2.2; Mason 1986; Hall 1998, 2000).

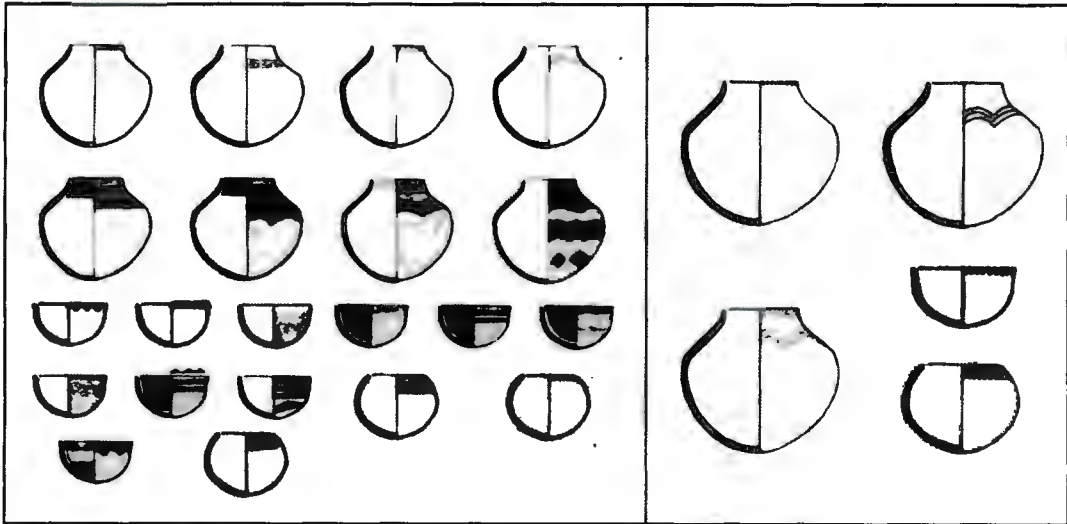


Figure 2.1. Drawings of typical early Moloko (left) and late Moloko (right) pottery classes. Note the significant decline frequency of design elements represented with the shift to stone-walled architecture in the later period (adapted from Hall 1998: 252-253).

In contrast, in the late Moloko town phase, it is clear that the stylistic complexity of vessels decreases notably and it seems that some vessels increase in size. The frequency of decoration declines markedly (Hall 1998). A simple, single band of notching on the rim is sometimes the only design on the majority of decorated pots at these late Moloko sites (Figure 2.3; Mason 1973; Mason 1986; Hall 1998; Huffman 2007b).

Hall (1998) suggests that as people aggregated in large towns, resulting in a centralised population as compared to that of early Moloko villages, there was also a significant, qualitative increase in the size of pottery manufacture and a decrease in the variety of ceramic shapes and decorative motifs produced. He argues that differences in the decorative intensity of pottery between the pre- and post-town periods of the Moloko indicate shifts in time and labour expenditure on ceramic manufacture and perhaps greater standardisation. Because women make pottery, it is their time and labour that is potentially altering. One possibility for this is that consolidated town living had implications for the scale of agricultural production and women had more to do, particularly if the division of labour became firmer. Further, he proposes that the changes in pottery production might reflect administrative

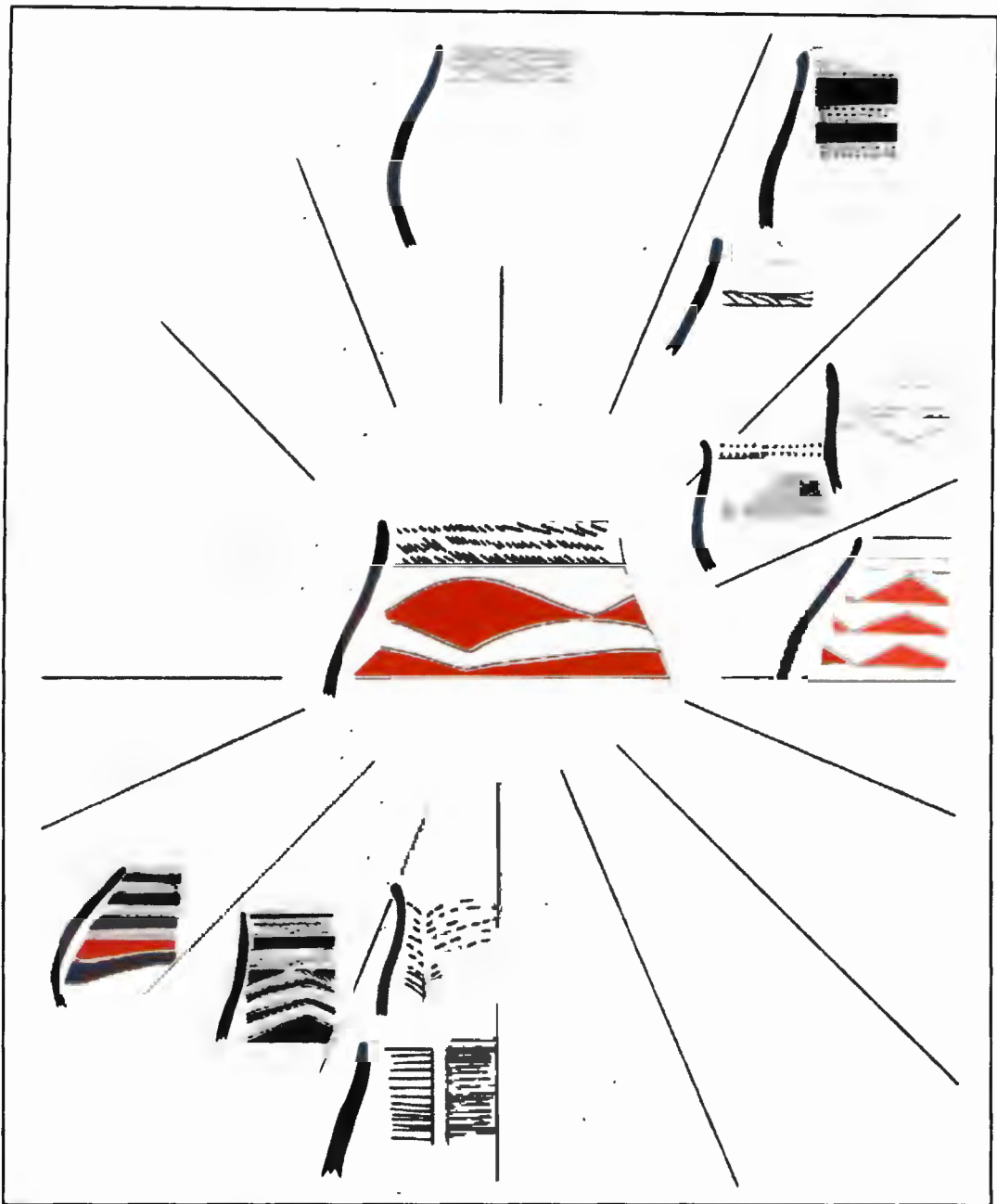


Figure 2.2. Ceramic shapes and styles typical of early Moloko pottery (*Madikwe* types, modified from Huffman 2007a: Figure 15.20A).

strategies for managing the residents of the newly aggregated communities. Another implication of standardization is specialization, in which fewer women are dedicated to manufacturing more pots for community consumption (Hall 1998). These theories are in accord with the efficient, large-scale ceramic production that would be required to sustain the needs of a population numbering several thousand or more.

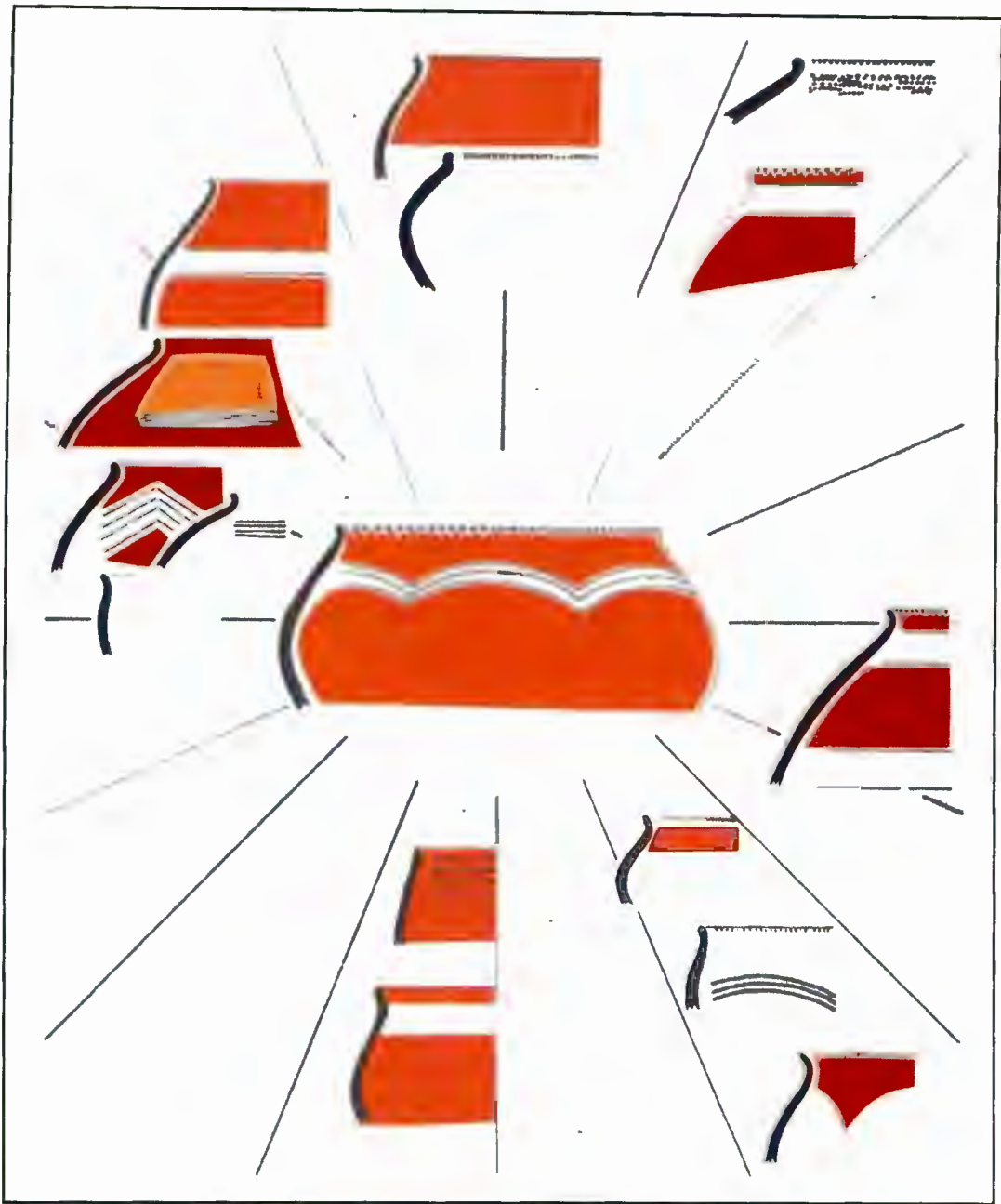


Figure 2.3. Ceramic shapes and styles typical of late Moloko pottery (*Buispoort* types, modified from Huffman 2007a: Figure 15.21A). Compare to Figure 2.2; from the early to late Moloko, the stylistic complexity of vessels decreases (Hall 1998).

This stylistic shift provides a framework by which to consider the Moloko ceramic sequence from a technological perspective. From the early to late Moloko, there is a clear inversion between the complexity of pottery decoration (well-decorated to

sparsely decorated) versus that of settlement architecture (no or few walls to completely stone-walled). Interpretation of the differences in ceramic style and possible trends toward standardization can be developed with attention to issues of chronology, technological choice and social identity. In this thesis, I consider these ideas through petrographic investigations of change in Western Tswana ceramic production over the Moloko period.

LATE MOLOKO CERAMIC ANALYSIS

My preliminary petrographic and chemical study of ceramic samples compared pottery production from early and late-phase sites and focused on technological characteristics of late Moloko pottery that might indicate a trend toward greater efficiency or standardisation in ceramic manufacture. That research found notable differences in the technology of ceramic production between the early and late Moloko periods (Rosenstein 2002) that correspond to the stylistic distinctions defined previously (Hall 1998). The ceramic sherds from the early 19th century town of Marothodi analysed in this study do not fit that pattern, however, and in this chapter I explore this inconsistency.

Petrographic and chemical analytical methods are valuable tools in the analysis of archaeological ceramics and assessment of ceramic provenance. The 'provenance hypothesis' describes the scientific principles employed in the interpretation of petrographic and chemical results (see discussion by Wilson & Pollard 2001). Provenance determination is most robust when there is systematic control over geologic variability between sites. At each site location, the researcher should study the local mineralogy to determine which minerals can be expected as natural inclusions in local clay as compared to uncharacteristic inclusions that likely derive from non-local geology.

Identification of clay fabrics that are derived from the surrounding geology, as is the case in the early Moloko samples analysed in this study, indicates that nearby clay sources were exploited for raw material and thus that pottery was manufactured

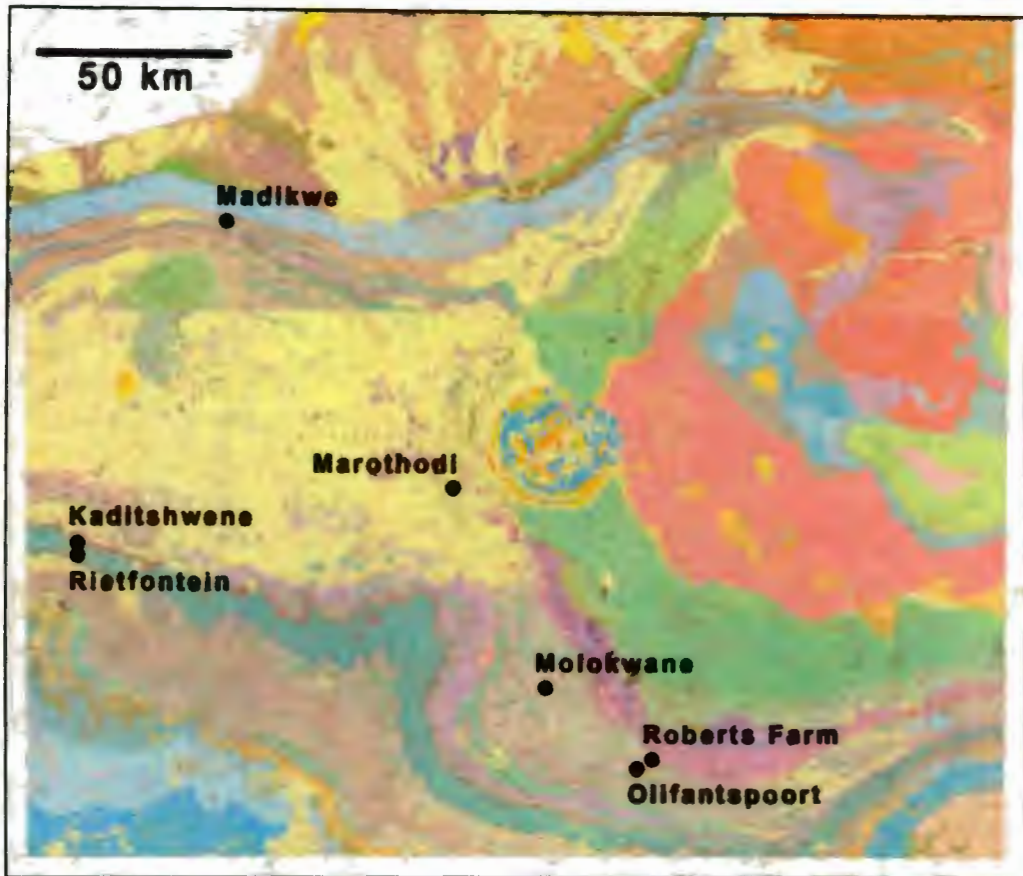


Figure 2.4. 1: 250 000 geologic map of the research region (adapted from Jansen *et al.* 1974; and Walraven 1981). The locations of the Moloko period Late Iron Age sites under discussion are located generally northwest to south of the Pilanesberg Complex, at centre.

locally. Non-local mineral inclusions within a local clay suggest that a specific temper was sought for use in ceramic production, as in some late Moloko sherds sampled in this study. Significant variation from expected clay composition may indicate ceramics made elsewhere and imported. Petrographic observations of pot sherd type and other attributes, including clay matrix and grain size, and type and number of inclusions are useful for broad characterisation of ceramic groups according to mineral composition and tempers.

These are general rules, however, for which there are innumerable individual exceptions. Bulk chemical analyses can be useful as an additional line of evidence when attempting to characterise clay and temper types in pottery. This can complement, but not replace, petrographic examination of a sample set. Analytical



Figure 2.5. An outcrop of weathered, dark grey graphitic schist at Kaditshwene, adjacent to a stone-walled enclosure.

determination of the bulk elemental composition of inhomogeneous clay cannot be informative if one does not also know the individual mineral components that produce the chemical signature of that clay.

Geology of the Rustenburg-Zeerust region

An examination of the geology in the Rustenburg-Zeerust region helps to establish the availability of different mineral types. Early and late Moloko sites are geographically proximate all over the region; in the early study (Rosenstein 2002) specifically,



Figure 2.6. Sampling a light-coloured, lustrous, talcaceous schist at Molokwane.

ceramics were analysed from both the early and late phases of Olifantspoort, which were directly contiguous, and Rietfontein, which is an early Moloko site approximately 3 km from the early 19th century town of Kaditshwene. A geologic map of the research area is presented in Figure 2.4. The sedimentary rocks of the Transvaal System, a supergroup of varying detrital and dolomitic rock types with locally observed volcanic layers, underlie the area (Haughton 1969; Engelbrecht 1990). Located to the east is the immense Bushveld Igneous Complex, a layered mafic body approximately 65 000 km² in aerial extent and 7-9 km in depth, which intruded the Transvaal sediments. The hills of the Pilanesberg Complex, a distinctive

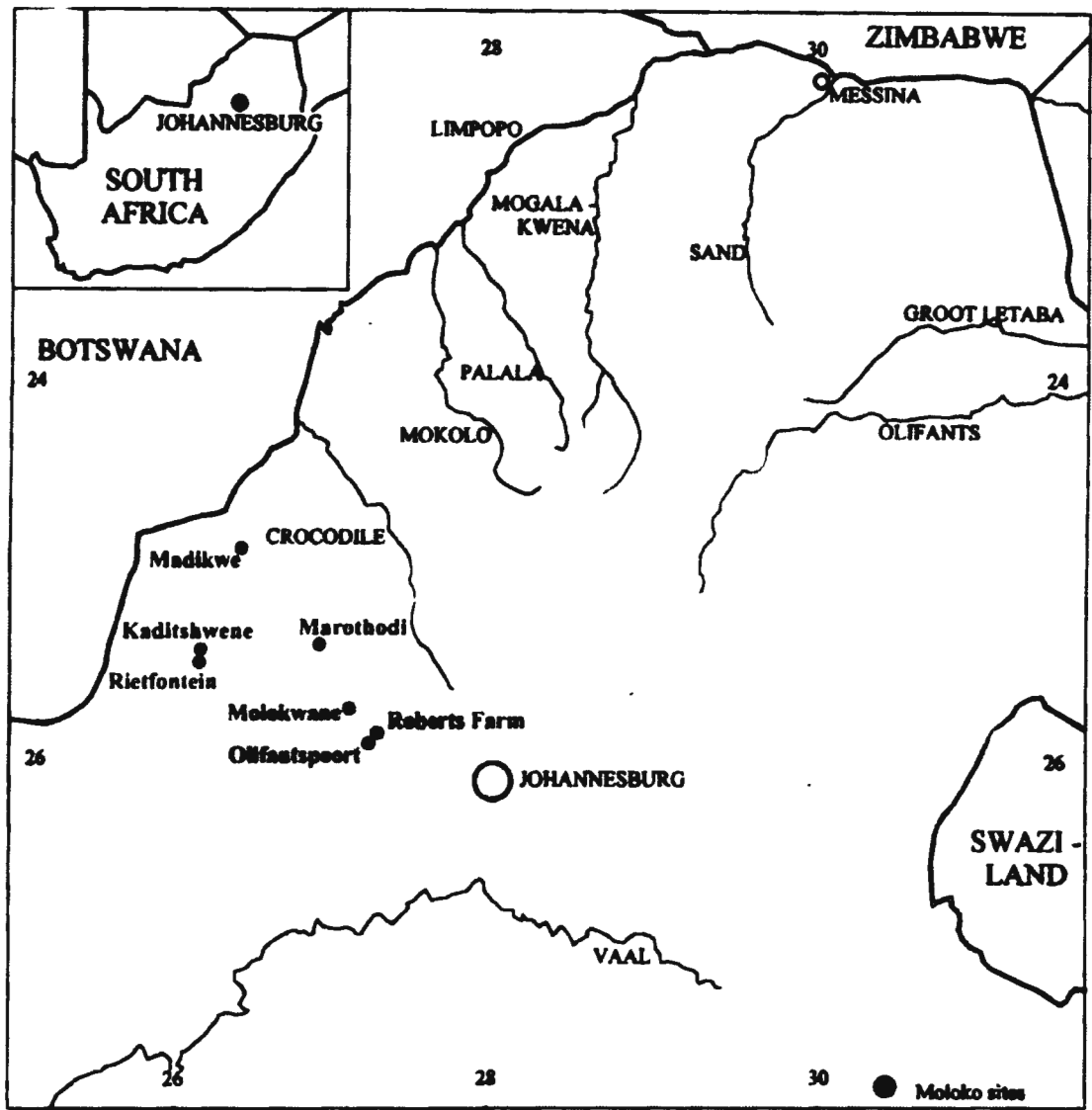


Figure 2.7. Map showing the geographic region under discussion and the location of early and late Moloko period Late Iron Age sites from which ceramic samples were analysed for Rosenstein (2002) and this thesis (map modified from Hall 1998: 237).

round alkali intrusive body measuring 25 km across, are less than 10 km east of Marothodi (Walraven 1981; Eales & Cawthorn 1996; Kiefer & Viljoen 2006).

Geologic outcrops of the dark grey to black Transvaal group graphitic schists, from which graphite-talc nodules are released by weathering, have been identified on-site at Molokwane and Kaditshwene (Figure 2.5) and near Olifantspoort and Marothodi.

Table 2.1. Summary of Appendix B: natural and added ceramic inclusion types in early and late Moloko potsherds (Rosenstein 2002).

Site	N	None	Lustrous or Platy Inclusions		Graphite-Talc Nodules	Mixed Inclusion Fabrics	
			Mica	Fibrous		Mica / Graphite	Mica / Fibrous / Graphite
<i>Early Moloko</i>	20						
Olifantspoort (OE)	6	2		4			
Roberts Farm (RO)	1	1					
Rietfontein (R)	4	4					
Madikwe (MD)	9	6		3			
<i>Late Moloko</i>	30						
Olifantspoort (OL)	10	2	3	1	3	1	
Molokwane (M)	10	1			4	5	
Kaditshwene (KF)	10		2		2	4	2

Occurrences of the light-coloured schists and igneous bodies from which lustrous minerals and lithic fragments can be obtained are common across this region. This is due to metamorphism of the original sedimentary geology by emplacements of the Bushveld Igneous Complex, including dykes that formed across the region and beyond Zeerust, and of the Pilanesberg Complex intrusions (Jansen *et al.* 1974; Walraven 1981). Schistose outcrops have even been observed on-site at Molokwane (Figure 2.6).

Petrography of early and late Moloko ceramics

Preliminary petrographic and chemical analyses on ceramic samples from three early and three late Moloko sites was carried out in a previous study (Rosenstein 2002). The pilot sample was composed of fifty sherds: seven from early Moloko sites at Rietfontein (Boeyens 2003); and nine from Madikwe (Hall 2000; Huffman 2000). Ten samples were analysed from each of the late Moloko sites, Olifantspoort, Molokwane and Kaditshwene (Appendix A). These sites were chosen for their geographic and geologic proximity to each other in order to have as direct a comparison as possible of ceramic production between the early and late Moloko periods (Figure 2.7). This was especially successful at Olifantspoort, where both the

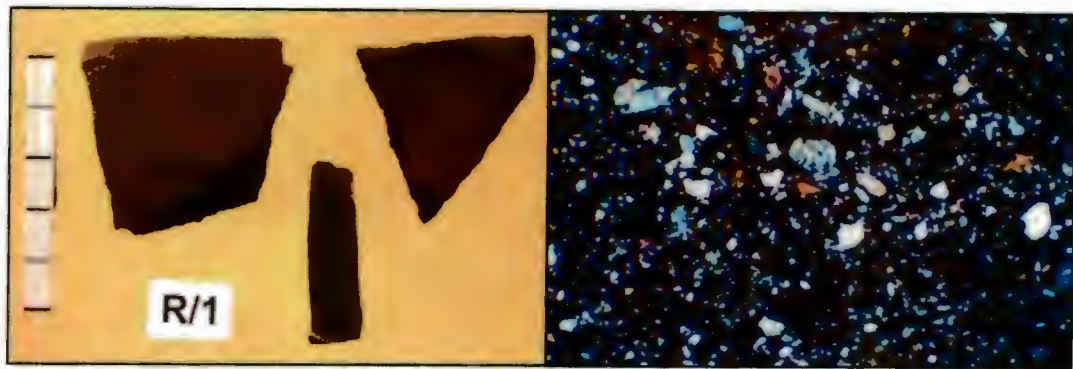


Figure 2.8. Photograph and petromicrograph (XPL, width = 7.5 mm) of a ceramic sherd from Rietfontein, an early Moloko site near Kaditshwene. Note the lack of prominent or atypical inclusions or added temper.

earlier and later phases occur, and at Kaditshwene, where the early component at Rietfontein is only three km distant.

Results of petrographic and chemical analyses (Appendix B and summarized in Table 2.1) revealed that early Moloko ceramics were produced from clays containing mineral inclusions characteristic of the local geology, including some weathered fibrous minerals. Furthermore, clays from early Moloko sites were not refined or reworked and there are no added minerals or other tempers in the samples (Figure 2.8; Rosenstein 2002).

In comparison, two major types of inclusions, graphite-talc nodules and lustrous mineral grains that do not occur in early Moloko samples, are found in the sampled sherds at each late Moloko site (Olifantspoort, Molokwane and Kaditshwene). Graphite-talc nodules occur as rounded, coarse grains, indicating that the lithic fragments are detrital. Graphitic schists are common in the geology underlying this agriculturally productive, mixed Bushveld and Thornfeld region. Platy, fibrous and lustrous minerals, most commonly muscovite mica but also other mineral varieties, occur as very angular, coarse grains, indicating the material was crushed and added as a temper (Figure 2.9; Rosenstein 2002).

Grains of the lustrous inclusions in ceramic samples from all three late Moloko sites were analysed by SEM-EDS for bulk chemical analysis in order to identify the minerals added. This was undertaken with a Leica S440 digital scanning electron

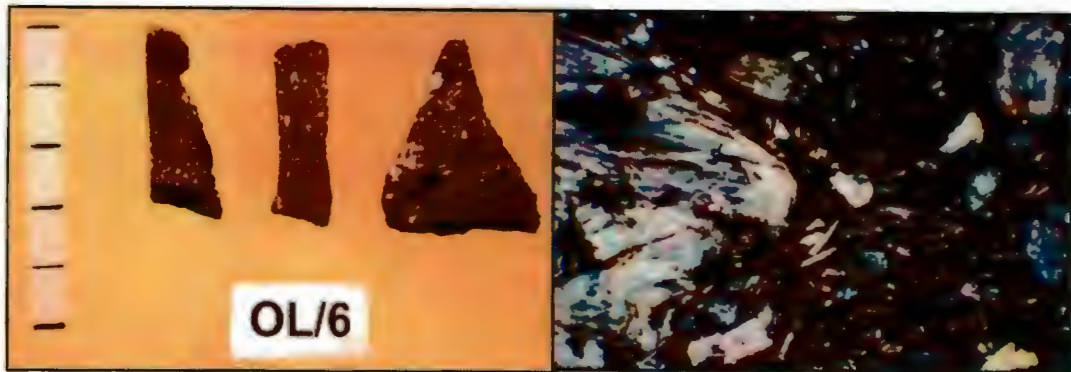


Figure 2.9. Photograph and petromicrograph (XPL, width = 7.5 mm) of a ceramic sherd from the late Moloko component at Olifantspoort. Note the presence of very coarse sand and pebble-sized grains of muscovite mica that were crushed and added as temper to the clay material. Also note the distinct sparkly effect the inclusion of mica has on the exterior of the ceramic.

microscope located in the Electron Microscope Unit at the University of Cape Town. Preliminary results indicate that muscovite and biotite micas, talc schists and asbestiform amphiboles were used, along with other as yet unidentified inhomogeneous lithic materials; interpretation of the SEM-EDS data is ongoing.

Petrography of Marothodi ceramics

The results from late Moloko ceramic thin section analysis of Olifantspoort, Molokwane and Kaditshwene samples (Rosenstein 2002) were compared with 42 pot sherds from Marothodi, another early 19th century Western BaTswana town, for this study. During the initial field survey completed by archaeologists from the University of Cape Town in 2002, ceramic samples were collected from a total of 66 localities at the site. The 42 sherds for microscopic analysis were chosen strategically to include samples from both high- and commoner-status homesteads. When possible, multiple rim, body, and lid samples from the same pot were analysed (Appendix C). The general fabric, inclusion character and composition of each sherd, including both individual minerals and lithic fragments, was determined and recorded on a presence/absence list of the continually recurring grain types (Appendix D).

Petrography was undertaken in the Materials Laboratory of the Department of Archaeology at the University of Cape Town, South Africa. A Reichert-Jung

Table 2.2. Marothodi ceramic sherd type according to petrographic group.

Petrographic Group	N	Sherd Type			Characteristics of Clay Fabric
		Body	Rim	Pot Lid	
A	24	15	4	5	Weathered qtz and fsp.
B	10	6	3	1	Weathered fsp.
C	2	2			Added micaceous temper.
D	1	1			Amphibole inclusions.
E	2	1	1		Unweathered qtz, little fsp.
F	3	1	1	1	Naturally occurring mica.

Polyvar-Pol dual petrographic-metallographic polarising microscope was used to analyse standard, ceramic thin sections with coverslip. Petromicrograph images (all 2.5x) were obtained in the Multipurpose Laboratory of the Department of Anthropology at the University of Arizona, Tucson, Arizona, USA, with an Olympic BH-2-UMA dual petrographic-metallographic polarising microscope and attached digital camera.

Petrographic analysis of the Marothodi ceramics revealed six clay groups among the 42 samples, each characterised by particular fabrics or inclusions (Figure 2.10). Table 2.2 reports on the petrographic group as correlated to sherd type and Appendix C compares petrographic group to provenience of vessels at the site, according to the collection reference.

Petrographic group A, composed of 24 samples, represents the most common clay fabric present at Marothodi. It is typified by weathered subangular to subrounded quartz and feldspar inclusions with white to grey first-order interference colours. Ten samples comprise group B, characterised by heavily weathered, subangular to subrounded sericitic grains of feldspar that appear yellow both in plane- and cross-polarised light.

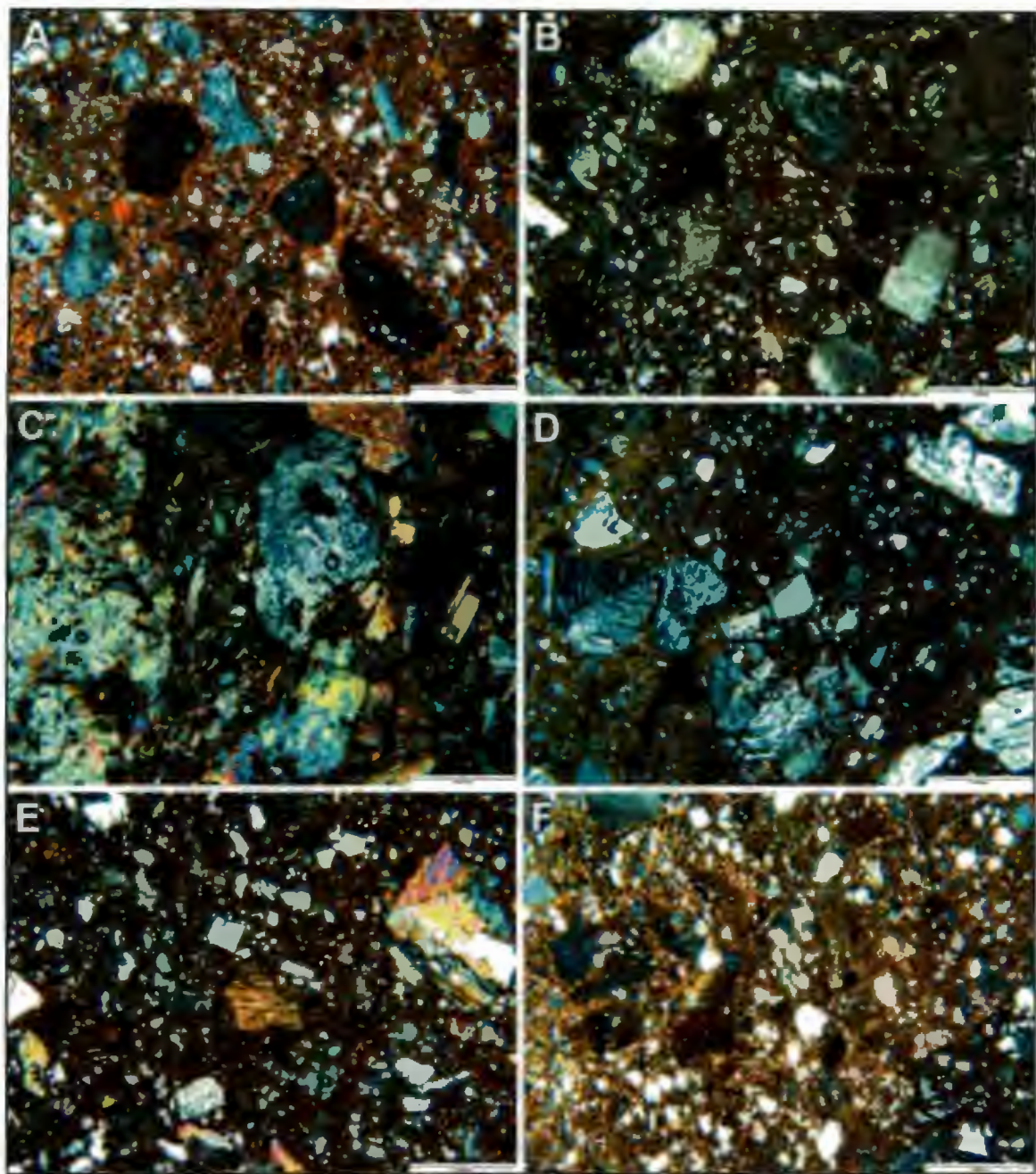


Figure 2.10. XPL petromicrographs representing typical petrographic groups of Marothodi ceramics as defined in Table 2.2 and Appendix D. Scale bar = 1 mm.

Group A	n = 24	VL-11-MDA
Group B	n = 10	VL-6-MD1
Group C	n = 2	VL-11-MDB
Group D	n = 1	VL-3-M11A
Group E	n = 2	VL-3-M5C
Group F	n = 3	VL-4-M1A

Only two samples contain crushed and added, pebble-sized (greater than 2 mm), micaceous temper, and these comprise Group C. The one sherd in petrographic group D is unique because it contains coarse-sized, angular, light-coloured, pleochroic green to pink-brown amphibole inclusions displaying the characteristic 124° cleavage. The fabric of samples in group E are similar to that of A, subangular to subrounded quartz grains, except that the inclusions in E are generally unweathered and there is little feldspar. Group F consists of sherds with at least one coarse mica grain in the section that is part of the natural temper of the clay. In this case, it is possible that local clay was mixed with another containing coarse-grained mica fragments.

Some issues warrant further investigation. Simon Hall (pers. comm.) has asked whether Moloko potters used different clays to construct different parts of the vessel, according to observed attributes of strength, structure and appearance. Evidence from samples VL-11-M14 A and B and VL-3-M5 A, B and C suggests that this does occur at Marothodi, although not frequently. There does not seem to be any correlation between different clay types and high- or commoner-status areas of the site (see Appendix C). Perhaps of most interest is the relative absence of sherds tempered with graphitic nodules (none) or added lustrous inclusions (two). This compares with the 90% of vessels from the other late Moloko sites that do have these inclusions (see Table 2.1). There are several hypotheses - environmental, technological and social - that could help to explain why Marothodi ceramics were not tempered with lustrous inclusions.

The pottery analysed for this study represent a direct geographic and temporal correlation to the early and late Moloko sites from which they were excavated. This precludes the possibility that regional geologic differences determined either, firstly, the observed change over time in the technology of ceramic production at Olifantspoort, Molokwane and Kaditshwene, or secondly, the absence of lustrous temper in potsherds from Marothodi. Having ruled out that differences in observed ceramic clay fabrics both within the Moloko sequence and between contemporary settlements are attributable to discrete geologic distribution of temper types, I now consider issues of ceramic technology, specialization, technological style and social identity.

TECHNOLOGICAL AND SOCIAL ASPECTS OF LATE MOLOKO POTTERY PRODUCTION

Sillar and Tite (2000), in a discussion of technological choices as social constructs, assert that materials science researchers in archaeology are bound by the same theoretical considerations as their colleagues in social science. They suggest that the holistic context – environmental, technological, social, economic, and ideological – in which an artefact was produced must be appreciated also, because it will greatly affect the interpretations made by the archaeometrist. It is with this understanding that the following ideas on technological choice, craft specialization, technological style and social identity are presented. Together they help develop an interconnected explanation for the change in ceramic manufacturing techniques observed between the early and late Moloko periods and for the break in pattern that occurs when data from Marothodi is considered.

Technological choice

I have suggested that the graphite- and lustrous inclusion-rich clay fabric common in late Moloko ceramics from Olifantspoort, Molokwane and Kaditshwene relates to innovation toward more efficient ceramic production in the town phase (Rosenstein 2002). The desire for a greater success rate in pottery manufacture would be heightened if production of vessels was for thousands of people in an urban settlement, rather than for hundreds in a village. This would link to the preference for larger pot sizes, as evidenced in the late Moloko ceramic assemblages. Steps toward permanence and stability are reflected in other technologies, as well, such as the use of stone, instead of wood, to demarcate space in the large towns. The use of stone likely was necessary in order to manage and sustain the local environment and landscape as the towns grew (Boeyens 2003). The wood consumption of a large town like Molokwane or Marothodi must have been substantial.

If the long-term availability of wood for fuel was a concern, then pyrotechnologies such as pot making might be adapted mechanically as a response. One alternative fuel for firing pottery and smelting metal is cattle dung, which can reach burning

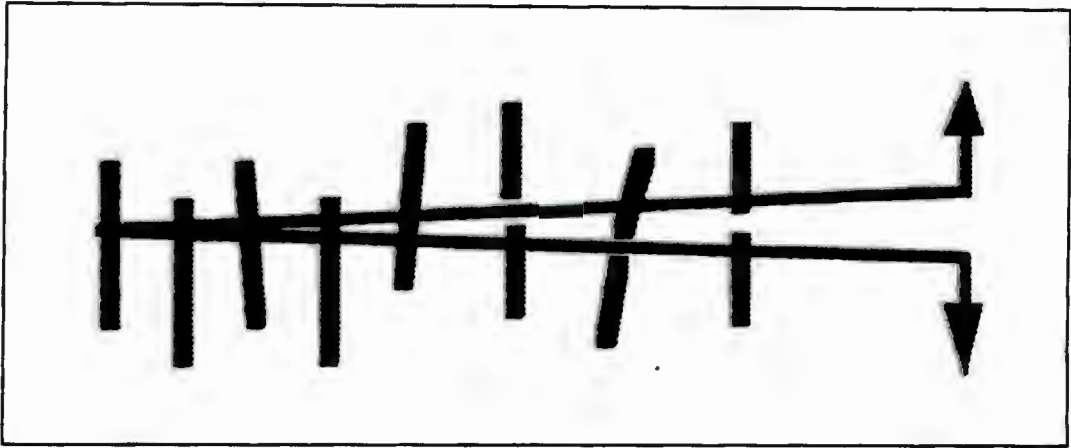


Figure 2.11. Platy inclusions bridge the opening of a crack as it proceeds through the clay matrix, forcing crack closure and enhancing the fracture resistance of the clay (modified from Becher 1991: 258).

temperatures of 1000°C. Ceramic mosaic hearths, such as those at Olifantspoort (Mason 1986), further suggest an interest in heat efficiency, insulation and fuel use. These innovations point to shifts in labour time, particularly for female tasks. The implication is that as the towns formed, women were altering the way they do work. One solution for craft production that fulfils the needs of large populations, as compared to small family units, is to ensure greater success in manufacturing, progressing toward a kind of ‘mass’ ceramic production. Late Moloko potters chose to collect clays with natural graphite-talc nodules and to source platy, fibrous and lustrous minerals and lithics to add as temper. Potential technological effects of these materials in clay include changes in parameters of physical strength, including fracture strength, toughness and thermal shock resistance, and alterations in the hydrous and thermodynamic properties of the ceramic, increasing the likelihood that a vessel survives the drying and firing process.

Tite *et al.* (2001) review the three major material properties of clays and tempers that underlie the technological choices potters make in ceramic production. Fracture strength is the maximum stress that a material can withstand at a particular point before the propagation of cracks causes failure, or breakage. The resistance of a material to stress is its toughness. In a homogenous clay ceramic, without added temper, the fracture strength is based on the size and packing of the clay particles and the level of vitrification of the clay body, which is a result of the firing temperature.

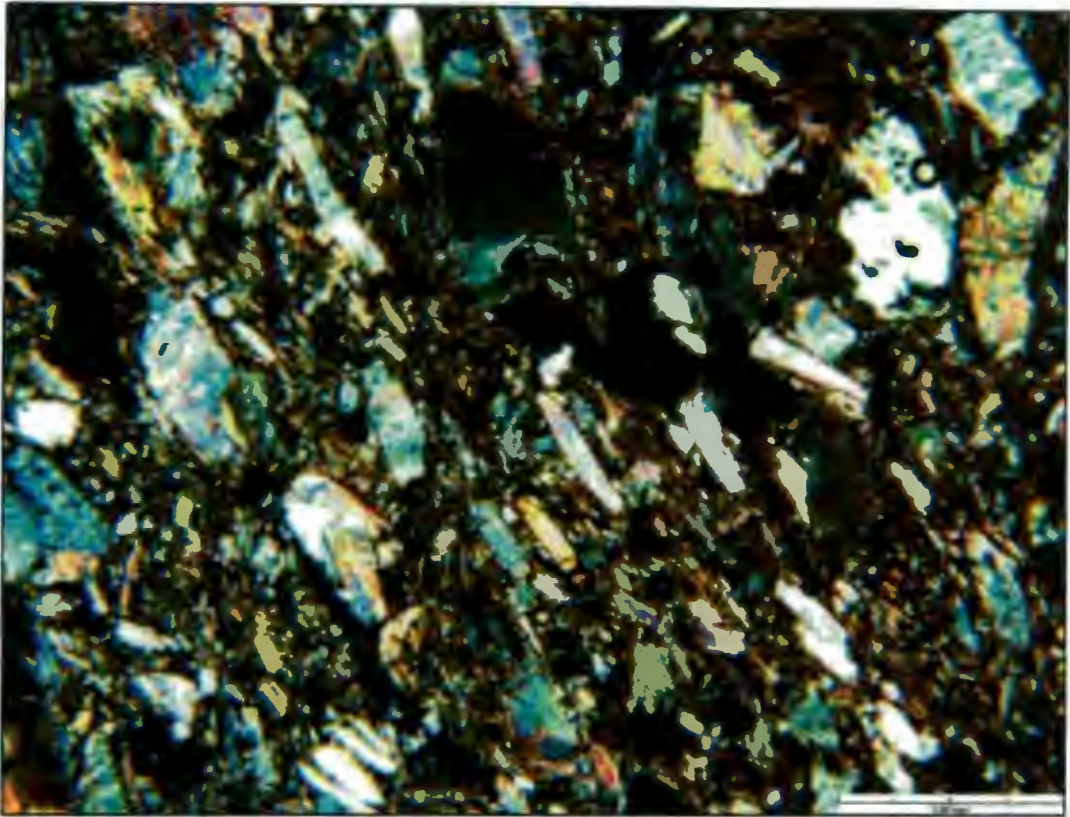


Figure 2.12. XPL petromicrograph of added mica inclusions aligned parallel to the working direction of the clay, or horizontally to an upright vessel, perpendicular to the exterior wall (VL-11-MDB).

Very little energy is required for cracks to initiate and grow in a relatively glassy matrix, even at low firing temperatures. Conversely, in a low-fired clay with added temper, these inclusions dissipate crack energy, and therefore the ceramic has greater toughness.

Thermal shock resistance, the amount and rate of temperature change a material can withstand before the initiation and propagation of cracks, is altered with the presence of different tempers in a clay fabric. In addition, platy and fibrous inclusions can help impede the propagation of cracks from the surface toward the interior as a clay body dries, is fired or is reheated, as in a cooking pot, by imposing closure and providing an obstruction that terminates an advancing crack (Figure 2.11). Elongate mineral and rock fragments align parallel to the working direction in a clay body (perpendicular to the exterior surface in coil-formed vessels; Figure 2.12).

Tite *et al.* (2001) compare the results of several studies in which the strength, toughness and thermal shock resistance of various tempers in ancient ceramics are evaluated experimentally. The published papers include data on quartz, grog, shell and limestone tempers, and West (1992) included platy and fibrous tempers. West (1992) provides a complete discussion of the effect of different tempers on fracture toughness, the primary factor in thermal shock resistance relevant to low-fired ceramics. He shows that the presence of platy and fibrous tempers in increasing amounts and greater size ranges in a clay body maximizes the fracture toughness and thermal shock resistance, and therefore the structural integrity, of a low-fired ceramic vessel with high temper concentration (above 20%).

In addition, phyllosilicate class minerals, including micas and talc, are hydrous sheet silicates that hold water molecules between the layers of their platy structure. The addition of platy minerals to a clay body will therefore affect the amount of water it is able to absorb and the length of time required for it to dry. It will also change the plasticity of the clay; the property of a wet material that allows it to be shaped and to hold that shape without further support. Natural and added tempers may alter the thermodynamic properties of the clay fabric, due to varying specific heat capacities of the temper materials and the clay mineral that makes up the matrix. The specific heat capacity of a material, the amount of energy required to raise the temperature of one gram one degree Kelvin, contributes to its behaviour during heating.

Historic accounts reveal that more recent BaTswana potters added platy and fibrous minerals to their clay to enhance the technological properties of the material. An observation by Sentker (1968) in the Braklaagte area approximately 10 km from the stone-walled site of Kaditshwene, indicates that Rosina Sukui, a BaHurutshe potter, added 'asbestos' to her clay to stiffen it. The relevant section translates as follows:

The clay (*moraga*) is acquired in the proximity, in the flats. It is kept in small dry pieces in a big pot. The clay is used as it is found and is not purified or prepared in any other way. It is moistened and kneaded until it is well kneaded and like plastic. Whilst kneading asbestos is added. The ratio is roughly 3 fist-sized pieces of asbestos in 1 ½ gallon of dry clay. The asbestos is ground on a grindstone, ground to powder and then added to the wet clay

and mixed well. Rosina maintains that the asbestos firms the clay [emphasis original].

A second observation by Grant (1968) in the Kgatleng region, Botswana, describes how Mina Kwapa, one of three potters in Morwa village, mixes her clay:

Unlike her predecessors who obtained their clay (tsopane) from behind the Phaphane Hill at Mochudi, she goes to the banks of a small stream in Morwa itself. In order to give additional strength to the clay she has to roam the Morwa hillsides for a certain type of stone, called Moshalakane – which turned out to be asbestos. Both clay and stone are ground down to a powder, a smooth hand stone, the thitelo, acting as the pestle. With water, the two powders are mixed together in the proportions of two clay to one asbestos (Grant 1968: 93).

In Lawton's extensive field and literature survey of southern African potters (1967), she reports:

A number of potters interviewed mixed a non-plastic material with the clay, which they said was to strengthen it. Skilled potters are able to tell from the feel and appearance of the clay whether it is necessary to add anything or not. (The effect of the addition of a non-plastic material, or filler, is to prevent excessive shrinking while drying, thus producing a stronger material. The amount of filler has to be carefully judged, as the addition of too much will have a weakening rather than strengthening effect.) Fillers used by Bantu potters include finely ground potsherds, sand, and earth containing asbestos. The asbestos acts as a binder as well as a filler and increases the cohesion of the clay (Lawton 1967: 8).

In her classification of pottery techniques and types according to tribe, Lawton describes an asbestos-bearing ore material added to clay by BaHurutshe, BaKwena and Kgalagadi potters (1967: 133-146).

The accuracy of these identifications of 'asbestos' as the temper material is unknown, but amphiboles and serpentines, silicate minerals that can have asbestiform (fibrous or platy) structure, do occur in the geology of the region (Jansen *et al.* 1974; Walraven 1981). Similarly to mica and talc minerals, the thin, strong fibres of asbestiform minerals are characteristically flexible, heat resistant and chemically inert.

Future research may include experimental clay firing at controlled temperatures with different proportions of graphitic and platy, lustrous, and asbestiform tempers to evaluate the technology used to manufacture pottery. Technical features related to the functioning of a vessel, such as building technique and temper material, as well as effectiveness in portability, cooling, heating and resistance to thermal shock, impact and abrasion have been compared successfully through experimental archaeology (Schiffer & Skibo 1987, 1997). All these issues are potentially relevant in the context of 'mass' production of ceramics in the late phase of the Moloko sequence.

Though a study of technological impact can be done successfully through experimental archaeology and other techniques strictly following the scientific method, it will always be confounded by the complexity of human nature and reasoning. A clay fabric experiment, as a pilot study to begin thinking about the technological behaviour of a *pot*, would be informative. The technology of an artefact is indivisible from the cultural system within which it is embedded, however, which influences the sociocultural behaviour of the *potter* and the decisions made when manufacturing artefacts. One must avoid a narrow focus only on technological change instead of a broader consideration on technological choice (*cf.* Lemmonier 1992; Pfaffenberger 1992; Schiffer 1992; Childs 1994; Gosselain 1998; Sillar & Tite 2000; Killick 2004).

To illustrate this I outline an ethnoarchaeological example from southern Africa. Lindahl and Matenga (1995) undertook a study of five women potters among the Shona, southeastern Bantu-speakers in Zimbabwe. The potters made deliberate choices in selecting the specific local, naturally tempered clay with which a particular sort of vessel should be formed. One woman used silty, fine-grained material only for small cooking and drinking pots, because the fine clay did not support large-sized vessels. Her coarse-grained clay was technologically suitable for making all sizes of

vessels. She did not use it for cooking pots, however, explaining that coarse grains in the wall of the vessel loosen during cooking and stirring, allowing gravel to mix into the food (Lindahl & Matenga 1995). Without acting as a potter or being a user of pot technology (for example, cooking food in a pot during an experiment), one cannot begin to evaluate these kinds of factors.

The technological choices potters make in selecting their clays and manufacturing their wares also involve social and environmental situational factors. Recognizing that the interactions between people and the artefacts they produce and use are influenced by many more attributes than simple, practical utility also is important in understanding technological change. Results of an ethnoarchaeological study in West Africa (Gosselain 1994) show that, in addition to raw material quality and performance, cultural and economic factors are considered for the collection of clay and the firing of vessels. These include time and energy available for pot making, so that clays are systematically exploited where other activities, such as farming, fishing, hunting, markets, already are taking place. Ceramic production is supplementary to these other tasks but never the main source of income or responsibility for a potter, because the benefits are not great enough. For this reason, investment in clay prospecting, which is uncertain and time consuming, is avoided. A potter is likely to use a substandard clay, decreasing the technological and functional success of ceramic manufacture, in order to also decrease the overall effort expended in time-consuming clay collection (Gosselain 1994). Any interpretation of the change in Moloko pottery production over time and space must integrate all of these concepts.

Craft specialization

It was also suggested previously that the demonstrated change in pottery manufacturing technology between the early and late Moloko periods, analogous to the decrease in number of ceramic classes and frequency of decoration and concurrent with the shift in settlement pattern from dispersed village homesteads to large, aggregated stone-walled towns, is evidence for specialization of ceramic production (Hall 1998; Rosenstein 2002). Several scholars over recent decades have contributed to a theory for understanding the advent of craft specialization via interconnected social, environmental and regional factors, such as the culture of technology and

materials, organization of production, political economy and exchange (cf. Brumfiel & Earle 1987; Costin 1991; Longacre 1999; Costin 2001; David & Kramer 2001a). The following discussion draws from these sources, based on information from a range of ethnographic, historic and archaeological examples.

Costin (1991) argues that the advent of craft specialization is a response to needs and demands that arise under economic and environmental constraints. Systems of production and distribution cannot be evaluated independently from these factors, which underpin the social and political function, role and demand for a craft.

Theory on the emergence of craft specialization incorporates the social, economic, political and environmental factors that effect the organization of production. These include the context of manufacture, the concentration of manufacturing sites on the landscape, and the scale and intensity of production, including time spent, efficiency, risk, scheduling, division and control of labour, and levels of technology and skill. Other important factors include the political economy of production, consumption, distribution and exchange, the location and control of natural resources and the specific type of craft technology.

If specialization is defined as differential involvement in craft activities, in the archaeological record it will be directly evidenced by the proportionally unequal distribution of manufacturing debris, used and unused tools and facilities associated with behaviours of production. This type of specialist production is suggested by high ratios of specific artefact concentrations in particular households, communities, or regions, for example, or among certain social classes or contexts (Costin 2001). The original research design for this project included a search for the archaeological correlates of ceramic specialization. For the Moloko period, this kind of data is robust for metal production but not ceramic manufacture, because production and firing sites are not apparent in the Iron Age. It seems incongruously difficult to recover evidence for women's contributions. Thus site formation processes must be considered, also, when evaluating the validity of this kind of data.

Indirect evidence of specialization in craft manufacture includes indication of standardization (Arnold 2000), increased efficiency or skill, or geographical variation,

as will be discussed here for the late Moloko context. This type of information is useful for understanding the relative degree of specialization for a particular craft and generally in the regional economy. Costin (2001) maintains that in order for indirect evidence to be used in a qualified argument for specialization, however, it must be shown that regularity in production was an appropriate economic response to cultural, social, political and environmental conditions.

At Late Iron Age sites in southern Africa, potsherds are ubiquitous on the landscape. The high degree of self-sufficiency in Western Tswana homesteads implies that ceramics were manufactured at every Moloko site. In the early Moloko village period, with about a hundred people at each site, potters produced a range of well-decorated vessel types. In comparison, during the late Moloko, when thousands of people inhabited the stone-walled settlements, potters made few varieties of ceramic class and decorated them sparsely, if at all. While it is thought that the organization of pottery manufacture in the early Moloko was at the household level, it is possible that the trend seen in the late Moloko, coeval with the shift in scale of settlement size, was related to specialized ceramic production. The addition of tempers that improve the technological properties of vessels, as discussed in the previous section, suggests both increased skill and efficiency in ceramic manufacture. It seems that this innovation was geographically constrained, since these tempers occur in late Moloko pottery at Olifantspoort, Kaditshwene and Molokwane, but not at Marothodi.

In a framework of craft specialization theory, standardization in late Moloko pottery manufacture can be interpreted as a reaction to the considerable social, political and environmental pressures facing the BaTswana during this time, as discussed in Chapter 1. Craft production in both the early and late Moloko included gendered tasks, and women manufactured pottery; the significance is in the degree of manufacture in the late Moloko (Hall 1998). Specialized ceramic production would parallel increasing importance of the male craft, metalworking, as a prospect for expanding economic opportunity through trade in a time of hardship. Segregation of women's production areas would also be in accord with the designation, by scalloped stone-walling, of separate, female-oriented domestic areas in the town settlements. These precisely defined back courtyards are most probably where ceramics were



Figure 2.13. ‘The potter and her apprentice,’ an ethnographic photograph taken at a homestead in Mochudi, Botswana, settled by the BaKgatla in AD 1871 (Duggan-Cronin 1929). The back courtyards are where primary pot construction takes place.

made (Figure 2.13). Comparatively, in the early phase, the proximity of men and women and their work spaces was much closer (Hall 1998).

Specialization of women’s craft would have a notable effect on the nature and efficiency of ceramic manufacture due to changes in division of labour and time allocated to particular tasks. The character of the pottery might change in response to transformations in these other social, political and economic relationships. It could be the result of a concentration of ceramic production with specialized women’s workgroups that supplied the craft to the entire settlement (Hall 1998; Costin 2001: 295-296).

Alternatively, the occurrence of few vessel forms and limited decoration in the late Moloko ceramic assemblage can be explained due to standardization of craft production (Hall 1998; Costin 2001: 301-303). The simplification of pottery manufacture in the late Moloko would allow women more time for other work. For

example, early Moloko pottery is decorated with a superficial application of ochre or graphite, and there is a significant reduction in their use in the later pottery. The lustrous inclusions characteristic of late Moloko ceramics are internal, incorporated into the clay fabric in the initial steps of formation of the vessel, but have a conspicuous effect on the external appearance of the pot. Thus adding lustrous temper not only increases the efficiency of production, but considering the limits on female time for labour, also is an effective way of 'decorating' the vessel by eliminating the need to apply ochre and graphite in a final step.

Technological style

There are numerous ways in which technological style has been explained in archaeological context (cf. Lechtman 1977; Hegmon 1992 for a review of early research; Dietler & Herbich 1998; Gosselain 1998; Hegmon 1998; Wobst 1999). Presented here is a somewhat synthesized definition, drawing from a combination of these theoretical frameworks.

There are two related 'style' concepts in material culture studies. First, style is the specific way that one does something, as in the manufacture of an artefact. This is also called the *chaîne opératoire*, a term introduced by Leroi-Gourhan (1965) to describe the ordered sequence of gestures and actions that takes place in the chain of production to transform a concept into finished product, including raw material procurement and fashioning technique. This is sometimes called 'technological style' (Lechtman 1977) or 'technological choice' (Lemmonier 1992). Second, style refers to the characteristics of an object that reflect or are a result of those processes, such as the shape of or decoration on a ceramic vessel. The meaning imbued in these attributes is associated with one's identity, as discussed in the next section; the concepts of style and identity are inextricably linked, but presented here separately for ease of explanation. There are also environmental, manufacturing and functional constraints on the number of technological alternatives available to a potter, and therefore on the stylistic expression on the artefact. An obvious example would be the type of clay local to the geology of the region affecting the technological or decorative choices of a potter.

Implicit in research on the *chaîne opératoire* of material production are the learning frameworks through which technological knowledge is passed, for example in apprenticeship, through kin lines or in workshops (Dietler & Herbich 1998; Gosselain 1998, 2000; Killick 2004). Ethnoarchaeology has been a useful and powerful method for recognizing and explaining stylistic and social identity markers in the archaeological record (David & Kramer 2001b). It has been especially successful in helping to expand the types of evidence considered reflective of style, from specific iconographic motifs to broader technological behaviour. During his fieldwork in Cameroon, Gosselain (1998) observed the techniques of ceramic manufacture of nearly one hundred potters among different language groups. He recorded the process, the *chaîne opératoire* of pottery production, according to each potter and determined through interviews which individual steps were skills learned in apprenticeship and which were the result of individual choices. Thus he links technological behaviour to social identity. He maintains that the style of decoration on a ceramic vessel is a changing external expression related to the more superficial aspects of a potter's identity. The formation of a pot is the result of a primary learning process, and therefore the style or manner in which it is done is a reflection of socialization, embedded with "enduring aspects of social identity, such as kinship, language, gender, and class subdivisions" (Gosselain 2000: 193).

Wobst (1999: 120) argues that people use style in material artefacts to represent intentions that cannot be expressed by other, non-artefact means, such as by speech, gesture, odour and touch. In this way, the presence of specific graphitic and lustrous, platy temper materials in late Moloko pottery can be interpreted not only as decorative and formative choices, but also as having a social role for the people producing and using the vessels. Each temper has an effect on the outward appearance as well as on the mechanical performance of a pot. The extent to which this type of technological style, as in decorative choice, can be closely related to symbolism and social identity, or affiliation, will be discussed in the next section.

Social identity

A social identity is a definition, connecting a person to or differentiating a person from others with a group framework. It varies over time and geographic space. The

recognition of identity from artefacts in the archaeological record is a particularly difficult problem, as it necessarily requires a 'thick' understanding (in Geertz 1973 terms) of the social and environmental context in which the artefact was designed.

A social identity is also a practice, observed through selection of, or preference for, particular characteristics. Because craft production is underpinned by economic, societal, political and ritual systems, the artefacts manufactured reflect social processes and behaviours inherent to the artisan (*cf.* Costin 1998; Gosselain 1998, 2000). In this way, identity can be identified in artefacts through technological style and technological choice.

The relationship between technological style and identity relates to another aspect of social communication, in which, because of distinct markers in their method of manufacture, form or decoration, objects are used to define or regulate social boundaries between individuals or groups (Dietler & Herbich 1998; Gosselain 1998, 2000). For Late Iron Age in southern Africa, the close link between the archaeology and the ethnography provides the basis for using these records to amplify our interpretations. Ethnographic accounts from South Africa describe how the decoration of ceramic vessels reflects gender identities and thereby identifies the contexts and ways in which people may interact. Among the BaPedi, for example, a group closely related linguistically to the BaTswana, vertical straight lines symbolically replicate maleness, and axes and spears can be manipulated outside of their specific use context to represent men. In contrast, femaleness is depicted by triangles and chevrons, which, among other things, represent the tips of the vulva and the rear skirt, a short skirt with a pointed hem at front and in back. The designs, which decorate BaPedi ceramics and correspond to the motifs seen on Moloko pottery of the Late Iron Age, provide a continual symbolic backdrop on decorated vessels. These patterns are often also found together in contexts where men and women interact and, accordingly, adorn the walls of the public courtyard where both sexes are permitted to congregate. In addition, the symbols are used to mark vessels purposely for gendered use, for example in beer drinking or rituals (Evers and Huffman 1988: 740, citing Vogel 1985).

African ethnography and ethnoarchaeology provide a framework through which the social meaning of crafts and craft production can be examined. Pyrotechnology, the transformation of earth raw materials (ore and clay) into metal and ceramics, is an important element of the social system, used to communicate the boundaries, roles and responsibilities of men and women in a group. As explained by Herbert, “the equation potters = women and smiths = men is virtually a given in Africa” (1993: 203). Further, expressive aspects of these processes, in all steps of the *chaîne opératoire*, reflect human physical, sexual and social characteristics, such that the artefacts themselves can represent people; this is especially the case with pottery (David *et al.* 1988; Evers & Huffman 1988; Berns 1990; Herbert 1993).

In southern Africa, pottery is inextricably linked to metaphors that describe and embody social meaning and interaction. Vessels are often purposefully moulded in a ‘womanly’ form, with a rounded neck, shoulder, body, a womb-like interior and sometimes breasts (Aschwanden 1982: 191). Discourse about pottery and its creation is rich in female symbolism, relating ‘creation’ from the soil of the earth, ‘gestation,’ or firing, and the ‘birth’ of a vessel from the pit kiln. When a child dies among Xitsonga speakers, he or she is buried in a pot, in a ‘return’ to the womb (de Heusch 1980). It is possible that similar general concepts of death and rebirth were held at the site of Broederstroom, west of Johannesburg, where Revil Mason excavated juvenile pot burials (Mason 1981).

Thus through the basic ethnographic metaphor of ‘pots are people’ (David *et al.* 1988: 365; Berns 1990; Herbert 1993: Chapter 8) ceramic sociologists and archaeologists in southern Africa are beginning to attempt to understand the social context of vessel production and use. It is especially important to consider how pottery and the human body can be treated in the same manner, reflecting and mediating the categories and boundaries of social identity.

In the Moloko context, it is probable that the choice of lustrous tempers with exceptionally visible exterior qualities can be interpreted not only as a technological innovation, but also as an identity marker. Travellers to the Rustenburg-Zeerust region during the early 19th century describe a sparkly substance, *sebilo*, valued by the BaTswana as a bodily adornment and traded widely, over hundreds of kilometres



Figure 2.14. Engraving after an original 1812 portrait by Burchell of Mahútu, a BaTlapin woman. Burchell writes (as in original), "... the bonnet-like appearance on her head, is produced by the peculiar mode in which the Bachapin women dress their *hair*. The color here shown, is occasioned by the *sibiilo* with which it is powdered (Burchell 1824: 494, Plate 8)

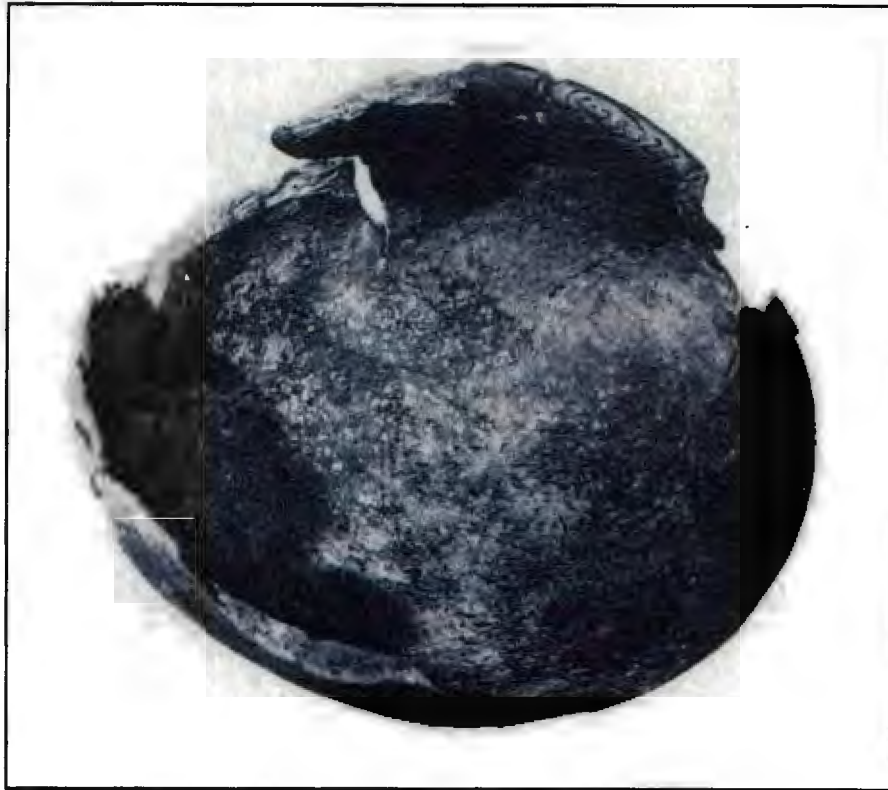


Figure 2.15. Broken ceramic vessel with *sebilo* still cached inside, excavated from the late Moloko site Olifantspoort (Mason 1987: 80).

(Campbell 1815; Lichtenstein 1815; Campbell 1822b; Burchell 1824). The material was finely crushed, mixed with fat, and applied to hair “in the same way as hair powder is used in Europe” (Campbell 1815: 169) and to skin (Figure 2.14).

Specularite, a crystalline form of hematite (ochre), is a glittering, silver-grey or silver-black mineral mined by people in southern Africa for more than 40 000 years (Middle Stone Age at Lion Cavern, Swaziland: Beaumont 1973). Late Iron Age specularite exploitation for more than 1 000 years through the early 20th century, in what is now the Northern Cape province of South Africa, is evidenced in the Postmasburg region (Beaumont & Boshier 1974; Thackeray *et al.* 1983). A broken ceramic vessel with specularite, or *sebilo*, still cached inside was excavated at the late Moloko site on Olifantspoort farm (Figure 2.15). A *sebilo* quarry, exploited from about AD 1700, was located at Ifafi, on the southern edge of the Magaliesberg Valley approximately 50 km from Olifantspoort (Mason 1987: 80).

Bodily decoration with glittery *sebito* was a notable marker of social identity among the BaTswana. The inclusion of shiny, lustrous temper in the form of various mineral and lithic materials in late Moloko ceramics had beneficial effects on the technological function of the clay body. Further, there was an important association between the sparkly exterior surface of a vessel with lustrous inclusions and the shimmering skin and hair of a person ornamented with *sebito*. Burchell observed, “A Bachapin whose head is thus covered, considers himself as most admirably adorned, and in full dress” (1824: 256). The human body and pots were treated in the same way; in principle, the body is not fully dressed without *sebito* nor is a pot that needs decoration finished without the application of a lustrous temper, red ochre or graphite. The principle underlying this relationship demonstrates the implication of ‘pots are people,’ such that the appearance of one signifies the other, and the pot is a symbol of social identity.

CERAMICS AT MAROTHODI: A STUDY IN VARIATION

This chapter has outlined a change in BaTswana ceramic production techniques that occurred between the early and late Moloko periods as evidenced by graphitic and lustrous tempers in pottery from the sites at Olifantspoort farm, Molokwane and Kaditshwene. Petrographic data of analyzed potsherds from the stone-walled town of Marothodi, however, reveal only two of 42 ceramic samples contain micaceous inclusions and none were made of graphitic clay. I have presented several technological and theoretical concepts, drawn from experimental archaeology and ethnographic analogy, to help understand this variation. No artefact is manufactured in a simple context for utilitarian purposes. There are underpinning technological, social, political, economic, environmental and ideological factors that must be considered in understanding and interpreting the production and use of an object. An artefact is a cultural item; implicit in the *chaîne opératoire* of its creation is human behaviour, technological choice, function, style and social identity. Complex systems such as the advent of craft specialization must be evaluated in comparison to these other structures and aspects of a dynamic society.

I have shown that the lack of graphitic or lustrous tempers at Marothodi is not related to availability of those materials in the local geology. Their inclusion in a clay body, however, improves the technological performance of the vessel. It is curious, therefore, that potters at Marothodi would not choose to add those materials when manufacturing ceramics. The settlement is of the same type and at the same scale as the other late Moloko stone-walled towns, and according to oral-historical and archaeological evidence, essentially contemporary. Therefore, the intensity of ceramic production at these late Moloko sites would have been equivalent.

It is possible that manufacture of ceramics with particular tempers was a specialized craft in the late Moloko, in which Marothodi potters did not participate because of cultural affiliation and social identity. For example, the high concentration of metal production at Marothodi in comparison to the other towns might reflect a special technological expertise of its inhabitants. Thus the dominant population at each late Moloko town is important to consider. While the social identities of the inhabitants of Olifantspoort (BaKwena), Molokwane (BaKwena), Kaditshwene (BaHurutshe) and Marothodi (BaTlokwa) are known, the ancestral linkages between the groups are not clear. As understood through the oral-historical record, the BaKwena and BaHurutshe are archetypal western BaTswana in heritage and culture. The origins of the BaTlokwa are more ambiguous, and it is possible that they and the BaKgatla, who settled in the adjacent Pilanesberg area, have their origins in common with the Nguni. It is notable that the graphitic and lustrous inclusions do not occur in BaKgatla ceramics, either (Hall *et al.* 2007, 2008). Perhaps the preference for these tempers underpins a degree of relatedness in the western BaTswana lineage that would be manifest in, among other things, learning frameworks of craft manufacture and the artefacts produced.

In addition, there is no direct historical, ethnographic or archaeological evidence that the BaTlokwa ornamented themselves with *sebito*, as there is for the BaKwena and BaHurutshe (Campbell 1815; Mason 1987). The presence of particular tempers in pottery can be a reflection of the application of glittering *sebito* to the person. If the BaTlokwa at Marothodi did not use *sebito* for bodily embellishment, it would be another critical consideration in interpreting their cultural origins and the lack of graphitic and lustrous inclusions in ceramics from that site. Considering its

widespread use in the BaTswana world, however (Burchell 1824: 256), it is unlikely that *sebito* adornment was not practiced at Marothodi.

Thus historical description, ethnographic research and archaeological evidence support both technological and cultural explanations for the difference in pottery production between Marothodi and the other late Moloko stone-walled towns investigated. An additional factor, that of chronology, must be considered. Although oral accounts indicate Marothodi was inhabited at the beginning of the 19th century, one must assess carefully the accuracy and reliability of historical information. When and where did these new technological attributes first appear in late Moloko ceramics, and what was the timing of their adoption across the BaTswana landscape?

Because of the imprecision of the radiocarbon calibration curve over the past three centuries, establishing an accurate chronology of the late Moloko sites is problematic, yet the sequence becomes crucial to understanding the technological development of ceramic manufacture in the Late Iron Age. For this reason, continuing research on this project has included evaluation of published radiocarbon and oral-historical dates for the late Moloko and an experiment in applying optically stimulated luminescence as a dating technique for the recent past.

Chapter 3

Dating Method One:

Radiocarbon

Radiocarbon dating is the chronometric technique most frequently utilized by archaeologists worldwide. This is due to a number of factors, including the common occurrence of organic materials in the archaeological record, ease of sampling, relatively inexpensive cost and reliability of quality data from specialized laboratories. Before radiocarbon dates are applied to archaeological contexts, however, the parameters of radiocarbon on Earth must be understood. Fluctuations in the amount of radiocarbon present in the atmosphere over time can result in ambiguous or uninterpretable dating results.

CONSIDERATIONS FOR RADIOCARBON DATING

Willard Libby and colleagues introduced radiocarbon dating in 1949 (Arnold & Libby 1949; Libby *et al.* 1949). Radiocarbon dating is possible because in an atmosphere with two inert carbon isotopes (carbon-12, ^{12}C , and carbon-13, ^{13}C) a radioactive carbon isotope is produced also (carbon-14, ^{14}C). Natural ^{14}C is formed in very small quantities by the bombardment of nitrogen atoms (^{14}N), the most abundant isotope in the atmosphere, with free neutrons from cosmic ray influx (Figure 3.1). The current equilibrium state carbon content of the atmosphere is approximately 98.9% ^{12}C , 1.1% ^{13}C and $1.17 \times 10^{-12}\%$ ^{14}C .

A number of concise introductions to radiocarbon dating history, principles, methods, calculations and concerns have been published (*cf* Bowman 1990; Taylor 1997, 2000, 2001; Faure & Mensing 2005). My summary is drawn from these sources. It is by no means exhaustive, but provides basic background to the environmental and physical chemistry aspects of the technique.

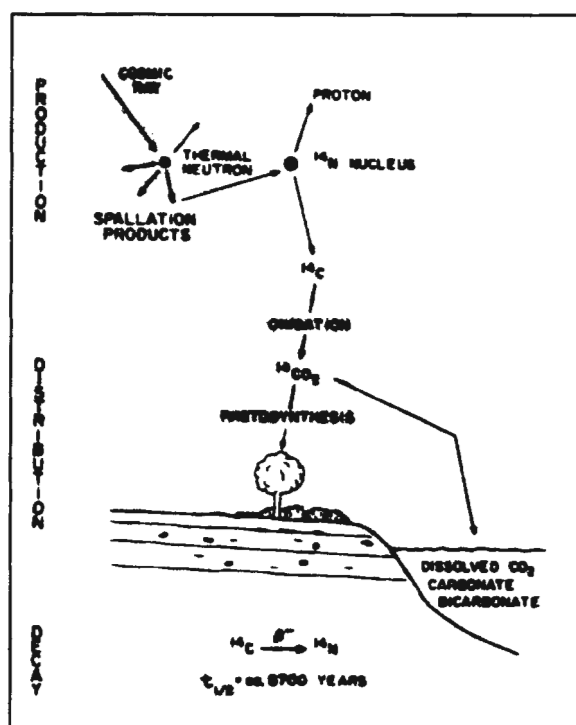


Figure 3.1. Radiocarbon production and dating, after Taylor (1997: Figure 3.1).

The basic principle of radiocarbon dating is that a living organism maintains a consistent concentration of ^{14}C , equal to that occurring in a rapidly mixing atmosphere, during the time it is alive and photosynthesising or metabolising. Upon death, the ^{14}C begins to decay to ^{14}N , thereby emitting atomic radiation in the form of beta particles at a constant rate over time, the ^{14}C half-life of 5730 ± 40 years. For conventional and historical purposes, however, Libby's standard, 5568 ± 30 years, is the half-life used for calculating radiocarbon dates. For radiocarbon dating to be accurate, the ratio of ^{14}C to ^{12}C in the organism must not be altered after death, except by the expected rate of radioactive decomposition. A laboratory can estimate the length of time since the organism was alive directly, by measuring the amount of atomic ^{14}C remaining in the matter by accelerator mass spectrometry (AMS), or indirectly, by gas proportional or liquid scintillation counting of the beta particles emitted as ^{14}C atoms decay. These results are corrected for radiometric background noise and extrapolated according to the Libby half-life of the ^{14}C isotope.

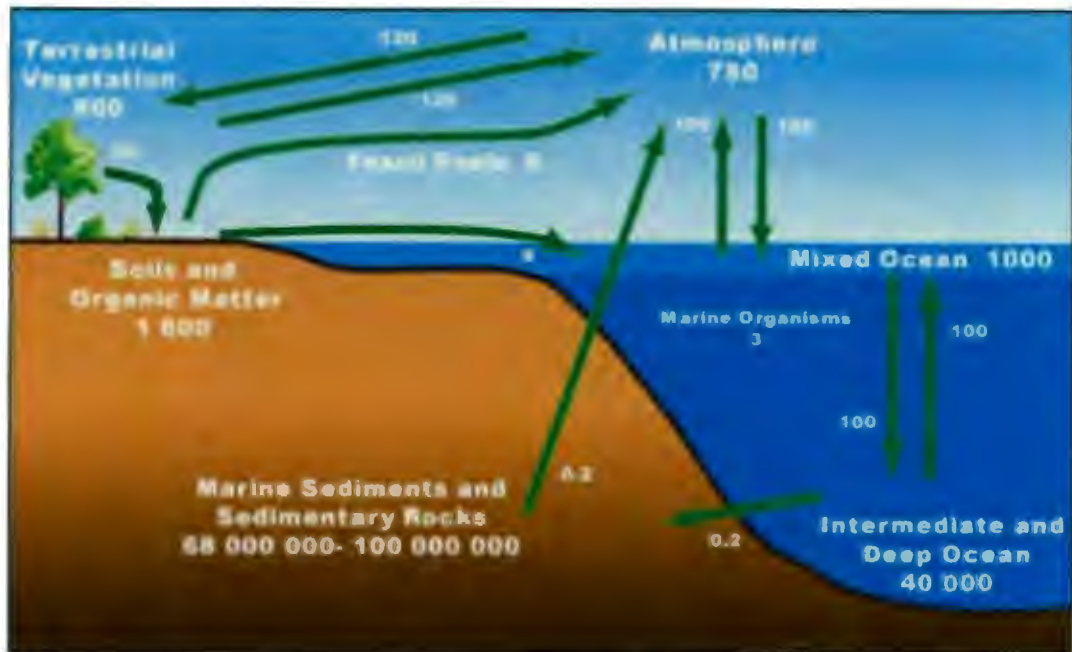


Figure 3.2. Major carbon reservoirs on Earth (in 10^{12} kg), with carbon exchange rates (10^{12} kg/year) (adapted from Ruddiman 2001: Figure 2-32b). Radiocarbon is produced and released at a rate of about 7.5 kg/year.

In actuality, radiocarbon dating is not so straightforward. There are several cosmic, climactic, environmental and archaeological factors that have influenced the production of ^{14}C in the Earth's atmosphere at different rates and at different times in history. For example, although in principle the atmospheric ratio of ^{14}C to elemental carbon (^{12}C) is assumed to be constant, in fact geographic effects on amounts of cosmic radiation, including latitude and altitude, change the ^{14}C production rate over time. The interaction of solar wind with the Earth's magnetic field, intensified during episodes of sun spot activity, and variations in the direction and intensity of the magnetic field affect the amount of free neutrons present in the atmosphere to bombard ^{14}N , altering the production rate of ^{14}C .

^{14}C is assumed to be constantly and equally mixed around the Earth in its various carbon reservoirs, including the biosphere, ocean, atmosphere and in living organisms, each of which contain relatively small concentrations of exchangeable ^{14}C as compared to stable carbon isotopes (Figure 3.2). But the amount of carbon exchange between the ocean and atmosphere has changed over time due to glaciation and the varying extent of polar ice caps in warmer and cooler periods of the Earth's

history. During ice ages, the rate of ocean-atmosphere carbon exchange is slowed, and during warm interglacial periods, melting ice releases 'old' carbon depleted in ^{14}C . Further, the amounts of radiocarbon contained in the different carbon reservoirs on Earth are not equivalent. The ratio of oceanic to atmospheric carbon is more than 40:1, due to the deep depth of the mid-ocean trenches and the amount of 'old' organic material preserved there, and the unequal distribution of land as compared to ocean in the northern versus southern hemispheres.

Humans also affect the atmospheric ratio of ^{14}C to ^{12}C ; industrial burning of fossil fuels increases atmospheric ^{12}C , while thermonuclear reactions release excess free neutrons, increasing ^{14}C production.

Each of the above conditions (geographic effects, mixing of carbon reservoirs and human impacts) cause difficulty in interpreting radiocarbon results and fluctuations in ^{14}C production over time. These de Vries effects, or 'wiggles,' are evidenced in specific inconsistencies between radiocarbon ages and independently dated materials for the entire 40 000 year period over which ^{14}C can be measured accurately and precisely in a sample. In recent centuries, sun spot activity has been cycling with a periodicity of approximately 200 years, leading to recent 'wiggles' in the radiocarbon calibration curve, clearly visible in Figure 3.3 at about 1350 cal AD (700 BP), 1550 cal AD (400 BP) and 1750 cal AD (200 BP). A second important recent depletion in the ratio of ^{14}C to ^{12}C is called the Suess effect. This is caused by the substantial influx of ancient carbon dioxide into the Earth's atmosphere from burning of fossil fuels, which no longer contain ^{14}C , which began with the Industrial Revolution beginning in the late 18th century. Suess effects, coupled with the significant de Vries effects in recent times due to solar cycles, result in acute inconsistencies in the curve of ^{14}C production over the last 300 years.

In addition, a correction for fractionation, or the preferential uptake by an organism of the lightest of the three carbon isotopes (^{12}C) over the middle-mass isotope (^{13}C) and of ^{13}C over the heaviest isotope (^{14}C), must also be applied to a radiocarbon age. The correction ratio of ^{13}C to ^{12}C , expressed as a $\delta^{13}\text{C}$ value in parts per thousand (‰),

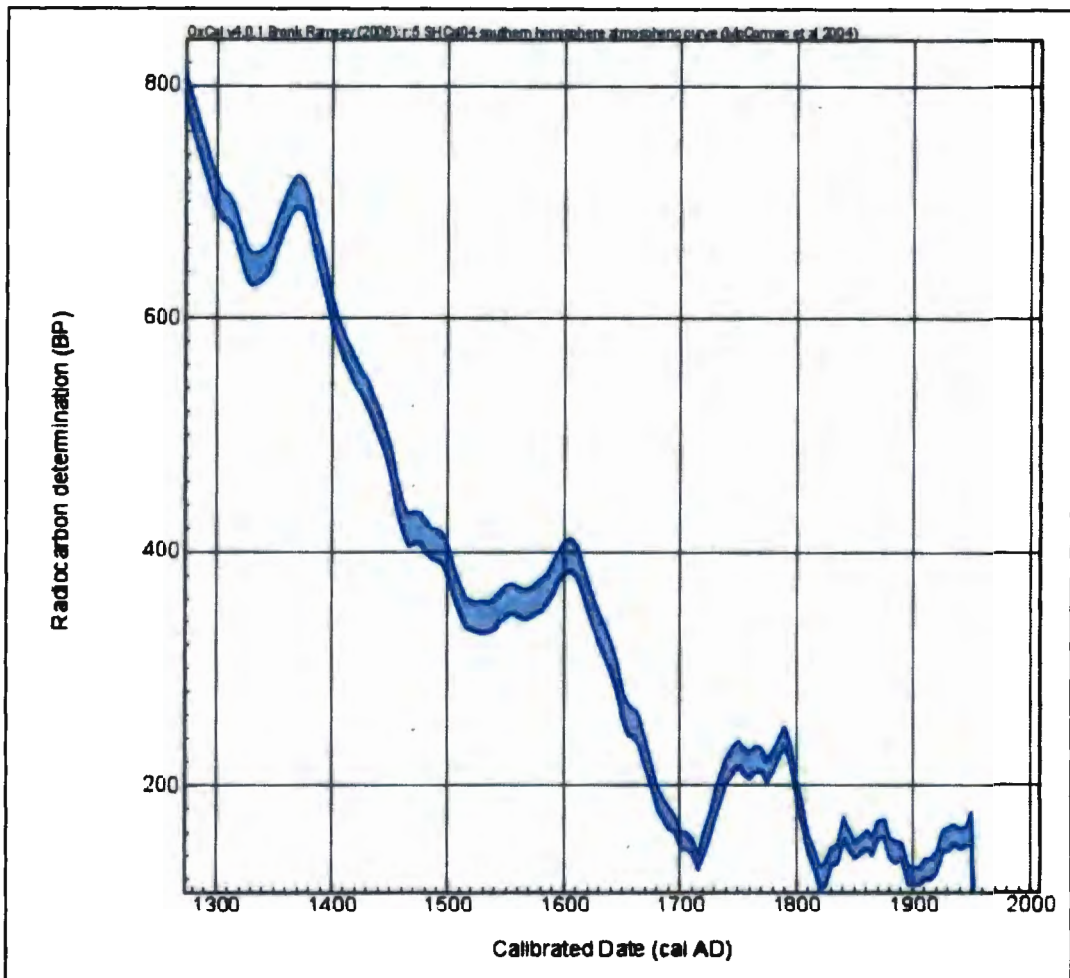


Figure 3.3. The radiocarbon calibration curve for the Late Iron Age, 800–0 years before present (BP, where ^{14}C 0 BP = cal AD 1950), in the southern hemisphere as developed with information from fourteen independent datasets (McCormac *et al.* 2004; Reimer *et al.* 2004). Suess and de Vries effects, or wiggles, can cause a single radiocarbon year (BP) to calibrate to a range of calendar years (cal AD).

measured by mass spectrometry and incorporated into a calibrated radiocarbon date result, helps to determine if a sample was subject to differential carbon reservoir effects.

The radiocarbon curve and the nature and extent of the wiggles detected therein have been continually researched and tested, particularly since the 1970s. Radiocarbon ages calculated on tree-rings of known dendrochronologic dates allow for direct comparison of radiocarbon results with calendric ages. Consequently, there are major revisions to the radiocarbon calibration curve, as discussed at International

Radiocarbon Conferences and reported in the journal *Radiocarbon* (Stuiver & Becker 1993; Stuiver & Pearson 1993; Stuiver *et al.* 1998). In the current calibration issue, published in 2004, it was reported that through multi-laboratory comparisons of ocean corals and foraminifera dated by the ratio of uranium-234 to thorium-230 and of varve chronologies cross-dated by organic material in the sediment layers, the radiocarbon calibration curve has been extended to approximately 26 000 cal BP, where 0 cal BP = AD 1950 (Figure 3.3; Reimer *et al.* 2004).²

Radiocarbon results must also be calibrated according to the kind of material dated. Inland terrestrial organic matter, both plants and animals, correlate to the carbon reservoir of the atmosphere, and are calibrated according to tree-ring data. Marine materials and samples from animals that exploited significant amounts of marine materials or were living at the coastline correlate to the mixed-carbon reservoir of the ocean, and are calibrated according to coral and varve sediment data. Lacustrine materials are also subject to carbon reservoir effects. Discrepancies between terrestrial, marine and lacustrine samples are due mainly to incorporation of 'old' or 'dead' carbon during carbonate formation and varied rates of air-water exchange. An age correction, dependent on time and geography, is required for marine and lacustrine samples; these samples are calibrated using different curves, resulting in an approximately 300 to 500 calendar year age difference from dates calibrated with the terrestrial curve (Stuiver & Braziunas 1993; Stuiver *et al.* 1998; Hall & Henderson 2001; Hughen *et al.* 2004).

A second calibration correction is required for samples taken from the southern hemisphere due to atmospheric and oceanic currents that carry 'old' radiocarbon from ocean carbon reservoirs preferentially to the southern hemisphere, in which there is less land mass. This discrepancy was discovered by the paired radiocarbon dating of known tree-ring-age wood samples from the northern and southern hemispheres. As many as 40 radiocarbon years, dependent on time and geography, must be subtracted from a southern hemisphere result before it is calibrated to a calendar date (Vogel *et*

² In this thesis, historical dates are reported as AD, for example, AD 1823. Uncalibrated radiocarbon dates are reported as BP, for example, 200 BP. Calibrated radiocarbon dates are reported as cal AD, for example, 1750 cal AD.

al. 1993; Vogel & Van der Plicht 1993; McCormac *et al.* 1998; McCormac *et al.* 2004).

Publicly available radiocarbon calibration programs, including CALIB (<http://www.calib.qub.ac.uk>; Stuiver & Reimer 1993; Stuiver *et al.* 2005), and OxCal (<http://c14.arch.ox.ac.uk/oxcal.html>; Bronk Ramsey 1995, 2001), based on the IntCal calibration series dataset (<http://www.radiocarbon.org/IntCal04.htm>; Reimer *et al.* 2004), allow the user to correct for fractionation and marine and geographic considerations when deriving a calendar date from a radiocarbon age.

Lastly, it is extremely important for the archaeologist to have stratigraphic and conceptual control over the material being dated, especially when that material could be non-cultural, such as charcoal (*cf* Dean 1978); of course this stipulation also applies to all other chronometric techniques. Artefacts and ecofacts, especially the small seeds, bones and other annual-growth samples preferable for a precise radiocarbon result, can easily move between strata in an archaeological site. Charcoal samples, for example, must be correlated to an archaeological event, as opposed to an environmental event such as a brush fire. In addition, as demonstrated by Michael Schiffer for the southwest of the United States, the rate of wood decay in a climactic region at the time of site occupation is extremely important in interpreting archaeological radiocarbon dates (Schiffer 1986). In arid or semi-arid environments, where wood can preserve for hundreds of years after dying or falling from a tree, and in tropical environments, where secondary chemicals in some woods repel termites and fungus, 'old wood' is often incorporated into sites as structural features or collected as firewood.

It is the responsibility of the archaeologist to understand the limitations of radiocarbon dating due to material, environment, calibration, and site formation processes when interpreting calendar ages for samples analysed. Other evidence, such as historical events or cross-dated artefacts, sometimes can help to narrow a poorly resolved radiocarbon date. Stratigraphic data can be used to chronologically sort a series of radiocarbon dates. Application of a technique such as Bayesian statistics is also useful for ordering chronometric results. In Bayesian analysis, prior information, such as clear stratigraphic evidence, is incorporated into a statistical model that

calculates posterior information, such as the probable distribution of chronometrically determined dates (Buck *et al.* 1996; Buck 2001). Bayesian statistical modelling can be invaluable for archaeologists using radiocarbon to date sites of ages that fall in sections of the calibration curve strongly affected by Suess and de Vries wiggles. This will be demonstrated in this chapter with examples from late Moloko period stone-walled towns. BCal, a Bayesian radiocarbon calibration software program, also is available publicly (<http://bcal.shef.ac.uk>). In the remainder of this chapter, I discuss some of the limitations and applications of radiocarbon dating for the chronology of the late Moloko.

RADIOCARBON IN THE LATE MOLOKO

Although the time range of the late Moloko period, from about the mid-17th century to the mid-19th century, corresponds exactly to a section of the radiocarbon calibration curve with pronounced Suess and de Vries effects, archaeologists commonly apply radiocarbon dating as the preferred chronometric technique. This is due to several factors: early development; wide applicability; good precision; the prohibitive cost of other methods of archaeometric dating; and the presence of the Quaternary Dating Research Unit (QUADRU) at the Council for Scientific and Industrial Research (CSIR) in Pretoria, South Africa, which runs a radiocarbon facility charging reasonable fees for gas proportional counting in local currency. AMS measurement of the radioactive ¹⁴C isotope is the best radiocarbon option for the late Moloko, however. Remains of minute samples such as annual-growth seeds and grasses can be analysed directly by AMS, which has greater detection efficiency and thus requires a very short counting time for a statistically equally valid result. Equally, control over the archaeological context of small samples becomes acute. Unfortunately, there is no AMS laboratory on the African continent, and AMS fees abroad generally are unaffordable on local research grants. John Vogel and Annemarie Fuls, who both retired recently as scientists at the QUADRU facility, have often expressed frustration at the inability to properly date the period of the Late Iron Age stone-walled settlements (*cf* Vogel & Fuls 1999). Late Iron Age archaeologists therefore have relied and sometimes continue to rely on radiocarbon dating as the most practical way to obtain age estimates for important sites, such as Olifantspoort, Molokwane and

Table 3.1. Published radiocarbon dates on charcoal for late Moloko stone-walled sites.

Calibrated ages were obtained using the CALIB program (Stuiver & Reimer 1993; Stuiver *et al.* 2005) according to the 2004 southern hemisphere radiocarbon calibration curve (McCormac *et al.* 2004). The original radiocarbon date records for lab numbers marked with † are ranges and therefore not calibratable. 1σ age ranges are given; [relative area] is the amount of space occupied by each range under the calibration curve of probability distributions. Ranges marked with * are suspect due to impingement on the end of the calibration data set.

Lab Number	Provenience	Radiocarbon Date (BP)	1σ Calibrated Radiocarbon Age Ranges (cal AD) [relative area under calibration curve]			
<i>Olifantspoort 20/71</i>						
GrN-5304	Midden I 0-15 cm	105 ± 35	1708-1721	[0.11]	1862-1866	[0.02]
			1810-1837	[0.28]	1879-1925	[0.49]
			1847-1857	[0.07]	*1950-1953*	[0.03]
GrN-5305	Midden I 50-60 cm	180 ± 30	1673-1711	[0.28]	1797-1812	[0.11]
			1719-1741	[0.15]	1836-1881	[0.27]
			1774-1776	[0.02]	1923-1951*	[0.18]
GrN-5306	Midden I 90 cm	105 ± 25	1711-1719	[0.07]	1883-1923	[0.57]
			1812-1836	[0.32]	*1950-1953*	[0.04]
RL-186	Midden VI base	400 ± 110	1449-1636	[1.00]		
RL-187	Hut N	330 ± 90	1464-1471	[0.02]	1789-1791	[0.01]
			1476-1667	[0.97]		
† RL-188	Hut W	320-250	-		-	
RL-189	Hut Bk	250 ± 90	1514-1543	[0.08]	1837-1848	[0.03]
			1624-1709	[0.34]	1855-1879	[0.06]
			1720-1811	[0.40]	1924-1950*	[0.08]
† RL-190	Hut Bi	< 200	-		-	
† RL-191	Hut Aj	< 240	-		-	
RL-201	Midden XI base	510 ± 90	1329-1335	[0.02]	1589-1616	[0.12]
			1391-1504	[0.86]		

Kaditshwene. I hope to illustrate the inadequacy of this chronometric technique for the Late Iron Age with examples of radiocarbon dates from these sites.

Conventional radiocarbon calibration of late Moloko dates

Radiocarbon dates have been obtained from midden and hut floor charcoal samples from the BaTswana stone-walled town at Olifantspoort (Vogel 1971; Mason 1986: 68-69). At Molokwane, charcoal samples were taken from several sites in the *kgosing*, or central settlement unit, including: burial areas; *kgotla*, or meeting areas;

Table 3.1 (continued). Published radiocarbon dates on charcoal for late Moloko stone-walled sites.

Lab Number	Provenience	Radiocarbon Date (BP)	1σ Calibrated Radiocarbon Age Ranges (cal AD) [relative area under calibration curve]			
<i>Molokwane</i>						
Pta-7168	SEL 2.10 burial area	150 ± 35	1694-1726	[0.23]	1828-1893	[0.47]
			1806-1816	[0.08]	1919-1950*	[0.23]
Pta-7162	SEL 2.2 private chamber	110 ± 45	1700-1722	[0.16]	1878-1929	[0.44]
			1809-1838	[0.24]	*1950-1953*	[0.01]
			1845-1867	[0.15]		
Pta-5404	SEL 2.1 <i>kgotla</i>	280 ± 50	1514-1542	[0.15]	1739-1798	[0.38]
			1624-1674	[0.47]		
Pta-7171	SEL 2.1 <i>kgotla</i>	250 ± 50	1637-1684	[0.39]	1729-1803	[0.61]
Pta-5403	SEL 2.4 cattle enclosure	110 ± 45	1700-1722	[0.16]	1878-1929	[0.44]
			1809-1838	[0.24]	*1950-1953*	[0.01]
			1845-1867	[0.15]		
Pta-7172	SEL 2.4 cattle enclosure	240 ± 45	1645-1680	[0.32]	1731-1802	[0.68]
Pta-5398	SEL 2.4 cattle enclosure	160 ± 50	1680-1731	[0.31]	1827-1893	[0.40]
			1801-1817	[0.09]	1917-1951*	[0.20]
Pta-5394	SEL 2.8 cattle enclosure	300 ± 40	1511-1552	[0.36]	1621-1666	[0.53]
			1557-1573	[0.11]	1790-1790	[0.01]
Pta-7169	SEL 2.3 kitchen	100 ± 45	1705-1722	[0.12]	1878-1928	[0.45]
			1810-1838	[0.26]	*1950-1954*	[0.03]
			1846-1867	[0.14]		
Pta-7173	SEL 2.3 kitchen	150 ± 50	1690-1727	[0.24]	1827-1894	[0.42]
			1805-1818	[0.08]	1909-1951*	[0.26]
Pta-7176	SEL 2.3 kitchen	140 ± 40	1698-1723	[0.18]	1877-1903	[0.18]
			1808-1819	[0.08]	1905-1946	[0.27]
			1825-1839	[0.10]	*1951-1951*	[0.01]
			1843-1869	[0.18]		
Pta-3488	SEL 1 midden	180 ± 50	1672-1713	[0.23]	1796-1814	[0.10]
			1717-1744	[0.15]	1834-1891	[0.30]
			1757-1762	[0.02]	1922-1951*	[0.16]
			1771-1779	[0.04]		
Pta-3492	SEL 1 hut	170 ± 45	1676-1736	[0.35]	1829-1892	[0.37]
			1799-1815	[0.10]	1921-1951*	[0.18]

cattle enclosures; and kitchen areas. In an outlying settlement unit, charcoal samples were dated from a midden and a hut floor (Pistorius 1997). Stratigraphically layered charcoal samples from a *kgotla* midden in the *kgosing* and an outlying midden at Kaditshwene have been dated by radiocarbon. Two Kaditshwene house floors also

Table 3.1 (continued). Published radiocarbon dates on charcoal for late Moloko stone-walled sites.

Lab Number	Provenience	Radiocarbon Date (BP)	1σ Calibrated Radiocarbon Age Ranges (cal AD) [relative area under calibration curve]			
<i>Kadiitshwene</i>						
Pta-5293	KLF1.1 midden 10-20 cm	180 ± 20	1675-1706	[0.33]	1859-1861	[0.01]
			1721-1738	[0.17]	1867-1878	[0.11]
			1798-1810	[0.12]	1925-1950*	[0.19]
			1838-1846	[0.07]		
Pta-5870	KLF1.1 midden 50-60 cm	180 ± 45	1672-1712	[0.24]	1797-1813	[0.10]
			1718-1743	[0.15]	1835-1890	[0.31]
			1759-1761	[0.004]	1922-1951*	[0.16]
			1772-1778	[0.04]		
Pta-5296	KLF1.1 midden 100-110 cm	200 ± 20	1671-1688	[0.25]	1752-1782	[0.35]
			1728-1748	[0.28]	1796-1804	[0.13]
Pta-7039	KLF3.1 midden 20-30 cm	160 ± 50	1680-1731	[0.31]	1827-1893	[0.40]
			1801-1817	[0.09]	1917-1951*	[0.20]
Pta-7046	KLF3.1 midden 40-50 cm	220 ± 45	1649-1696	[0.32]	1949-1950*	[0.004]
			1725-1807	[0.67]		
Pta-7033	KLF3.1 midden 100-110 cm	200 ± 40	1665-1699	[0.23]	1867-1878	[0.05]
			1722-1809	[0.61]	1931-1939	[0.03]
			1838-1844	[0.03]	1942-1950*	[0.04]
Pta-7047	BLF1.1 house floor	120 ± 45	1699-1722	[0.17]	1878-1930	[0.42]
			1809-1838	[0.23]	1940-1941	[0.01]
			1845-1867	[0.16]	*1950-1952*	[0.01]
Pta-7035	BLF1.2 house floor	180 ± 45	1672-1712	[0.24]	1797-1813	[0.10]
			1718-1743	[0.15]	1835-1890	[0.31]
			1759-1761	[0.004]	1922-1951*	[0.16]
			1772-1778	[0.04]		

were dated (Boeyens 2000, 2003). Published radiocarbon ages for these three excavated stone-walled towns are presented in Table 3.1, recalibrated with the CALIB program (Stuiver & Reimer 1993; Stuiver *et al.* 2005) according to the 2004 southern hemisphere radiocarbon calibration curve (McCormac *et al.* 2004).

It is important to remember that the outcome of a radiocarbon date calibration is not an exact calendar date, but a range of statistically probable calendar dates that correspond to that radiocarbon age and its accompanying error figure. The error conventionally reported by the radiocarbon laboratory is the one-sigma (1 σ) range, or the 67th percentile. I think it is wiser, rather, to consider the two-sigma (2 σ) range, or 95th percentile, as including the appropriate calendar age, since mathematically, one in

every three 1σ calendar date ranges will be incorrect! Standard radiocarbon calibration programs report both 1σ and 2σ ranges.

With this limitation in mind, note that in Table 3.1, only the 1σ probable calendar date ranges resulting from the recalibrated radiocarbon ages are given. These are less valid, for the reasons given above, but unfortunately at 2σ , the calendar date calibration extends solidly between the late 16th and mid-20th centuries. This range is absolutely inadequate for resolving the historical time frame in which the late Moloko stone-walled sites were inhabited. This is due to the extensive wiggle in the radiocarbon calibration curve over the last 300 years (see Figure 3.3), caused especially by sun spot activity and the introduction of ‘old’ carbon to the atmosphere as a result of the burning of fossil fuels at the beginning of the Industrial Revolution.

As noted above, independent archaeological and historical evidence can highlight a smaller range within a radiocarbon calibration as being the more likely date. Consequently, the centuries-wide range for calibrated late Moloko period radiocarbon dates can be restricted somewhat by oral-historical evidence, as will be discussed in Chapter 4. The events of the *difaqane*, for example, are known to have begun in the third decade of the 19th century, at which time many of the stone-walled settlements were abandoned. Thus radiocarbon dates that extend beyond AD 1820-1840 to the modern-age (AD 1955) are spurious.

This preliminary assessment of late Moloko radiocarbon dates demonstrates that conventional calibration methods are not useful for this time period, however, an alternative radiocarbon calibration method using Bayesian statistics can help sort radiocarbon results.

BAYESIAN RADIOCARBON CALIBRATION AT OLIFANTSPOORT AND KADITSHWENE

A Bayesian radiocarbon calibration incorporates archaeological information, such as stratigraphy, into the statistical analysis. In this section, I recalibrate stratified



Figure 3.4. John Vogel, right, at a midden excavation at the site on Olifantspoort farm in October 1967, collecting material for radiocarbon age determination (Vogel 1971). OSL dating samples for this study were collected from a different section of this same large midden, as described in Chapter 6. Photograph courtesy QUADRU.

radiocarbon dates from middens at the stone-walled site on Olifantspoort farm and from Kaditshwene to show how Bayesian statistics can be a useful tool for interpreting radiocarbon dates from the 17th to 19th centuries. It is not possible to use Bayesian radiocarbon calibration for dates from Molokwane, because there are no published results from stratified contexts.

Revil Mason extensively radiocarbon dated many different features at Olifantspoort (see Table 3.1). John Vogel (Figure 3.4; 1970) obtained radiocarbon dates from charcoal at three depths in a large midden near the centre of the settlement. These are GrN-5304 (0-15 cm), GrN-5305 (50-60 cm) and GrN-5306 (90 cm). During excavations undertaken by UNISA at Kaditshwene, Jan Boeyens selected charcoal from three depths in the large midden located at the top end of the main *kgotla* for radiocarbon dating (Figure 3.5; Boeyens 2000). These samples are Pta-5293 (10-20 cm), Pta-5870 (50-60 cm) and Pta-5296 (100-110 cm).



Figure 3.5. The large midden of the main *kgotla* at Kaditshwene, from the south. OSL dating samples for this study were collected from a different section of this same large midden, as described in Chapter 6. Photograph courtesy Jan Boeyens.

Figure 3.6 shows the radiocarbon calibration results, as reported to 2σ by the CALIB 5.01 program, for both sample sets. The calibration curves for each radiocarbon date are given in the stratigraphic order in which they were recovered. According to the principles of stratigraphy, it is unlikely, if the samples were not ‘old wood,’ contaminated, inverted, or poorly excavated, that the lowermost sample from the stratigraphic section is younger than the uppermost. The radiocarbon results overlap almost completely at both sites, however, and the age range of all samples is once again unworkable and of little value for the archaeologist.

We know that none of the samples can date after around AD 1840, because both Olifantspoort and Kaditshwene were abandoned during the *difaqane*. One might be tempted to simply discount all of the calendar ages younger than AD 1840, but this is a mathematically invalid approach. In radiocarbon calibration, a radiocarbon age yields a range of possible calendar dates, and the most probable occupy a greater relative proportion of the area under the calibration curve, to a total of 1.0 (see the

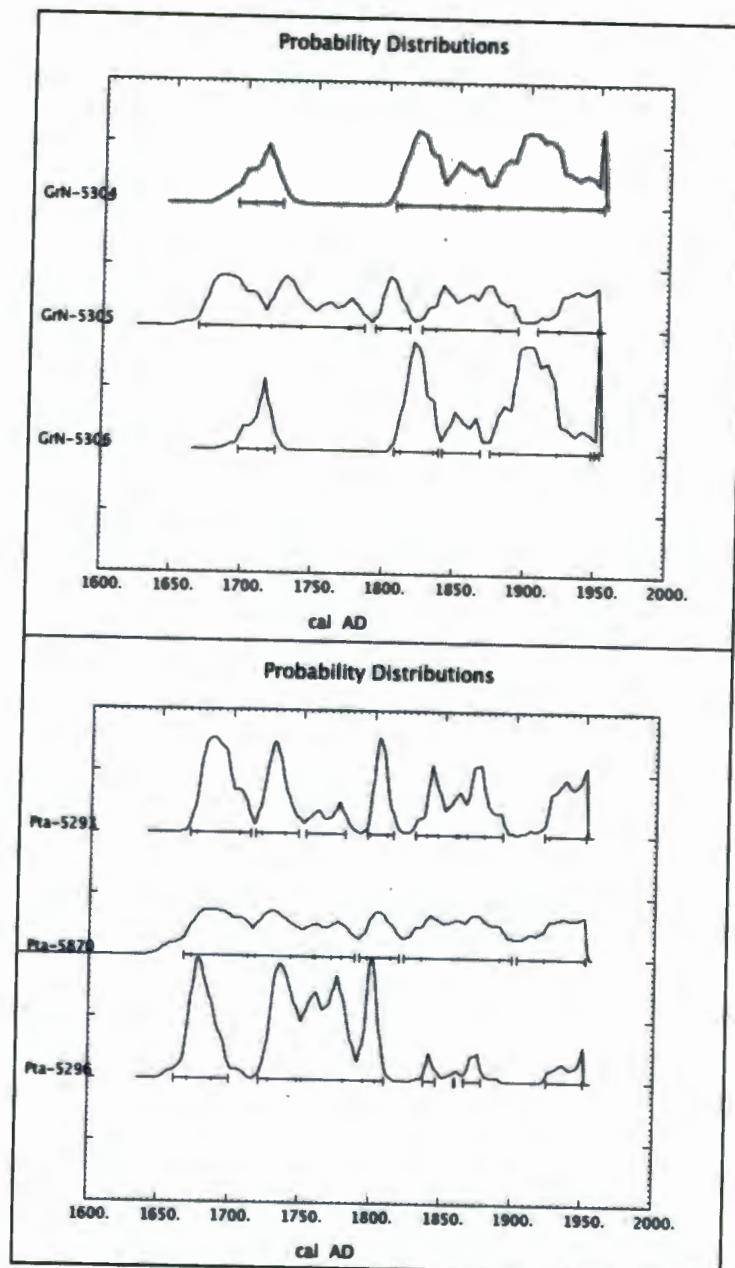


Figure 3.6. Radiocarbon date ranges for the middens at the site on Olifantspoort farm (above) and Kaditshwene (below). These results were calibrated with the Southern Hemisphere dataset (McCormac *et al.* 2004) of the CALIB 5.01 program (Stuiver & Reimer 1993), and the probability curves represent calculations made by traditional statistical methods, as presented in Table 3.1.

[relative probabilities] reported in Table 3.1 that correspond to the probability curves in Figure 3.6). In order to eliminate dates younger than *difaqane* age from the dataset, the entire calibration curve must be recalculated, so that the relative probabilities of calendar dates older than *difaqane* age are refigured and still total 1.0.

The statistical computations of conventional radiocarbon calibration cannot resolve these stratigraphic and boundary incongruities in dating, but the application of Bayesian statistics does help. Bayesian analysis is a model-based approach to statistics based on the 18th century contribution of Thomas Bayes, who suggested that in the process of data analysis, prior information can be incorporated with new data in the equation:

$$\text{posterior} \propto \text{likelihood} \times \text{prior}$$

Equation 3.1

where the **posterior** (result) is proportional to a relationship between the **likelihood** (probability of observing a value for data) and the **prior** (probability of those values occurring based on parameters known *before* obtaining the data) (see Buck *et al.* 1996; Buck 2001).

Traditional radiocarbon ages also are determined according to models of statistical probability. The dates in Table 3.1 are given with a relative area, or the area under a probability curve, such as those depicted in Figure 3.6, that corresponds to each calibrated date range. Bayesian radiocarbon calibration is simply an alternative statistical model for which archaeological contexts are an ideal application, because stratigraphic relationships are also chronological data. To apply the Bayesian approach to radiocarbon calibration, consider Equation 3.1. In archaeology, the **likelihood** is the radiocarbon age and error according to conventional radiocarbon calibration, and the **prior** is stratigraphic information on the ordering of archaeological events. Thus in a Bayesian radiocarbon calibration, the traditional calibration is adjusted to account for extra knowledge, for example, the probability that one sample collected above another is younger (high probability), or that late



Figure 3.7. A graphical representation of chronological information entered in the BCal calibration program. Alpha 1 and beta 1 represent boundaries. 'Midden' represents the group of radiocarbon results, ordered according to stratigraphy.

Moloko stone-walled towns were occupied in AD 1850, well after the *difaqane* (low probability).

BCal software, which uses the CALIB calibration dataset, allows the user to enter relative or absolute prior chronological information, or to use both. Figure 3.7 is a graphical representation of the data entered. The radiocarbon age results for the midden samples are entered as a group in relative stratigraphic order. Alpha 1 and beta 1 represent absolute time boundaries older and younger than the stratigraphically ordered group.

The Olifantspoort and Kaditshwene dates were calibrated according to the Southern Hemisphere dataset (McCormac *et al.* 2004) using two Bayesian methods for each dataset, and the date ranges are given in Table 3.2. A simple Bayesian calibration of only the ordered midden dates was performed for each. As explained earlier, the late 19th and early 20th century results are erroneous, because archaeological and historical evidence clearly indicate that the late Moloko sites were abandoned at the time of the *difaqane*, between 1820 and 1840.

Table 3.2. Bayesian calibrations for ordered radiocarbon data from the middens on Olifantspoort farm and at Kaditshwene.

Radiocarbon date results were calibrated in the BCal calibration program using the Southern Hemisphere dataset (McCormac *et al.* 2004) and prior information according to archaeological strata. Highest posterior density (HPD) regions, calculated at 95%, indicate the most likely calendar date ranges for each stratigraphic parameter.

Site; Ordered Group Label	Lab Number	¹⁴ C Date (BP)	Boundary (beta 1)	Parameter	HPD intervals (cal AD)	
Olifantspoort; Midden	GrN-5304	105 ± 35	no absolute prior information	0-15 cm	1811-1944	
	GrN-5305	180 ± 30		50-60 cm	1700-1742	1797-1939
	GrN-5306	105 ± 25		90 cm	1695-1725 1806-1869	1876-1922
Olifantspoort; Midden	GrN-5304	105 ± 35	normal distribution (mean = 120 ± 10 BP)	0-15 cm	1806-1852	
	GrN-5305	180 ± 30		50-60 cm	1716-1749 1751-1783	1795-1850
	GrN-5306	105 ± 25		90 cm	1695-1726	1804-1838
Kaditshwene; Midden	Pta-5293	180 ± 20	no absolute prior information	10-20 cm	1677-1713 1717-1782	1796-1816 1829-1891
	Pta-5870	180 ± 45		50-60 cm	1672-1820	1822-1863
	Pta-5296	200 ± 20		100-110 cm	1661-1703	1722-1807
Kaditshwene; Midden	Pta-5293	180 ± 20	exact year (127 BP; AD 1823)	10-20 cm	1721-1747 1752-1785	1793-1822
	Pta-5870	180 ± 45		50-60 cm	1680-1709	1720-1812
	Pta-5296	200 ± 20		100-110 cm	1666-1697 1725-1789	1791-1805

BCal can perform more complex calibrations that incorporate absolute prior chronological information as either a mean or an exact number. In the second calibration for the midden on Olifantspoort farm, the beta 1 boundary value is set to a normal distribution around AD 1830 ± 10 (120 ± 10 BP), to generally incorporate the years of the *difaqane*, since the year of abandonment of this site is unknown. Comparatively, oral-historical records reveal that Kaditshwene was abandoned in AD 1823 (Boeyens 2000, 2003), thus the beta 1 boundary in the second Kaditshwene calibration is set for that exact date.

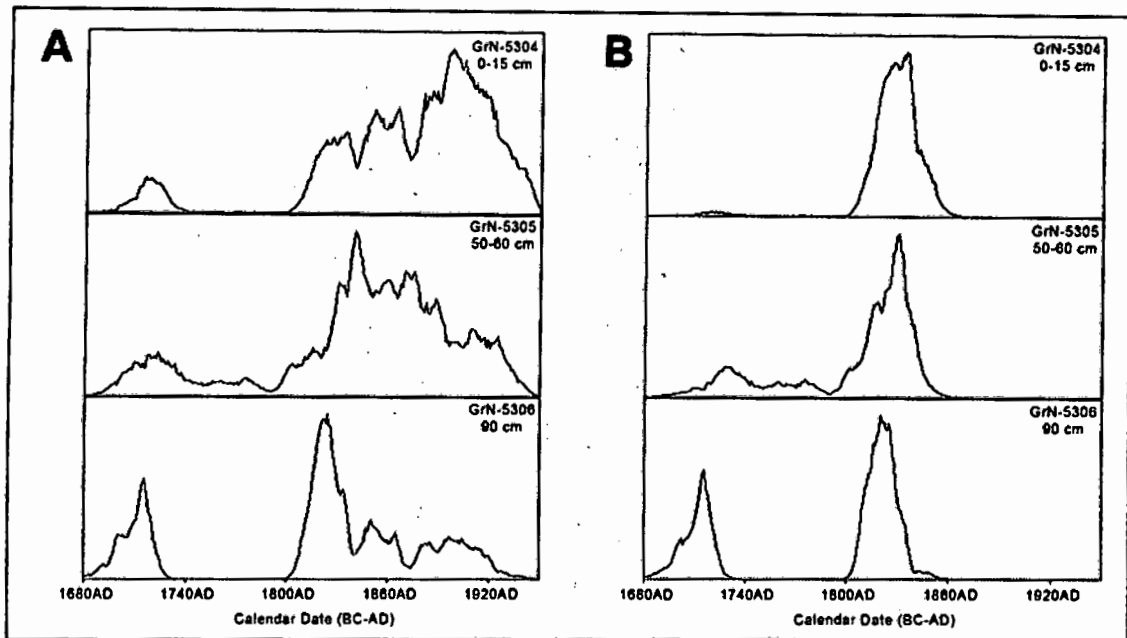


Figure 3.8. Probability curves for Bayesian radiocarbon calibration of dates from the midden on Olifantspoort farm, as presented in Table 3.2. Note in (a) how the input of prior stratigraphic information increases the probability that deeper samples yield older calendar dates. In (b) an upper chronological boundary (a normally distributed mean around AD 1830 \pm 10) was added to the stratigraphic results to incorporate another type of prior information - the abandonment event of the *difaqane*.

In basic terms, conventional radiocarbon calibrations translate a radiocarbon date directly into a range of calendar ages according to the probability that any given calendar age in that range is the correct result. To further refine a traditional calibration, Bayesian calibrations differentially weight those calendar ages according to archaeological evidence about stratigraphy. In order to appreciate the value of Bayesian radiocarbon calibration, an archaeologist must recognise that the results from traditional radiocarbon calibrations, such as those in Table 3.1 and Figure 3.6, also are probability curves. Bayesian analysis simply is an alternative statistical method available to calibrate radiocarbon ages; its validity is equal to that of conventional calibrations.

Figures 3.8 and 3.9 graphically represent the probability distributions of the two Bayesian calibrations for each late Moloko midden. In Figures 3.8a and 3.9a, stratigraphic information, the depths at which the samples were collected in the midden, was incorporated into the calibration, so that there is a high probability that

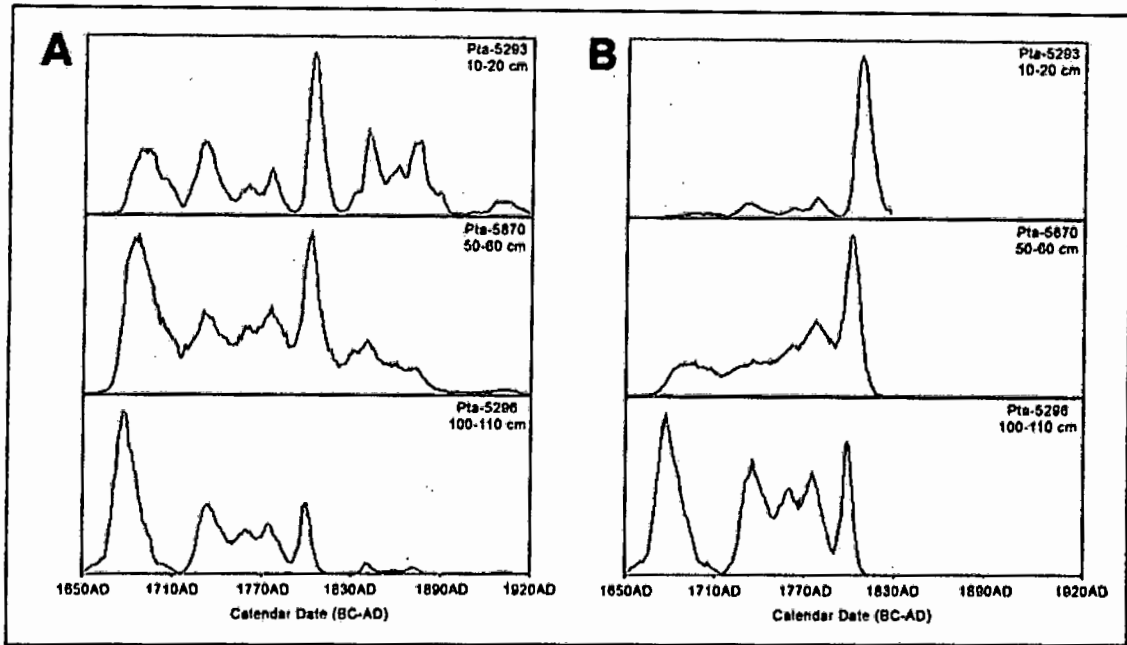


Figure 3.9. Probability curves for Bayesian radiocarbon calibration of dates from the midden at Kaditshwene, as presented in Table 3.2. Note in (a) how the input of prior stratigraphic information increases the probability that deeper samples yield older calendar dates. In (b), an upper chronological boundary (an exact date of AD 1823) was added to the stratigraphic results to incorporate another type of prior information - the abandonment event of the *difaqane*.

the shallowest sample is younger than the deepest sample. Compared to the results in Figure 3.6, there is a notable change in calibration results when these prior stratigraphic data are used in the analysis. The probability curves shift to the left as the samples get deeper, signifying the greater likelihood of an older age for the deepest sample.

Bounding the calibration according to the time of the *difaqane* further resolves the dates. To obtain the probability curves in Figures 3.8b and 3.9b, the date of site abandonment was incorporated into the calibration, so that there is a low probability that the sample is younger than AD 1830 ± 10 for Olifantspoort or AD 1823 for Kaditshwene. Accordingly, the probability curves are truncated at those dates, and they shift even further to the left as the samples get deeper, signifying the greater likelihood of an older age for the deepest sample.

Although the Bayesian outcomes are a great improvement compared to the centuries-long time span over which traditional radiocarbon calibrations range for these dates,

they still are not adequately precise for the late Moloko context. Ideally, for the relatively short-term historical processes that took place in the late Moloko, a generational time scale would be more appropriate in order to understand the chronology of settlement at the stone-walled towns, which underwent rapid population changes over a short period.

In some cases, the oral-historical record can be used effectively to achieve that type of resolution, as described in the following chapter. Those records are not available, or reliable, however, for every late Moloko settlement. With this example in mind, and, coupled with the essential nature of the technological questions discussed in Chapter 2 for understanding this era of BaTswana history, one of the major aims of this research was to apply a different chronometric technique, OSL dating, to the late Moloko context in an attempt to achieve better chronological control over this time period. This experiment, described in Chapters 5 and 6, included OSL sampling of these same two previously excavated middens, one at Olifantspoort and another at Kaditshwene. As indicated above, both have been dated by radiocarbon and this is obviously important in any assessment of the comparative value of alternative dating techniques.

Chapter 4

Dating Method Two:

The Oral-Historical Record

The aggregation of the Western BaTswana during the 18th and 19th centuries was a result of a complex interplay between historical and environmental events, including colonial encroachment and drought. Conflict between chiefdoms, pressure from population growth, periodic dry climate episodes and centralization of political power and cattle-wealth by rulers helped to effect the consolidation (Manson 1995).

Oral-historical records describe an intensification of inter-lineage conflict and competition over scarce natural resources. These records contextualize the archaeological evidence for changes in spatial organization, gender relations, and labour specialization, as evidenced in ceramic and metal production (Hall *et al.* 2006; Hall *et al.* 2007, 2008). Significant to this research, this 'oral geography' also can provide a chronology for the movement of BaTswana groups around the Rustenburg-Zeerust region during this time and for the appearance of these large towns.

There are two main sources for oral-historical information about the recent past in southern Africa. The first are diaries, travelogues and reports by early European missionaries and other travellers who ventured from the Cape into the interior beginning around AD 1800. Some travellers were helped by members of the groups encountered, and from those informants recorded testimony about migrations, genealogies and other aspects of local history. The descriptions and drawings in these records are useful for the interpretation of the corresponding archaeology. Further, the diaries often note the precise year and day on which travellers visited certain settlements, giving at least an earliest known date of occupation, though duration of occupation is more difficult to ascertain. These instances help establish chronological sequences for the archaeology. The travelogues are valuable for helping

Table 4.1. Comparing dating methods for late Moloko sites: radiocarbon dates calibrated with Bayesian statistics according to the beta 1 border of the *difaqane* and dates from the oral-historical record.

Bayesian-calibrated radiocarbon dates are reported to 2σ error.

Site	Radiocarbon date (BP)	Bayesian-calibrated radiocarbon date (cal AD)	Oral-historical date (AD)
Olifantspoort	105 ± 35 (GrN-5304)	1806-1852	18 th C to 1823-1838
	180 ± 30 (GrN-5305)	1716-1749 1751-1783 1795-1850	
	105 ± 35 (GrN-5306)	1695-1726 1804-1838	
Molokwane	See Table 3.1; calibrated dates range early 16 th - mid-20 th C		Mid-18 th C to 1828
Kaditshwene	180 ± 20 (Pta-5293)	1721-1747 1752-1785 1793-1822	About 1790 to 1823
	180 ± 45 (Pta-5870)	1680-1709 1720-1812	
	200 ± 20 (Pta-5296)	1666-1697 1725-1789 1791-1805	
	See Table 3.1; additional calibrated dates range late 17 th - mid-20 th C		
Marothodi	-	-	1800-1810 to 1823-1828

archaeologists to narrow wide radiocarbon date ranges for samples taken at a site and provide an important chronometric control over the initial exploration of new archaeometric methods.

In addition, exhaustive scholarly works by historians and anthropologists, compiling early traveller accounts with information from archival research, government documents, oral testimony, praise-songs and (sometimes) archaeology, can be good sources of chronology for archaeologists.

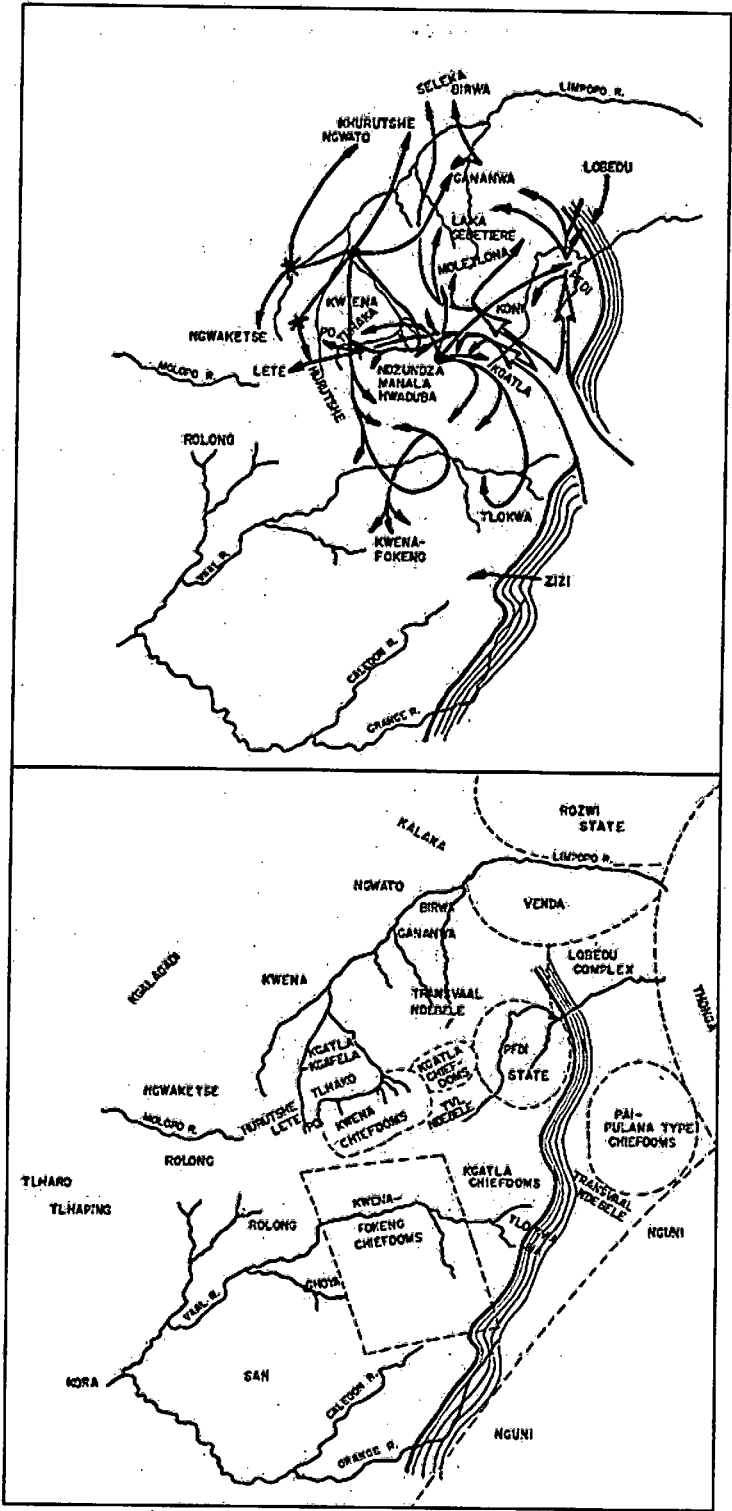


Figure 4.1. Above, dispersal of BaTswana and neighbouring BaSotho chiefdoms through the 16th - 18th centuries. Below, distribution of groups around AD 1800 (Legassick 1969: Figures 5 and 6).

ORAL-HISTORICAL DATING FOR THE LATE MOLOKO

It is fortunate that there were several early European travellers to the Rustenburg-Zeerust area and the wider BaTswana region whose writings can be explored for valuable information on the BaTswana and their way of life. For this thesis, the travelogues of John Campbell (1822aa; 1822b) and William Burchell (1824) have been most useful, but the accounts of Henry Lichtenstein (1812), Stephen Kay (1834), Robert Moffat (1842) and Henry Methuen (1846) also contain indispensable insights.

An oral-historical 'date' is based on either traveller chronicles or evidence from the historians and anthropologists who have studied the BaTswana in this region for more than half a century, establishing the dates and locations for lineages of chiefs, shifts in power and episodes of migration during this period of significant change in social and economic organization. Important early work includes that by Vivien Ellenberger (1939), Isaac Schapera (1942; 1953), Paul-Lenert Breutz (1953a; 1953b), and Martin Legassick (1969). The two maps presented in Figure 4.1 give some idea as to the complexity of the oral-historical sequence from the 16th to 18th centuries in the Rustenburg-Zeerust region and its surrounds. The oral records provide the general geography of ruling lineages in precolonial times.

The oral-historical dates for late Moloko stone-walled sites are presented in Table 4.1 with Bayesian-calibrated radiocarbon dates for comparison. These dates were determined from the research of the archaeologists who originally excavated the settlements and refined by recent syntheses of the oral-historical and archaeological records, particularly ceramic evidence (Manson 1995; Parsons 1995; Hall *et al.* 2007; Huffman 2007a; Hall *et al.* 2008).

Olifantspoort

The oral-historical record for Olifantspoort is the poorest of the late Moloko towns. There were no early travellers who visited this southern part of the Rustenburg area. The general identification of the inhabitants as BaKwena is secure (Mason 1986), but the sequence of settlement is much less so. The stone-walled site must have been

built in the 18th century and abandoned between AD 1823 and AD 1838 during the *difaqane*, but this is the best resolution currently available.

According to ceramic evidence, there is an early Moloko occupation on the hill stratigraphically below the stone walling (Huffman 2007b). This makes Olifantspoort an interesting case in the context of BaTswana aggregation. Did the people living there begin to build stone walls when the social, political and environmental climate became fragile; did a new group displace the earlier inhabitants at that time; or did the earlier inhabitants abandon the hill before the stone wall builders arrived? The chronology is clearly a key factor here, but the oral-historical record is not helpful in this regard.

Molokwane

Molokwane was occupied by the BaKwena ba Modimosana ba Mmatau from their arrival in the Rustenburg area until the *difaqane* (Breutz 1953a; Pistorius 1996, 1997). According to Pistorius (1997), the radiocarbon dates reported in Table 3.1 indicate the appearance of the Mmatau as early as the 17th century, although the oral-historical record does not place the group there before mid-18th century. It is possible that there is an earlier occupation at Molokwane, as at Olifantspoort, but it is also possible that the reliance on these earlier dates represent a misunderstanding of the radiocarbon calibration. Ceramic evidence supports the latter; none of the characteristic 17th century pottery types identified by Huffman (2002; 2007a) were recovered from the early deposits at Molokwane (Hall *et al.* 2007, 2008). This is an issue that must be addressed in future research on the settlement sequence at this site.

While some stone walls probably were erected at the beginning of occupation at Molokwane, it is more likely that the major period of building and site expansion, including the construction of the *kgosing* that remains today (see Figure 1.5), occurred during the rule of the very powerful and successful chief Kgaswane, from AD 1780-1828 (Hall *et al.* 2007, 2008). By potentially correlating the establishment of Molokwane and the influence of Kgaswane, better chronometric control of the sequence will influence the ceramic argument above.

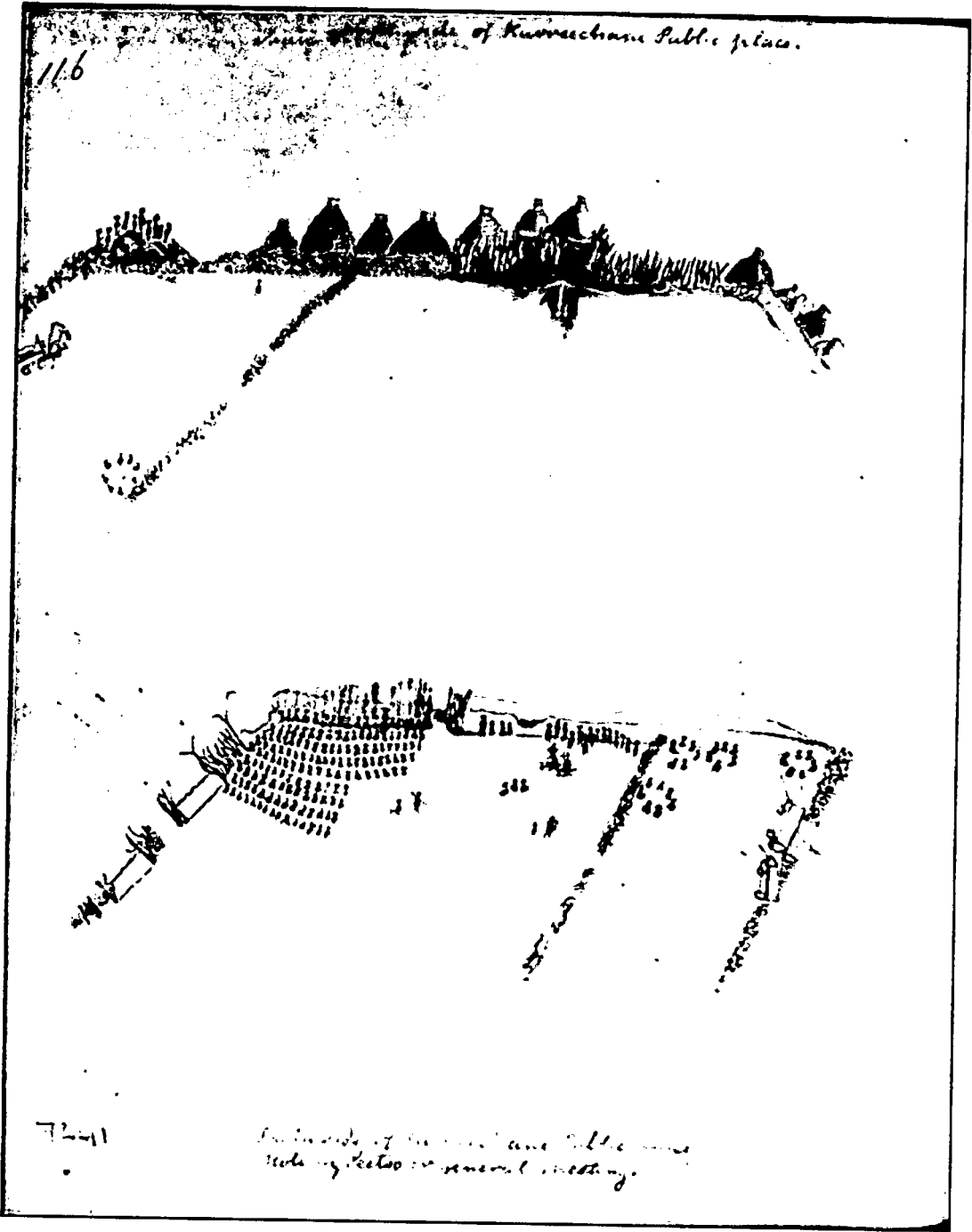


Figure 4.2. ‘Holding Peetso or general meeting;’ Campbell’s AD 1820 field sketch of the main *kgatla* in the *kgosing* of Kaditshwene. In the upper drawing, the ‘North side of Kurreechane Public Place,’ note the midden in the left corner (Campbell 1820b).

Kaditshwene

Kaditshwene was a late capital of the BaHurutshe booMenwe, one of two groups that formed when the followers of two brothers, Menwe and Manyane, splintered over right to succession in the middle of the 17th century. Oral traditions indicate that the BaHurutshe booMenwe had been living at Vergenoegd, about 10 km south of Zeerust, at the end of the 18th century. Their chief died and it is likely that the group moved their centre to the hill at Kaditshwene under the new leadership of Sebogodi. In AD 1823 during the strife of the *difaqane*, the Kololo, under Sebetwane, attacked the settlement and its inhabitants were forced to abandon it (Breutz 1953b; Boeyens 2000).

Kaditshwene is a unique example of an 'exact' oral-historical date, since John Campbell visited in AD 1820 and recorded some detailed information about the town and its inhabitants (Campbell 1822b: 222-277). For example, it is known that the chief died several years before Campbell's arrival, and that while waiting for the boy successor to come of age, the late chief's eldest brother, Diutlwileng, acted as regent (Campbell 1822b: 226-227).

Campbell also made field sketches, one of which is directly relevant to the archaeometric dating in this thesis. On 10 May 1820, Campbell observed what he called a 'peetso,' or general meeting, in the *kgosing* at Kaditshwene. In his depiction, Campbell detailed people standing on a large midden at the corner of the north side of the *kgotla*, the public gathering-place (Figure 4.2). Boeyens excavated this feature (Boeyens 2000), and the radiocarbon samples discussed in detail in Chapter 3 as well as an OSL sample discussed in Chapter 5 were collected from this midden. The midden obviously has a long chronology and it would be important to know what this is. The oral-historical record can provide precise dates by which to test chronometric methods.

Marothodi

The oral-historical records suggest that the BaTlokwa have their origins to the south and east of the central BaTswana region, perhaps indicating an Nguni lineage for this

group rather than classically western BaTswana (Hall *et al.* 2007; Huffman 2007b; Hall *et al.* 2008)

In the early 18th century, BaTlokwa ba ga Sedumedi occupied the area to the south of the Pilanesberg. AD 1780 marked the beginning of decades of struggle between the BaTlokwa and the BaFokeng, which lasted until the assassination of the BaFokeng chief around AD 1800. Shortly thereafter, the BaTlokwa established their capital at Marothodi, to the west of the Pilanesberg under Bogatsu, who was succeeded by his senior son Kgosi in about AD 1815.

Conflict continued throughout the time of settlement at Marothodi until about AD 1823, when the oral-historical records indicate that the BaTlokwa were attacked and removed from the town, either by the Kololo under Sebetwane in AD 1823 or the BaKgatlwa ba Mmatau under Motswasele in AD 1827 (Ellenberger 1939: 172-173; Breutz 1953a; Manson 1995; Hall *et al.* 2007, 2008).

EVALUATING ORAL-HISTORICAL DATES

Interpretation of the late Moloko stone-walled towns clearly is helped by the existence of the oral-historical record. Evidence from the oral geography can guide or even refine the archaeology. There are several concerns, however, some of which are addressed by Legassick (1969). For example, while abandonment dates are all well known, dates of original late Moloko settlement are imprecise. In this crucial period of BaTswana history, for which we are attempting to understand the chronology and duration of occupation, this ambiguity is inadequate. While there are some towns and groups about which a considerable amount has been written, for others there is relatively little. In addition, the record is often patchy and conflicting, and it is sometimes unclear which observations are quality information from primary sources and which are unsubstantiated, but perpetuated in the literature.

Of course, a final, crucial consideration is that even a concise, constructive oral-historical record is fallible and needs to be tested. It can be misleading by design, by

deliberate exaggeration according to the chronicler's agenda or by the informants' withholding of sensitive knowledge, or by default, through ignorance or by information lost or distorted as the generations pass. Uncritical archaeologists may fall prey to direct interpretation of the oral-historical record, and this is particularly disadvantageous in a research context in which we are trying to refine chronologies. Better dating of sequences, coupled with archaeological evidence, will potentially provide independent control over the oral geography and illuminate the contextual nature of its construction.

For this study, I investigated the applicability of OSL dating to the late Moloko context. Well controlled OSL dating can provide an opportunity to interrogate some of the chronologies and sequences claimed in the oral-historical record. The remainder of this thesis is devoted to describing OSL dating, reporting on OSL ages that were obtained for the four late Moloko stone-walled towns, and discussing the usefulness of OSL dating for the Late Iron Age.

Chapter 5

Dating Method Three:

Optically Stimulated Luminescence

There is great potential for use of optical dating in the Iron Age, and this research is among the first applications for this period in southern Africa. In order to adapt the technique, most commonly used in Stone Age archaeology, to relatively young and shallow archaeological sequences, there are several important factors to consider. In this chapter and the two following, I report on the method and findings of this pilot study using OSL to date the Late Iron Age. With a fundamental understanding of the technique and foresight in the field, OSL dating can be applied successfully to Late Iron Age contexts.

OPTICALLY STIMULATED LUMINESCENCE DATING IN SOUTHERN AFRICA

An OSL age indicates the last time a sample was exposed to levels of heat or light above a threshold value, and the technique is most straightforward on quartz grains from aeolian dune sands that have been buried for tens of thousands of years. Optical dating has been applied at archaeological sites in southern Africa only over the past decade; the cost of the optical dating, approximately four times or more than that of a conventional radiocarbon date and substantially more than that of an AMS date, is one reason for this.

Optical dating of old contexts in southern Africa

Among the first published luminescence ages for a southern African archaeological site are those on quartz sediment from relic sand dunes at sites around Dobe-toa, on the border of Botswana and Namibia in the northwest Kalahari Desert (Franklin & Hornyak 1990) and at a Middle to Late Stone Age site at White Paintings rock shelter

in the Tsodilo Hills, Botswana (Feathers 1997). Other early research occurred at the first test pit at Florisbad, near Bloemfontein, South Africa, where hominid remains were found (Grün *et al.* 1996). At Blombos Cave, on the southern Cape coast of South Africa, two deliberately engraved slabs of red ochre and 41 estuarine shell beads are dated by OSL, using individual quartz grains from dune sand and archaeological sediments, to 72.7 ± 3.1 ka. These artefacts are regarded as among the earliest evidence for modern human behaviour (Henshilwood *et al.* 2002; Jacobs *et al.* 2003a; Jacobs *et al.* 2003b; Henshilwood *et al.* 2004; Jacobs *et al.* 2006).

Luminescence studies on coastal Middle Stone Age archaeology in South Africa also include TL and OSL ages on quartz grains from Die Kelders on the southern Cape coast (Feathers & Bush 2000) and TL and OSL ages on quartz and feldspar grains from Klasies River Main Site on the south coast and Duinefontein on the west coast (Feathers 2002). Other OSL research in South Africa includes quartz ages from Sibudu Cave in KwaZulu-Natal (Wadley & Jacobs 2004, 2006), Rose Cottage Cave in the Free State (Woodborne & Vogel 1997; Pienaar 2005) and the open-air Sunnyside 1 Site, also in the Free State (Henderson *et al.* 2006). Currently, many luminescence projects are ongoing in South Africa, including further dating of Middle Stone Age sites, plus Later Stone Age sites and geological sites that can be used as indicators of the palaeoenvironment in which early modern humans were living.

Optical dating of young contexts in southern Africa

The coastal sediments of Middle Stone Age sites in southern Africa are ideal environments for optical dating, due to the aeolian nature of dune sands, discrete stratigraphy and long duration of burial. Samples for luminescence dating can be collected successfully from varied depositional environments, however, and there have been a few applications of optical dating on other types of samples at the younger end of the southern African sequence. In her PhD dissertation, Fumiko Ohinata worked with Edward Rhodes, then of the Research Laboratory for Archaeology and the History of Art (RLAHA), University of Oxford, to perform single-grain OSL dating on quartz extracted from burnt clay and stones from Iron Age smelting furnaces in Swaziland (Ohinata 2001). With meticulous sample collection coordinated between the excavator and the luminescence specialist, they achieved

high-precision OSL ages. Her early second millennium ages have errors of 160 years or less (as low as 40 years for some samples) and ages from the late 1700s and early 1800s have associated errors of 12 years or less (some as low as seven years). It is not known whether these results are at 1- or 2-sigma error intervals, but luminescence ages are typically reported with 1-sigma errors. The technical papers for this work are still forthcoming (Ohinata 2001). More recently, John Hobart, of the Pitt Rivers Museum at the University of Oxford, worked with Jean-Luc Schwenninger of RLAHA to obtain OSL dates on ceramics from Pitsaneng in Lesotho, a Later Stone Age herder-hunter-gatherer site (Hobart 2003, 2004); their methods and results are not yet published either (Hobart pers. comm. 2007).

These studies demonstrated the feasibility of OSL dating of younger archaeological samples, including ceramics and fired clay furnaces, from southern African sites. Other work in dating the very recent past with OSL includes research on young coastal dunes in the Netherlands, with success in obtaining accurate ages from 260 years to less than 10 years (Ballarini *et al.* 2003). The ages of sands deposited in recent tsunami events also have been measured accurately using optical dating (Huntley & Clague 1996; Banerjee *et al.* 2001). The applicability of optical dating to sediments from Iron Age midden deposits in South Africa still is not known, however, and is the focus of the chronometric aspect of my research.

In 2003, the UCT-UNISA excavation project started at the large stone-walled town on Vlakfontein farm, near the Pilanesberg in North West Province, South Africa. Using the oral-historical record, Jan Boeyens identified the site as that of Marothodi but at that early stage had not yet completed his exhaustive research. The archaeology clearly indicated a late Moloko association, and the oral geography suggested that the site was founded in the early 19th century and abandoned at the time of the *difaqane*. The exact dates of settlement and abandonment at the site were unknown. Charcoal and bone samples were collected with care during excavation, potentially for radiocarbon dating, but Simon Hall and his colleagues agreed that funds could be better spent in other ways. The poor chronological resolution of radiocarbon dating in this time period simply did not justify the expenditure when the oral-historical records were so promising.

Of course, every archaeologist hopes to have a secure archaeometric technique with which to successfully date a site, in this case, as a scientific 'check' on the oral-historical record. For late Moloko sites, there are very few useful and affordable options, and no chronometric technique besides radiocarbon has ever been applied to this context. In late 2003, Zenobia Jacobs, an archaeologist specializing in OSL dating and, at that time, a scientist in the QUADRU laboratory at the CSIR in Pretoria, agreed to help me undertake a pilot study in OSL dating of the late Moloko.

Thus this research is an investigation of two important concerns. The main goal is to understand the chronology of the late Moloko stone-walled towns, including verification of the oral-historical dates Boeyens has determined since for Marothodi. The oral-historical records describing events and genealogy at Kaditshwene, Marothodi and to some extent, Molokwane, offer a unique opportunity to compare results from the OSL dating technique to known historical ages.

Secondly, this study is a test of the appropriateness of OSL dating of quartz grains extracted from Iron Age midden and furnace features. It also, indirectly, is an assessment of the accuracy of OSL dating for the very recent past, on a scale of hundreds, rather than thousands or tens of thousands, of years. Because the dates for some late Moloko sites are known from the oral-historical record, they provide an independent verification for the accuracy of the OSL dates. The results of this research will indicate the feasibility of applying this chronometric technique to other southern African sites occupied during time periods with acute Suess and de Vries effects in the radiocarbon calibration curve.

CONSIDERATIONS FOR OPTICALLY STIMULATED LUMINESCENCE DATING

The earliest luminescence dating was thermoluminescence (TL) dating. A measurement of TL from a sediment or ceramic or stone artefact provides an estimate of the length of time since it was last heated to an approximate temperature greater than 300°C for slow-fired material or 500°C for quick-fired material. Farrington

Daniels and colleagues first suggested the technique could be applicable to dating in 1953 after measuring TL, energy stimulated by heat and emitted as light, from minerals, clays and rocks exposed to x-rays or radioactivity (Daniels *et al.* 1953). Martin Aitken and his students developed the use of TL for dating archaeological materials, including ceramics and burnt stone, in subsequent studies (Aitken *et al.* 1964; Aitken *et al.* 1968).

Huntley and colleagues introduced optical dating of sediments from South Australia in 1985 (Huntley *et al.* 1985), and OSL is now preferred over TL for sediment dating. Although OSL measures light emission from the sample after optical stimulation, rather than thermal, the fundamental principles of the two methods are the same. Each technique frees trapped electron charge from the crystal lattice of a mineral as light that is measurable in a controlled laboratory setting.

Martin Aitken published the first comprehensive text on luminescence dating (Aitken 1985), and the basic principles of the method also can be found in a number of more recent references (*cf* Aitken 1997; Aitken 1998; Grün 2001; Bøtter-Jensen *et al.* 2003; Feathers 2003; Duller 2004). The explanation of optical dating that follows is drawn from these basic references. In addition, the journals *Radiation Measurements* and *Quaternary Science Reviews* regularly publish new research, methods and applications, as well as the proceedings of the *International Conference on Luminescence and Electron-Spin Resonance Dating* that meets every three years.

Principles of optical dating

Luminescence dating is possible because common minerals, such as quartz and feldspar, absorb naturally occurring external energy in the form of alpha, beta, gamma and cosmic ionizing radiation. Although there are many minerals that absorb radiation and emit luminescence, the physical basis of signal production in quartz is the best understood (*eg* Bøtter-Jensen *et al.* 2003). The trapped-charge population in quartz grains accumulates in a measurable and predictable way, such that a quartz grain has its own internal energy ‘clock.’ Thus quartz is preferred for luminescence dating and was the mineral measured in this OSL study.

The ionizing radiation in the environment surrounding the quartz grain deposits extra energy in the crystal. Ionizing radiation creates free charge carriers (electrons or holes) that are trapped in crystalline defects that occur naturally in the quartz structural lattice. If an individual quartz grain is exposed to sunlight or heat during its continual lifecycle of erosion, transport and deposition, then the stored electron energy is released, in effect resetting the dating clock of that material by zeroing or 'bleaching' the grain. For sediment in nature, this can occur from exposure to sunlight or possibly a sustained veld fire. Human behaviour, such as the firing of ceramics, bricks, clay-lined hearths or lithics knapped from cryptocrystalline silicates, also will discharge the luminescence signal. Ideal OSL samples are quartz grains that were fully bleached, then deposited, buried and subsequently never exposed to heat or light. This can occur from natural burial, such as in the development of sedimentary layers, or in deposits accumulated by human activity. In addition, humans can build sediment into structural walls, bricks or thick-walled ceramics so that interior crystals are no longer exposed to sunlight or heat.

Upon deposition and burial, the bleached grains are hidden from light; the luminescence clock begins ticking as the energy stored increases through time. The rate of increase is determined by the rate of ionising radiation to which the quartz grain is exposed. Thus, in absorbing ionizing radiation and releasing trapped energy, each crystal is a potential chronometer. To obtain the depositional age of buried sediments, a sample is collected and processed in the dark because as indicated, exposure to light will lead to zeroing of the luminescence signal.

If the rate of radiation uptake over time can be determined and the amount of energy released can be measured, one can establish the length of time since a crystal was last reset. The age equation for luminescence dating is deceptively simple:

$$\text{age estimate (ka)} = \frac{\text{equivalent dose (Gy)}}{\text{estimated dose rate (Gy/ka)}}$$

Equation 5.1

where the **equivalent dose**, measured in Grays (the SI unit measuring the absorption of radiation energy by matter), is divided by the **estimated dose rate**, or average absorbed radiation in Grays per thousand years.

The luminescence age equation, however, actually is a complex calculation with many parameters consisting of both measured and estimated values. The equivalent dose (D_e), also called the paleodose, is the amount of dose generated by a controlled radioactive source in the laboratory that equals the amount in the sample when it was collected. It represents the total dose that the sample absorbed since it was last reset and is dependant on the luminescence sensitivity of the sample. The estimated dose rate, or annual dose, is the rate at which a sample absorbed radiation energy while it was buried and can be estimated by measurement in the field and in the laboratory.

Understanding and measuring equivalent dose

In the laboratory, the electrons trapped in the crystalline lattice of the quartz mineral can be released by stimulating the grain with a light source, causing luminescence that is measurable with specialized equipment. For this study, all luminescence measurements were carried out with an automated Risø TL/OSL reader (Bøtter-Jensen *et al.* 2000). The Risø reader has seven main components (Figure 5.1a-g). A removable, rotating carousel (a) holds up to 48 sample discs (b), where each disc represents a single aliquot, or division, of the sediment sample. This is placed inside the instrument chamber. Each aliquot can be individually beta-irradiated by a $^{90}\text{Sr}/^{90}\text{Y}$ source through a beryllium window (c). Thermal stimulation is by a heat source (d) up to 700°C, and optical stimulation is by blue light emitting diodes (LEDs) at 470 nm wavelength (e) or infrared LEDs at 875 nm wavelength (f). A photomultiplier tube measures luminescence through a detection filter (g). The luminescence scientist programs specialized computer software to run a unique measurement sequence on each aliquot in turn, such as in the measurement cycle of the single aliquot regenerative-dose (SAR) protocol (Murray & Wintle 2000) outlined in Table 5.1.

OSL, by definition, is the result of the release of electrons trapped in the crystal lattice of a quartz grain due to light exposure. Under conditions of constant stimulation, the

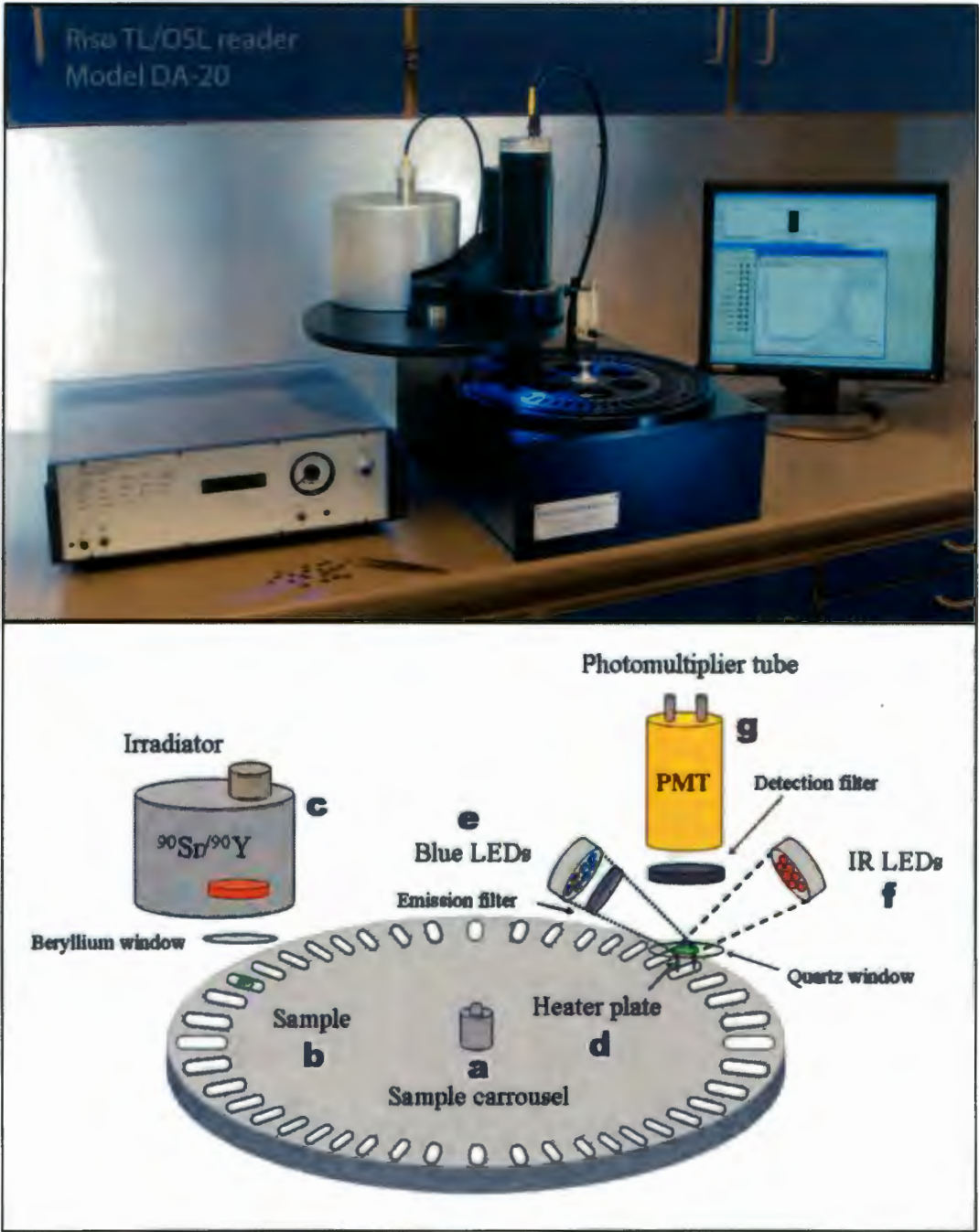


Figure 5.1. A photograph and schematic of the Risø TL/OSL reader (modified from Risø DTU February 2008: cover, 2)

release of luminescence from quartz grains in the Risø reader results in a characteristic OSL decay curve, the natural OSL signal (L_N). This measured natural luminescence is proportional to the number of trapped electrons accumulated since the last time the traps were emptied and therefore proportional to the last time the

Table 5.1. Typical measurement cycle D_e determination for late Moloko sample aliquots using the single aliquot regenerative dose (SAR) protocol (Murray & Wintle 2000).

Step	Principle
<i>Run 1 – Run 5</i>	
1. Beta dose Run 1 = (no dose), Run 2 = 2 s, Run 3 = 1 s, Run 4 = 5 s, Run 5 = 10 s	No dose for measuring natural luminescence in Run 1, then four regenerative doses bracketing expected D_e estimate
2. Preheat to 240° C, hold for 10 s; record TL glow curve	Removes unstable electrons and transfers charge from optically insensitive traps to sensitive ones
3. Measure OSL under blue LEDs at 125° C for 40 s; record OSL decay curve	Measures natural intensity (L_N) or regenerative intensities (L_X)
4. 2 s beta test dose	Fixed test dose (T_D)
5. Cutheat to 160° C for 0 s; record TL glow curve	Quick heat minimizes sensitivity change
6. Measure OSL under blue LEDs at 125° C for 40 s; record OSL decay curve	Measures luminescence intensities after test dose (T_N or T_X) to determine sensitivity
<i>Run 6</i>	
7. 0 s beta dose; repeat steps 2-6.	Monitors recuperation of signal
<i>Run 7</i>	
8. 2 s beta regenerative dose; repeat steps 2-6	Recycling ratio test; repeated regenerative dose to determine effectiveness of sensitivity correction
<i>Run 8</i>	
9. 2 s beta regenerative dose; measure OSL under IR diodes at 50° C for 100 s	Record OSL decay curve (L_X) to determine presence of feldspars
<i>Run 9</i>	
10. Repeat steps 2-6	OSL IR depletion ratio test; comparison of luminescence intensities before and after IR stimulation

grains were exposed to heat or light. The OSL reader records the luminescence counts per second over time as the grains are exposed to LEDs. It produces a decay curve for each aliquot that is essentially a graphical representation of sample bleaching inside the instrument. The shape of the curve reflects the sharp decrease in the number of luminescence counts after only a few seconds due to the rapid depletion of trapped electrons at first exposure (Figure 5.2).

The equivalent dose (D_e) is the amount of artificial laboratory beta radiation required to produce a luminescence signal in a sample that matches its L_N . The D_e is

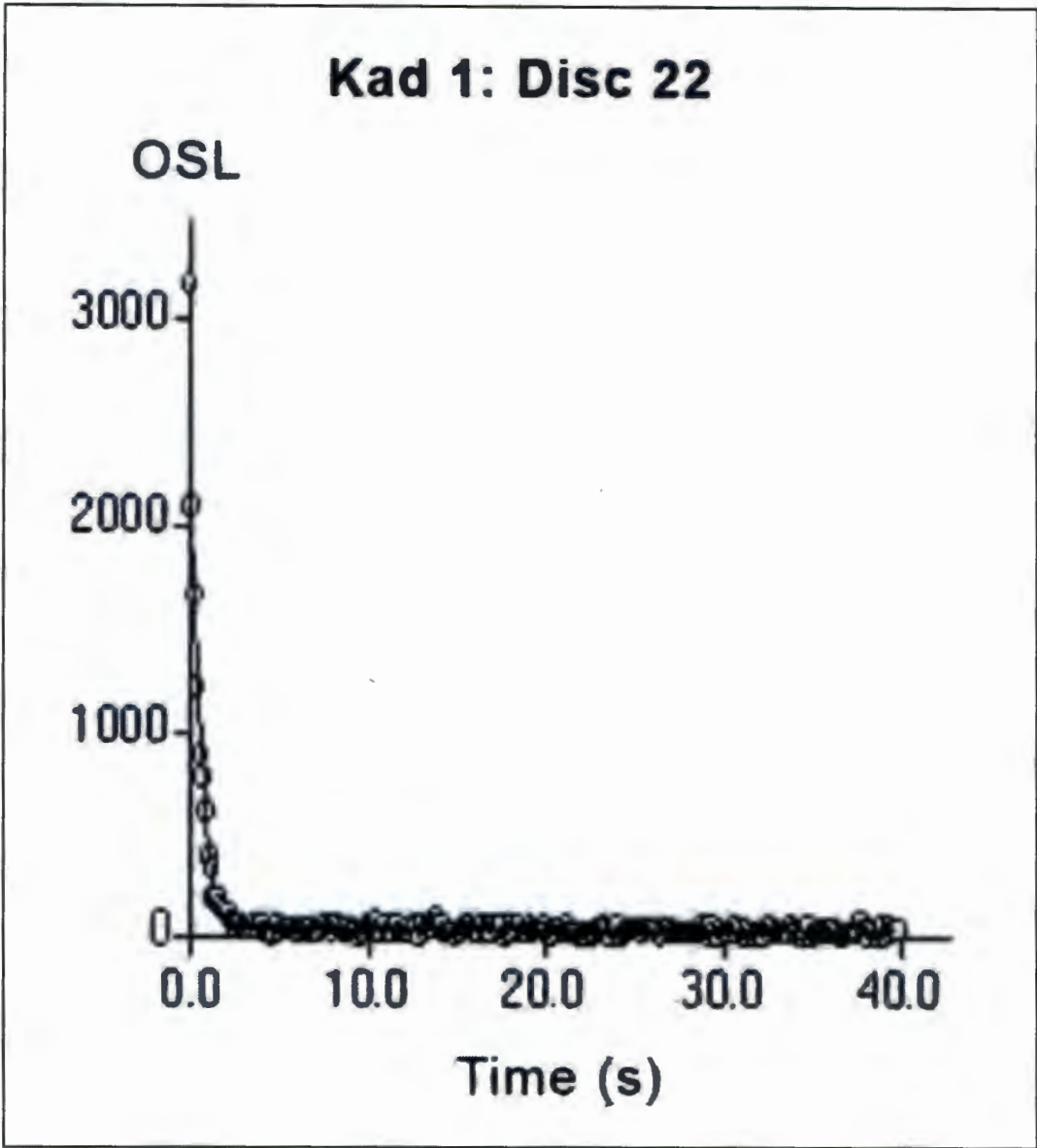


Figure 5.2. A typical decay curve for an aliquot from sample Kad 1, representing the number of OSL counts per second during exposure to blue LEDs. The shape of the curve reflects the rapid depletion of trapped electrons at first exposure.

determined by comparing the L_N to the OSL signals regenerated (L_X) after a range of beta doses are applied to the sample. The resulting plot, a dose response curve, shows the relationship between the natural luminescence measured and the dose administered. D_e is estimated by projecting the natural signal onto the dose response curve (Figure 5.3 and Table 5.2).

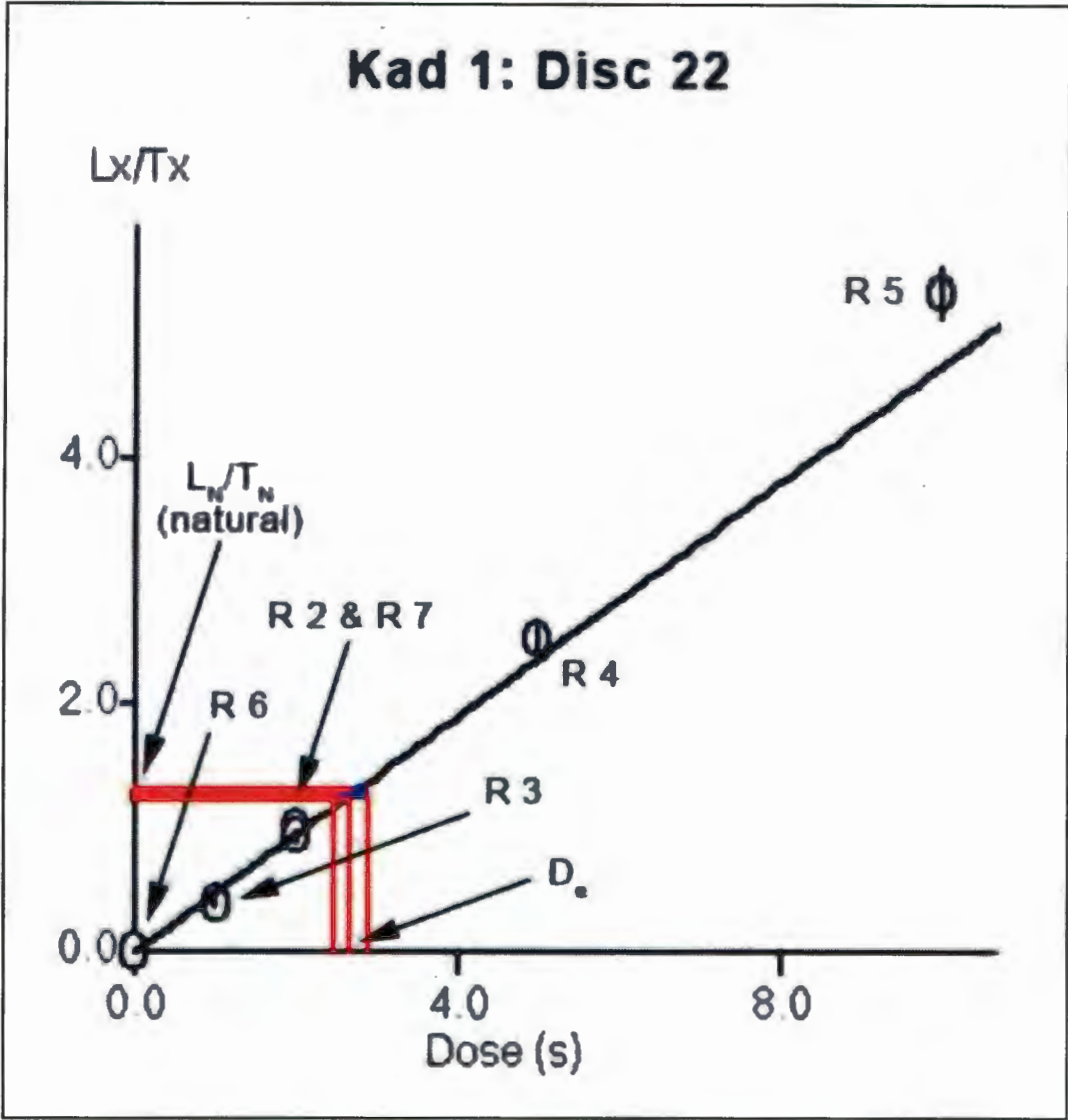


Figure 5.3. A dose response curve for one aliquot of sample Kad 1. R 2 - R 7 refer to Run numbers as described on Table 5.1. $D_e = 2.7 \pm 0.2$ Gy. The recycling ratio for this aliquot, calculated by comparing the OSL signals from Run 2 and Run 7, is 0.95 ± 0.06 . For every aliquot measured successfully, the D_e determined from its dose response curve is plotted on a radial diagram, as in Figures 6.14 - 6.17, to determine the mean D_e for the sample.

An important consideration for optical dating is controlling for the difference in the OSL sensitivity of quartz grains that have naturally accrued radiation over hundreds of years compared to the OSL sensitivity of those grains with only a few seconds of dose in the laboratory. These are changes in luminescence sensitivity that occur as a result of laboratory procedures (Wintle & Murray 1999). This issue was addressed in

Table 5.2. The OSL measurements used to build the dose response curve for one aliquot (Disc 22) of sample Kad 1, as shown in Figure 5.3, using the single aliquot regenerative dose (SAR) protocol (see Table 5.1; Murray & Wintle 2000). The dose is administered in seconds (1 Gy per s). L_X/T_X is a measurement of OSL intensity.

Run	Dose (s)	L_X/T_X
1	0 (natural)	1.275 ± 0.054
2	2	0.986 ± 0.042
3	1	0.384 ± 0.019
4	5	2.543 ± 0.101
5	10	5.345 ± 0.208
6	0	0.006 ± 0.003
7	2	0.989 ± 0.042

the SAR protocol {see Table 5.1; Murray, 2000 #264}, in which sensitivity change in the production of a dose response curve is monitored and compensated for during OSL measurement. Using the SAR protocol, D_e can be determined with greater precision and accuracy.

In optical dating, the natural OSL intensity (L_N) of each aliquot is measured first, followed by repeated OSL measurements at different beta regenerative dose rates (L_X), as shown in Table 5.1, steps 1-3. (The given beta doses for the late Moloko samples are very low because the estimated age is so young as compared to Middle Stone Age samples, where the given beta dose might be as high as 250 Gy.) In theory, the D_e is the average dose at which the natural luminescence intensity matches the regenerated luminescence intensity, except that this does not account for the known sensitivity changes in quartz due to laboratory radiation.

The improvement made in the SAR protocol was to add a test dose (T_D ; step 4), followed by a cut heat that removes spurious OSL signals (step 5) and a second OSL measurement (step 6). In the SAR protocol, the D_e calculation is a ratio of the OSL measurements of the natural signal before and after the first test dose (L_N/T_N) to the OSL measurements of intensity after regeneration doses and subsequent test doses that equalize sensitivity change (L_X/T_X). The background signal is subtracted, and the result is represented as a dose response curve, which shows the sensitivity corrected

L_X/T_X ratio for each regenerative dose. To obtain the D_e for an aliquot, its corrected L_N/T_N (the natural intensity) is plotted against its dose response curve (see Figure 5.3). The sample D_e is the mean of all of the aliquot D_e determinations.

The SAR protocol also includes several internal tests for sensitivity and contamination that demonstrate the reliability of the derived equivalent dose values (Murray & Wintle 2003; Wintle & Murray 2006), developed in part for high-precision OSL measurements of sediments at Blombos Cave, South Africa (Jacobs *et al.* 2003b; Jacobs *et al.* 2006).

In the SAR protocol, a dose recovery test is performed before measuring an OSL sample (Murray & Wintle 2003; Wintle & Murray 2006). The dose recovery test investigates the ability of the newly bleached quartz grains in that sample to accurately reflect the known laboratory doses applied in subsequent OSL measurement. For the late Moloko samples, one aliquot of the sample was bleached completely by 100 s of blue LED exposure, then reradiated with alternating 2, 5 and 10 s beta regeneration doses and measured for OSL by SAR as in steps 2-10 in Table 5.1. If the zeroed sample cannot recover the known laboratory dose, it is improbable that the sample will give an accurate D_e in a dating experiment. Thus the dose recovery is a test of reliability of the SAR protocol and therefore of the reliability of a date measurement on that sample.

Another sensitivity test in the SAR protocol is to examine OSL response according to preheat temperature. For this, the sample is preheated in a stepwise fashion in step 2, increasing by 20° C for every three aliquots in a 24 aliquot measurement, instead of at a constant temperature as described in Table 5.1. Changes in luminescence sensitivity as a function of preheat temperature can be revealed through OSL measurement of the natural signal before and after a test dose (T_X/T_N) and through D_e determination. In Figure 5.4, T_X/T_N clearly shows a large sensitivity change at higher preheat temperatures, likely due to the young age of the sample. The corresponding plot of D_e according to preheat temperature, a 'preheat plateau,' shows that D_e remained similar at preheat temperatures from 180-280° C. Because of these data from the preliminary dating runs of the late Moloko samples, we chose a constant preheat of 260° C for the final dating measurements in this study

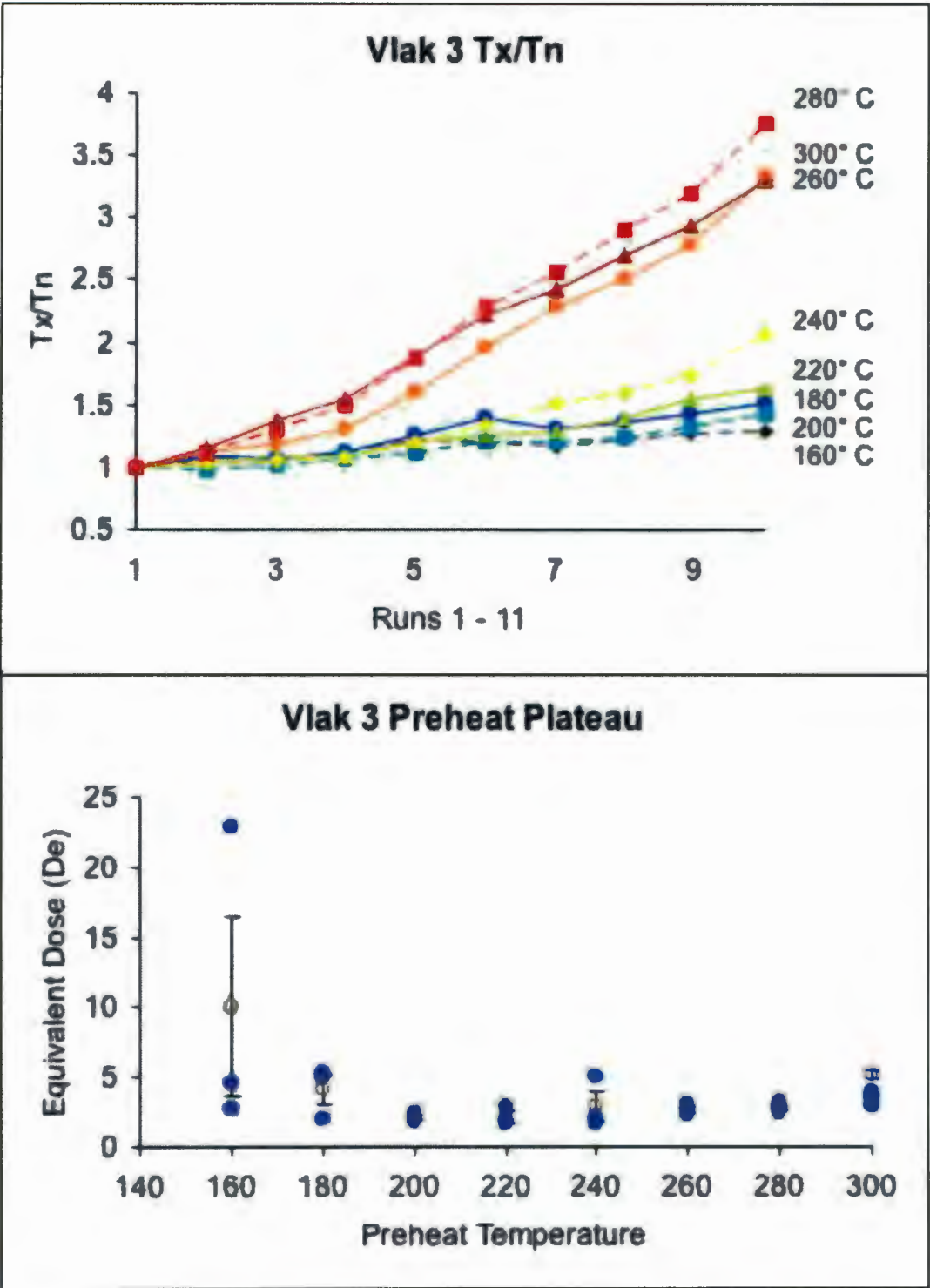


Figure 5.4. Sensitivity tests according to preheat temperature in the SAR protocol. Above, comparing the OSL measurement after the test dose T_X/T_N over 11 runs of different regenerative doses. Below, the change in D_e .

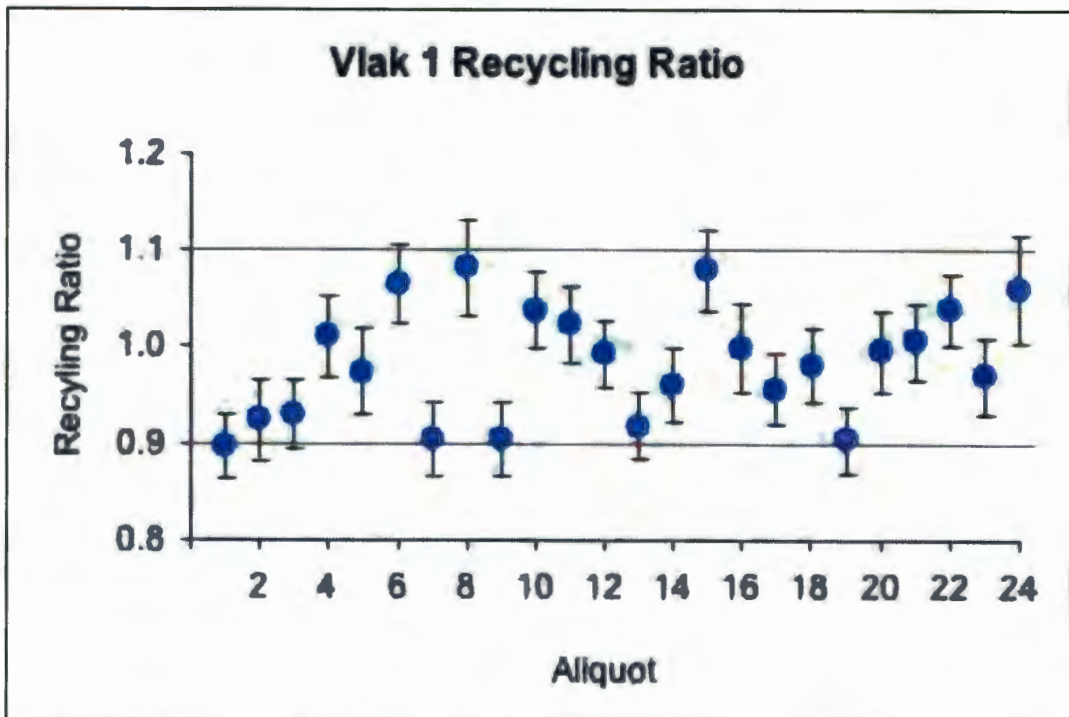


Figure 5.5. Recycling ratio test. An aliquot fails the test if the ratio of L_x/T_x from Run 7 to L_x/T_x from Run 2 is not within 10% error around unity, or 1.0. Here, aliquots 1, 7, 9 and 19 fail the recycling ratio test.

In addition, there are two tests of the reliability of the D_e result within the SAR measurement cycle. The recycling ratio (RR) test, Run 7, is a repetition of Run 2, the first regenerative dose point in the measurement cycle (Murray & Wintle 2000). The recycling runs are placed at the end of the experiment sequence because sensitivity change in quartz is more rapid at the beginning of measurement than at the end. If using the test dose OSL measurements to correct for sensitivity changes in the grains during measurement has been successful, then a ratio of L_x/T_x from Run 7 to L_x/T_x from Run 2 should be at unity, or 1.0. Murray and Wintle allow for 10% error around unity ($0.9 \leq RR \leq 1.1$) before rejecting aliquots due to failure of the recycling ratio test (Figure 5.5.).

Finally it is imperative to test aliquots for presence of feldspar grains remaining among the quartz, which occurs even though the pre-treatment of samples is so rigorous (see Chapter 6 for a description of sample pre-treatment for this project). Feldspar grain contamination is a major cause of scatter and imprecision in optical

dating of quartz for several reasons. Feldspar characteristically has a bright luminescence that can overwhelm the weaker quartz signal during measurement. Also, while quartz has a simple crystalline structure (SiO_2), feldspar has a much more complex structure ($\text{XAl}_{1-2}\text{Si}_{3-2}\text{O}_8$, where X can be K, Na or Ca). The potassium content will increase the internal beta dose in K-feldspars relative to quartz grains of similar size, increasing the annual dose rate of a sample and causing age underestimation. In addition, feldspar exhibits anomalous fading, in which electrons are released from defect sites through electrical conduction while the grains are still buried and absorbing natural radiation (Wintle 1973). This 'leakage' of electrons is due to quantum tunneling, a phenomenon in which a subatomic particle violates the laws of physics by penetrating a barrier stronger than the kinetic energy contained in that particle. Anomalous fading means that the sample loses dose (potential luminescence) over time, decreasing measured D_e and underestimating the age. Finally, it has been shown that single grains from the same feldspar sample can have different fading properties, further complicating a date measurement (Aitken 1998). Thus while it is not necessary to avoid feldspar dating altogether, anomalous fading must be accounted for in the luminescence measurement. For quartz aliquots, it is crucial to test for feldspar contamination.

The SAR protocol includes a test for the presence of feldspar grains on each sample aliquot. Feldspar has a bright luminescence under blue LED stimulation and a distinctive luminescence under infrared (IR) stimulation, but quartz has very weak or no luminescence under IR stimulation (Godfrey-Smith & Cada 1996). In the SAR protocol, these properties are exploited to detect feldspar contamination. Runs 8 and 9 in Table 5.1 constitute the OSL IR depletion ratio test (Duller 2003). The OSL measurement L_X/T_X from Run 9 is compared to that from Run 7, the difference being stimulation by IR diodes in Run 8. If feldspar is present on the aliquot, it will produce a signal during the IR exposure, effectively bleaching the feldspar grains. Then, the OSL ratio L_X/T_X from Run 9, a normal SAR measurement after blue LED exposure, will be reduced, because the zeroed feldspar will not produce a signal. As with the recycling ratio, the ratio of L_X/T_X from Run 9 to L_X/T_X from Run 7 should be unity, or 1.0. An aliquot fails the OSL IR depletion ratio test if it does not reach unity within two standard deviations of the error of its Run 9 / Run 7 intensity ratio (Figure 5.6).

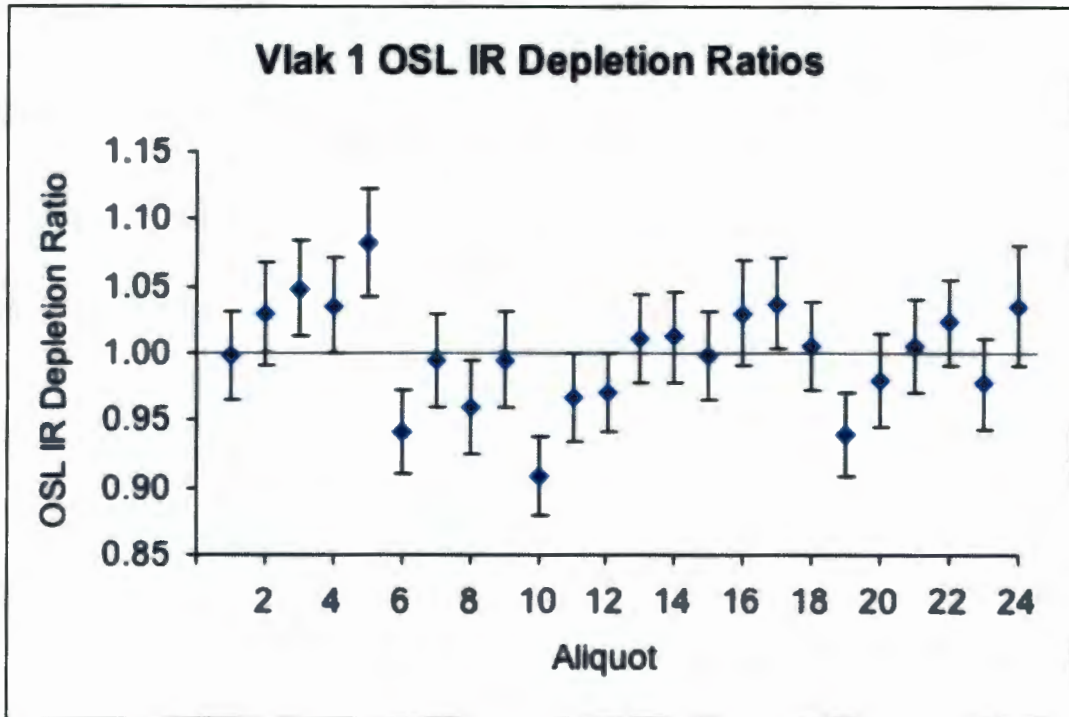


Figure 5.6. OSL IR depletion ratio test (Duller 2003). An aliquot fails the test if the ratio of L_x/T_x from Run 9 to L_x/T_x from Run 7 is not within two standard deviations of error around unity, or 1.0. Here, aliquots 5, 10 and 19 fail the OSL IR depletion ratio test.

In some studies it has been possible to measure feldspar luminescence and, using a modified SAR protocol, to recover the applied radiation dose (Blair *et al.* 2005), however, anomalous fading of feldspars continues to be a crucial concern. Quartz OSL is better understood, and the quartz OSL signal bleaches more rapidly than both the quartz TL signal and the feldspar IRSL signal (Godfrey-Smith & Cada 1996). Because of its predictable behaviour, plus advances in equipment, particularly automation and the use of powerful blue LEDs (Bøtter-Jensen *et al.* 1999; Bøtter-Jensen *et al.* 2000; Bøtter-Jensen *et al.* 2003), the most accurate and precise method of optical dating is by quartz OSL measurements.

Understanding and measuring dose rate

In Equation 5.1 for estimated luminescence age, the equivalent dose determination is divided by the estimated dose rate over time. Naturally occurring ionizing radiation, primarily from the decay of uranium (U) and thorium (Th) and their daughter

products, plus potassium (K), is responsible for the movement of electrons into traps in the crystal lattice of a mineral grain. These trapped electrons are stored and build up through time. The rate at which trapped electrons, and therefore OSL signals, accumulate is predictable; it is proportional to the rate at which energy is absorbed by a grain from the radiation flux (from U, Th and K) to which it is exposed. The half-lives of the U and Th parent isotopes and of ^{40}K are very long, in the order of 10^9 years, such that their natural abundance is in effect constant over the time range of OSL dating interest, from 10 years to ~200 ka. This allows estimation of past radiation dose rates by the measurement of the current radioactive flux in the sample and the environment.

There are four types of environmental radiation: alpha (α) from the decay chains of U and Th; beta (β) from the decay chains of U, Th, K and rubidium (Rb); gamma (γ) from the decay chains of U, Th, and K; and cosmic radiation from the sun. Alpha particles are heavy, energetic particles of short penetration range, in the order of only a few microns. Beta rays have an intermediate penetration range, about 2 mm, and gamma rays a long penetration range, up to about 30 cm. Cosmic ray radiation is highly penetrating, and it is calculated as a function of sample latitude, longitude, elevation and sediment overburden (Figure 5.7).

A sample acquires this environmental radiation in two ways, internally and externally. In quartz, the internal dose rate represents alpha and beta radiation from natural impurities and minerals within the grain itself, such as zircon. The external dose rate is derived from alpha, beta and gamma radiation from the bulk sediment matrix surrounding the grain, plus a contribution from cosmic rays. An estimate of the current radioactive flux, the sample dose rate, is calculated from an estimate of internal U and Th concentration of the grain plus external U, Th, and K concentration from a bulk sediment sample surrounding the grain.

Understanding the dose rate of a sample is complex and affected by a number of additional factors. Particularly in moist environments, such as on the coast or in wet cave deposits, soluble radioactive elements have the potential to become mobile. The sensitivity of minerals to acquiring radiation can vary significantly, even within one

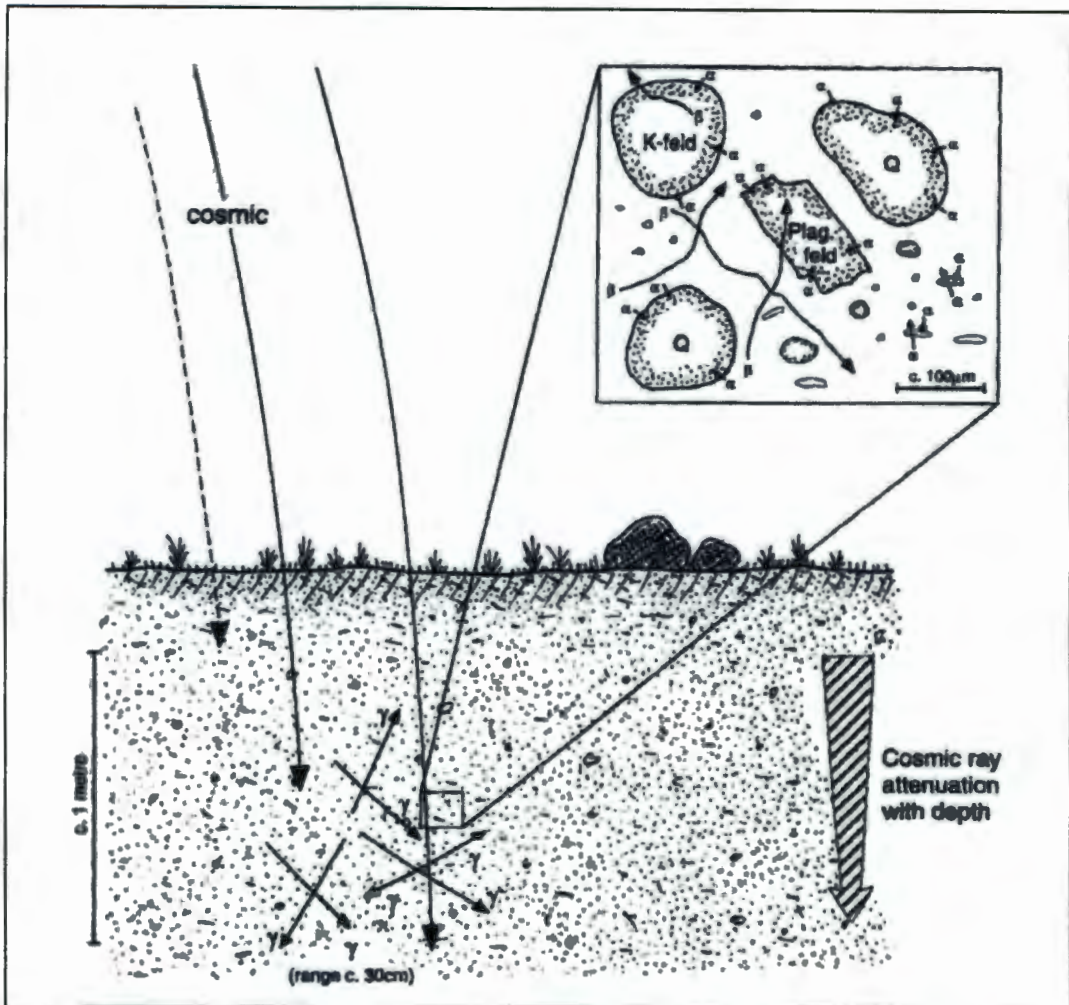


Figure 5.7. Radiation accumulation by a sample measured to determine dose rate. Short-range alpha and beta particles from natural impurities in the sample comprise the internal component and long-range gamma particles and cosmic radiation from the surrounding environment comprise the external dose (Aitken 1998: Figure 2.2).

sample, depending on the geologic history of each grain. Water attenuates radiation; therefore if a sample is damp or waterlogged its ability to accumulate dose is reduced, resulting in an older age estimate. Equation 5.1 for luminescence age is a ratio; if the value of the denominator, the estimated dose rate, decreases, then the value of the numerator, the equivalent dose, increases, resulting in an increase in age.

Also significant is the location of the sample in the ground. Because gamma radiation has a range of penetration of about 30 cm, any object or material present within a

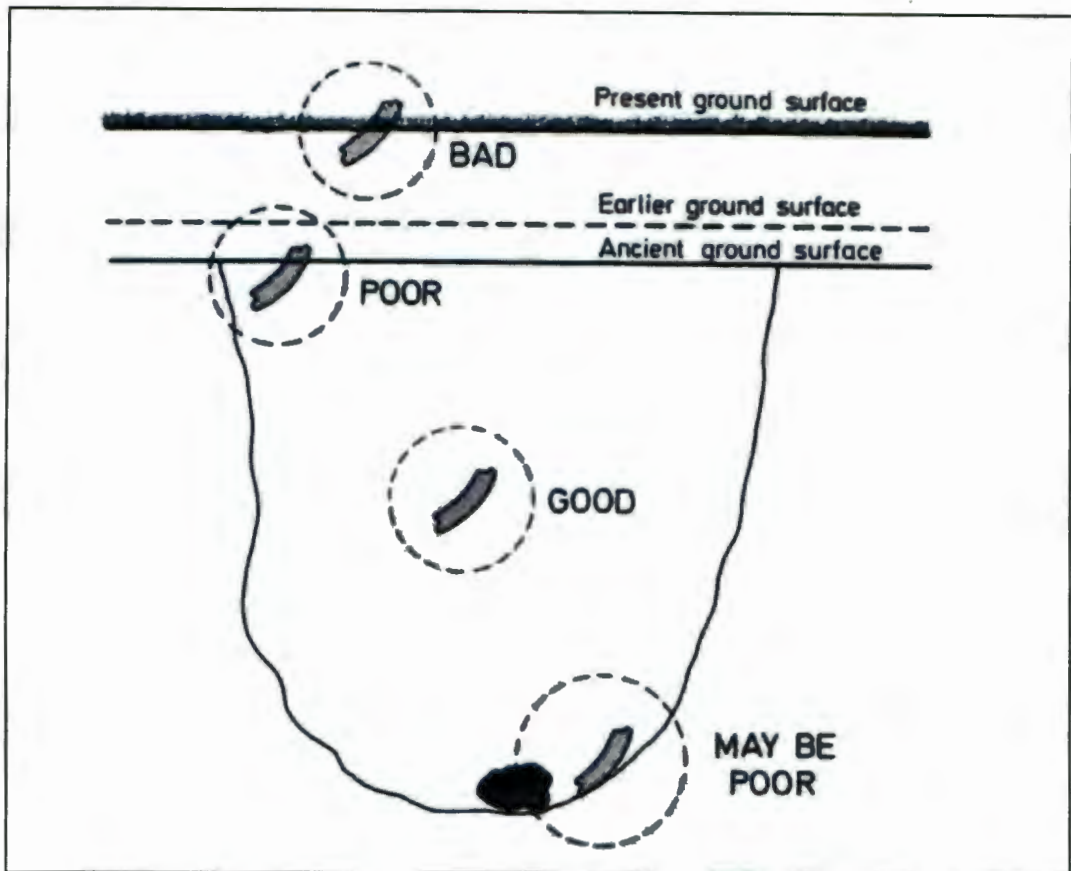


Figure 5.8. Positioning and environment of luminescence samples in relation to acquisition of environmental dose. Gamma radiation penetrates 30 cm. A good sample is 30 cm below an ancient ground surface and is not close to any objects or materials that might emit spurious radiation (Aitken 1997: Figure 7.2).

30 cm radius sphere around the sample is contributing to the radiation dose received by the sample. Close proximity to particularly emissive objects, for example, uranium-bearing rocks, or to a stratum containing sediments of different radioactivity than those of the sample will skew the dose rate. Distance to open air is also a factor because of the gamma contribution from cosmic radiation, so the ideal sample is collected from a minimum depth of 30 cm (Figure 5.8). In some instances, it is possible to measure surface samples accurately, if one assumes that a sample collected from the surface has always been on the surface and accounts for radon fallout and higher cosmic dose (James Feathers, pers. comm.).

Luminescence age is estimated by dividing only two factors: the equivalent dose determination and the estimated rate of absorbed radiation dose over time. Thus

assessment and calculation of the radioactivity of the sample and its surroundings is equally important as measuring the luminescence it releases. Dose rate can be determined chemically or radiometrically, and those calculations are increased by the estimated radiation contribution by cosmic rays. If time and funding permits, two or more of the four methods of dosimetry described here can be employed.

In the field, a dosimeter can be buried in or as close as possible to the space from which the sample was or will be removed. Typically, the dosimeter is constructed of a high-purity, water-tight copper capsule containing calcium sulphate doped with dysprosium, a mixture that readily accumulates radiation. Before burial the dosimeter is heated to release any trapped charge. Over time, radioactivity from the sediment builds up a latent luminescence signal in the calcium sulphate. Optimally, a buried dosimeter remains in place for a year. This allows for a long-term measurement of dose through all the varied environments the sample experiences in that time, including periods of wet and dry conditions. Upon removal of the dosimeter, a second 'companion' dosimeter is heated; the two are kept together so that contribution from background radiation, for example, from shipping and security x-rays, can be subtracted accurately. In the laboratory, the luminescence signal intensity of the material inside the dosimeter is measured by thermoluminescence.

A second field method for determining dose rate is by *in-situ* gamma spectrometry, which measures radiation at present. By counting gamma rays emitted from the soil, the spectrometer determines the concentration of U, Th and K present in a 30 cm sphere around its sensitive sodium iodide (NaI) crystal tip. The tip of the portable *in-situ* gamma spectrometer should be placed in the exact location from which the sample was removed (Figure 5.9). The spectrometer amplifies and stores the elemental information in the form of an energy spectrum, and it is retrievable from a computer. The count data are adjusted according to the background radiation of the detector crystal in the *in-situ* gamma spectrometer, which is calibrated for each individual instrument, and then converted into ppm U and Th and %K. There are several disadvantages of *in-situ* gamma spectrometry over dosimeters. Most portable *in-situ* gamma spectrometers are able to detect only strong gamma signals from far



Figure 5.9. *In-situ* gamma spectrometry at an OSL sample location (Molo 1) in a Molokwane midden. The spectrometer, in the sample hole, is measuring U, Th and K concentrations from a 30 cm sphere around its sensitive crystal tip.

down the decay chain (see Figures 6.9-6.12), thus one has to assume there is secular equilibrium of the radioactive isotopes to get an accurate dose rate determination. Secular equilibrium occurs when the half-life of a parent radioactive isotope is much longer than that of the daughter, so that production and decay rates of the daughter are equal. This means that over the time scale in which luminescence dating is useful, the relative quantity of each isotope should remain constant, but environmental factors, such as water-rock interaction, can cause chemical reactions that disrupt secular equilibrium. Comparatively, dosimeters are less problematic. A dosimeter measures

the total gamma dose rate, so secular equilibrium is not a factor. In addition, as shown in Figure 5.9, *in-situ* gamma spectrometers can be large and bulky, making it difficult to place them in the exact location of the sample and sometimes resulting in significant destruction of the archaeological stratigraphy.

If field dosimetry is not possible, the best alternative is to collect bulk sediments from within the 30 cm sphere surrounding the sample that are representative of the different soils and environments in which a sample is situated, including artefacts. The radiation dose these emit can be measured in the laboratory, resulting in a model of the sediment geometry around the sample and the annual dose it experienced.

In addition, a portion of the sample sediment itself can be very finely ground and measured in laboratory alpha and/or beta counters, which count gross alpha and beta particle emission. %K can be quantified by several methods. X-ray fluorescence (XRF) spectroscopy measures the unique x-ray energies emitted by an element under x-ray excitation. Inductively coupled plasma mass spectrometry (ICP-MS) detects concentration of particular atomic ions based on their unique mass-to-charge ratio. Flame photometry is an inexpensive optical technique that detects and measures the emission of light at wavelengths characteristic for each element.

Two final factors are important in estimating the annual dose to which a sample was exposed. A portion of the sample sediment is monitored in a drying oven to establish moisture content at present, and that is used as a proxy for past wetness, because water attenuates radiation, as described above. Lastly, latitude, altitude and depth of sample are important data for determining the cosmic ray contribution. Cosmic ray influx varies over the Earth by latitude, dependant on the planet's axial tilt toward the sun, and by altitude, where higher elevations receive more contribution. Cosmic ray intensities also change over time and due to solar modulation. In addition, because some subatomic components of cosmic rays are negatively or positively charged, fluctuations in the Earth's geomagnetic field cause influx variation over time (Prescott & Hutton 1994).

In summary, the seemingly simple equation for OSL age represents quite a complex calculation with many parameters and both measured and estimated values that are important to understand before sampling for OSL at an archaeological site. For this

reason, close collaboration between the archaeologist and dating scientist, as occurred in this study, is absolutely necessary to minimize variability and maximize precision of the resultant OSL dates. If the dating specialist cannot visit the site, the archaeologist should bring an *in-situ* gamma spectrometer or several dosimeters to the field, and plan excavations carefully so that the equipment can be properly placed. A simple study of the regional geology will reveal if there is feldspar in the local rocks, minerals containing radioactive elements or sediments that could be a contamination concern. Considering the nature of Late Iron Age deposits, where there are no pure quartz sand dunes, this is especially important. It is helpful to have discussions about datable features, so that informed decisions can be made about sampling for such an expensive technique. The collaboration might include conversations about the cultural significance and sedimentological and archaeological characteristics of different midden deposits, for example, and whether luminescence dating is a viable option if a feature is less than 30 cm deep.

The value of an expensive OSL date is thus greatly enhanced by careful and deliberate sampling and dose rate measurement to minimize error and maximize precision. And because of the ubiquitous occurrence of quartz grains in sediment and the capability for high precision age determination, OSL is potentially the best chronometric method for absolute dating of late Moloko sites. This research was a pilot study to test that hypothesis.

Chapter 6

Late Moloko OSL:

Sampling, Analysis and Results

There are five fundamental components of optical dating: OSL measurement and dosimetry, as described in Chapter 5, plus field sampling, sample pre-treatment, calculations to estimate the OSL age and data interpretation. The principles of equivalent dose determination and dose rate estimation were discussed generally in the previous chapter. In this chapter, I describe specifically the field contexts and dosimetry of the OSL samples collected for the late Moloko dating project. I also explain the laboratory procedures and measurement methods and report the OSL ages, as well as the relevant data used to calculate the date for each sample.

OSL DATING THE LATE MOLOKO

A major goal of this research is to provide a detailed comparison of three different ways to obtain dates from late Moloko sites: Bayesian-calibrated radiocarbon dating, dating using information from the oral-historical record, and OSL dating, a new method for this period in South Africa. Table 6.1 outlines results from the three techniques.

In this chapter and the next, I comprehensively discuss the OSL results and assess the value and validity of each OSL age. An OSL date is affected by many factors, as explained in Chapter 5, and late Moloko midden and furnace samples provide an excellent case study for understanding specific issues in collecting and measuring OSL samples from Late Iron Age archaeological contexts. I should note that recently, TL, rather than OSL, has been used successfully for dating fired features, such as furnace walls and tuyères, (Hagihara *et al.* 2001; Godfrey-Smith & Casey 2003; Zacharias *et al.* 2006a; Zacharias *et al.* 2006b). This research was pilot study

Table 6.1. Comparing dating methods for late Moloko sites: radiocarbon dates calibrated with Bayesian statistics according to the beta 1 border of the *difaqane*, dates from the oral-historical record and OSL ages.

Bayesian-calibrated radiocarbon dates and OSL ages are reported to 2σ error.

Site	Radiocarbon date (BP)	Bayesian-calibrated calendar date (AD)	Oral-historical date (AD)	OSL age (years); calendar range (AD)
Olifantspoort	105 ± 35 (GrN-5304)	1806-1852	18 th C to 1823-1838	237 ± 28 (Olif 1); 1738-1794
	180 ± 30 (GrN-5305)	1716-1749 1751-1783 1795-1850		
	105 ± 35 (GrN-5306)	1695-1726 1804-1838		
Molokwane	See Table 3.1; calibrated dates range early 16 th - mid-20 th C		Mid-18 th C to 1828	195 ± 14 (Molo 1); 1794-1822
Kaditshwene	180 ± 20 (Pta-5293)	1721-1747 1752-1785 1793-1822	About 1790 to 1823	192 ± 38 (Kad 1); 1773-1849
	180 ± 45 (Pta-5870)	1680-1709 1720-1812		247 ± 44 (Kad 2); 1712-1800
	200 ± 20 (Pta-5296)	1666-1697 1725-1789 1791-1805		
	See Table 3.1; additional calibrated dates range late 17 th - mid-20 th C			
Marothodi	-	-	1800-1810 to 1823-1827	302 ± 34 (Vlak 1); 1667-1735 303 ± 38 (Vlak 2); 1662-1738 186 ± 56 (Vlak 3); 1761-1873

specifically to test the applicability of OSL for Late Iron Age samples, however; in Chapter 7, I will discuss the advantages and disadvantages of each luminescence method for measuring fired samples.

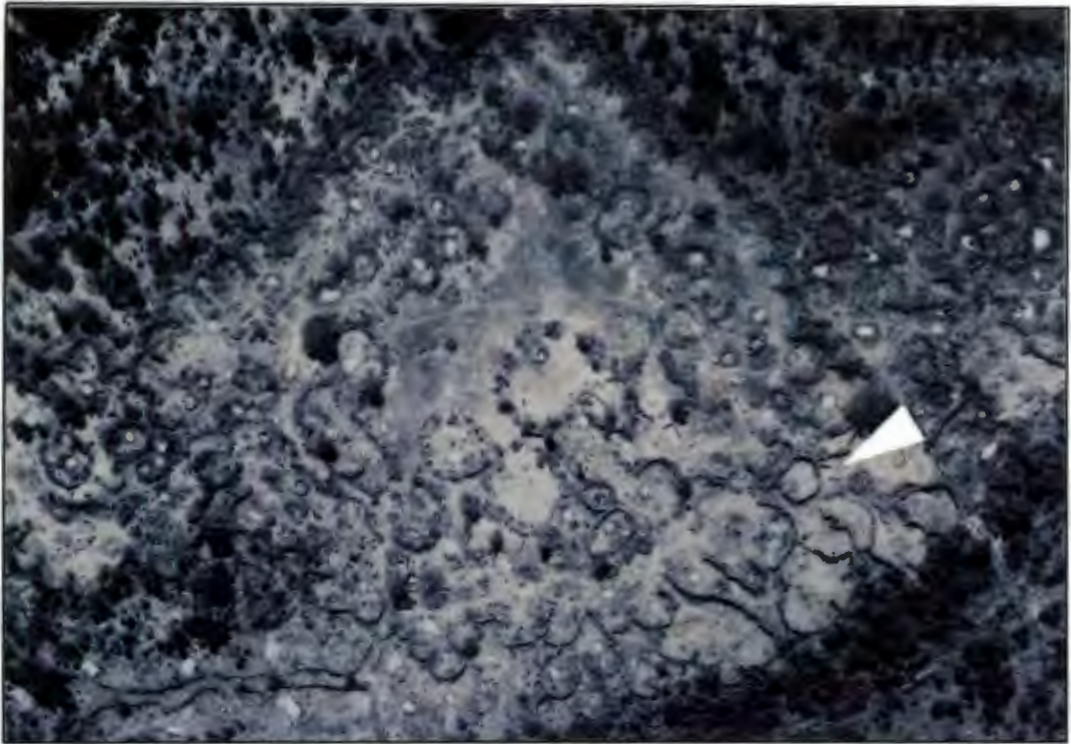


Figure 6.1. The white arrow points to the ash heap midden at the site on Olifantspoort farm excavated and radiocarbon dated by Revil Mason and John Vogel and where the OSL sample Olif 1 was collected (image adapted from Mason 1987: Figure 36).

Sample selection

While there are several materials occurring on late Moloko sites that are suitable for optical dating, the major concern in dating these recent contexts is sample depth. It can be a challenge to locate middens with enough sediment accumulation over the past few hundred years to bury potential samples 30 cm or more for the most accurate dosimetry. I collected four sediment samples from deep midden deposits and one from a relatively shallow midden deposit. I also collected two samples from copper smelting furnace walls, which are made of clay that becomes ceramic during the smelt due to the high temperature. Collection, laboratory preparation and analysis of late Moloko OSL samples were undertaken as a QUADRU project with the guidance of Zenobia Jacobs, Gill Collett and Stephan Woodborne.

Middens at late Moloko sites are trash heaps formed from two processes: the discard of broken pots, bone and other debris associated with their consumption and use in the

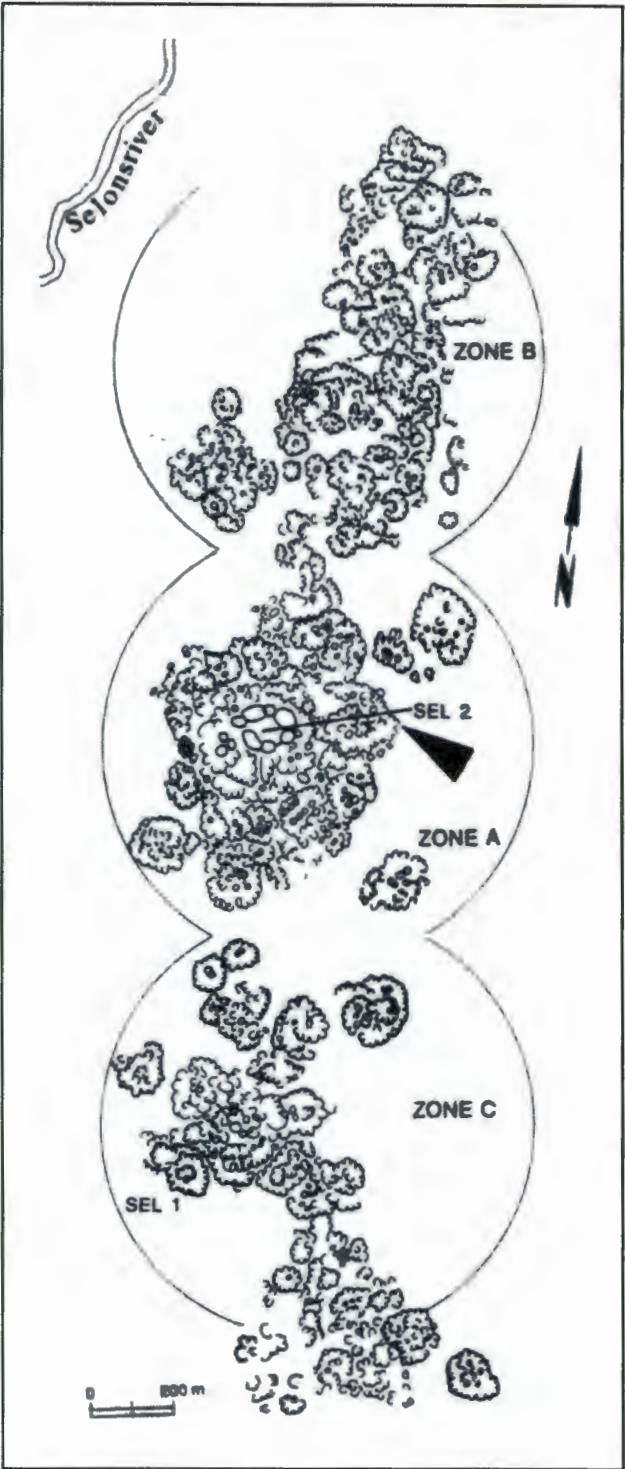


Figure 6.2. The black arrow points to the area in the central section of Molokwane, just east and down slope of the *kgosing*, where the midden sample Molo 1 was collected (image adapted from Pistorius 1994: Figure 3).

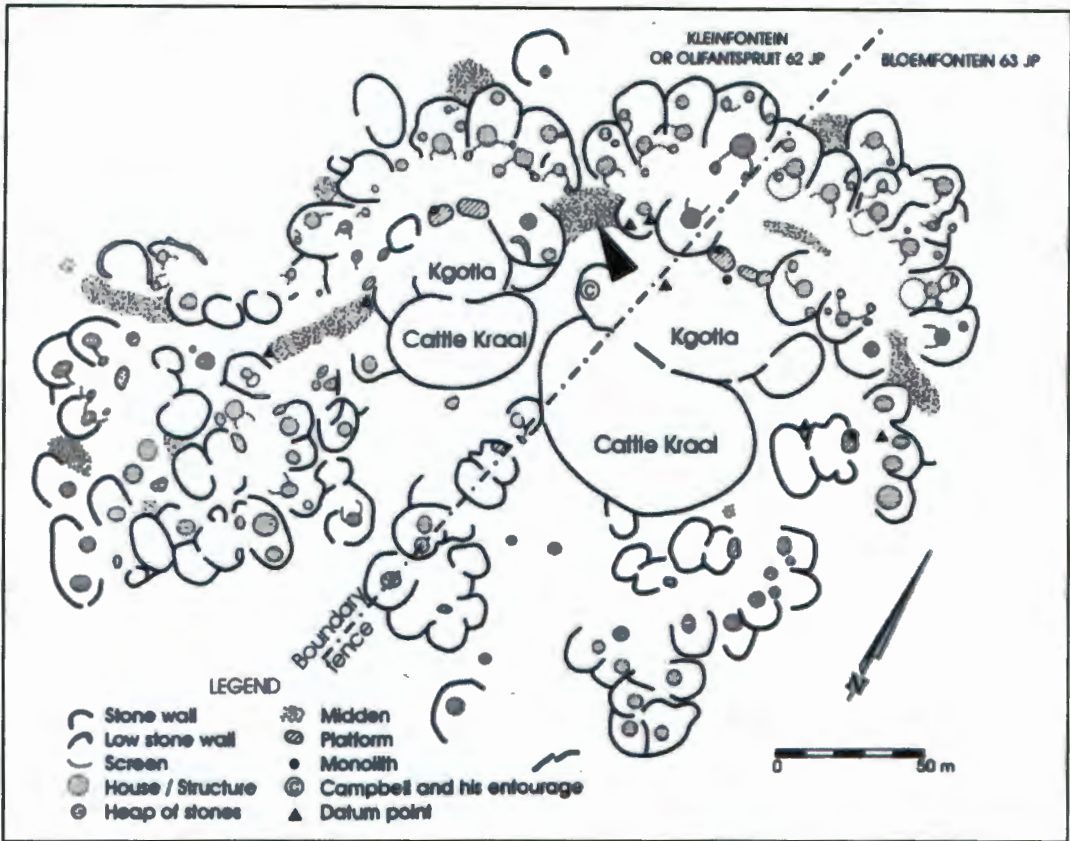


Figure 6.3. The black arrow indicates the position of the central midden at Kaditshwene from which OSL sample Kad 1 was collected. In John Campbell’s field sketch (Figure 4.2), the midden is depicted in the upper left corner. Note the symbol ●, to the left of the arrow here. This indicates the location of Campbell’s wagon, drawn adjacent to the midden in the sketch. Sample Kad 2, a copper furnace wall, was collected on the northwest perimeter of this area in an unexcavated section of the site (image adapted from Boeyens 2003: Figure 5).

nearby structures, and the sweeping and cleaning of hearth ash and other sediment from hut floors and verandas. Dating of quartz grains incorporated in these deposits cannot result in a discrete date, therefore, but should be interpreted as a range of years over which the midden formed. The substantial depth of most middens means that obtaining samples from 30 cm below surface to obtain an accurate dose rate usually is not difficult. The midden OSL results are assessed against formation processes in a more detailed discussion in Chapter 7.

Comparatively, OSL yield on quartz grains extracted from the ceramic wall of copper smelting furnaces will be proportional to the time elapsed since its last firing event. This model situation is countered by the problem of obtaining good dosimetry for a

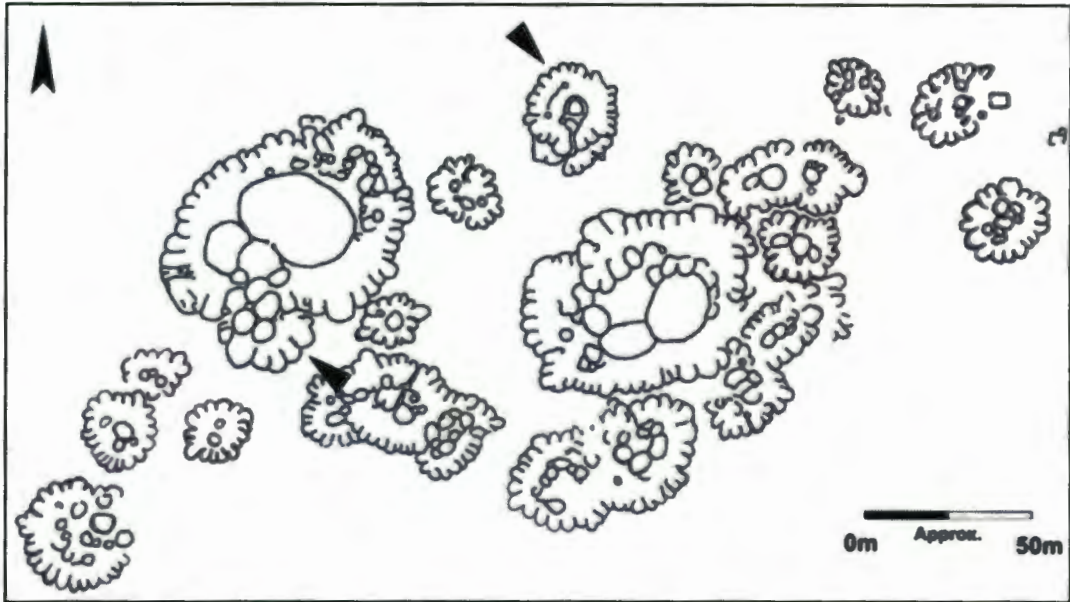


Figure 6.4. At Marothodi, two samples were collected from SU25, marked by the black arrow at the north: Vlak 1, sediment from a midden, and Vlak 2, a copper furnace wall. For sample Vlak 3, sediment was collected from a midden in the area marked by the lower arrow, near the *kgosing* (image adapted from Hall *et al.* 2006: Figure 2).

furnace feature. Ideally, the furnace would be unexcavated, so that dose rate measurements can be taken of all the fill and debris surrounding the sample before it is removed. Without excavation, however, it is difficult to know anything about the furnace or its size and shape! A dedicated archaeologist and dating scientist would have to pre-plan an essentially vertical excavation around the furnace to be dated so that a dosimeter or *in-situ* gamma spectrometer can be properly placed before the fill and surrounding sediment is removed. An alternative might be to choose a furnace for dating that is currently on the surface, and presumably always has been, thus consistently incorporating the gamma dose rate over time. These considerations again stress the importance of close collaboration between the archaeologist and the luminescence specialist.

The samples for this study were collected in September 2003, during the dry season in the summer rainfall region. The sampling rationale was to obtain OSL dates from as many contexts as possible where the age of the feature was already estimated from either radiocarbon and/or oral-historical dates.

Table 6.2. Samples collected for OSL dating.

Site	Sample Designation	Lab Number	Material; Provenience	Depth	Position of <i>in-situ</i> gamma spectrometer
Olifantspoort	Olif 1 (A & B)	C8098 PL-0345	sediment; midden	30 cm	sample hole A
Molokwane	Molo 1 (A & B)	C8099 PL-0346	sediment; midden	30 cm	sample hole A
Kaditshwene	Kad 1 (A & B)	C8103 PL-0350	sediment; midden	40 cm	sample hole A
	Kad 2	C-8104 PL-0351	ceramic wall; copper furnace	18 cm, exposed	tip at sample position
Marothodi	Vlak 1 (A & B)	C8100 PL-0347	sediment; SU25 midden	25 cm	sample hole B
	Vlak 2	C8101 PL-0348	ceramic wall; SU25 copper furnace	13 cm, exposed	tip at sample position
	Vlak 3 (A & B)	C8102 PL-0349	sediment; midden	40 cm	sample hole B

Sample collection

One midden sample (Olif 1) was collected from an unexcavated section of the large deposit Mason excavated as ‘ash heap Midden I’ at the site on Olifantspoort farm, where radiocarbon samples were collected in the 1960s as described in Chapter 3 (Figure 6.1). A second midden sample (Molo 1) was collected from a large deposit just east and down slope of the small hill on which the *kgosing* at Molokwane was built (Figure 6.2). Pistorius identified the *kgosing* as Zone A SEL 2, and the radiocarbon dates for this area of the settlement are listed in Table 3.1. At Kaditshwene, a sediment sample (Kad 1) was collected from the large midden in the central *kgosing*, depicted by John Campbell in 1820 and radiocarbon dated by Jan Boeyens as described in Chapter 4 (Figure 6.3). Also, a wall sample was removed from a copper furnace (Kad 2) on the northwest perimeter of the *kgosing* that had not been excavated by Boeyens. Three samples were collected at Marothodi, each named ‘Vlak’ for the farm on which the site is located. One sediment sample (Vlak 1) came from the small midden excavated in 2003 in settlement unit SU25 at the north side of the site. A copper furnace sample (Vlak 2) came from just outside the perimeter wall of this settlement unit. A second sediment sample (Vlak 3) came from the midden



Figure 6.5. Collecting a midden sediment sample (Vlak 3) at Marothodi. The opaque PVC pipe, blocked at the far end with black plastic, is inserted horizontally into a cleaned section until the plastic appears at the near end.

associated with the primary *kgosing* located at the centre of the site (Figure 6.4). Table 6.2 displays information about the sample locations and their collection.

At Olifantspoort, Molokwane and Marothodi, I collected samples with the invaluable help and patience of Gill Collett from QUADRU. At Kaditshwene, Jan Boeyens accompanied me. Sample collection was as follows. For midden samples, an opaque white length of PVC pipe was stuffed at one end with an opaque black plastic sheet. This blocked end was inserted horizontally into a newly-cleaned section and



Figure 6.6. Collecting a wall sample from a copper furnace (Kad 2) at Kaditshwene. The thick black plastic tarp ensures that the sample remains as much in the dark as possible. Photograph courtesy Jan Boeyens.

hammered inward such that as the tube filled with sediment, the black plastic sheet was pushed toward the open, exposed end of the pipe (Figure 6.5). When the tube was full of sediment, it was removed, the end quickly covered with several layers of black plastic, and sealed. For each midden, two side-by-side samples (*ie* Kad 1A and Kad 1B) were taken to ensure enough total quartz was collected in the ashy substrate, although in all cases only one tube was needed. For the copper furnace samples, the furnace wall was cleared of dirt and then, under a black plastic cover, to ensure the sample was exposed to as little light as possible, a portion of the interior wall was removed by hammer-and-chisel and wrapped in black plastic (Figure 6.6).

After the samples were removed, the *in-situ* gamma spectrometer was set up in one of the two sample holes in each midden, or in the space from which the furnace wall was removed, and left to collect data for at least 3000 counts, usually about one hour.

There were two major limitations to this dosimetric method for this study. Because the intensity of occupation at late Moloko sites is not always extensive, some deposits



Figure 6.7. *In-situ* gamma spectrometry in the SU25 midden at Marothodi (Vlak 1). The deposit is sterile after 25 cm, thus it is not possible to collect a sample deep enough for the ideal 30 cm sphere of gamma ray penetration.

are very shallow. The midden in SU25 at Marothodi, for example, is only 25 cm deep and lies above natural turf soil. It is not possible in that situation to collect a sample deep enough to account for gamma ray penetration in a 30 cm sphere (Figure 6.7).

The field dosimetry for the furnace samples also is inferior, because the gamma spectrometer is unduly influenced by cosmic radiation from the sun (Figure 6.8). Placing the gamma spectrometer into a hole dug behind the furnace wall before the feature is excavated can rectify this problem, but this would require knowing the dimensions of the furnace before it is exposed. Also, if field dosimetry is compared to laboratory measurements, scientifically valid refinements can be made considering both types of information.

Determining sample dosimetry

Quantification of the radioactive dose absorbed annually by a sample is integral for



Figure 6.8. *In-situ* gamma spectrometry of a sampled copper furnace at Kaditshwene (Kad 2). The placement of this instrument is not ideal, because of the 30 cm spherical geometry over which the crystal collects information. Another option would be to place the spectrometer into an access hole dug behind the furnace wall before the sample is removed, however, this would have to be done before the furnace is excavated and its dimensions are known.

accurate and precise optical dating results. The principles of dose rate estimation were described in Chapter 5. For this study, once back in the QUADRU laboratory, we used several methods to determine different dose rate factors. Dose rate determinations for the late Moloko samples are presented in Table 6.3. Although

Table 6.3. Dose rates for late Moloko OSL samples.

	Olif 1	Molo 1	Kad 1	Kad 2	Vlak 1	Vlak 2	Vlak 3
<i>In-situ gamma spectrometry</i>							
K (%)	0.93 ± 0.01	1.105 ± 0.014	0.313 ± 0.007	0.255 ± 0.007	0.345 ± 0.008	0.079 ± 0.004	0.397 ± 0.008
U (ppm)	1.89 ± 0.06	1.382 ± 0.053	1.610 ± 0.057	0.920 ± 0.043	0.572 ± 0.034	0.492 ± 0.031	0.404 ± 0.028
Th (ppm)	7.47 ± 0.19	5.849 ± 0.169	4.770 ± 0.153	4.395 ± 0.147	2.757 ± 0.116	2.253 ± 0.105	1.824 ± 0.095
<i>X-ray fluorescence</i>							
K (%)	1.05 ± 0.01	1.84 ± 0.01	0.61 ± 0.01	0.60 ± 0.01 sediment 2.14 ± 0.01 glass	7.72	0.45 ± 0.01 sediment 0.71 ± 0.01 glass	0.70 ± 0.01
<i>Thick source alpha counting</i>							
U (ppm)	2.02 ± 0.09	1.09 ± 0.06	1.54 ± 0.07	-	0.64 ± 0.03	-	0.54 ± 0.03
Th (ppm)	7.55 ± 0.33	6.76 ± 0.21	6.86 ± 0.26	-	1.98 ± 0.10	-	1.95 ± 0.10

Table 6.3 (continued). Dose rates for late Moloko OSL samples.

	Olif 1	Molo 1	Kad 1	Kad 2	Vlak 1	Vlak 2	Vlak 3
<i>Water content (%)</i>							
	7.9	9.1	4.6	5.0	6.6	0.1	7.5
<i>Dose rate (Gy/ka)</i>							
Beta	1.06 ± 0.06	1.42 ± 0.08	0.70 ± 0.03	0.38 ± 0.02	0.42 ± 0.03	0.17 ± 0.01	0.53 ± 0.02
Gamma	0.76 ± 0.04	0.80 ± 0.04	0.53 ± 0.02	0.36 ± 0.01	0.28 ± 0.01	0.18 ± 0.01	0.28 ± 0.01
Cosmic	0.27 ± 0.03	0.28 ± 0.03	0.26 ± 0.03	0.27 ± 0.03	0.27 ± 0.03	0.27 ± 0.02	0.26 ± 0.02
<i>Total dose rate</i>	2.12 ± 0.08	2.53 ± 0.08	1.53 ± 0.03	1.03 ± 0.03	1.01 ± 0.04	0.66 ± 0.02	1.10 ± 0.03

Dose rates include a 0.034 ± 0.001 Gy/ka assumed contribution for the internal alpha dose rate from U and Th inside the quartz grains.

All elemental and dose rate measurements and errors are rounded off to two decimal places, but the total dose rate and ages were calculated before rounding.

dosimeters are preferable for estimating dose rate, they were not available for this research, and an *in-situ* gamma spectrometer was used for all samples.

The NaI crystal in the *in-situ* gamma spectrometer detects gamma radiation. When a gamma ray produced during radioactive decay of U, Th or K is detected, the crystal emits an electrical pulse that is delivered to an amplifier (the white box visible in Figures 5.9 and 6.7), then to computer software that analyzes the height of each pulse that enters it. The computer application used at QUADRU is the Aptec PCMCA /Super Basic Display and Acquisition Software, a multichannel analyzer that produces an energy spectrum reporting the counts received, or number of pulses, in log scale on the y-axis for each pulse voltage channel (keV) on the x-axis (Figures 6.9 - 6.12).

If the user defines a region of interest (ROI), Aptec will calculate the number of counts in that region. Here we are interested in the counts for K, U and Th (the number of times one of these radioactive elements decayed and released a gamma ray), and the peaks for these elements occur in known channels on the x-axis. The K peak has the lowest keV and the Th peak has the highest; each ROI, the area under the energy peak, is filled in. The counts for each radioactive element in a sample are normalized and calibrated according to the background radiation from the NaI crystal.

These results are converted into amounts, %K and ppm U and Th, in an Excel spreadsheet by mathematical matrix analysis that integrates the range of energies in each elemental channel of the sample and the crystal background.

Measurement of alpha and beta radiation can be accomplished in a thick source alpha counter. To do this a subsample of each sediment was finely ground in a mortar and pestle and spread evenly over a filter in a holder that was placed in the instrument. Each sample was left in the instrument for at least 3000 counts, usually about two days. Gross alpha and beta counts were calibrated according to the size of the sample holder (the amount of sediment being measured) and the background radiation of the filter that was measured beforehand. It was not possible to count the alpha radiation of the copper furnace wall samples, because they were too vitrified to grind into a fine powder by hand in a mortar and pestle.

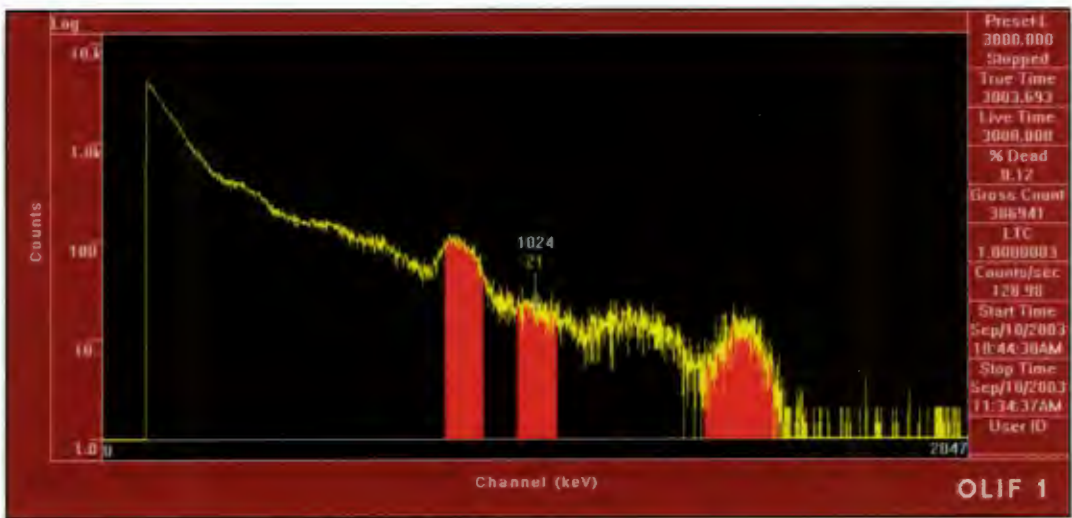


Figure 6.9. The Aptec spectrum for sample Olif 1. Counts under each peak are as follows: K 7783, U 1852 and Th 1569.

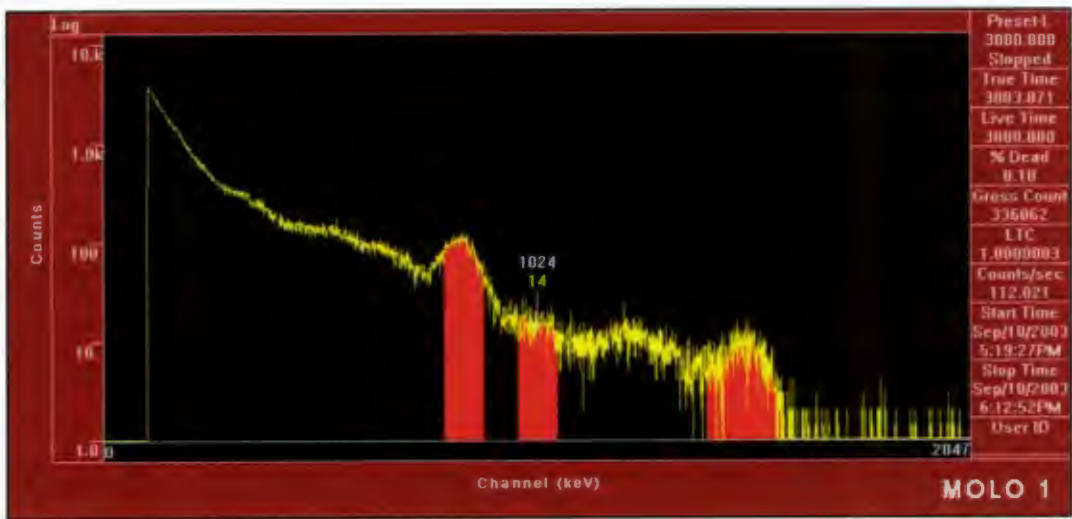


Figure 6.10. The Aptec spectrum for sample Molo 1. Counts under each peak are as follows: K 8283, U 1402 and Th 1231.

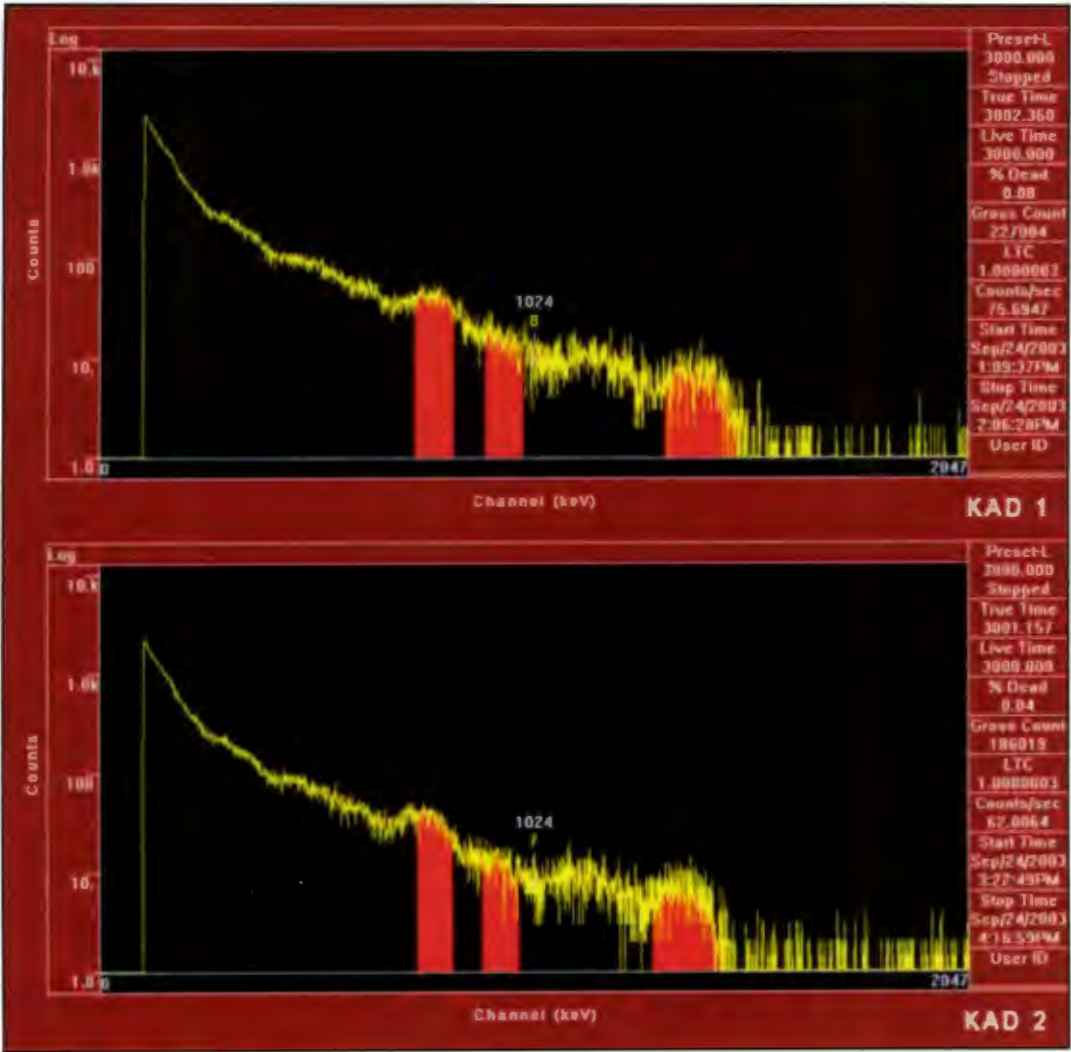


Figure 6.11. The Aptec spectra for samples Kad 1 and Kad 2. Counts under each peak for Kad 1 are as follows: K 3525, U 1382 and Th 1007; and for Kad 2: K 2731, U 991 and Th 917.

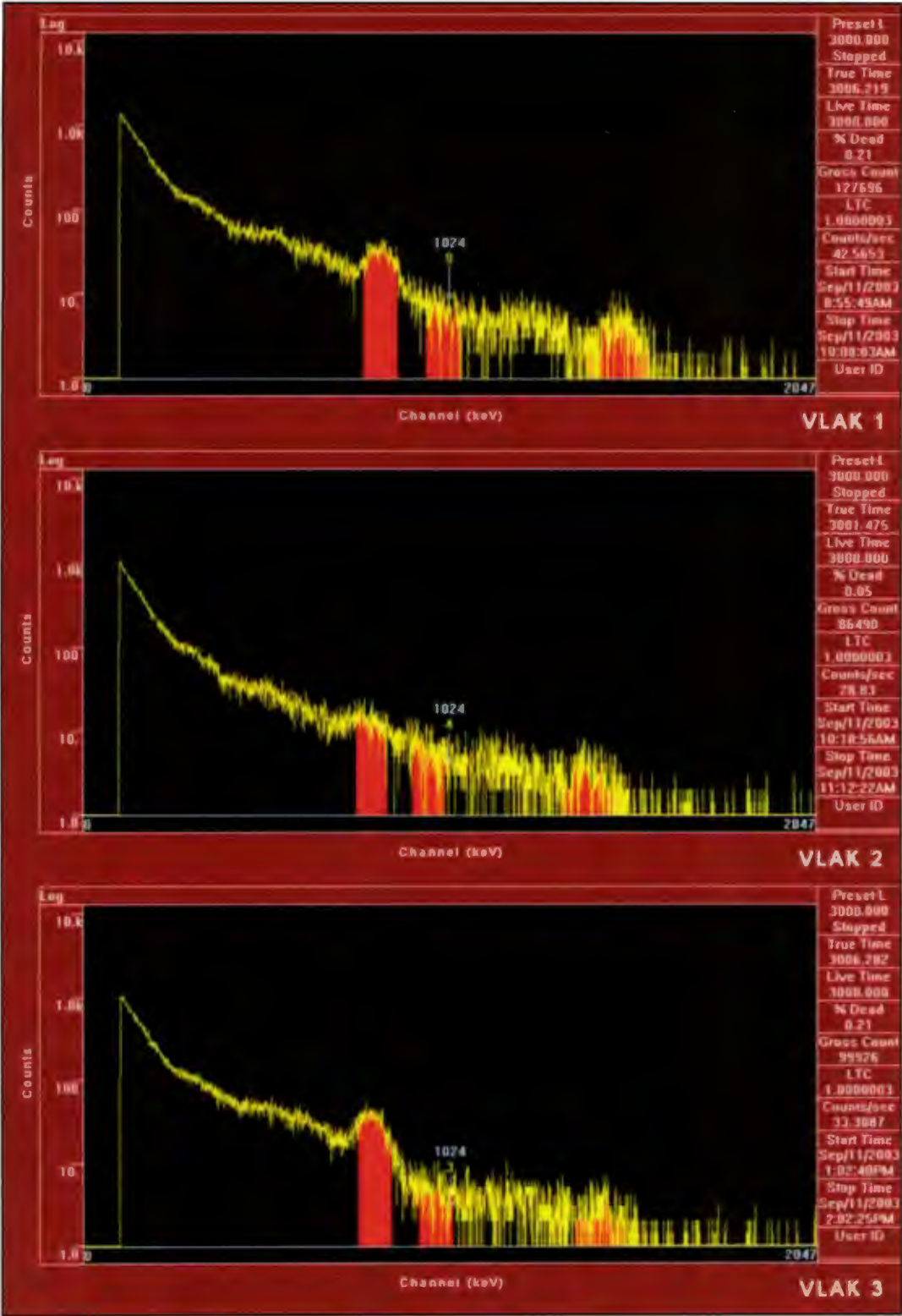


Figure 6.12. The Aptec spectra for samples Vlax 1, Vlax 2 and Vlax 3. Counts under each peak for Vlax 1 are as follows: K 2812, U 620 and Th 577; Vlax 2: K 1106, U 518 and Th 470; and Vlax 3: K 2882, U 424 and Th 384.

A subsample of each sediment also was sent to an outside laboratory for fused disc XRF analysis of %K₂O. These results were stoichiometrically reduced to %K as in Equation 6.1,

$$\%K = \%K_2O * 0.83$$

Equation 6.1

where 0.83 equals the portion of the K₂O molecule, by atomic weight, that is K₂. Two analyses were performed on each furnace wall sample, one on the loose sediment-like portion of the ceramic that fell loose in the sample bag and one on the glassy, slaggy, vitrified portion. Moisture content was measured by weight loss on drying. A subsample of each sediment was weighed, left in a 50° C drying oven for several days, and weighed again when dry, as in Equation 6.2:

$$\% \text{ weight loss} = \frac{\text{mass wet (g)} - \text{mass dry (g)}}{\text{mass dry (g)}} \times 100$$

Equation 6.2

Water content is the most variable dosimetric factor, as sediment moisture can fluctuate day-to-day as well as seasonally and over long time periods. The water content measured here is a record only of the subsurface conditions in the field on the day of sampling. If the final OSL age determination is calculated using *in-situ* field dosimetry, such as by gamma spectrometer or dosimeter, these methods measure the present moisture of the sediment, and it is not necessary to add a moisture content factor calculated in the laboratory.

Finally, the cosmic dose is calculated for each sample according to the methods of Prescott and Hutton (1994), which consider the penetration potential of cosmic rays into a sample by latitude, elevation and depth of overburden with a standard average bulk sediment density (1.5 g/cm³).

Sample pretreatment

Samples for optical dating must undergo a lengthy physical and chemical pre-treatment to extract pure quartz grains of the appropriate size for measurement. This process can take several weeks. Pre-treatment methods have been refined over the decades, but the basic steps remain the same (see Aitken 1985, 1997; Wintle 1997). All pre-treatment at QUADRU is done in a luminescence laboratory room under strict red-light conditions.

When sediment sample tubes from the field were opened for the first time, the outer few cm of sediment from each end of the pipe was removed due to possible light contamination during collection. This sediment was used for laboratory dosimetry as described above. Quartz extraction from solid materials, such as furnace wall and pottery, is more involved than quartz separation from loose sediments. For furnace wall 'ceramic,' the first step was removal of the outer 2-3 mm of the body by steel brush. This eliminates exterior grains that potentially were bleached by light since the ceramic was last heated and also grains that may have been contaminated by beta particles, with a penetration depth of about 3 mm, in the transmission zone between the ceramic and the surrounding sediment. The remaining ceramic wall was then crushed in a vice and ground with mortar and pestle until it became generally loose sediment.

Once crushed, wall samples were pre-treated by the same method as sediment samples. The first procedure is a wet chemistry series. The samples were reacted in concentrated hydrochloric acid to leach carbonates, then reacted in sodium hydroxide or concentrated hydrogen peroxide to remove organic material, then finally rinsed in a small amount of concentrated hydrochloric acid to remove any carbonates that might have formed when the organic solution in the previous step came into contact with air.

For physical separation, the dried sample was gently disaggregated with a mortar and pestle, then placed in a mechanical sieve shaker including stacked sieves of mesh sizes 300, 212, 180 and 150 μm , which are the desired particle size fractions for OSL dating. It is important to know the exact grain size fraction measured by OSL when

calculating the final age, because different grain sizes attenuate external dose at different rates.

The 150-180, 180-212 and 212-300 μm fractions were collected and run through a Franz Magnetic Separator to remove the magnetic grains. For these samples, most of which came from metallurgical contexts, there was a high proportion of magnetic grains in the sediment. Two heavy liquid separations were used on each size fraction to divide the potassium feldspar grains from the quartz grains by specific gravity (sg). The specific gravity of the heavy liquid, sodium polytungstate, can be altered with addition or evaporation of distilled water. This property was exploited first to force quartz (sg 2.65) to sink in sodium polytungstate where sg is 2.62, separating the feldspars (sg 2.55-2.63) in the float, then floating the quartz in sodium polytungstate where sg is 2.70, sinking any remaining heavy minerals.

The final pre-treatment before luminescence measurement is etching of the quartz grains from each size fraction in concentrated hydrofluoric acid. This removes a micron-thick outer layer of alpha particle irradiation on the grains, breaks up grains with unstable crystalline structures that might have irregular luminescence and dissolves any feldspar grains that remain with the quartz. The stripping of this outer alpha layer in HF etching affects the dosimetry, because dose rates were measured before it was removed. This is corrected in the final OSL age calculation.

A rinse in hydrochloric acid removed any fluorides that formed during the etch, and the grains were resieved to remove any broken or small crystals. The final result was three fractions of pure quartz sand, 150-180, 180-212, and 212-300 μm , that could be used for OSL dating. Measurement was on the size fraction with the highest mass weight so that the greatest number of aliquots could be tested.

In preparation for luminescence measurement, multiple sample grains were mounted on 9.7 mm diameter aluminum discs with a sticky silicone oil spray. Each disc represents a single aliquot, or division, of the sample. Aliquot size was determined by masking the disc so that only a specific spot size is covered with silicone spray, either 2 or 3 mm (Figure 6.13). As many as one thousand grains can fit on a disc if it is not

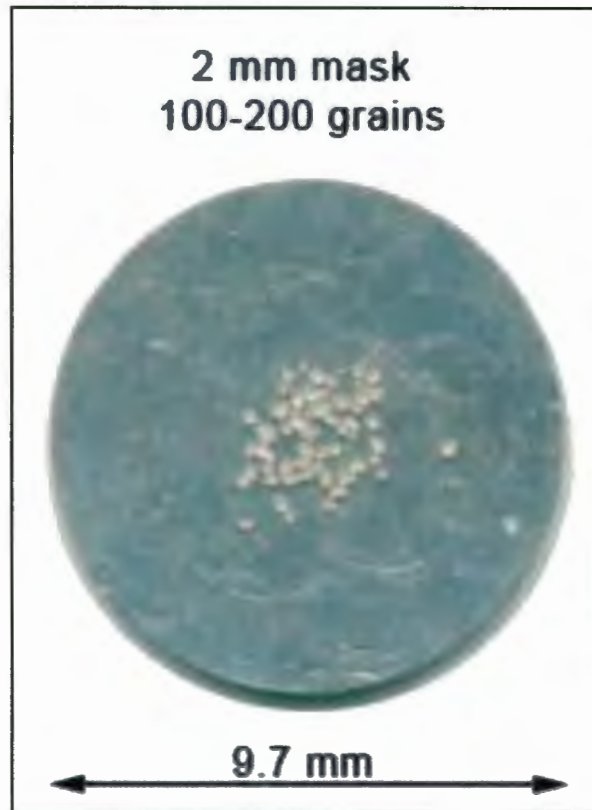


Figure 6.13. A 9.7 mm diameter aluminum sample disc sprayed with silicone oil through a 2 mm mask, on which quartz grains are mounted for luminescence measurement. Photograph courtesy of Marc Pienaar.

masked, but with smaller aliquots fewer grains contribute to the luminescence signal, resulting in a more accurate measurement of D_e . With a smaller size sand fraction, more grains will fit on the sample disc.

OSL MEASUREMENT AND RESULTS

The major consideration for OSL dating of the late Moloko samples was their young age. After examining the sensitivity of the quartz grains during preliminary D_e measurements with stepped preheats (see Chapter 5 and Figure 5.4), a lower, constant preheat temperature was used for the final dating runs. Low regeneration doses compensate for the low expected luminescence of the quartz. In addition, all of the

samples, except the one from Molokwane, were heavily contaminated with feldspar. This is not surprising, given the heterogeneity of middens and the clay deposits people mined for furnace wall material, plus the feldspars are the most common mineral group on Earth. The preliminary OSL measurements were performed without HF etching of the grains because that acid is particularly dangerous and unpleasant to use. Those early results showed clearly that the samples required an HF etch to be accurately datable because of the high number of aliquots that failed the OSL IR depletion ratio test, indicating presence of feldspars.

The SAR protocol, used to measure the OSL and determine the equivalent dose (D_e) of the late Moloko samples, was described in Chapter 5. The final dating measurements for the late Moloko samples were run on between twenty-four and sixty 2 or 3 mm size aliquot discs for each sample. This high number of aliquots ensured that even if when discs were rejected according to the criteria of the recycling ratio or OSL IR depletion ratio tests, there were enough well-behaved aliquots to have a statistically valid D_e result.

In order to determine the age of a sample, the D_e result for every individual sample aliquot that passed the sensitivity and contamination tests was plotted on a radial plot. A radial plot is a graphical presentation that compares estimates with different precisions (Galbraith 1990, 1994; Galbraith *et al.* 1999). Simply, it is an x, y scatter plot in which y is a standardized estimate of $D_e \pm 2 \sigma$ and x is the precision of the D_e result. To obtain the D_e for any point, a line is drawn from the origin (0, 0) through (x, y) to the circular scale. Figures 6.14 - 6.17 present the radial plot for each late Moloko OSL sample. The shaded line indicates the mean D_e estimate.

Partial bleaching is another possible source of error in optical dating. Partial bleaching occurs when quartz grains were exposed to light or heat for only a short length of time before deposition at a site. The OSL signal is incompletely zeroed, meaning that not all of the trapped electrons were released before the grain was buried. Thus the D_e obtained in the laboratory is a measurement of luminescence signal accrued since burial plus the signal remaining from the previous history of the grain, resulting in spuriously old ages. Sample mixing, or the presence of quartz

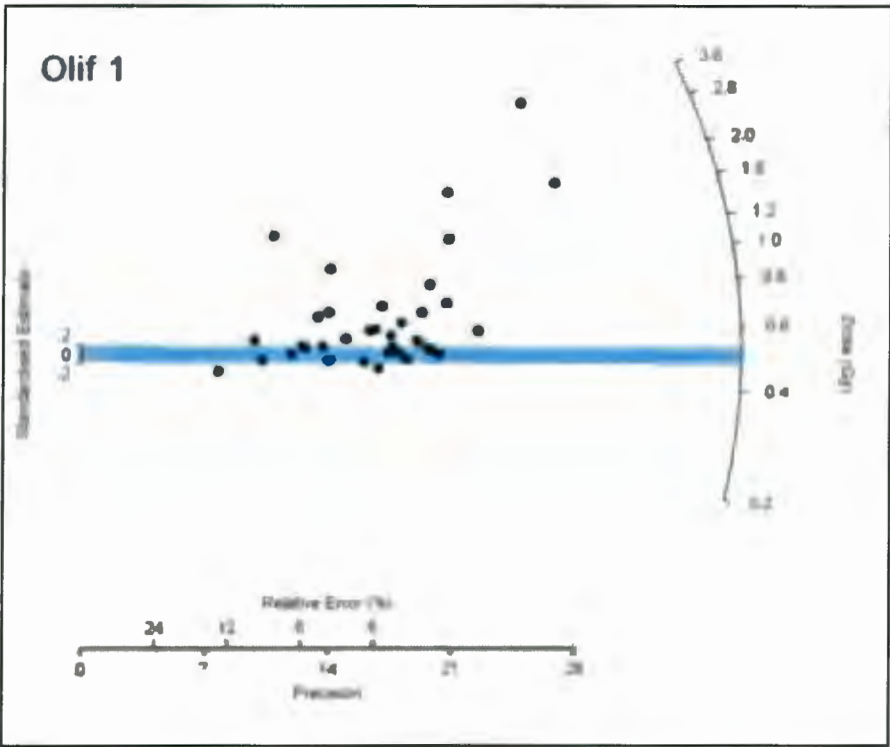


Figure 6.14. Radial plot of D_e for sample Olif 1 ($n = 37$). Because of high overdispersion, characteristic of partial bleaching, the minimum age model was used to estimate D_e .

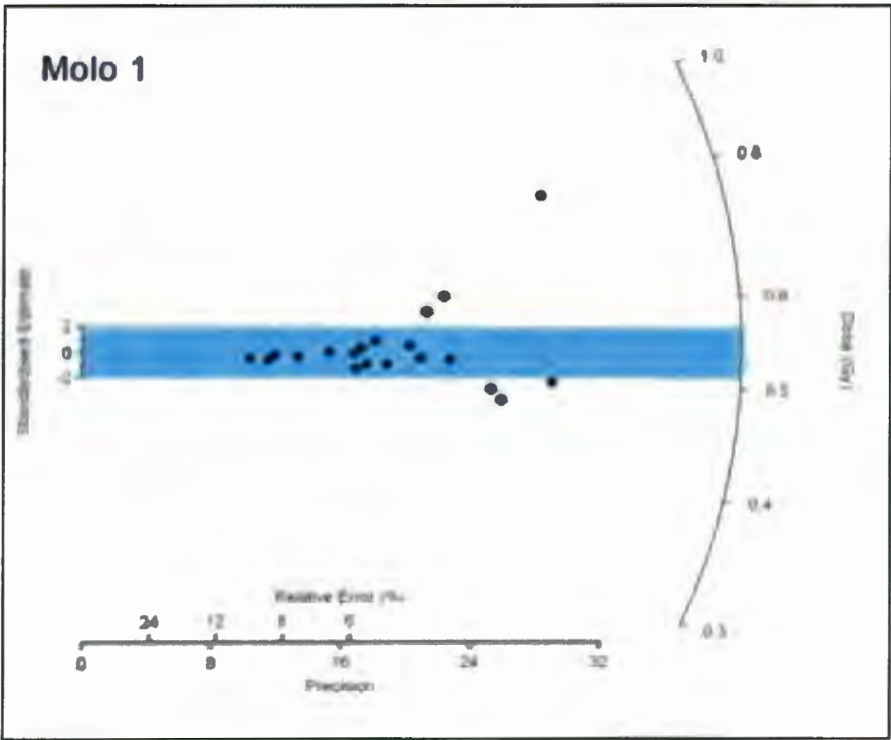


Figure 6.15. Radial plot of D_e for sample Molo 1 ($n = 23$). The central age model was used to estimate D_e .

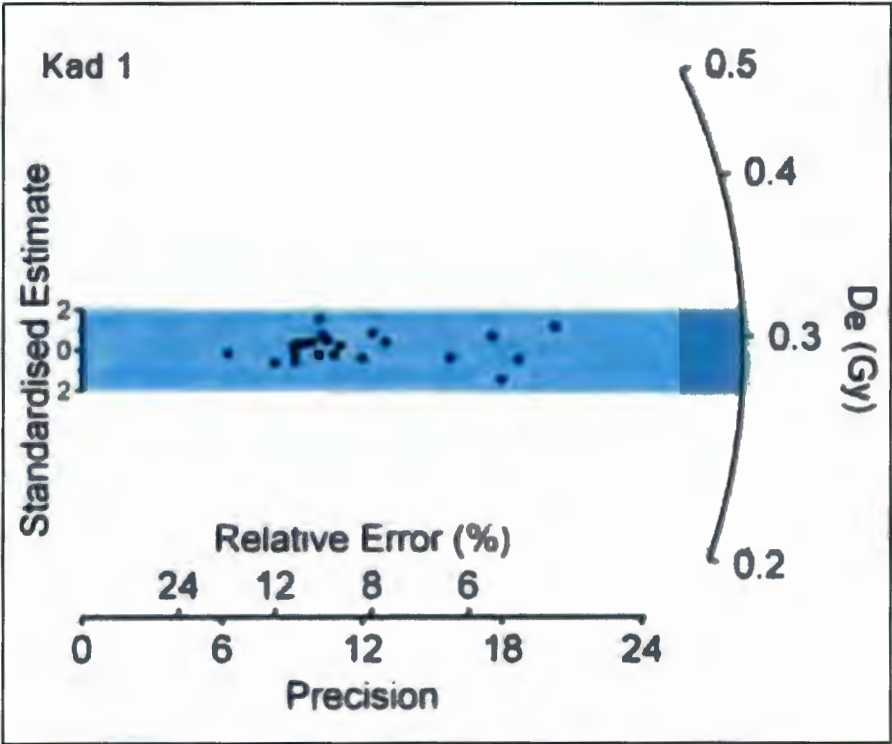


Figure 6.16a. Radial plot of D_e for sample Kad 1 (n = 24). The central age model was used to estimate D_e .

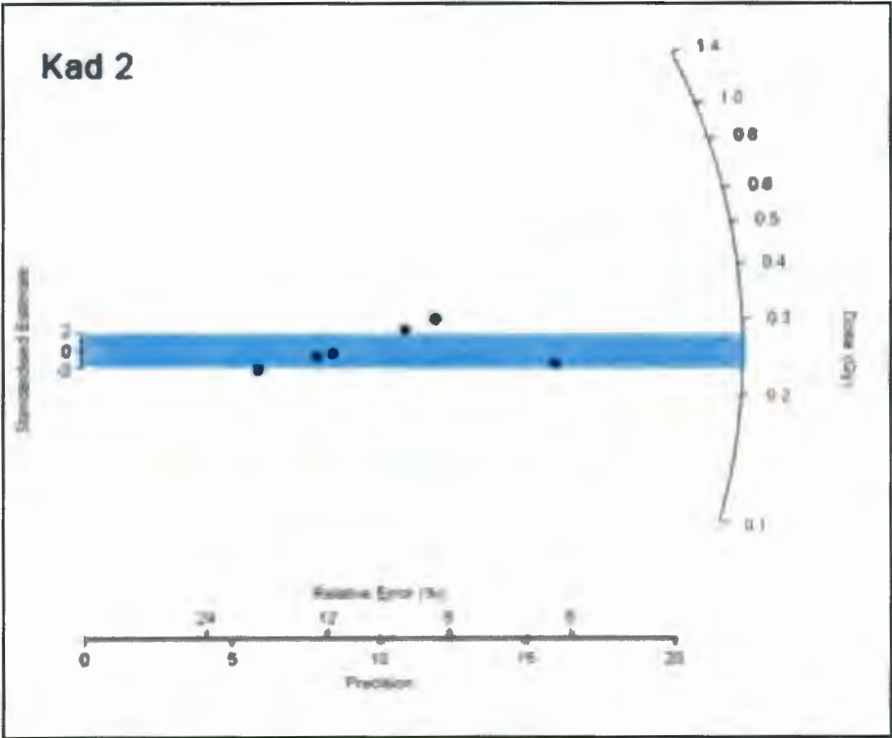


Figure 6.16b. Radial plot of D_e for sample Kad 2 (n = 6). The central age model was used to estimate D_e .

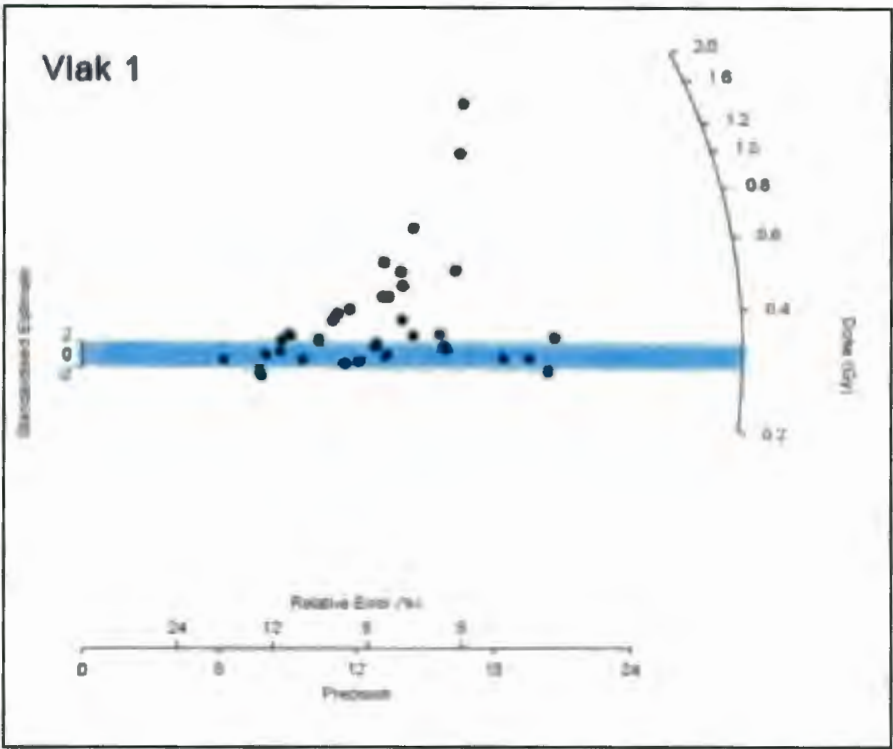


Figure 6.17a. Radial plot of D_e for sample Vlæk 1 ($n = 38$). Because of high overdispersion, characteristic of partial bleaching, the minimum age model was used to estimate D_e .

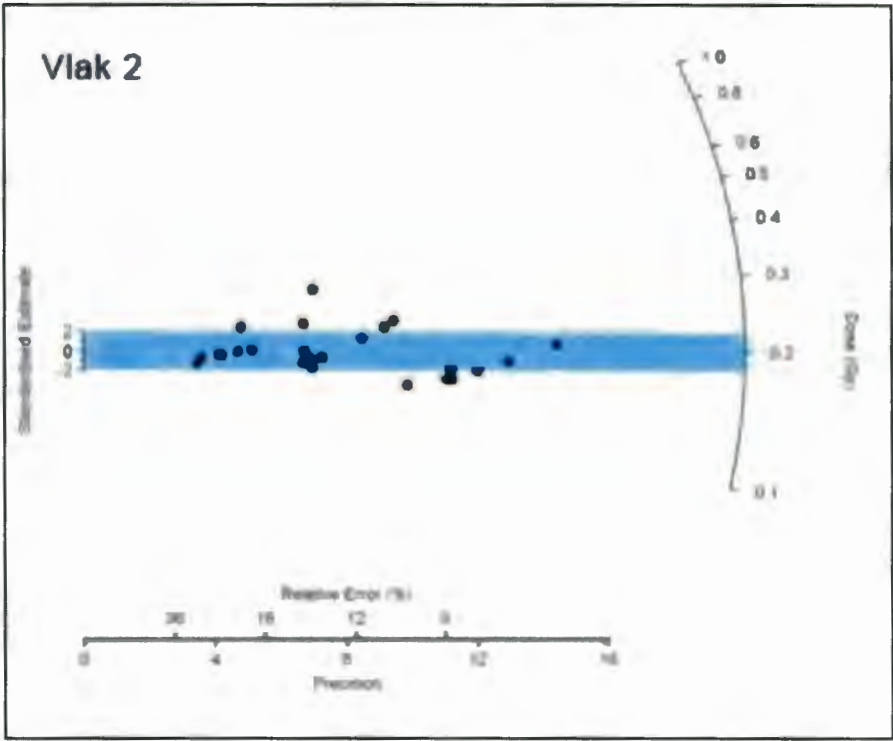


Figure 6.17b. Radial plot of D_e for sample Vlæk 2 ($n = 23$). The central age model was used to estimate D_e .

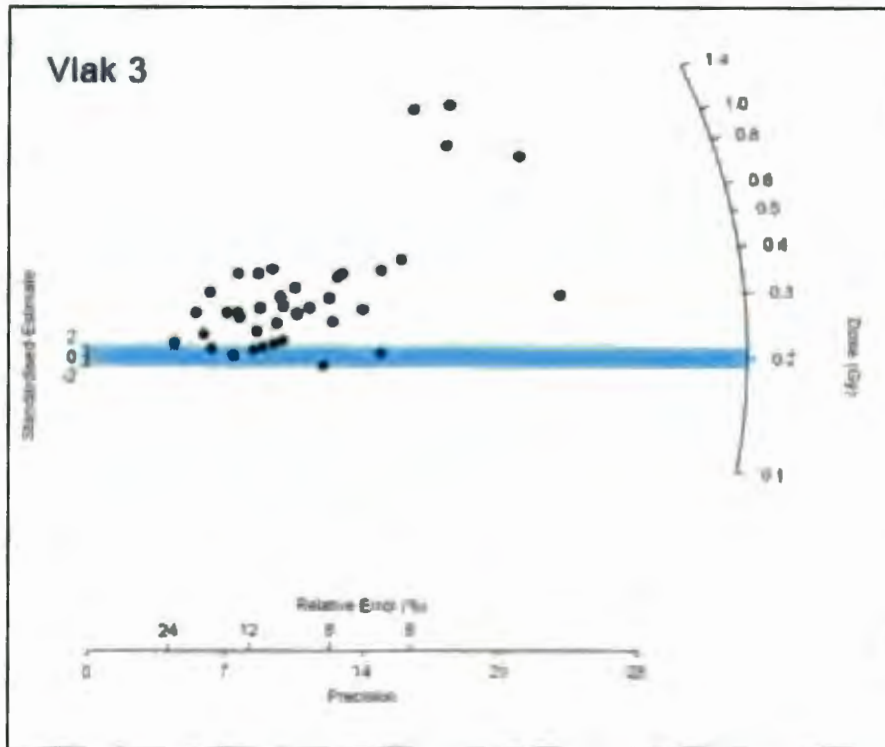


Figure 6.17c. Radial plot of D_e for sample Vlax 3 ($n = 40$). Because of high overdispersion, characteristic of partial bleaching, the minimum age model was used to estimate D_e .

grains with different ages of deposition, is also a source of error that can be visualized on a radial plot.

Thus the visual presentation of D_e points on the radial plot is very informative. The spread of D_e points such as those seen for samples Olif 1, Vlax 1 and Vlax 3 (Figures 6.14, 6.17a and 6.17b) are characteristic of partial bleaching of grains. The curvilinear shape of the points on these radial plots reflects the aberrantly bright luminescence of quartz grains that retain some of their old electrons. The discrete cluster of larger D_e measurements for four aliquots in Vlax 3 (Figure 6.17c), for example, possibly suggests sample mixing, or a second population of grains with ages older than the true midden age.

There are two statistical models of dispersion developed by Galbraith *et al.* (1999) used to obtain a final D_e and age of a sample. For these age models, when the observed range of the D_e values for all aliquots is within 20% of the expected

Table 6.4. Evaluation of the central and minimum age models (Galbraith *et al.* 1999) to determine final equivalent dose (D_e) for each late Moloko OSL sample.

For the convenience of comparison to OSL ages, the oral-historical date ranges AD from Table 6.1 are artificially recalculated to BP where ‘present’ is AD 2003, the year of OSL measurement.

Oral-historical date (BP)	Overdispersion (%)	Model	D _e (Gy)	Age (years)
<i>Olif 1 midden</i>				
~303-204 to 180-165	67 ± 8	Central	0.79 ± 0.09	372 ± 44
		minimum	0.502 ± 0.025	237 ± 14
Overdispersion and the curvilinear shape of points on the radial plot indicate that the minimum age model is most appropriate.				
<i>Molo 1 midden</i>				
~278-228 to 175	12 ± 2	central <i>a</i>	0.541 ± 0.015	204 ± 12
		minimum <i>a</i>	0.526 ± 0.014	203 ± 9
		central <i>b</i>	0.504 ± 0.008	195 ± 7
Low overdispersion and statistical overlap of the central <i>a</i> and minimum <i>a</i> age model results (n = 23) indicate that the central age model is most appropriate. The central <i>b</i> result is a refinement by removal of three high dose points (n = 20).				

variance, it indicates that the grains are fully bleached and represent a single depositional event. If overdispersion of the range of D_e values on the radial plot is less than 20%, we assume that all quartz grains were sufficiently bleached by exposure to sunlight or heat prior to deposition and use a central age model to calculate the final D_e . If overdispersion on the radial plot is greater than 20%, this indicates that some sample grains were only partially bleached prior to deposition or that the sample is of mixed ages, and we use a minimum age model to calculate the final D_e . For the late Moloko samples, we evaluated D_e according to one or both age models as appropriate and the results are presented in Table 6.4.

Recall Equation 5.1, the age equation for luminescence dating:

$$\text{age estimate (ka)} = \frac{\text{equivalent dose (Gy)}}{\text{estimated dose rate (Gy/ka)}}$$

Table 6.4 (continued). Evaluation of the central and minimum age models (Galbraith *et al.* 1999) to determine final equivalent dose (D_e) for each late Moloko OSL sample.

Oral-historical date (BP)	Overdispersion (%)	Model	D _e (Gy)	Age (years)
<i>Kad 1 midden</i>				
~204-180	0	central	0.293 ± 0.007	192 ± 19
There is no overdispersion in this sample, thus the central age model is applied.				
<i>Kad 2 furnace wall</i>				
~204-180	19 ± 7	central	0.254 ± 0.022	247 ± 22
Though overdispersion is near 20%, the central age model is applied because the high temperature of the copper smelt, around 1000° C, would have sufficiently zeroed the luminescence signal.				
<i>Vlak 1 midden</i>				
223-193 to 180-176	58 ± 7	central	0.457 ± 0.042	445 ± 43
		minimum	0.310 ± 0.014	302 ± 17
High overdispersion and the curvilinear shape of points on the radial plot indicate that the minimum age model is most appropriate.				
<i>Vlak 2 furnace wall</i>				
223-193 to 180-176	19 ± 4	central	0.198 ± 0.010	303 ± 19
Though overdispersion is near 20%, the central age model is applied because the high temperature of the copper smelt, around 1000° C, would have sufficiently zeroed the luminescence signal.				
<i>Vlak 3 midden</i>				
223-193 to 180-176	80 ± 9	central	0.557 ± 0.070	507 ± 65
		minimum	0.204 ± 0.030	186 ± 28
High overdispersion and the curvilinear shape of points on the radial plot indicate that the minimum age model is most appropriate.				

The final D_e for each sample was based on repeated laboratory OSL measurements and statistical analysis by either the central or minimum age model. The total dose rate was based on measurement of U and Th from *in-situ* gamma spectrometry in the field and on measurement of K from XRF in the laboratory. The final age results for the late Moloko OSL samples are presented in Table 6.5.

Table 6.5. Final age calculation for late Moloko OSL samples.

	Olif 1	Molo 1	Kad 1	Kad 2	Vlak 1	Vlak 2	Vlak 3
<i>Grain size (μm)</i>							
	150-180	150-180	180-212	212-300	180-212	212-300	180-212
<i>Number and size of aliquots</i>							
	37 x 2 mm	20 x 3 mm	24 x 3 mm	6 x 3 mm	38 x 3 mm	23 x 3 mm	30 x 2 mm 10 x 3 mm
<i>Overdispersion (%)</i>							
	67 ± 8	12 ± 2	0	19 ± 7	58 ± 7	19 ± 4	80 ± 9
<i>Statistical age model</i>							
	minimum age	central age	central age	central age	minimum age	central age	minimum age

Table 6.5 (continued). Final age calculation for late Moloko OSL samples.

	Olif 1	Molo 1	Kad 1	Kad 2	Vlak 1	Vlak 2	Vlak 3
<i>Equivalent dose (D_e) (Gy)</i>							
	0.502 ± 0.025	0.504 ± 0.008	0.293 ± 0.007	0.254 ± 0.022	0.310 ± 0.014	0.198 ± 0.010	0.204 ± 0.030
<i>Total dose rate (Gy/ka)</i>							
	2.121 ± 0.073	2.532 ± 0.093	1.528 ± 0.059	1.030 ± 0.061	1.011 ± 0.029	0.655 ± 0.023	1.099 ± 0.025
<i>Age (1 σ error)</i>							
years	237 ± 14	195 ± 7	192 ± 19	247 ± 22	302 ± 17	303 ± 19	186 ± 28
calendar range	1752-1780	1801-1815	1792-1830	1734-1778	1684-1718	1681-1719	1789-1845
<i>Age (2 σ error)</i>							
years	237 ± 28	195 ± 14	192 ± 38	247 ± 44	302 ± 34	303 ± 38	186 ± 56
calendar range	1738-1794	1794-1822	1773-1849	1712-1800	1667-1735	1662-1738	1761-1873

Chapter 7

Optically Stimulated Luminescence:

Interpretation and Discussion

As explained in Chapters 5 and 6, there are several potential sources of error in OSL age estimates, including accuracy of annual dose rate determination, sensitivity of electron traps in quartz grains to radiation absorption and attenuation, contamination by feldspars, partial bleaching of quartz grains and sample mixing. In this chapter, I discuss some of these issues more directly in relation to the late Moloko OSL results.

OSL DATING OF THE LATE MOLOKO

The sites dated in this thesis were chosen because the dates of their occupation are generally known through the oral-historical record, thus there is some independent control with which to compare the OSL ages. This research was an exercise to determine if OSL results for the recent past can be more accurate and precise than radiocarbon dates and therefore help to improve and fill gaps in the oral-historical chronologies.

As presented in Table 6.1, the OSL ages for the late Moloko stone-walled sites compare favourably to the known oral-historical dates, particularly for the midden samples. They provide a scientific basis on which to refine the interpretation of calibrated radiocarbon dates. Also, consider that in this thesis, dates are reported to 2σ error, whereas conventionally a laboratory reports dates to 1σ error. If the OSL age errors reported are halved, as one would find in a standard archaeology publication, the dates draw even closer to the oral-historical dates (Table 6.5). This is exciting for the potential application of OSL dating to periods in the Late Iron Age where radiocarbon is ineffectual.

In the following sections, I explain the specific OSL age results in the context of sample type and position (see Tables 6.1, 6.2 and 6.5), and review some other general archaeological and geological considerations for OSL dating at Late Iron Age sites.

Midden samples

One major difference between the midden sediment samples dated in this study as compared to typical OSL dating samples is their environment of formation. Whereas quartz dune sand, for example, is deposited by natural geologic processes and usually subject to few disturbances over time, quartz grains in a midden are mainly deposited by human action and often are subject to many disturbances. Several archaeologists have studied middens to evaluate rates of artefact accumulation and duration of site occupation (see Varien & Mills 1997; Beck & Hill 2004 for review of this literature), but formation processes on a granular level has been examined by fewer researchers (see Courty 2001; Stein 2001 for microfacies analysis). In order to evaluate an OSL date on quartz sand from an Iron Age archaeological midden, one must contemplate the manner in which grains are deposited there.

Middens at late Moloko sites are refuse heaps of broken pots, bone and other debris generated mostly from nearby domestic contexts, such as hearth ash and other sediment collected during sweeping and cleaning of hut floors, verandas and courtyards. In theory, a quartz grain would be bleached upon exposure to sunlight before it is blown into a hut, for example, and any grains associated with a hearth should be completely bleached, or 'zeroed,' from the heat. Midden deposits are subject to post-depositional bioturbation frequently because of their unconsolidated nature and high organic content. Geologically older grains from underlying sediments can be incorporated into the deposit by disturbance from domestic animals, rodents, insects and other burrowing creatures. Conversely, bleached grains from the surface can be reintroduced into lower layers.

For future OSL sampling of Iron Age middens, archaeologists should locate deep, well-consolidated deposits, collect from the centre of the stratigraphy (at least 30 cm deep but not too close to the bottom) and, if possible, collect near a horizontal lens or other feature that indicates no or little bioturbation has occurred. This sampling

strategy is possible because although middens are generally stratified, we assume that late Moloko midden deposits represent one chronological event. As related to sample Olif 1 and described below, this might not always be the case, but the length of time that late Moloko features were in use is usually relatively short and within the standard error of archaeometric dating techniques. If the researcher is sequence-aware and culturally oriented, the archaeology itself will alert an excavator about a multi-component site. One can try to establish the time represented by the bottom and the top of single component middens, considering issues of geologic inclusions and bioturbation.

Olifantspoort

The OSL age for the Olifantspoort midden sample Olif 1 (AD 1738-1794) can be compared to the broad oral-historical date (18th century to AD 1823-1838), but there is little known about the site from the oral-historical record. The age correlates directly with the Bayesian-calibrated radiocarbon date from the middle layer of the midden (1716-1850 cal AD; 50-60 cm), but does not overlap with radiocarbon dates from the upper layer (0-15 cm) or the lowermost (90 cm). OSL sample Olif 1 was collected at a depth of 30 cm, between the middle and upper radiocarbon samples.

This OSL result fits with the current hypothesis for the sequence of BaTswana aggregation into stone-walled towns (see Chapter 1 and Figure 1.3) and the complex cultural and archaeological context of the site on the hill at Olifantspoort farm. Huffman (2007) argues that there is an early or middle Moloko settlement component stratigraphically below the stone walled site, reflective of the major cultural shifts that occurred in this region over this period. The size of the ash heap sampled could be indicative of many hundreds of years of deposit, in which case Olif 1 might represent an admixture of different Moloko-age quartz grains from a midden location that was used consistently over time. This type of long stratigraphic sequence will not be the case for most Late Iron Age middens, since even deep examples usually represent a chronologically short duration of occupation. It does offer an opportunity for further testing of OSL dating for the Late Iron Age, if stratigraphically ordered samples can be retrieved from other deep midden features at Olifantspoort.

In addition, the Olifantspoort result may well be a reminder to practice archaeology carefully. As we know, Revil Mason previously excavated this feature. Though the midden is wide and deep, it is possible that, when collecting my sample, I did not move far enough away from his trench or sieve pile to avoid incorporation of stray old quartz grains from below and/or quartz grains that were partially bleached during his excavation. Both of these suppositions are supported by the high overdispersion of the range of D_e values for the Olif 1 sample ($67 \pm 8\%$).

Molokwane

The OSL age for the Molokwane midden sample Molo 1 (AD 1794-1822) can be compared to the broad oral-historical date (mid-18th century to AD 1827), but the oral-historical record is not exact for this settlement. The radiocarbon dates for Molokwane range from the early 16th to mid-20th century, but none are in stratified context, so it is not possible to use Bayesian radiocarbon calibration for these results. The deep and compacted OSL midden sample from Molokwane was collected at a depth of 30 cm and is an example of a deposit ideal for OSL dating. The defined ash lens through which the sample was collected implies minimal disturbance of the deposit in that position (see Figure 5.3) and the low overdispersion of the range of D_e values for the sample ($12 \pm 2\%$) indicated little mixing or partial bleaching of quartz grains.

This is the first precise chronometric result ever obtained for Molokwane. It supports the argument of Hall *et al.* (2007; 2008), developed from the archaeology and the oral-historical record, that the *kgosing* was in its final, impressive post-aggregation size and form between AD 1780-1827, during the rule of the powerful chief Kgaswane, and not earlier.

Kaditshwene

The OSL age for the Kaditshwene midden sample Kad 1 (AD 1773-1849) overlaps the oral-historical date (AD 1790-1823) and notably, at 1σ error, matches it almost exactly (AD 1792-1830). Because an OSL date is not calibrated, but is a direct

calendar age, the result can be truncated at AD 1823, the time of abandonment during the *difaqane*. The age correlates with the Bayesian-calibrated radiocarbon dates on charcoal from all three layers of the midden. This is expected, because the three radiocarbon ages are so close (200-180 BP plus associated errors), and because OSL sample Kad 1 was collected at a depth of 40 cm, between the upper and middle radiocarbon samples.

The deep and compacted midden sample from Kaditshwene was example of a deposit ideal for OSL dating. There was no overdispersion of the range of D_e values for the sample, indicating no mixing or partial bleaching of quartz grains. This OSL result can be used to refine the Bayesian-calibrated radiocarbon chronology for Kaditshwene. The earliest calibrated date ranges for the upper two charcoal samples (10-20 cm and 50-60 cm) can be disregarded outright. It is more difficult to interpret the result for the bottom half of the midden. There is no indication of a occupation at Kaditshwene earlier than the stone-walled town, and, as evidenced by the archaeology and in the oral-historical record, it is unlikely that the midden accumulated over many decades because of the generally short occupation time of Late Iron Age settlements. Therefore, it is reasonable to disregard the earliest calibrated radiocarbon date range for the lowermost charcoal sample as well, eliminating the possibility that the midden was deposited before the mid-18th century.

This imprecision can be resolved easily with a second OSL sample from the bottom half of the midden, which is included in plans for future work. I expect that the second OSL sample will correlate closely with the first, proving that the central *kgosing* at Kaditshwene was established in the late 18th century, and that in general, Late Iron Age middens accumulate over a short time, within the standard error range of chronometric dating techniques.

Marothodi

The OSL ages for the Marothodi samples are the first chronometric results for this site. The age for the Marothodi midden sample Vlak 1 (AD 1667-1735) does not correlate to the oral-historical date (AD 1800-1810 to AD 1823-1827), and Vlak 3 (AD 1761-1873) overlaps it very broadly. These results are less straightforward than

those for the other late Moloko sites and require archaeological and geomorphological explanation.

Sample Vlak 1 was collected near the base of a shallow midden (see Figure 6.7) at a depth of 25 cm. Incorporation of old quartz grains via bioturbation is more of a concern with shallower middens and for OSL samples collected close to the bottom of such deposits. It is difficult to predict the slope of the ground below a shallow deposit, and it is easy to scrape sterile sediment from a rising stratum into the collection tube accidentally. These are likely causes of the high overdispersion of the range of D_e values for Vlak 1 ($58 \pm 7\%$). Shallow midden deposits are not ideal for OSL dating, and samples collected from them by necessity should be taken from several cm above the base. In addition, dosimetry was not exact for this sample, as I already have mentioned, and generally the soil surface at Marothodi is subject to acute changes in water saturation over the year, as evidenced by the buckling of stone walls and other structural features. Nevertheless, the Vlak 1 midden result compares almost exactly with the age of the associated Vlak 2 furnace sample. This will be discussed further in the next section on the OSL dating of furnace samples.

OSL sample Vlak 3 was collected at a depth of 40 cm from a deep and below an ashy layer (see Figure 6.5). Vlak 3 has an extremely high overdispersion of the range of D_e values ($80 \pm 9\%$) for the 40 aliquots measured. This indicates that many quartz grains in this sample were only partially bleached, and therefore the luminescence intensity of those grains swamped the intensity of the fully bleached grains. It is also possible that old quartz grains were incorporated from bioturbation, or that the ashy layer represents a time near the beginning of the deposit, so that old grains were incorporated from below during sampling. Removing the four outlying aliquots (see Figure 6.17c) would decrease the overdispersion significantly and refine the OSL age. Because the D_e values of those aliquots are highly precise, however, discounting them would require sound justification either from the archaeology, the oral geography (which we have for this case, but not for many other sites in the region) or the geomorphology. This example underscores the importance of the archaeologist and luminescence specialist working closely together to interpret OSL results.

Furnace samples

For the furnace wall samples, the major consideration is correction of the luminescence sensitivity change in the quartz grains. These are not pottery specimens, but partly vitrified furnace wall ceramics. The more vitrified a furnace feature is, the more difficult it is to separate a piece from the rest of the furnace in the field, and the more physical force required to disaggregate the fragments in the laboratory. I suspect that this energy might have caused extra damage to the quartz crystalline structure or electron traps, not unlike the way that physical friction between two materials can cause an electrostatic discharge. Perhaps a less vigorous quartz extraction method can be devised for partly vitrified samples. A separation procedure that alternates between several physical and chemical separations might be more successful, but would increase pre-treatment time substantially.

In the SAR protocol for measuring OSL, the recycling ratio test evaluates the level of luminescence sensitivity change in the quartz grains on each aliquot. The recycling ratio failure rate of many furnace sample aliquots indicates that sensitivity change did occur. For the future, TL will be a better option for luminescence dating of furnace features, because the samples are simulated by heat, rather than light. The relatively low overdispersion for both furnace samples (about 19%) indicates that the temperature of a metallurgical smelt is sufficiently high to fully bleach the quartz grains in the furnace wall.

Kaditshwene

The OSL age for the Kaditshwene furnace sample Kad 2 (AD 1712-1800) overlaps the oral-historical date (AD 1790-1823) by about 10 years and correlates with the Bayesian-calibrated radiocarbon dates on charcoal from all three layers of the midden. Of the 24 aliquots of sample Kad 2 that were measured by OSL to obtain D_e , only six passed the recycling ratio test. The furnace at Kaditshwene was very highly vitrified and required very forceful extraction to disaggregate quartz grains from the sample. Although a statistically valid age can be obtained with only six data points, the result would be significantly more robust if there were more successful aliquots included in the analysis.

It is important to note that this sample was collected from an unexcavated feature at Kaditshwene, and we do not know anything about its archaeological context or contemporaneity with the *kgosing* midden. At 2σ error, and with correlation to the oral-historical date, we can say with 95% confidence that the young range of the OSL age (approximately AD 1790-1800) might represent an early episode of copper working at the settlement.

Marothodi

The age for the Marothodi furnace sample Vlak 2 (AD 1662-1738) does not correlate to the oral-historical date (AD 1800-1810 to AD 1823-1827), but compares almost exactly to the OSL result for midden sample Vlak 1 (AD 1667-1735), which is from the same homestead. Of the 24 aliquots of sample Vlak 2 that were measured by OSL to obtain D_e , only 10 passed the recycling ratio test, but the precision of 13 additional aliquots were sufficiently high to include in the statistical analysis. Before it can be accepted, this OSL result needs to be re-examined with more rigorous statistical methods.

Nevertheless, the exact age agreement between samples Vlak 1 and Vlak 2 is intriguing, and if the OSL results are indeed correct, archaeological and geological evidence might help interpret the presence of this small homestead at the site more than a century earlier than the *kgosing*. These samples were collected from settlement unit SU25, which, as described by Hall *et al.* (2006) is unlike any other homestead at Marothodi. SU25 was originally built with an internal cattle track, the remaining walls of which form something like a keyhole shape on the site plan (see Figure 6.4). The cattle entered the homestead from the south and walked around the central kraal before going inside. There is no other homestead at Marothodi with this architectural feature, and they do not occur at Molokwane or in the *kgosing* area at Kaditshwene. There is a major cattle track linking the hilltop site at Olifantspoort to the valley, visible in Figures 1.5 and 6.1, but none recorded within an individual homestead. In fact, the layout of SU25, coupled with the presence of surface metallurgical remains, is so unique that it made the homestead the first target for excavation by the UCT team (Hall, pers. comm.)

In addition, the archaeology at SU25 offers some stratigraphic information regarding the use of the internal cattle track. The path was blocked off in two places before the homestead was abandoned, as evidenced by the abutment of the midden (sampled for OSL age Vlak 1) with the obstructing wall. This suggests that neither the track nor the central kraal were used for cattle when the homestead was last inhabited (Hall *et al.* 2006: 30).

Lastly, the geology at Marothodi is unique, because there are copper ore sources directly adjacent to the site. While the artisans at Marothodi certainly used ore from this source, analytical and archaeological evidence indicate that the majority of quality ore was removed before the BaTlokwa ever arrived at the location (Hall *et al.* 2006: 28).

These observations, when coupled with the 17th-18th century OSL dates for SU25, support several interesting possible interpretations for that homestead. If it predates the large *kgosing*, then it is likely that SU25 was occupied before the period of BaTswana aggregation that began in about AD 1750. The structure of the internal cattle track might suggest that the first inhabitants of the homestead were not BaTswana, since its architectural form deviates from the characteristic settlement pattern of other late Moloko and modern ethnographic examples. Perhaps it represents an early exploitation of the nearby copper ore by an earlier group, and then reuse of the existing metallurgical setup (anvil stones, distinct furnace area) by one or more subsequent groups until the arrival of the BaTlokwa in the late 18th century. Certainly the presence of the copper ore at this site could have drawn metal workers to the area for centuries before Marothodi was established. After his recent rereading of the oral geography, Jan Boeyens notes that renowned anthropologist Isaac Schapera thought Marothodi was occupied as early as AD 1750 (Boeyens pers. comm. 2008). These are important issues that have to be considered with close collaboration between the archaeologist and dating specialist before the early OSL ages can be accepted.

Archaeological and geological considerations for OSL dating in the Late Iron Age

There are several general archaeological and geological considerations in OSL dating that are unique to the Late Iron Age context. Perhaps most important, as evidenced by the preceding discussion, an OSL age (as with any archaeometric result) must be evaluated carefully according to archaeological evidence on the integrity of the stratigraphy from which it was sampled and the security of its association with cultural artefacts.

It is important to note the depositional environment from which sediment was sampled. Determining the dose rate in a midden can be very complex. Whereas a quartz sand dune deposit is usually well sorted and nearly completely homogenous, an Iron Age midden, by definition, is a coarse, inconsistent feature full of artefacts and often rocks, tree roots or other debris. These inhomogeneities potentially can cause the dose rate to vary significantly from one sample location to another only a metre away.

Also, it is interesting to note how the chemistry of sample environments can be reflected directly in the amount of radioactive elements in the sediment. For example, midden sample Molo 1 was collected across an ash lens, and Mason described the midden at the site on Olifantspoort farm as an 'ash heap.' The high %K is indicative of the greater ash content in these samples as compared to those at Kaditshwene and Marothodi (see Figures 6.9-6.12). These examples highlight the value of planting *in-situ* dosimeters to measure the dose rate for a sample over a year, rather than relying on laboratory measurements to make an estimate, so that these incongruities can be incorporated into the final equivalent dose determination. The more control one has over all the potential sources of error in estimating equivalent dose, the more precise the resultant OSL age will be.

An additional consideration for dating in the Late Iron Age is the potential of veld fires to zero or partially bleach the luminescence signal of grains in a feature after a site is abandoned but before it is buried. In a pilot study on using archaeomagnetism to date late Moloko features, I determined that a hut door slide at Marothodi was

adequately fired (presumably when the hut burned naturally after abandonment) to have an archaeomagnetic signal (Rosenstein *et al.* in press). The alignment of iron-rich minerals that produces an archaeomagnetic signal occurs when ferromagnetic grains have been heated above their Curie temperature. The Curie temperature varies for different minerals, but generally is between 580°C - 680°C, well above the temperature that releases the luminescence signal from quartz grains, about 500 °C for quick-fired material (Feathers 2003: 1495).

This is not a concern for a hut that burned upon, or just after, abandonment, because the error inherent in the luminescence measurements will eclipse the difference between the true age of human occupation and a fire one or two years later. A fire that occurred a decade or two after abandonment is a greater concern, however, if the datable features are only shallowly buried at that time and the high heat of the fire is sustained. Additionally, if a tree that has grown into a midden burns, and its root system smoulders, that heat might also partially bleach the luminescence signal of buried quartz grains. These are difficult problems to plan for or perhaps even identify, but again, the value of close collaboration between the archaeologist and dating specialist cannot be stressed enough.

Another factor for the interpretation of OSL dates is the particular geologic history of the local quartz grains. It is useful to be familiar with the regional geology and potential quartz sources in order to evaluate the ages of discrete age populations in mixed samples, although partial bleaching can obscure the original geologic age of a grain. If there is feldspar in the local geology, this is also advantageous to know, since anomalous feldspar fading is a significant source of error in quartz OSL dating.

For the late Moloko samples, I am particularly interested in how the luminescence signal of quartz can be affected by micro-inclusions of other minerals in its crystalline structure. In my petrographic analyses of ceramics from early and late Moloko phase sites (this study, and see Rosenstein 2002), I found that rutilated quartz grains, for example, occur frequently in pottery from sites near the Bushveld Igneous Complex. Studies have shown that rutile exhibits weak luminescence at low temperature (up to 100°) in wavelengths from 350-600 nm, which includes blue light at 470 nm (Addiss *et al.* 1968; Melnyk *et al.* 2005). It is also possible that etching in HF acid fractures

rutilated grains where the rutile needles cause weakness in the crystalline structure. If this is true, the broken grains, reduced in size, would be removed from the dating sample in the resieving process after the etch and would not affect the D_e determination. Clearly, physical and luminescence properties of rutilated quartz are a potential problem for OSL dating in this context and worth investigating in the future.

THE FUTURE OF OSL DATING FOR THE LATE IRON AGE

By using OSL to date sediments at late Moloko settlements for which the age is generally known by the oral-historical record, this pilot study has shown that luminescence can be used to date Late Iron Age sites for which there is no or little oral-historical information, and that this technique is a good chronometric alternative to radiocarbon for the 17th-19th centuries. OSL ages for sediments sampled from clear stratigraphic contexts, yielding results with high precision and low overdispersion, can be very accurate. The results of this research are informative in several other aspects, offering insights on the use of optical dating for the recent past and how archaeologists can apply OSL more successfully in Iron Age chronometric studies in the future.

Besides midden sediment and furnace wall, other possible sample materials for OSL dating include potsherds, the most common artefacts at late Moloko sites, but their mobility makes them less optimal than an *in-situ* object or feature. It is difficult to be sure that a potsherd comes from a pot that was made at the site of interest and therefore contemporary with it. Pots commonly migrate with people, are reused and become heirlooms.

Comparatively, successful OSL or TL dates might be obtained from fragments of tuyère, the clay pipe manufactured to transmit air between the bellows and the interior of a metal smelting furnace. In fact, given the difficulty of obtaining precise OSL dates on the two late Moloko furnace samples, I expect that TL will continue to be a more successful method for dating fired features. Ideally, a single fired sample could

be dated by both luminescence techniques, as a way to compare the resolution and applicability of each for archaeometallurgical remains.

At sites where smelting took place, tuyère samples are preferable to pottery or furnace wall dating for several reasons. Generally, tuyère pipes are produced of local clay, often a poor quality fabric full of quartz sand that is unsuitable for pottery manufacture but perfectly functional for the smelting process, and in almost every instance, tuyères are used and discarded at the place of smelting. Prefabricated tuyères are kept nearby to replace failed pipes, and used and broken tuyères almost always are found near the furnace at which they were employed; tuyères are large and bulky to transport around the landscape or even the smelting site. Thus, whereas the age or provenance of a pot in relation to where it is excavated can be dubious, a tuyère is unlikely to be found far from its context of use. In a smelting atmosphere that commonly reaches 1000°C or more, tuyères are fired well above the temperature needed to zero a luminescence signal in quartz, about 300°C for slow-fired material (Feathers 2003: 1495).

Another avenue to explore is luminescence dating of quartz grains from the interior of structural features, such as hearths, door slides and daga walls, which are often heated in natural fires or in intentional hut fires upon or after site abandonment. Treating the sample as a low-fired ceramic, researchers have successfully dated adobe (mudbrick) walls from archaeological sites in the southwest United States by luminescence (Feathers 2007). Given the difficulties in understanding the luminescence sensitivity change in quartz grains from partly vitrified furnace samples, the low-fired nature of door slides and daga walls might make them a better option for OSL dating.

It is clear that luminescence will be a valuable chronometric tool for dating the Iron Age. OSL dating is a developing method, only a few decades old, and this research has contributed to assessing the applicability of OSL dating in the recent past. Control over many of the issues and difficulties with OSL dating described in this chapter can be established in the field. Just as the value of a radiocarbon date is only as good as the security of the archaeological context in which it was sampled, the same holds for OSL ages. In order to make best use of the substantial expense for an OSL date, Iron Age archaeologists need to understand luminescence in terms of the

nature of Iron Age deposits. These are not pure quartz sand dunes, but complicated cultural units from complex sites. By targeting carefully selected features, such as deep middens with long stratigraphic sequences, we can begin to use OSL to obtain archaeometric dates for many of the major sites in southern Africa that were occupied during a time over which radiocarbon dating is ineffective and oral-historical records are unavailable or unreliable.

Chapter 8

Conclusion

The archaeological and oral-historical records of the late Moloko in the 18th and early 19th centuries point towards the strategies used by the BaTswana to manage a sociopolitical crisis brought on by competition for land and leadership, the advance of the colonial frontier, desire for colonial trade goods, environmental pressures, and, beginning in the 1820s, reactive militarism of the Ndebele under Mzilikazi (Manson 1995). The aggregation of thousands of people into several stone-walled towns in the Rustenburg-Zeerust area during this period attests to the remarkable scale of change in political power and the regional economy. Shifts are recognizable at a smaller scale, as well, as evidenced by innovation and standardization of late Moloko ceramic technology at western BaTswana towns.

SORTING OUT CERAMICS

The lack of added lustrous, platy or asbestiform tempers in pottery from Marothodi, as determined in this research, may hint at important questions about the identity of the town's inhabitants. While some of the oral-historical records associate the BaTlokwa at Marothodi with the other western BaTswana lineages, including the BaKwena at Olifantspoort and Molokwane and the BaHurutshe at Kaditshwene, recent reinterpretation of the record and the archaeology suggests that the origins of the BaTlokwa are ambiguous and likely of Nguni ancestry (Hall *et al.* 2007; Huffman 2007; Hall *et al.* 2008). Both Ellenberger (1939) and Breutz (1953) note that the oral testimony do not obviously place the BaTlokwa or the BaFokeng within the western BaTswana world. The ceramic data suggests that this expression of uncertainty was correct. The oral-historical record raised an issue to which the ceramics intimate an answer. While the classically western BaTswana potters shifted towards adding these characteristic inclusions to the clay body, the BaTlokwa maintained a technological style without distinctive temper.

These scales of analysis require more chronological control than is offered by radiocarbon dating or the oral-historical record. As I have shown in this thesis, OSL dating is a viable chronometric method to use for the Late Iron Age, and it offers the precision necessary for resolving the 18th and 19th century settlement sequence in the Rustenburg-Zeerust region.

FUTURE DIRECTIONS

This study has opened up several future avenues of research. There is interesting work to be done mapping the wider distribution of different types of temper and scientifically characterizing the specific inclusions late Moloko potters used to temper a clay body. The addition of mineral tempers can be interpreted at different scales. Generally, on a macroscopic scale, lustrous inclusions relate to the principle of 'pots are people' and body decoration, and can be identified by visual inspection of a pot sherd with a hand lens. On a microscopic scale, the provenance of a vessel can be determined according to classification of specific lustrous or graphitic minerals, matching it either to the source location of the temper or to the clay used in manufacture. The local variability of minerals and clay sources, based on geology, help to answer questions about trade, mobility and identity. Future research will include macro- and microscopic analysis of additional vessels from different but strategically located sites chosen according to the oral geography as explained in Chapter 4.

BaTswana potters purposefully added lustrous, platy and asbestiform minerals into clay for ceramic manufacture. They were aware that these easily recognizable minerals directly correlated to more efficient ceramic production, and I have argued that these qualities were inseparable from distinct aesthetic properties. Once the range of minerals used is identified, their thermodynamic properties can be modeled, identifying the specific ways in which those tempers affect the strength and firing of the vessel.

Understanding this change in ceramic technology requires future sampling of sites for pottery through the 18th and 19th centuries that unequivocally relate to Nguni-speakers, for example the BaPo. It also is necessary that the chronology of site settlement is refined. For accurate interpretation of the late Moloko ceramic sequence, it is worthwhile to determine if the added tempers comprise technological changes that developed through the 18th century or that arise abruptly in the 19th century. If the dating resolution can be improved for a site like Olifantspoort, for example, at which there are ceramics representing the entire Moloko sequence for the Rustenburg-Zeerust region, the resulting chronology could be used to accurately cross-date pottery from all the other Moloko settlements. More generally, there are other issues in the Late Iron Age linked directly to the timing and progression of shifts on the regional landscape. These include central arguments related to the availability of resources, migration and adoption of new agricultural methods, and it is important to assess how these events relate to dated fluctuations in climate, and to cooler and drier conditions (see Figure 1.3 and the associated discussion).

The prospects for continuing to use luminescence for dating Late Iron Age sites in southern Africa are exciting. There are two additional date ranges during the last millennium where de Vries effects cause a small plateau in the radiocarbon calibration radiocarbon curve, although much less acute than the effects beginning in about AD 1650 (see Figure 3.3). These are roughly AD 1300-1400 and AD 1500-1600. Notably, the former range encompasses the demise of the powerful state at Mapungubwe and the subsequent emergence of a new centre at Great Zimbabwe. Although methods such as Bayesian radiocarbon calibration improve the interpretation of overlapping dates, greater chronometric precision at the outset can help refine the dating of the entire Late Iron Age.

Luminescence dating is expensive, however, and it is not feasible, or even perhaps necessary, to re-date all of the most important sites of the Late Iron Age. But for the recent past, luminescence dating is significantly more accurate than is possible with radiocarbon, and this is the basis of the chronometric aspect of a newly funded research project under the African Origins Platform of the National Research Foundation. The goal of the Five Hundred Year Initiative is to understand the last 500 years of southern African history through an interdisciplinary research program

involving archaeologists, anthropologists, linguists, historians and climate scientists. With an explicit, well-planned sampling strategy, luminescence can be used as an anchor for archaeomagnetic dating, a relative dating technique.

On ongoing objective of the Five Hundred Year Initiative is to establish an archaeomagnetic master curve for this region of southern Africa, and my work provides an initial contribution to this.² The construction of an archaeomagnetic master curve requires the location of *in-situ* archaeological features that can be measured for archaeomagnetic direction at time of last exposure to heat above about 600 °C and also dated by an absolute dating method, such as luminescence. For this project, I will focus on hearths, door slides, daga walls and furnaces. In a pilot study, I determined that these types of features are sufficiently fired to obtain archaeomagnetic directions (Rosenstein *et al.* in press). Extrapolation of records for magnetic declination and inclination at Cape Town beginning in AD 1595 suggests that the drift of magnetic field in the region and time of interest would be sufficiently rapid to yield high precision archaeomagnetic dates over a short period (Brock 1977).

Archaeomagnetism is potentially the best method for relative, and eventually absolute, dating of sites in this temporal and geographic context. This research will be an important contribution to our field, because it will become possible to obtain meaningful archaeometric dates for Late Iron Age sites. This is essential, because the cost of one OSL date is the same as that of three or four archaeomagnetic dates. Once this initial outlay of time and money for an extensive suite of luminescence dates is concluded, and the archaeomagnetic master curve is complete, archaeomagnetism can replace luminescence as the preferred chronometric method for the second half of the Late Iron Age.

² This research is a shared effort with two dating scientists, Dr James Feathers, a luminescence specialist, and Dr Stacey Lengyel, an archaeomagnetic dating specialist. Already, our collaboration has raised interesting possibilities at Smelterskop, a tin production site in the Rooiberg valley, Limpopo Province, where archaeological work is ongoing with Dr Simon Hall, Dr David Killick and Dr Shadreck Chirikure.

Appendix A

**Table of Previous Early and Late Moloko
Ceramics Analysed (Rosenstein 2002)**

Excavated reference	Study reference	Phase; site	Vessel type	Decoration	Comments
29/72 (2527CD35) A. Pot 5	OE/1	Early Moloko; Olifantspoort	unknown	plain	
29/72 (2527CD35) Hut J	OE/2	Early Moloko; Olifantspoort	unknown	plain	
29/72c	OE/3	Early Moloko; Olifantspoort	bowl?	plain	Incision on interior wall.
29/72c Hut I pot 3	OE/4	Early Moloko; Olifantspoort	bowl?	plain	Black graphite interior, red ochre exterior – possibly a bowl?
29/72 (2527CD35)	OE/5	Early Moloko; Olifantspoort	bowl?	plain	Red ochre inside and outside – indeterminate body sherd.
29/72 I (2527CD35)	OE/6	Early Moloko; Olifantspoort	unknown	plain	
55/75	RO/1	Early Moloko; Roberts farm	unknown	plain	
20/71 Hut J	OL/1	Late Moloko; Olifantspoort	unknown	plain	
20/71 Hut Ai	OL/2	Late Moloko; Olifantspoort	unknown	plain	
20/71 Hut G	OL/3	Late Moloko; Olifantspoort	unknown	plain	
20/71 Hut B4?	OL/4	Late Moloko; Olifantspoort	unknown	plain	
20/71 Hut B	OL/5	Late Moloko; Olifantspoort	unknown	plain	
20/71 I/O/F (midden)	OL/6	Late Moloko; Olifantspoort	unknown	plain	
20/71 VI/N/W (midden)	OL/7	Late Moloko; Olifantspoort	unknown	plain	
20/71 unprovenanced	OL/8	Late Moloko; Olifantspoort	unknown	plain	
20/71 II/0-10 (midden)	OL/9	Late Moloko; Olifantspoort	unknown	plain	
20/71 VII/30-40 (midden)	OL/10	Late Moloko; Olifantspoort	unknown	plain	Red ochre exterior.

Excavated reference	Study reference	Phase; site	Vessel type	Decoration	Comments
SEL2.3/A.5	M/1	Late Moloko; Molokwane	unknown	plain	Strongly curved plain body sherd.
SEL2.8/C.2	M/2	Late Moloko; Molokwane	unknown	plain	
SEL2.1/A.1.2	M/3	Late Moloko; Molokwane	jar?	plain	Profile suggests shoulder-body sherd
SEL2.8/F.3	M/4	Late Moloko; Molokwane	unknown	plain	Curved body sherd.
SEL2.3/F.2	M/5	Late Moloko; Molokwane	unknown	plain	Curved body sherd.
SEL2.10/A.1	M/6	Late Moloko; Molokwane	globular pot	plain	Beaded rim with exterior burnish.
SEL2.10/A.1	M/7	Late Moloko; Molokwane	globular pot?	plain	Slightly concave sherd from just below rim of globular pot?
SEL2.6(C) (a-c) 3 hut front <i>malapa</i>	M/8	Late Moloko; Molokwane	globular pot	plain	Large rim sherd.
SEL2.1/Z.2	M/9	Late Moloko; Molokwane	unknown	plain	Thick body sherd.
SEL2.3/D.1	M/10	Late Moloko; Molokwane	unknown	plain	
RFN 2.1	R/1	Early Moloko; Rietfontein	bowl	comb stamped & incised	Rim band of fine diagonal comb stamping with two incised zigzag bands below separated by horizontal incision. From lip, color order is: graphite, graphite, ochre, graphite, ochre. Interior red ochre.
RFN 2.1	R/2	Early Moloko; Rietfontein	bowl	punctates & incision	Incised band below rim, filled with punctates. Interior red ochre.
RFN 2.1	R/3	Early Moloko; Rietfontein	bowl?	diagonally incised bands	Body sherd from bowl? With two bands filled with diagonal incision separated by graphite bands. Interior black graphite.
RFN 2.1	R/4	Early Moloko; Rietfontein	unknown	plain	Thick walled body sherd – possibly jar or globular pot.

Appendix B

Table of Early and Late Moloko Ceramic Data (Rosenstein 2002)

Sample	Munsell Colour Designation <i>interior</i> <i>centre</i> <i>exterior</i>	Sherd Thickness	Modal % of Inclusions	Incl. Sizes - Mode; Max	Mineral Inclusions						Lithic Inclusions				Probable Geologic Correlation; Other Comments
					Ms	And	Qtz	Fsp	Pyx	Amp	Gra-talc	Gran	Met/Wea	Opq	
OE/1	2.5YR 4/6 red 7.5YR 3/1 very dark gray 7.5YR 3/2 dark brown	10.5	45	0.3; 1.1		++	++	++				++	+	-	Bushveld; abundant fibrous/needle-like metamorphic mineral; also possibly chrome spinel
OE/3	7.5YR 3/2 dark brown 5YR 4/3 reddish brown 5YR 2.5/1 black	9.0	35	0.3; 2.3			++	++	++	+		++	-		
OE/4	2.5YR 4/8 red 7.5YR 2.5/1 black 2.5YR 5/8 red	8.0	45	0.2; 1.4			++	++		++		++	+		
OE/5	5YR 5/8 yellowish red 7.5YR 4/1 dark gray 5YR 5/6 yellowish red	7.3	30	0.3; 2.4			++	++	+	++		+	++	+	
OE/6	5YR 5/4 reddish brown 7.5YR 2.5/1 black 7.5YR 4/3 reddish brown	11.0	35	0.4; 1.5			++	++	+	+					Bushveld; possibly same clay as OL/3 and OL/5

Appendix B

Sample	Munsell Colour Designation <i>interior</i> <i>centre</i> <i>exterior</i>	Sherd Thickness	Modal % of Inclusions	Incl. Sizes - Mode; Max	Mineral Inclusions						Lithic Inclusions				Probable Geologic Correlation; Other Comments
					Ms	And	Qtz	Fsp	Pyx	Amp	Gra- talc	Gran	Met/ Wea	Opq	
OE/2	5YR 5/6 yellowish red 7.5YR 6/4 light brown 5YR 5/6 yellowish red	12.3	40	0.5; 2.8				++						-	Bushveld; smaller inclusions; possibly vitrified fabric
RO/1	5YR 5/4 reddish brown 7.5YR 4/2 brown 5YR 5/4 reddish brown	7.0	25	0.1; 0.8				++	+				-		
R/1	GLEYS 1 2.5/N black GLEYS 1 2.5/N black GLEYS 1 2.5/N black	9.0	30	0.1; 0.9			++	++		++				-	Bushveld (Transvaal mix?); generally finer inclusions; quartz also occurs as chert and possibly rutilated locally
R/3	2.5YR 5/6 red 5YR 3/3 dark reddish brown 2.5YR 4/6 red	9.0 - 10.0	45	0.2; 1.4			++	+		+		+			
R/2	2.5YR 4/6 red 5YR 5/6 yellowish red 5YR 5/6 yellowish red	7.0	30	0.3; 1.3			++	++		+		+	-		Bushveld; generally coarser inclusions; quartz possibly rutilated locally
R/4	2.5YR 5/8 red 7.5YR 4/4 brown & 5YR 5/6 yellowish red 2.5YR 5/6 red	12.5 - 17.0	45	0.2; 2.0		++	++	+		+		+	-		Bushveld (Transvaal mix?); green-to-brown hornblende, neoblastic quartz

Appendix B

Sample	Munsell Colour Designation <i>interior</i> <i>centre</i> <i>exterior</i>	Sherd Thickness	Modal % of Inclusions	Incl. Sizes - Mode; Max	Mineral Inclusions						Lithic Inclusions				Probable Geologic Correlation; Other Comments
					Ms	And	Qtz	Fsp	Pyx	Amp	Gra- talc	Gran	Met/ Wea	Opq	
MD/3	5YR 4/6 yellowish red 7.5YR 4/4 brown 7.5YR 4/4 brown	10.0	30	0.3; 2.1		++	++	++	++	++					TV and BV mix; twinned plagioclase plus weathered amphibole;
MD/5	5YR 5/8 yellowish red 7.5YR 5/4 brown 7.5YR 5/4 brown	7.0 - 8.0	30	0.3; 1.4		++	++	++	++	++				-	'dirty' fabric - many micron-sized grains in clay; many fibrous overgrowths, alterations, inclusions
MD/6	5YR 5/8 yellowish red 7.5YR 4/4 brown 5YR 5/8 yellowish red	8.5 - 10.0	25	0.2; 1.7		?	++	++	++	++				-	
MD/1	2.5 YR 4/6 red 5YR 3/2 dark reddish brown 2.5YR 4/6 red	12.0 - 14.0	40	0.3; 1.9			++	++		++				++	BV; twinned plagioclase; significant opaque content; MD/4 - vry weathered microcline suggests additional, unknown source
MD/4	2.5YR 4/6 red 2.5YR 4/4 reddish brown 2.5YR 4/4 reddish brown	7.0 - 8.0	40	0.3; 2.1		++	++	++	++	++				++	
MD/7	5YR 2.5/1 black 5YR 3/3 dark reddish brown 5YR 3/3 dark reddish brown	9.0	35	0.3; 2.2		++	++	++						++	

Appendix B

Sample	Munsell Colour Designation <i>interior</i> <i>centre</i> <i>exterior</i>	Sherd Thickness	Modal % of Inclusions	Incl. Sizes - Mode; Max	Mineral Inclusions						Lithic Inclusions				Probable Geologic Correlation; Other Comments
					Ms	And	Qtz	Fsp	Pyx	Amp	Gra- talc	Gran	Met/ Wea	Opq	
MD/2	10R 4/8 red 7.5YR 3/1 very dark gray 2.5 YR 4/8 red	12.0	35	0.3; 2.4		-	++	++		++		++			TV; quartzite inclusions?; possible BV source of significant quartz and feldspar, but not determinable
MD/8	2.5YR 4/4 reddish brown 7.5 YR 4/4 brown & 10YR 3/2 v dark grayish brown 2.5YR 4/6 red	9.0 - 11.0	30	0.2; 2.6		?	++	++		++					
MD/9	5YR 3/3 dark reddish brown 7.5YR 3/2 dark brown 2.5YR 4/6 red	8.0 - 11.0	45	0.4; 1.2		++	++	++		-					TV; ncoblastic quartz; quartz- and feldspar- dominated fabric
OL/3	7.5YR 2.5/1 black 5YR 4/1 dark gray & 7.5YR 5/4 brown 2.5YR 5/6 red	7.0 - 8.0	45	0.5; 1.3			++	++	++	+			+		BV; possibly same clay as OE/6; OL/5 - large rock fragment inclusions with fibrous/needle-like metamorphic mineral inclusion
OL/5	5YR 5/6 yellowish red 7.5YR 2.5/1 black 5YR 5/6 yellowish red	6.0 - 6.5	40	0.4; 0.9			++	++	+	++					
OL/6	5YR 4/6 yellowish red 5YR 4/6 yellowish red 5YR 4/6 yellowish red	9.0	40	0.6; 2.5	++			-			-	-	+	+	TV and BV mix?; dominant mica with one granophyre and a few weathered plagioclase incls.

Appendix B

Sample	Munsell Colour Designation <i>interior</i> <i>centre</i> <i>exterior</i>	Sherd Thickness	Modal % of Inclusions	Incl. Sizes - Mode; Max	Mineral Inclusions						Lithic Inclusions				Probable Geologic Correlation; Other Comments
					Ms	And	Qtz	Fsp	Pyx	Amp	Gra- talc	Gran	Met/ Wea	Opq	
OL/2	5YR 5/6 yellowish red gray 4/N very dark gray 7.5 YR 5/6 strong brown	5.0 - 6.0	35	0.3; 1.9			+	+			++		++		TV-dominated (graphite-talc and mica); some weathered BV grains; M/7 - more graphite-talc than OL samples; OL/4 - red inclusions - possibly grog, garnet, or vitrification?
OL/4	5Y 5/1 gray 7.5YR 4/4 brown 7.5YR 4/4 brown	10.5 - 11.5	25	0.4; 2.2							++		++	+	
OL/7	5YR 4/4 reddish brown 5YR 4/4 reddish brown 5YR 4/6 yellowish red	9.3	25	0.3; 2.1			-	-	-		++		++		
M/7	10YR 6/3 pale brown gray 1 3/N very dark gray 10YR 5/3 brown	8.0 - 10.0	30	0.4; 4.5							++		++	+	
OL/9	2.5YR 3/4 dark reddish brown 2.5YR 3/4 dark reddish brown 2.5YR 3/4 dark reddish brown	8.5 - 9.0	30	0.3; 3.4	++										TV; clay is fibrous, 0.1 mm fibers define orientation of fabric; round, dark, slightly reflective aggregates of clay body - vitrification?
M/3	5YR 4/4 reddish brown 5YR 3/3 dark reddish brown 5YR 4/3 reddish brown	7.0	20	0.2; 2.2	++						+		++	?	

Appendix B

Sample	Munsell Colour Designation <i>interior</i> <i>centre</i> <i>exterior</i>	Sheet Thickness	Modal % of Inclusions	Incl. Sizes - Mode, Max	Mineral Inclusions						Lithic Inclusions				Probable Geologic Correlation; Other Comments
					Ms	And	Qtz	Fsp	Pyx	Amp	Gr- talc	Gran	Met/ Wea	Opq	
OL/1	5YR 5/4 reddish brown GLE 4/N very dark gray 7.5YR 6/6 reddish yellow	9.3	25	0.4; 2.2	++ bt?		+					-	+		TV and some BV; dominated by intergrown micaceous incls. and quartz with unidentified prismatic inclusions.
OL/8	7.5YR 6/4 light brown 7.5YR 2.5/1 black 7.5YR 6/6 reddish yellow	6.0	25	0.3; 2.1			++	++					?	-	Unknown, anomalous fabric; possibly chert, possibly severely metamorphosed or weathered grains
OL/10	5YR 5/4 reddish brown 5Y 5/1 gray 2.5YR 5/6 red	8.3 - 9.0	25	0.3; 3.0	++ bt	++							+		TV; few inclusions besides mica and andalusite; muscovite locally intergrown with biotite
M/4	5YR 5/3 reddish brown 10YR 4/1 dark gray 5YR 5/8 yellowish red	7.5 - 8.0	45	0.3; 3.0	++	++	+			-	++			-	TV; andalusite grains with reaction 'glimmer' rims
M/10	5YR 4/4 reddish brown 10YR 4/1 dark gray 2.5YR 4/8 red	8.0 - 8.7	25	0.3; 2.2	+	++					++		++		

Appendix B

Sample	Munsell Colour Designation interior centre exterior	Sherd Thickness	Modal % of Inclusions	Incl. Sizes Mode: Max	Mineral Inclusions						Lithic Inclusions				Probable Geologic Correlation; Other Comments
					Ms	And	Qtz	Fsp	Pyx	Amp	Gra- talc	Gran	Mét/ Wea	Opq	
M/8	5YR 4/6 yellowish red 5YR 5/4 reddish brown 10YR 6/3 pale brown	8.0 - 9.0	30	0.5; 2.0			++	++		-			-		Anomalous sample; possibly very weathered BV and TV mix?; neoblastic quartz, plagioclase
M/1	5YR 5/8 yellowish red 7.5YR 3/1 very dark gray 5YR 4/6 yellowish red	9.5	40	0.5; 3.2	-	++	+				++		+	-	TV; M/1, M/2, M/9 - high % of talc fragments; M/1 - geometrically structured graphite-talc fragments; M/2 - red-brown to green amphibole possible hornblende?; M/9 - rounded, yellow, isotropic inclusions - possibly garnet, spinel, or vitrification?
M/2	2.5YR 5/6 red GLEY 1 5/N gray 2.5YR 5/8 red	8.0 - 9.0	25	0.3; 3.0	+	++				-	++		+	-	
M/5	7.5YR 6/4 light brown GLEY 1 3/N very dark grey 5YR 5/6 yellowish red	7.0 - 8.0	25	0.2; 1.9		++					++		+	-	
M/6	5YR 5/6 yellowish red GLEY 1 3/N very dark grey 5YR 5/6 yellowish red	7.5 - 8.0	25	0.3; 2.3		+	+				++		++	-	
M/9	2.5YR 5/6 red GLEY 1 3/N very dark gray 2.5YR 4/1 dark reddish gray	13.0 - 14.5	30	0.4; 3.0							++		+	-	

Appendix B

Sample	Munsell Colour Designation interior centre exterior	Sherd Thickness	Modal % of Inclusions	Incl. Sizes - Mode; Max	Mineral Inclusions						Lithic Inclusions				Probable Geologic Correlation; Other Comments
					Ms	And	Qtz	Fsp	Pyx	Amp	Gra- talc	Gran	Met/ Wea	Opq	
KF/2	2.5YR 4/6 red 5YR 4/1 dark gray 2.5YR 4/6 red	9.0 - 11.0	45	0.3; 2.8	++		++	++		++					TV; high quartz and feldspar content but no twinned plagioclase; possible BV component but not conclusive; orientation of mica grains defines clay fabric direction;
KF/4	2.5YR 4/4 reddish brown 7.5YR 4/4 brown 2.5YR 4/6 red	11.5 - 15.0; 8.5 rim	40	0.3; 1.6	++		++	++		+	+				polygranular quartz aggregates with needle- like inclusions overlying - weathering?; altered amphibole, pyroxene
KF/6	7.5YR 3/1 very dark gray 7.5YR 3/2 dark brown 5YR 4/6 yellowish red	12.5 - 13.5	40	0.3; 2.4	++		++	++		+	-		-		
KF/7	2.5YR 4/6 red 5YR 3/3 dark reddish brown 2.5YR 4/6 red	7.0 - 8.0	45	0.4; 3.2	++		++	++			+		-		
KF/9	5YR 3/3 dark reddish brown 5YR 2.5/1 black 5YR 3/3 dark reddish brown	12.5; 8.0 rim	45	0.3; 1.9	++		++	++		+	-		+		
KF/10	2.5YR 3/3 dark reddish-brown 5YR 2.5/1 black 5YR 3/3 dark reddish brown	8.0 - 8.5	45	0.4; 1.1			++	++			-		+		

Appendix B

Sample	Munsell Colour Designation interior centre exterior	Sherd Thickness	Modal % of Inclusions	Incl. Sizes - Mode: Max	Mineral Inclusions						Lithic Inclusions				Probable Geologic Correlation; Other Comments
					Ms	And	Qtz	Fsp	Pyx	Amp	Gra- talc	Gran	Met/ Wea	Opq	
KF/1	2.5YR 4/8 red 7.5YR 4/2 brown 2.5YR 4/6 red	12.5; 4.0 rim	45	0.3; 3.6	++		++	++		++	+	+	+		TV; very high % of inclusions; large polygranular calcic amphiboles, up to 1.4 mm, some needle-like
KF/8	5YR 3/1 dark reddish brown 5YR 3/1 dark reddish brown 5YR 3/1 dark reddish brown	9.0; 6.0 rim	45	0.2; 1.8	++		++	++		++	+		-		
KF/3	5YR 2.5/1 black 5YR 2.5/1 black 5YR 3/1 very dark gray	6.5; 5.0 rim	45	0.5; 2.8	++		++	-							TV; long mica laths define orientation of clay fabric; angular quartz up to 1 mm; relatively coarser fabric compared to other Kaditshwene samples
KF/5	2.5YR 4/6 red GLEY1 3/N very dark gray 2.5YR 5/8 red	9.0 - 9.7; 8.0 rim	25	0.5; 3.6		++	-	++			++				TV; needle-like talc in graphite-talc nodules; possible vitrification; relatively coarse andalusite grains up to 1.4 mm

Notes on Appendix B

The site and sample designations are as follows:

OE	Olifantspoort, early Moloko component
RO	Roberts Farm, early Moloko (2 km from Olifantspoort)
R	Rietfontein, early Moloko
MD	Madikwe, early Moloko
OL	Olifantspoort, late Moloko
M	Molokwane, late Moloko
KF	Kaditshwene, late Moloko

The color of ceramic sherds is described from the exterior surface to the interior surface. For example, 'red br/yell or - dark br - red or' denotes a red-brown and yellow-orange mixed-color exterior rind, a dark brown center section, and a red-orange interior rind.

All measurements are in millimeters (mm).

Relative amounts of inclusions present are symbolized as follows:

-	Trace
+	Medium
++	Rich
?	Possibly present, more analysis needed.

Mineral inclusion abbreviations are as follows:

Ms	Muscovite	Pyx	Pyroxene
And	Andalusite	Amp	Amphibole
Qtz	Quartz	Bt	Biotite
Fsp	Feldspar	Plag	Plagioclase feldspar

Lithic inclusion abbreviations are as follows:

Gra-talc	Graphite-talc nodules
Gran	Granophyres (quartz and feldspar intergrowths)
Met/Wea	Unidentifiable metamorphosed or extremely weathered rock fragments, some micaceous (possibly schists).

'Opq' is the abbreviation for Opaques, most likely metal oxides.

'BV' denotes likely association with igneous and locally metamorphosed Bushveld Complex source material.

'TV' denotes likely association with sedimentary and locally metamorphosed Transvaal Supergroup source material.

Appendix C

Table of Marothodi Ceramics Analysed

Sample	Group	Collection Reference Label	Provenience Label	Sherd Type	Comments
VL-11-M4A	A	SU1/KG1/M4	Back right verandah	Body	
VL-11-M4B	A	SU1/KG1/M4	Back right verandah	Pot Lid	
VL-11-M11A	A	SU1/KG1/M11	Hut mound, back right	Body	High status area.
VL-11-M11B	A	SU1/KG1/M11	Back hut? mound	Rim	High status area.
VL-11-M11C	B	SU1/KG1/M11	Back hut? mound	Thick Body	High status area.
VL-11-M12A	B	SU1/KG1/M12	Hut? mound for front	Body	
VL-11-M12B	B	SU1/KG1/M12	Stone circle, back right	Rim	
VL-11-M12C	A	SU1/KG1/M12	Stone circle, back right	Thick Body	
VL-11-M14A	A	SU1/KG1/M14	From pot stand	Rim	Matching section VL-11/M14B in Group 3.

Appendix C

Study Reference	Group	Collection Reference	Provenience Label	Sherd Type	Comments
VL-11-M14B	B	SU1/KG1/M14	From pot stand	Thick Body/Base?	Potter built up thickness? Matching section VL-11/M14A in Group 1.
VL-11-MDA	A	SU1/KG1/MID	Midden enclosure, east side	Body	Decorated.
VL-11-MDB	C	SU1/KG1/MID	Midden enclosure, east side	Body	Micaceous.
VL-11-MDC	B	SU1/KG1/MID	Midden enclosure, east side	Body	Feldspar tempered?
VL-12-M2A	B	SU1/KG2/M2	Hoe pot	Rim	Matching section VL-12-M2B.
VL-12-M2B	B	SU1/KG2/M2	Hoe pot	Body	Matching section VL-12-M2A.
VL-13-M11A	A	SU1/KG3/M11	Hut mound front	Body	High status area.
VL-13-M11B	F	SU1/KG3/M11	Hut mound front	Pot Lid	High status area.
VL-13-M11C	A	SU1/KG3/M11	Front of hut mound	Body	High status area. Laminated? Matching section VL-13-M11D.
VL-13-M11D	A	SU1/KG3/M11	Front of hut mound	Body	High status area. Cut across 'lamination.' Matching section VL-13-M11C.
VL-14-M7A	A	SU1/KG4/M7	Front left, stone circle	Rim	Decorated. Matching sections VL-14-M7B, VL-14-M7C.

Appendix C

Study Reference	Group	Collection Reference	Provenience Label	Sherd Type	Comments
VL-14-M7B	A	SU1/KG4/M7	Front left, stone circle	Upper Body	Decorated. Matching sections VL-14-M7A, VL-14-M7C.
VL-14-M7C	A	SU1/KG4/M7	Front left, stone circle	Lower Body	Not decorated. Matching sections VL-14-M7A, VL-14-M7B.
VL-3-M5A	B	SU3/M5	Back of hut mound	Rim	Matching sections VL-3-M5B, VL-3-M5C.
VL-3-M5B	A	SU3/M5	Back of hut mound	Pot Lid	Matching sections VL-3-M5A, VL-3-M5C.
VL-3-M5C	D	SU3/M5	Back of hut mound	Body	Matching sections VL-3-M5A, VL-3-M5B.
VL-3-M8A	A	SU3/M8	Back of hut mound with pot stand	Pot Lid	
VL-3-M9A	B	SU3/M9	From hut? mound	Body	Decorated with red ochre.
VL-3-M11A	F	SU3/M11	From stone circle, front left	Rim	Complete pot profile. Black rounded particles (minerals or rock fragments?) loose in bag.
VL-3-M11B	F	SU3/M11	From stone circle, front left	Body	Complete pot profile. Black rounded particles (minerals or rock fragments?) loose in bag.
VL-3-M18A	A	SU3/M18	Back of hut mound	Thin Body	Complete pot (matching section VL-3-M18B).

Study Reference	Group	Collection Reference	Provenience Label	Sherd Type	Comments
VL-3-M18B	A	SU3/M18	Back of hut mound	Thick Body	Complete pot (matching section VL-3-M18A).
VL-4-M1A	E	SU/M1	Hut mound in front of furnace	Rim	Matching section VL-4-M2B
VL-4-M1B	E	SU/M1	Hut mound in front of furnace	Body	Matching section VL-4-M2A
VL-4-M2A	A	SU/M2	Hut back	Body	
VL-5-M3A	A	SU5/M3	Between two stone circles	Pot Lid	
VL-5-M3A (2)	A	SU5/M3	Between two stone circles	Pot Lid	
VL-5-M5A	C	SU5/M5	Front stone circle	Body	Micaceous.
VL-6-M1A	A	SU6/M1	Behind forge furnace	Thin Body	
VL-6-M1B	A	SU6/M1	Behind forge furnace	Thick Body	
VL-6-M4A	A	SU6/M4	Front right verandah	Rim	Matching section VL-6-M4B.
VL-6-M4B	A	SU6/M4	Front right verandah	Body	Matching section VL-6-M4A.
VL-6-MD1	B	SU6/MID	Midden that has been scraped next to fence line	Pot Lid Handle	Smelter settlement unit midden

Appendix D

Table of Marothodi Ceramic Data

Sample	Group	Sherd Thickness	Modal % of Inclusions	Incl. Sizes - Mode; Max	Mineral Inclusions				Lithic Incls		Comments
					Qtz	Fsp	Amp	Mica	Met/Wea	Grog ?	
VL-11-M4A	A	11.0	25	0.1; 1.6	+	++	-(g) -(l)		++	+	Weathered. Rutilated qtz.
VL-11-M4B	A	15.0	30	0.1; 1.6	++	+	-(g)		++	+	Weathered.
VL-11-M11A	A	12.0	20	0.1; 3.0	+	+	-(g)		++	+	Weathered. Rutilated qtz.
VL-11-M11B	A	8.0	20	0.1; 1.6	+	+	-(g)		++	+	Weathered. Fine grained.
VL-11-M12C	A	11.5	20	0.1; 1.6	+	+	-(g)		+	+	Weathered.
VL-11-M14A	A	8.0	20	0.1; 1.8	+	+	-(g)		++	+	Weathered. Rutilated qtz.
VL-11-MDA	A	8.0	25	0.2; 2.0	+	++	-(g)		++	+	Weathered.

Appendix D

Sample	Group	Sherd Thickness	Modal % of Inclusions	Incl. Sizes - Mode; Max	Mineral Inclusions				Lithic Incls		Comments
					Qtz	Fsp	Amp	Mica	Met/Wea	Grog?	
VL-13-M11A	A	13.0	25	0.2; 2.0	+	+	-(g)		++	+	Weathered.
VL-13-M11C	A	20.0	20	0.1; 2.2	+	++	-(g)		++	+	Weathered.
VL-13-M11D	A	19.0	20	0.1; 2.4	+	++	-(g)		++	+	Weathered.
VL-14-M7A	A	7.0	20	0.1; 2.0	+	+	-(g)		++	+	Weathered.
VL-14-M7B	A	7.5	20	0.1; 1.5	+	+	-(g)		++	+	Weathered.
VL-14-M7C	A	7.0	20	0.1; 2.0	+	+	-(g)		++	+	Weathered. Rutilated qtz.
VL-3-M5B	A	20.0	25	0.1; 2.3	++	++	-(g)		++	+	Weathered. Rutilated qtz.
VL-3-M8A	A	13.5	20	0.1; 1.2	+	+	-(g)		++	+	Weathered. Section poorly ground.
VL-3-M18A	A	7.0	30	0.1; 0.8	+	+	-(g) -(l)	-(ms)	++	+	Weathered. Few coarse inclusions.
VL-3-M18B	A	10.0	25	0.1; 1.4	+	+	-(g) -(l)	-(ms)	++	++	Weathered. Rutilated qtz.

Appendix D

Sample	Group	Sherd Thickness	Modal % of Inclusions	Incl. Sizes - Mode; Max	Mineral Inclusions				Lithic Incls		Comments
					Qtz	Fsp	Amp	Mica	Met/Wea	Grog?	
VL-4-M2A	A	10.5	25	0.1; 1.6	+	+	-(g)		++	+	Weathered. Rutilated qtz.
VL-5-M3A	A	19.0	30	0.1; 1.8	++	++	-(g)		++	+	Weathered.
VL-5-M3A (2)	A	11.5	25	0.1; 1.2	+	+	-(g)		++	+	Weathered. Poly qtz frag.
VL-6-M1A	A	11.0	30	0.1; 2.4	+	+	-(g)		++	+	Weathered. Poly qtz frag.
VL-6-M1B	A	19.5	25	0.2; 1.6	+	+	-(g)		++	+	Weathered. Rutilated qtz.
VL-6-M4A	A	8.0	25	0.1; 3.6	+	+	+(g)		+	+	Weathered. One 3.6 igneous rock frag; next max 1.2.
VL-6-M4B	A	10.0	25	0.1; 1.4	+	+	+(g)		+	+	Weathered. Rutilated qtz.
VL-11-M11C	B	12.0	40	0.2; 1.8	++	++		-	++	+	Heavily weathered. Micaceous grog(?) frag.
VL-11-M12A	B	13.0	30	0.1; 2.8	++	++		-	++	+	Heavily weathered.
VL-11-M 12B	B	7.5	35	0.1; 3.2	+	++		-	++	-	Heavily weathered.
VL-11-M14B	B	20.0	25	0.2; 2.1	++	++	-(g)		++	++	Heavily weathered. Rutilated qtz.

Appendix D

Sample	Group	Sherd Thickness	Modal % of Inclusions	Incl. Sizes - Mode; Max	Mineral Inclusions				Lithic Incls		Comments
					Qtz	Fsp	Amp	Mica	Met/Wea	Grog?	
VL-11-MDC	B	10.5	25	0.3; 4.0	+	++			++		Heavily weathered.
VL-12-M2A	B	7.0	35	0.2; 1.4	+	++			++		Heavily weathered.
VL-12-M2B	B	12.0	35	0.2; 2.0	+	++		-	++	++	Heavily weathered.
VL-3-M5A	B	10.5	25	0.2; 3.0	+	++			++	++	Heavily weathered.
VL-3-M9A	B	10.0	30	0.1; 1.8	++	++			++	+	Heavily weathered.
VL-6-MD1	B	19.0	40	0.2; 2.0	++	++			++	+	Heavily weathered.
VL-11-MDB	C	12.0	35	0.4; 6.0	+			++			30% mica (bt and ms). Rutilated qtz.
VL-5-M5A	C	15.0	40	0.4; 5.0	-			++		+	35% mica (bt and ms). Rutilated qtz.
VL-3-M5C	D	9.5	35	0.2; 2.2	++	+	++ (1)		-	-	Weathered. Rich in lithic frags.

Appendix D

Sample	Group	Sherd Thickness	Modal % of Inclusions	Incl. Sizes - Mode; Max	Mineral Inclusions				Lithic Incls		Comments
					Qtz	Fsp	Amp	Mica	Met/Wea	Grog?	
VL-4-M1A	E	6.5	25	0.2; 1.2	++	-			-	+	Unweathered. Few coarse inclusions.
VL-4-M1B	E	8.5	25	0.2; 1.0	++	-	-(l)		-	+	Slightly weathered. Few coarse inclusions.
VL-13-M11B	F	10.0	20	0.1; 2.4	++	++	-(g) -(l)	+(ms)	++	+	Heavily weathered. Section poorly ground. Opaques. Granophyres.
VL-3-M11A	F	7.5	25	0.3; 3.6	+	+	+(l)		+	+	Weathered. Very coarse inclusions. Rutilated qtz.
VL-3-M11B	F	12.0	20	0.2; 1.5	+	++	-(l)	+(ms)	++	+	Weathered. Coarse inclusions. Rutilated qtz.

Notes on Appendix D

The sample designation VL refers to Vlakfontein, the name of the farm on which Marothodi is located.

All measurements are in millimeters (mm). Maximum inclusions measurement does not include possible grog inclusions.

Mineral inclusion abbreviations are as follows:

Qtz	Quartz
Fsp	Feldspar
Amp	Amphibole
Ms	Muscovite
Bt	Biotite

Relative amounts of inclusions present are symbolized as follows:

-	Trace
+	Medium
++	Rich
?	Possibly present, more analysis needed.

Amphibole occurs in two forms:

- (g) Fine grains that are strong in color, pleochroic dark green to light green
- (l) Coarse grains that are light in color, pleochroic light green to light pink/brown

Lithic inclusion abbreviations are as follows:

Met/	Unidentifiable metamorphosed or extremely weathered mineral or rock
Wea	fragments, commonly sericitised feldspar and quartz.

Grog? The possible presence of 'grog' in some sherds is denoted with a '?'. There are two reasons an inclusion might display a characteristic 'grog' appearance, and it is extremely difficult to differentiate between the two. (1) An area of the ceramic paste, or a clay nodule, overfires due to the particular chemical characteristics of the minerals occurring there. (2) A temper of crushed, previously fired pottery sherds (grog) is added to the clay. In both cases, one might observe in thin section how the region in question shrunk, or pulled in, from its surrounding matrix. If small grains are observed that overlap the boundary between the area and the matrix, the area is not grog, however, this distinction is often difficult to resolve. I hope to conduct further petrographic research and perhaps some experimental 'chemical' archaeology in the future to better understand the difference between these two types of inclusions.

References Cited

- Addiss, R.R., Ghosh, A.K. & Wakim, F.G. 1968. Thermally stimulated currents and luminescence in rutile (TiO₂). *Applied Physics Letters* 12: 397-400.
- Aitken, M.J. 1985. *Thermoluminescence dating*. London: Academic Press.
- Aitken, M.J. 1997. Luminescence dating. In: Taylor, R.E. & Aitken, M.J. (eds) *Chronometric dating in archaeology*: 183-216. New York: Plenum Press.
- Aitken, M.J. 1998. *An introduction to optical dating: the dating of Quaternary sediments by the use of photon-stimulated luminescence*. New York: Oxford University Press, Inc.
- Aitken, M.J., Tite, M.S. & Reid, J. 1964. Thermoluminescent dating of ancient ceramics. *Nature* 202: 1032-1033.
- Aitken, M.J., Zimmerman, D.W. & Fleming, S.J. 1968. Thermoluminescent dating of ancient pottery. *Nature* 219: 442-445.
- Anderson, M. forthcoming. The Late 'Iron Age' Tswana towns of the Bankenveld: towards an understanding of variability, complexity and identity. Unpublished PhD thesis, University of Cape Town, Cape Town.
- Arnold, D.E. 2000. Does the standardization of ceramic pastes really mean specialization? *Journal of Archaeological Method and Theory* 7: 333-375.
- Arnold, J.R. & Libby, W.F. 1949. Age determinations by radiocarbon content: checks with samples of known age. *Science* 110: 678-680.
- Aschwanden, H. 1982. *Symbols of life: an analysis of the consciousness of the Karanga*. Gewru, Zimbabwe: Mambo Press.
- Ballarini, M., Wallinga, J., Murray, A.S., van Heteren, S., Oost, A.P., Bos, A.J.J. & van Eijk, C.W.E. 2003. Optical dating of young coastal dunes on a decadal time scale. *Quaternary Science Reviews* 22: 1011-1017.
- Banerjee, D., Murray, A.S. & Foster, I.D.L. 2001. Scilly Isles, UK: optical dating of a possible tsunami deposit from the 1755 Lisbon earthquake. *Quaternary Science Reviews* 20: 715-718.
- Beaumont, P.B. 1973. The ancient pigment mines of southern Africa. *South African Journal of Science* 69: 140-146.
- Beaumont, P.B. & Boshier, A.K. 1974. Report on test excavations in a prehistoric pigment mine near Postmasburg, northern Cape. *South African Archaeological Bulletin* 29: 41-59.
- Becher, P.F. 1991. Microstructural design of toughened ceramics. *Journal of the American Ceramic Society* 74: 255-269.
- Beck, M.E. & Hill, M.E. 2004. Rubbish, relatives, and residence: the family use of middens. *Journal of Archaeological Method and Theory* 11: 297-333.
- Berns, M.C. 1990. Pots as people: Yungur ancestral portraits. *African Arts* 23: 50-102.
- Blair, M.W., Yukihiro, E.G. & McKeever, S.W.S. 2005. Experiences with single-aliquot OSL procedures using coarse-grain feldspars. *Radiation Measurements* 39: 361-374.
- Boeyens, J.C.A. 1999. Kaditshwene: what's in a name? In: Finlayson, R. (ed.) *African Mosaic*: 250-284. Pretoria: University of South Africa Press.
- Boeyens, J.C.A. 2000. In search of Kaditshwene. *South African Archaeological Bulletin* 55: 3-17.

- Boeyens, J.C.A. 2003. The Late Iron Age sequence in the Marico and early Tswana history. *South African Archaeological Bulletin* 58: 63-78.
- Boeyens, J.C.A. 2004. Oral tradition and historical identity at Marothodi. Paper presented at the Southern African Association of Archaeologists Biennial Conference, Kimberly.
- Bowman, S. 1990. Radiocarbon dating. London: British Museum Press.
- Breutz, P.-L. 1953a. The tribes of Rustenburg and Pilanesberg districts. *Ethnological Publications* No. 28. Pretoria: Government Printer.
- Breutz, P.-L. 1953b. The tribes of the Marico district. *Ethnological Publications* No. 30. Pretoria: Government Printer.
- Breutz, P.-L. 1989. A history of the Batswana and origin of Bophuthatswana. Ramsgate: Breutz.
- Brock, A. 1977. Magnetic dating methods in prehistory. *South African Archaeological Bulletin* 32: 5-13.
- Bronk Ramsey, C. 1995. Radiocarbon calibration and analysis of stratigraphy: the OxCal program. *Radiocarbon* 37: 425-430.
- Bronk Ramsey, C. 2001. Development of the radiocarbon calibration program OxCal. *Radiocarbon* 43: 355-363.
- Brumfiel, E.M. & Earle, T.K. 1987. Specialization, exchange and complex societies: an introduction. In: Brumfiel, E.M. & Earle, T.K. (eds) *Specialization, Exchange and Complex Societies*: 1-9. Cambridge: Cambridge University Press.
- Buck, C.E. 2001. Applications of the Bayesian statistical paradigm. In: Brothwell, D. & Pollard, A. (eds) *Handbook of archaeological sciences*. New York: John Wiley & Sons.
- Buck, C.E., Cavanagh, W.G. & Litton, C.D. 1996. *The Bayesian approach to interpreting archaeological data*. Chichester: John Wiley & Sons.
- Burchell, W.J. 1824. *Travels in the interior of southern Africa*. vol. 2. London: Longman, Hurst, Rees, Orme and Brown.
- Bøtter-Jensen, L., Andersen, C.E., Duller, G.A.T. & Murray, A.S. 2003. Developments in radiation, stimulation and observation facilities in luminescence measurements. *Radiation Measurements* 37: 535-541.
- Bøtter-Jensen, L., Bulur, E., Duller, G.A.T. & Murray, A.S. 2000. Advances in luminescence instrument systems. *Radiation Measurements* 32: 523-528.
- Bøtter-Jensen, L., Mejdahl, V. & Murray, A.S. 1999. New light on OSL. *Quaternary Science Reviews* 18: 303-309.
- Campbell, J. 1815. *Travels in South Africa*. Corrected 3rd ed. London: Missionary Society.
- Campbell, J. 1820a. 'Lion House where children sleep for safety from lions' / Wild flowers / 'Kurreechane from the East'. ARP9 John Campbell Album INIL7234. Cape Town: National Library of South Africa.
- Campbell, J. 1820b. 'N Side of Kurrechane Public Place' / 'S Side of Kurrechane Public Place, holding Peetso or General Meeting'. ARP9 John Campbell Album INIL7241. Cape Town: National Library of South Africa.
- Campbell, J. 1822a. *Travels in South Africa undertaken at the request of the London Missionary Society; being a narrative of a second journey in the interior of that country* (1820). vol. 2. London: Westley.
- Campbell, J. 1822b. *Travels in South Africa undertaken at the request of the London Missionary Society; being a narrative of a second journey in the interior of that country* (1820). vol. 1. London: Westley.

- Childs, S.T. 1994. Society, culture and technology in Africa: an introduction. In: Childs, S.T. (ed.) *Society, culture and technology in Africa MASCA Research Papers in Science and Archaeology*, Supplement to Volume 11: 7-14. Philadelphia: University of Pennsylvania.
- Costin, C.L. 1991. Craft specialization: issues in defining, documenting and explaining the organization of production. In: Schiffer, M.B. (ed.) *Archaeological method and theory*, vol. 3: 1-56. Tucson: University of Arizona Press.
- Costin, C.L. 1998. Introduction: craft and social identity. In: Costin, C.L. & Wright, R. (eds) *Craft and social identity Anthropological Papers No. 8*. Washington, DC: American Anthropological Association.
- Costin, C.L. 2001. Craft production systems. In: Feinman, G. & Price, T.D. (eds) *Archaeology at the millennium: a sourcebook*: 273-327. New York: Kluwer Academic/Plenum Publishers.
- Courty, M.-A. 2001. Microfacies analysis assisting archaeological stratigraphy. In: Goldberg, P., Holliday, V.T. & Ferring, C.R. (eds) *Earth sciences and archaeology*: 205-239. New York: Kluwer.
- Daniels, F., Boyd, C.A. & Saunders, D.F. 1953. Thermoluminescence as a research tool. *Science* 117: 343-349.
- David, N. & Kramer, C. 2001a. Style and the marking of boundaries: contrasting regional studies. In: *Ethnoarchaeology in action*: 168-224. Cambridge: Cambridge University Press.
- David, N. & Kramer, C. 2001b. Specialist craft production and apprenticeship. In: *Ethnoarchaeology in action*: 303-359. Cambridge: Cambridge University Press.
- David, N., Sterner, J. & Gavua, K. 1988. Why pots are decorated. *Current Anthropology* 29: 365-389.
- de Heusch, L. 1980. Heat, physiology and cosmogeny: *rites de passage* among the Thonga. In: Karp, I. & Bird, C. (eds) *Explorations in African systems of thought*: 27-43. Bloomington: Indiana University Press.
- Dean, J.S. 1978. Independent dating in archaeological analysis. In: Schiffer, M.B. (ed.) *Advances in archaeological method and theory*, vol. 1: 223-255. New York: Academic Press.
- Denbow, J. 1990. Congo to Kalahari: data and hypotheses about the political economy of the western stream of the Early Iron Age. *African Archaeological Review* 8: 139-176.
- Dietler, M.D. & Herbich, I. 1998. *Habitus*, techniques, style: an integrated approach to the social understanding of material culture and boundaries. In: Stark, M.T. (ed.) *The archaeology of social boundaries*. Washington, DC: Smithsonian Institution Press.
- Duggan-Cronin, A.M. 1929. The Bantu tribes of South Africa: reproductions of photographic studies. vol. 2, sect. 1 (The Suto-Chuana tribes). Cambridge: Deighton, Bell & Co.
- Duller, G.A.T. 2003. Distinguishing quartz and feldspar in single grain luminescence measurements. *Radiation Measurements* 37: 161-165.
- Duller, G.A.T. 2004. Luminescence dating of quaternary sediments: recent advances. *Journal of Quaternary Science* 19: 183-192.
- Eales, H.V. & Cawthorn, R.G. 1996. The Bushveld Complex. In: Cawthorn, R. (ed.) *Layered intrusions*: 181-229. Amsterdam: Elsevier.

- Ellenberger, V. 1939. History of the Batlokwa of Gaberones (Bechuanaland Protectorate). *Bantu Studies* XIII: 165-198.
- Engelbrecht, J. 1990. Contact metamorphic processes related to the aureole of the Bushveld Complex in the Marico District, western Transvaal, South Africa. *South African Journal of Geology* 93: 339-349.
- Evers, T.M. 1981. The Iron Age in the eastern Transvaal. *Proceedings of the Prepared for the Southern African Association of Archaeologists excursion*, pp. 64-109. Guide to archaeological sites in the northern and eastern Transvaal.
- Evers, T.M. 1983. "Oori" or "Moloko"? The origins of the Sotho-Tswana on the evidence of the Iron Age of the Transvaal, reply to RJ Mason. *South African Journal of Science* 79: 261-264.
- Evers, T.M. 1984. Sotho-Tswana and Moloko settlement patterns and the Bantu cattle patterns. In: Hall, M., Avery, G., Avery, D.M., Wilson, M. & Humphreys, A.J. (eds) *Frontiers: southern African archaeology today*. Oxford: British Archaeological Reports, International Series, No. 207.
- Evers, T.M. & Huffman, T.N. 1988. On why pots are decorated the way they are. *Current Anthropology* 29: 739-741.
- Faure, G. & Mensing, T.M. 2005. Cosmogenic radionuclides: carbon-14 (radiocarbon). In: *Isotopes: principles and applications*, 3rd ed.: 614-624. Hoboken, New Jersey: John Wiley and Sons, Inc.
- Feathers, J.K. 1997. Luminescence dating of sediment samples from White Paintings Rockshelter, Botswana. *Quaternary Science Reviews* 16: 321-331.
- Feathers, J.K. 2002. Luminescence dating in less than ideal conditions: case studies from Klasies River Main Site and Duinefontein, South Africa. *Journal of Archaeological Science* 29: 177-194.
- Feathers, J.K. 2003. Use of luminescence dating in archaeology. *Measurement Science and Technology* 14: 1493-1509.
- Feathers, J.K. 2007. Luminescence dating of ceramics from Los Alamos Country, New Mexico -- summary report. Los Alamos National Laboratory.
- Feathers, J.K. & Bush, D.A. 2000. Luminescence dating of Middle Stone Age deposits at Die Kelders. *Journal of Human Evolution* 38: 91-119.
- Franklin, A.D. & Hornyak, W.F. 1990. Isolation of the rapidly bleaching peak in quartz TL glow curves. *Ancient TL* 8: 29-31.
- Galbraith, R.F. 1990. The radial plot: graphical assessment of spread in ages. *Nuclear Tracks and Radiation Measurements* 17: 207-214.
- Galbraith, R.F. 1994. Some applications of radial plots. *Journal of the American Statistical Association* 89: 1232-1242.
- Galbraith, R.F., Roberts, R.G., Laslett, G.M., Yoshida, H. & Olley, J.M. 1999. Optical dating of single and multiple grains of quartz from Jinmium rock shelter, northern Australia: Part I, experimental design and statistical models. *Archaeometry* 41: 339-364.
- Geertz, C. 1973. Thick description: toward an interpretive theory of culture. *The interpretation of cultures: selected essays*: 3-30. New York: Basic Books.
- Godfrey-Smith, D.I. & Cada, M. 1996. IR stimulation spectroscopy of plagioclase and potassium feldspars, and quartz. *Radiation Protection Dosimetry* 66: 379-385.
- Godfrey-Smith, D.I. & Casey, J.L. 2003. Direct thermoluminescence chronology for Early Iron Age smelting technology on the Gambaga Escarpment, Ghana. *Journal of Archaeological Science* 30: 1037-1050.
- Gosselain, O.P. 1994. Skimming through potters' agendas: an ethnoarchaeological study of clay selection strategies in Cameroon. In: Childs, S.T. (ed.) *Society*,

- culture and technology in Africa MASCA Research Papers in Science and Archaeology, Supplement to Volume 11: 99-107. Philadelphia: University of Pennsylvania.
- Gosselain, O.P. 1998. Social and technical identity in a clay crystal ball. In: Stark, M.T. (ed.) *The archaeology of social boundaries*: 78-106. Washington, DC: Smithsonian Institution Press.
- Gosselain, O.P. 2000. Materializing identities: an African perspective. *Journal of Archaeological Method and Theory* 7: 187-217.
- Grant, L.H. 1968. Pot making. *Botswana Notes and Records* 1.
- Grün, R. 2001. Trapped charge dating (ESR, TL, OSL). In: Brothwell, D.R. & Pollard, A.M. (eds) *Handbook of archaeological sciences*: 47-62. Chichester: John Wiley & Sons, Ltd.
- Grün, R., Brink, J.S., Spooner, N.A., Taylor, L., Stringer, C.B., Franciscus, R.G. & Murray, A.S. 1996. Direct dating of Florisbad hominid. *Nature* 382: 500-501.
- Hagihara, N., Miono, S., Manabe, S. & Nakanishi, A. 2001. A discovery of suitable layers for the thermoluminescence (TL) dating of ancient iron manufacturing furnace to investigate the origin of iron manufacturing in Japan. *Quaternary Science Reviews* 20: 987-991.
- Hall, B.L. & Henderson, G.M. 2001. Use of uranium-thorium dating to determine past ^{14}C reservoir effects in lakes: examples from Antarctica. *Earth and Planetary Science Letters* 193: 565-577.
- Hall, M. 1976. Dendroclimatology, rainfall and human adaptation in the later Iron Age of Natal and Zululand. *Annals of the Natal Museum* 22: 693-703.
- Hall, M. 1986. The role of cattle in southern African agropastoral societies: more than bones alone can tell. In: Hall, M. & Smith, A.B. (eds) *Prehistoric pastoralism in southern Africa* Goodwin Series 5: 83-87. Claremont, South Africa: South African Archaeological Society.
- Hall, M. 1987. *The changing past: farmers, kings and traders in southern Africa, 200 - 1860*. Cape Town: David Philip.
- Hall, S. 1981. Iron Age sequence and settlement in the Rooiberg, Thabazimbi area. Unpublished M.A. thesis, University of the Witwatersrand, Johannesburg.
- Hall, S. 1985. Excavations at Rooikrans and Rhenosterkloof, Late Iron Age sites in the Rooiberg area of the Transvaal. *Annals of the Cape Provincial Museums* 1: 131-210.
- Hall, S. 1995. Archaeological indicators for stress in the western Transvaal region between the seventeenth and nineteenth centuries. In: Hamilton, C. (ed.) *The mfecane aftermath: reconstructive debates in southern African history*: 307-322. Johannesburg: Witwatersrand University Press.
- Hall, S. 1998. A consideration of gender relations in the Late Iron Age "Sotho" sequence of the western highveld, South Africa. In: Kent, S. (ed.) *Gender in African prehistory*: 235-258. Walnut Creek, CA: AltaMira Press.
- Hall, S. 2000. Forager lithics and early Moloko homesteads at Madikwe. *Natal Museum Journal of Humanities* 12: 33-50.
- Hall, S., Anderson, M., Boeyens, J. & Coetzee, F. 2007. The archaeology and oral history of the Tlokwa and their neighbours in the Rustenburg and Pilanesburg region. Seminar of the Five hundred Year Research Group. University of the Witwatersrand, Johannesburg.
- Hall, S., Anderson, M., Boeyens, J. & Coetzee, F. 2008. Towards an outline of the oral geography, historical identity and political economy of the late precolonial Tswana in the Rustenburg region. In: Swanepoel, N., Esterhuysen,

- A. & Bonner, P. (eds) Five hundred years rediscovered: southern african precedents and prospects: 55-85. Johannesburg: Wits University Press.
- Hall, S., Miller, D., Anderson, M. & Boeyens, J. 2006. An exploratory study of copper and iron production at Marothodi, an early 19th century Tswana town, Rustenburg District, South Africa. *Journal of African Archaeology* 4: 3-35.
- Hanisch, E.O.M. 1979. Excavations at Icon, northern Transvaal. In: Van der Merwe, N.J. & Huffman, T.N. (eds) *Iron Age studies in southern Africa*. Goodwin Series 3: 72-79. Claremont, South Africa: South African Archaeological Society.
- Haughton, S.H. 1969. *Geological history of southern Africa*. Cape Town: Geological Society of South Africa.
- Hegmon, M. 1992. Archaeological research on style. *Annual Review of Anthropology* 21: 517-536.
- Hegmon, M. 1998. Technology, style, and social practices: archaeological approaches. In: Stark, M.T. (ed.) *The archaeology of social boundaries*: 264-279. Washington, DC: Smithsonian Institution Press.
- Henderson, Z., Scott, L., Rossouw, L. & Jacobs, Z. 2006. Dating, paleoenvironments, and archaeology: a progress report on the Sunnyside 1 Site. *Anthropological Papers of the American Anthropological Association* 16: 139-149.
- Henshilwood, C.S., d'Errico, F., Vanhaeren, M., Van Niekerk, K. & Jacobs, Z. 2004. Middle Stone Age shell beads from South Africa. *Science* 304: 404.
- Henshilwood, C.S., d'Errico, F., Yates, R., Jacobs, Z., Tribolo, C., Duller, G.A.T., Mercier, N., Sealy, J.C., Valladas, H., Watts, I. & Wintle, A.G. 2002. Emergence of modern human behavior: Middle Stone Age engravings from South Africa. *Science* 295: 1278-1280.
- Herbert, E.W. 1993. *Iron, Gender and Power: rituals of transformation in African societies*. Bloomington: Indiana University Press.
- Hobart, J.H. 2003. Forager-farmer relations in southeastern southern Africa: a critical reassessment. Unpublished D.Phil. thesis, University of Oxford, Oxford.
- Hobart, J.H. 2004. Pitsaneng: evidence for a neolithic Lesotho? *Before Farming* 2004/4: article 4.
- Huffman, T.N. 1980. Ceramics, classification and Iron Age entities. *African Studies* 39: 123-174.
- Huffman, T.N. 1982. Archaeology and ethnohistory of the African Iron Age. *Annual Review of Anthropology* 11: 133-150.
- Huffman, T.N. 1990. Broederstroom and the origins of cattle-keeping in southern Africa. *African Studies* 49: 1-12.
- Huffman, T.N. 1996. Archaeological evidence for climatic change during the last 2000 years in southern Africa. *Quaternary International* 33: 55-60.
- Huffman, T.N. 1998. The antiquity of *lobola*. *South African Archaeological Bulletin* 53: 57-62.
- Huffman, T.N. 2000. Archaeological survey of Madikwe Game Reserve, North West Province. Unpublished report. Johannesburg: Archaeological Resources Management, Department of Archaeology, University of the Witwatersrand.
- Huffman, T.N. 2001. The central cattle pattern and interpreting the past. *Southern African Humanities* 13: 19-35.
- Huffman, T.N. 2002. Regionality in the Iron Age: the case of the Sotho-Tswana. *Southern African Humanities* 14: 1-22.
- Huffman, T.N. 2004. The archaeology of the Nguni past. *Southern African Humanities* 16: 79-111.

- Huffman, T.N. 2006. Maize grindstones, Madikwe pottery and ochre mining in pre-colonial southern Africa. *Southern African Humanities* 18: 51-70.
- Huffman, T.N. 2007a. Handbook to the Iron Age: the archaeology of pre-colonial farming societies in southern Africa. Scottsville: University of KwaZulu-Natal Press.
- Huffman, T.N. 2007b. The last 500 years in the Trans-vaal. Seminar of the Five hundred Year Research Group. University of the Witwatersrand, Johannesburg.
- Hughen, K.A., Baillie, M.G.L., Bard, E., Beck, J.W., Bertrand, C.J.H., Blackwell, P.G., Buck, C.E., Burr, G.S., Cutler, K.B., Damon, P.E., Edwards, R.L., Fairbanks, R.G., Friedrich, M., Guilderson, T.P., Kromer, B., McCormac, G., Manning, S., Ramsey, C.B., Reimer, P.J., Reimer, R.W., Remmele, S., Southon, J.R., Stuiver, M., Talamo, S., Taylor, F.W., van der Plicht, J. & Weyhenmeyer, C.E. 2004. Marine04 marine radiocarbon age calibration, 0-26 cal kyr BP. *Radiocarbon* 46: 1059-1086.
- Huntley, D.J. & Clague, J.J. 1996. Optical dating of tsunami-laid sands. *Quaternary Research* 46: 127-140.
- Huntley, D.J., Godfrey-Smith, D.I. & Thewalt, M.L. 1985. Optical dating of sediments. *Nature* 313: 105-107.
- Jacobs, Z., Duller, G.A.T. & Wintle, A.G. 2003a. Optical dating of dune sand from Blombos Cave, South Africa: II - single grain data. *Journal of Human Evolution* 44: 613-625.
- Jacobs, Z., Duller, G.A.T., Wintle, A.G. & Henshilwood, C.S. 2006. Extending the chronology of deposits at Blombos Cave, South Africa, back to 140 ka using optical dating of single and multiple grains of quartz. *Journal of Human Evolution* 51: 255-273.
- Jacobs, Z., Wintle, A.G. & Duller, G.A.T. 2003b. Optical dating of dune sand from Blombos Cave, South Africa: I - multiple grain data. *Journal of Human Evolution* 44: 599-612.
- Jansen, H., Schifano, G. & Schutte, I.C. 1974. 2426 Thabazimbi Geological Map. Explanatory notes by H. Jansen. Geological Survey of South Africa. Pretoria: Government Printer; scale 1:250 000.
- Kay, S. 1834. Travels and researches in Caffraria: describing the character, customs, and moral conditions of the tribes inhabiting that portion of southern Africa. New York: Harper and Brothers.
- Kiefer, R. & Viljoen, M.J. 2006. PGE exploration targets to the west of the Pilanesberg, South Africa. *South African Journal of Geology* 109: 459-474.
- Killick, D. 2004. Social constructionist approaches to the study of technology. *World Archaeology* 36: 571-578.
- Lane, P. 1994/95. The use and abuse of ethnography in the study of the southern African Iron Age. *Azania* 29-30: 51-64.
- Lawton, A.C. 1967. Bantu pottery of southern Africa. *Annals of the South African Museum* 49: 1-440.
- Lechtman, H. 1977. Style in technology - some early thoughts. In: Lechtman, H. & Merrill, R.S. (eds) *Material culture: styles, organization, and dynamics of technology*: 3-20. St. Paul, MN: West.
- Legassick, M. 1969. The Sotho-Tswana peoples before 1800. In: Thompson, L. (ed.) *African societies in southern Africa*. London: Heinemann.

- Legassick, M. 1970. The Griqua, the Sotho-Tswana, and the missionaries, 1780-1840: the politics of a frontier zone. Unpublished PhD thesis, University of California, Los Angeles.
- Lemmonier, P. 1992. Elements for an anthropology of technology. Ann Arbor: Anthropological Papers of the Museum of Anthropology, University of Michigan, No. 88.
- Leroi-Gourhan, A. 1965. *Le geste et la parole: la mémoire et les rythmes*.
- Libby, W.F., Anderson, E.C. & Arnold, J.R. 1949. Age determination by radiocarbon content: world-wide assay of natural radiocarbon. *Science* 109: 227-228.
- Lichtenstein, H. 1812. *Travels in South Africa in the years 1803, 1804, 1805 and 1806*. Vol. 2. London: Henry Colburn.
- Lichtenstein, H. 1815. *Travels in South Africa in the years 1803, 1804, 1805 and 1806*. Vol. 2. vol. Henry Colburn, London. Cape Town (1930): Van Riebeeck Society.
- Lindahl, A. & Matenga, E. 1995. Present and past: ceramics and homesteads. Uppsala: Studies in African Archaeology 11.
- Longacre, W.A. 1999. Standardization and specialization: what's the link? In: Skibo, J.M. & Feinman, G.M. (eds) *Pottery and people: a dynamic interaction*: 44-58. Salt Lake City: University of Utah Press.
- Maggs, T.M. 1976. Iron Age communities of the southern Highveld. Pietermaritzburg: Natal Museum (Occasional Publication 2).
- Maggs, T.M.O.C. 1984. The Iron Age south of the Zambezi. In: Klein, R.J. (ed.) *Southern African prehistory and paleoenvironments*: 329-360. Rotterdam: Balkema.
- Maggs, T.M.O.C. & Davidson, P. 1981. The Lydenburg Heads and the earliest African sculpture south of the equator. *African Arts* 14: 28-33.
- Manson, A. 1995. Conflict in the western highveld/southern Kalahari c. 1750-1820. In: Hamilton, C. (ed.) *Mfecane aftermath: reconstructive debates in southern African history*: 351-361. Johannesburg: Witswatersrand University Press.
- Map. 1994. 2526 Johannesburg Topo-Admin. edition. Mowbray: Chief Directorate: Surveys and Land Information; scale 1:500 000.
- Mason, R.J. 1968. Transvaal and Natal Iron Age settlement revealed by aerial photography and excavation. *African Studies* 27: 167-179.
- Mason, R.J. 1973. Iron Age research in the western Transvaal, South Africa, 1971-72. *Current Anthropology* 14: 485-487.
- Mason, R.J. 1981. Early Iron Age settlement at Broederstroom 24/73, Transvaal, South Africa. *South African Journal of Science* 77: 401-416.
- Mason, R.J. 1986. Origins of Black people of Johannesburg and the southern western Transvaal, AD 350-1880. Johannesburg: Occasional Paper 16 of the Archaeological Research Unit, University of the Witswatersrand.
- Mason, R.J. 1987. Origins of the African people of the Johannesburg area. Johannesburg: Skotaville.
- McCormac, F.G., Hogg, A.G., Blackwell, P.G., Buck, C.E., Higham, T.F.G. & Reimer, P.J. 2004. SHCal04 southern hemisphere calibration, 0-11.0 cal kyr BP. *Radiocarbon* 46: 1087-1092.
- McCormac, F.G., Hogg, A.G., Higham, T.F.G., Baillie, M.G.L., Palmer, J.G., Xiong, L., Pilcher, J.R., Brown, D. & Hoper, S.T. 1998. Variations of radiocarbon in tree rings: southern hemisphere offset preliminary results. *Radiocarbon* 40: 1153-1159.

- Melnyk, V., Shymanovska, V., Puchkovska, G., Bezrodna, T. & Klishevich, G. 2005. Low-temperature luminescence of different TiO₂ modifications. *Journal of Molecular Structure* 744-747: 573-576.
- Methuen, H.H. 1846. *Life in the wilderness; or, wanderings in South Africa*. London: Richard Bentley.
- Moffat, R. 1842. *Missionary labours and scenes in southern Africa*. London: John Snow.
- MSB77. 1820. Campbell Collection. Unpublished journal and water-colour sketches of John Campbell, Vol. 3. Cape Town: National Library of South Africa.
- Mucina, L. & Rutherford, M.C. (eds) 2006. *The vegetation of South Africa, Lesotho and Swaziland*. Strelitzia 19. Pretoria: South African National Biodiversity Institute.
- Murray, A.S. & Wintle, A.G. 2000. Luminescence dating of quartz using an improved single-aliquot regenerative-dose protocol. *Radiation Measurements* 32: 57-73.
- Murray, A.S. & Wintle, A.G. 2003. The single-aliquot regenerative-dose protocol: potential for improvements in reliability. *Radiation Measurements* 37: 377-381.
- Norström, E., Holmgren, K. & Mörh, C.-M. 2008. A 600-year-long $\delta^{18}\text{O}$ record from cellulose of *Breonadia salicina* trees, South Africa. *Dendrochronologia* 26: 21-33.
- Ohinata, F. 2001. *Archaeology of iron-using farming communities in Swaziland: pots, people and life during the first and second millennia AD*. Unpublished PhD thesis, University of Oxford, Oxford.
- Parsons, N. 1995. Prelude to *difaqane* in the interior of southern Africa c. 1600 - c. 1822. In: Hamilton, C. (ed.) *The mfecane aftermath: reconstructive debates in southern African history*: 323-349. Johannesburg: Witswatersrand University Press.
- Pfaffenberger, B. 1992. Social anthropology of technology. *Annual Review of Anthropology* 21: 491-516.
- Phillipson, D. 1977. *The later prehistory of eastern and southern Africa*. London: Heinemann.
- Pienaar, M. 2005. *Dating the stone age at Rose Cottage Cave, South Africa: an exercise in optically dating cave sediments*. Unpublished MA thesis, University of Pretoria, Pretoria, South Africa.
- Pistorius, J.C.C. 1992. Molokwane, an Iron Age Bakwena village: early Tswana settlement in the western Transvaal. Johannesburg: Perskor Printers.
- Pistorius, J.C.C. 1994. Molokwane, a seventeenth century Tswana village. *South African Journal of Ethnology* 17: 38-54.
- Pistorius, J.C.C. 1996. Spatial expressions in the *kgosing* of Molokwane. *South African Journal of Ethnology* 19: 143-164.
- Pistorius, J.C.C. 1997. Diachronic evidence from the *kgosing* of Molokwane. *South African Journal of Ethnology* 20: 118-132.
- Prescott, J.R. & Hutton, J.T. 1994. Cosmic ray contributions to dose rates for luminescence and ESR dating: large depths and long-term time variations. *Radiation Measurements* 23: 497-500.
- Reimer, P.J., Baillie, M.G.L., Bard, E., Bayliss, A., Beck, J.W., Bertrand, C.J.H., Blackwell, P.G., Buck, C.E., Burr, G.S., Cutler, K.B., Damon, P.E., Edwards, R.L., Fairbanks, R.G., Friedrich, M., Guilderson, T.P., Hogg, A.G., Hughen, K.A., Kromer, B., McCormac, F.G., Manning, S., Ramsey, C.B., Reimer, R.W., Remmele, S., Southon, J.R., Stuiver, M., Talamo, S., Taylor, F.W., van

- der Plicht, J. & Weyhenmeyer, C.E. 2004. IntCal04 terrestrial radiocarbon age calibration, 0-26 cal kyr BP. *Radiocarbon* 46: 1029-1058.
- Risø DTU. February 2008. A guide to "The Risø TL/OSL Reader". Roskilde, Denmark: Risø Technical University of Denmark, National Laboratory for Sustainable Energy.
- Rosenstein, D.D. 2002. Ceramic production as a reflection of technological and social complexity in the Late Iron Age of South Africa: an ethnographic and petrographic study. Unpublished B.A. Hons thesis, George Washington University, Washington, DC.
- Rosenstein, D.D., Lengyel, S. & Jacobs, Z. in press. Chronometry beyond carbon: a pilot study using OSL and archaeomagnetism to date late Moloko sites in South Africa. *Proceedings of the 36th International Symposium on Archaeometry*, Quebec City, Canada.
- Ruddiman, W.F. 2001. *Earth's climate: past and future*. New York: W.H. Freeman & Sons.
- Schapera, I. 1942. A short history of the Bakgatla-bagaKgafela of Bechuanaland Protectorate. Cape Town: Communications from the School of African Studies, University of Cape Town, New Series No. 3.
- Schapera, I. 1953. *The Tswana*. London: International African Institute.
- Schiffer, M.B. 1986. Radiocarbon dating and the "old wood" problem: the case of the Hohokam chronology. *Journal of Archaeological Science* 13: 13-30.
- Schiffer, M.B. 1992. *Technological perspectives on behavioral change*. Tucson: University of Arizona Press.
- Schiffer, M.B. & Skibo, J.M. 1987. Theory and experiment in the study of technological change. *Current Anthropology* 28: 595-622.
- Schiffer, M.B. & Skibo, J.M. 1997. The explanation of artifact variability. *American Antiquity* 62: 27-50.
- Seddon, J.D. 1968. An aerial survey of settlement and living patterns in the Transvaal Iron Age: preliminary report. *African Studies* 27: 189-194.
- Sentker, H.F. 1968. Hurutshe fieldwork file and Vergenoegd collection. Museum of Anthropology and Archaeology, University of South Africa, Pretoria.
- Sillar, B. & Tite, M.S. 2000. The challenge of "technological choices" for materials science approaches in archaeology. *Archaeometry* 42: 2-20.
- Stein, J.K. 2001. Archaeological sediments in cultural environments. In: Stein, J.K. & Farrand, W.R. (eds) *Sediments in archaeological context*: 1-28. Salt Lake City: University of Utah Press.
- Stuiver, M. & Becker, B. 1993. High-precision decadal calibration of the radiocarbon time scale, AD 1950-6000 BC. *Radiocarbon* 35: 35-65.
- Stuiver, M. & Braziunas, T. 1993. Modeling atmospheric ^{14}C influences and ^{14}C ages of marine samples to 10,000 BC. *Radiocarbon* 35: 137-189.
- Stuiver, M. & Pearson, G.W. 1993. High-precision bidecal calibration of the radiocarbon time scale, AD 1950-500 BC and 250-6000 BC. *Radiocarbon* 35: 1-23.
- Stuiver, M. & Reimer, P.J. 1993. Extended ^{14}C database and revised CALIB radiocarbon calibration program. *Radiocarbon* 35: 215-230.
- Stuiver, M., Reimer, P.J., Bard, E., Beck, J.W., Burr, G., Hughen, K.A., Kromer, B., McCormac, G., Van der Plicht, J. & Spurk, M. 1998. Intcal98 radiocarbon age calibration, 24,000-0 cal BP. *Radiocarbon* 40: 1041-1083.
- Stuiver, M., Reimer, P.J. & Reimer, R.W. 2005. CALIB 5.0. WWW program and documentation: www.calib.org.

- Taylor, R.E. 1997. Radiocarbon dating. In: Taylor, R.E. & Aitken, M.J. (eds) *Chronometric dating in archaeology*: 65-96. New York: Plenum Press.
- Taylor, R.E. 2000. Fifty years of radiocarbon dating. *American Scientist* 88: 60-67.
- Taylor, R.E. 2001. Radiocarbon dating. In: Brothwell, D.R. & Pollard, A.M. (eds) *Handbook of archaeological sciences*: 23-34. Chichester: John Wiley & Sons, Ltd.
- Thackeray, A., Thackeray, J.F. & Beaumont, P.B. 1983. Excavations at the Blinkklipkop specularite mine near Postmasburg, Northern Cape. *South African Archaeological Bulletin* 38: 17-25.
- Tite, M.S., Kilikoglou, V. & Vekinis, G. 2001. Strength, toughness and thermal shock resistance of ancient ceramics, and their influence on technological choice. *Archaeometry* 43: 301-324.
- Tyson, P.D., Karlén, W., Holmgren, K. & Heiss, G.A. 2000. The Little Ice Age and medieval warming in South Africa. *South African Journal of Science* 96: 121-126.
- Tyson, P.D., Lee-Thorp, J., Holmgren, K. & Thackeray, J.F. 2002. Changing gradients of climate change in southern Africa during the past millennium: implications for population movements. *Climate Change* 52: 129-135.
- Varién, M.D. & Mills, B.J. 1997. Accumulations research: problems and prospects for estimating site occupation span. *Journal of Archaeological Method and Theory* 4: 141-191.
- Vogel, C.A.M. 1985. The traditional mural art of the Pedi of Sekhukhuneland. Unpublished M.A. thesis, University of the Witwatersrand, Johannesburg.
- Vogel, J.C. 1970. Groningen radiocarbon dates IX. *Radiocarbon* 12: 444-471.
- Vogel, J.C. 1971. Radiocarbon dating of Iron Age sites in the southern Transvaal. In: Mason, R.J. (ed.) *Prehistoric man at Melville Koppies*: 59-63. Johannesburg: Occasional Paper 6 of the Department of Archaeology, University of the Witwatersrand.
- Vogel, J.C. & Fuls, A. 1999. Spatial distribution of radiocarbon dates for the Iron Age in southern Africa. *South African Archaeological Bulletin* 54: 97-101.
- Vogel, J.C., Fuls, A., Visser, E. & Becker, B. 1993. Pretoria calibration curve for short-lived samples, 1930-3350 BC. *Radiocarbon* 35: 73-85.
- Vogel, J.C. & Van der Plicht, J. 1993. Calibration curve for short-lived samples, 1900-3900 BC. *Radiocarbon* 35: 87-91.
- Von Bezings, K.L. & Inskeep, R.R. 1966. Modelled terracotta heads from Lydenburg, South Africa. *Man* 1: 102.
- Wadley, L. & Jacobs, Z. 2004. Sibudu Cave, KwaZulu-Natal: Background to the excavations of Middle Stone Age and Iron Age occupations. *South African Journal of Science* 100: 145-151.
- Wadley, L. & Jacobs, Z. 2006. Sibudu Cave: background to the excavations, stratigraphy and dating. *Southern African Humanities* 18: 1-26.
- Walraven, F. 1981. 2526 Rustenburg Geological Series. Explanatory notes by F. Walraven. Geological Survey of South Africa. Pretoria: Government Printer; scale 1: 250 000.
- West, S.M. 1992. Temper, thermal shock and cooking pots: a study of tempering materials and their physical significance in prehistoric and traditional cooking pottery. Unpublished MSc thesis, Unpublished MSc thesis, University of Arizona, Tucson.

- Wilson, L. & Pollard, A.M. 2001. The provenance hypothesis. In: Brothwell, D.R. & Pollard, A.M. (eds) *Handbook of Archaeological Sciences*: 507-517. Chichester: John Wiley & Sons, Ltd.
- Wintle, A.G. 1973. Anomalous fading of thermoluminescence in mineral samples. *Nature* 245: 143-144.
- Wintle, A.G. 1997. Luminescence dating: laboratory procedures and protocols. *Radiation Measurements* 27: 769-817.
- Wintle, A.G. & Murray, A.S. 1999. Luminescence sensitivity changes in quartz. *Radiation Measurements* 30: 107-118.
- Wintle, A.G. & Murray, A.S. 2006. A review of quartz optically stimulated luminescence characteristics and their relevance in single-aliquot regeneration dating protocols. *Radiation Measurements* 41: 369-391.
- Wobst, H.M. 1999. Style in archaeology or archaeologists in style. In: Chilton, E.S. (ed.) *Material meanings: critical approaches to the interpretation of material culture*: 118-132. Salt Lake City: University of Utah Press.
- Woodborne, S. & Vogel, J.C. 1997. Luminescence dating at Rose Cottage Cave: a progress report. *South African Journal of Science* 93: 467-470.
- Zacharias, N., Michael, C., Philaniotou-Hadjianastasiou, O., Hein, A. & Bassiakos, Y. 2006a. Fine-grain TL dating of archaeometallurgical furnace walls. *Journal of Cultural Heritage* 7: 23-29.
- Zacharias, N., Michael, C.T., Georgakopoulou, M., Kilikoglou, V. & Bassiakos, Y. 2006b. Quartz TL dating on selected layers from archaeometallurgical kiln fragments: a proposed procedure to overcome age dispersion. *Geochronometria* 25: 29-35.